Chemistry of functionalised macrocycles

Matthes, Karen Elizabeth

CHEMISTRY OF FUNCTIONALISED MACROCYCLES

by

KAREN ELIZABETH MATTHES, B.Sc. (Hons), G.R.S.C.

A thesis submitted for the degree of Doctor of Philosophy
of the University of Durham.

September 1987

MEMORANDUM

The work for this thesis has been carried out in the Department of Chemistry at the University of Durham between October 1984 and September 1987. It is the work of the author unless otherwise stated. None of the work has been submitted for any other degree.

To my parents and Ian

I cannot tell you why the thing went wrong;

Recriminations though were hot and strong.

"Well", said my lord, "There's nothing more to do.

I'll note these dangers for another brew;

I'm pretty certain that the pot was cracked.

Be that as may, don't gape! We've got to act.

Don't be alarmed, help to sweep up the floor

Just as we always do, and try once more.

Pluck up your hearts!" The muck was gathered up,

A canvas then was laid to form a cup

And all the muck was thrown into a sieve;

He sifted it for what it yet might give.

from *The Canon's Yeoman's Tale,*

The Canterbury Tales by Geoffrey Chaucer

(Translated into Modern English by Nevill Coghill)

ACKNOWLEDGEMENTS

I am indebted to the following people:

Dr. David Parker for his guidance and patience during the course of this research. I shall miss his eternal optimism and endless enthusiasm;

Professor George Ferguson for his rapid determination of the X-ray crystal structures reported in this thesis. It was a pleasure to meet Professor Ferguson in April of this year, and to "see the face" at the other end of the terminal;

Dr. Hans-J. Buschmann for the determination of stability constants of complexation by titration calorimetry.

I would like to thank the SERC for financial support, particularly for providing the finance to attend the XI International Symposium on Macrocyclic Chemistry, Firenze, Italy in September 1986.

Throughout the course of this research Dr. Stephen Whittleton has been a great friend. I wish to thank him for all his encouragement and belief in my work.

Finally I would like to thank my parents and Ian for their love and support and friendship.

CHEMISTRY OF FUNCTIONALISED MACROCYCLES

by

Karen Elizabeth Matthes

ABSTRACT

The work reported in this thesis is divided into two distinct areas. The first involves the synthesis of monoaza- and diaza-[12]-ring macrocycles, with differing side-arm *N*-substituents. The twelve-membered macrocycles possess a convenient ring-size for exploring the stability and selectivity of complexation of small cations, in particular those from groups IA and IIA. Amide substituents on nitrogen were expected to function as effective σ-donors to cations with high charge density (*e.g.* Li^+, Ca^{2+}), because of their high ground state dipole moments. The effect of the length of the side-arms attached to nitrogen on the complexation has also been studied. Complexation behaviour has been probed using ^{13}C NMR spectroscopy, titration calorimetry, and fast-atom bombardment mass spectroscopy. Copper(II) complexes of three of the [12]-ring cycles have also been characterised by X-ray crystallographic analysis.

The second area involves the study of a series of macrocyclic ligands capable of forming homo- and hetero-dinuclear complexes. In particular, ligands containing the pyridyl-dithio (PyS_2) binding unit and a polyether chain linking the two sulphur atoms have been examined. The three binding atoms of each PyS_2 group define three corners of a fairly rigid square planar environment which favours the formation of square planar d^8 complexes. Accordingly, complexation with rhodium(I) [and (III)], palladium(II), and platinum(II) has been investigated: the structural properties of these complexes have been determined by the use of FT NMR and X-ray crystallography.

CONTENTS Page No.

CHAPTER ONE - INTRODUCTION

1.1 Applications for Lithium and Calcium Ion-Selective Macrocyclic Ionophores

In 1967, Pedersen reported on the ability of macrocyclic crown ethers to bind to metal cations.[1] This initial observation has prompted a mass of literature on the use of macrocyclic polyether analogues as selective ionophores for both lithium and calcium ions. This interest was stimulated by the similarity in behaviour of the macrocyclic ligands to naturally occurring ionophorous antibiotics.[2,3] The development of such lithium and calcium ion carriers could have a diverse range of applications, as discussed below.

1.1.1 *Ion-selective electrodes*

The natural antiobiotic valinomycin has an exceptionally high selectivity for potassium ions over sodium ions of 10,000 to 1.[4] The structure of valinomycin is represented in Figure 1.1 and the structural features which give rise to this high selectivity are discussed in

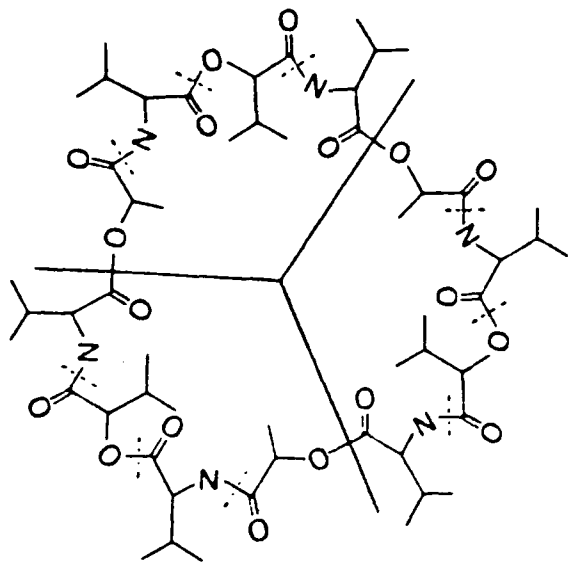

Figure 1.1

Primary structure of valinomycin

section 2.1. Consequently valinomycin is widely used as a sensing element in potassium-selective electrodes.[2,5]

There is a great deal of research into the design of neutral lithium-selective ionophores for incorporation into a lithium-selective solvent polymeric membrane electrode.[6-16] Such a device would permit the convenient measurement of lithium ion activity in both physiological and environmental systems.[13-19] For example, it would be useful to measure lithium ion activity in blood during therapy of manic depressive psychosis. The structures of the lithium ionophores, (1) and (2), currently available from Fluka, for incorporation into solvent polymeric membrane electrodes[6,11,20] are given below.

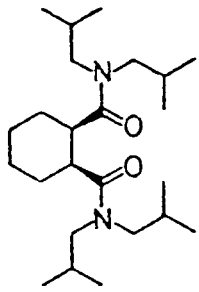

(1)

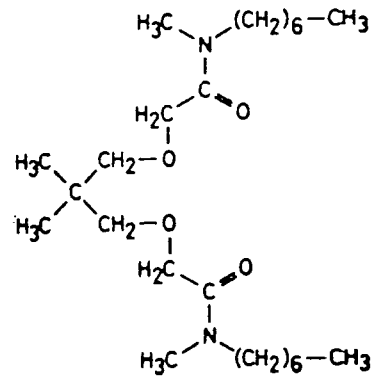

(2)

Compound (1), when incorporated into polymeric membranes, selectively binds lithium ions over alkaline earth metal cations and alkali cations by approximately 1,000 and 100 respectively.[9] Variation of the amide groups in (1) modifies selectivity markedly,[16] so much so that the selectivity exhibited by (1) has now been superceded by (3).[16]

Synthetic neutral carrier-based calcium-selective electrodes based on the ligand (4)[21,22] are currently used widely for clinical and

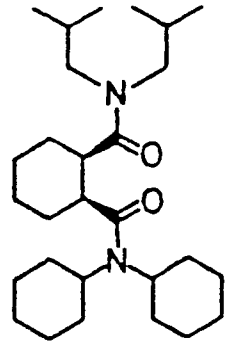

(3)

electrophysiological calcium activity measurements.[23] Compound (4) is also available from Fluka. However, a continued and extensive effort has been maintained in the design of calcium ion-selective electrodes with improved selectivity and sensitivity.[24-27] The selectivity exhibited by (4) has been further improved by the use of ionophore (5).[28]

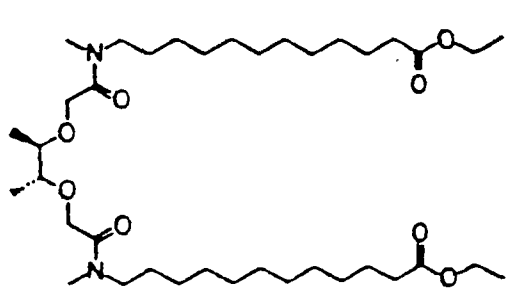

(4)

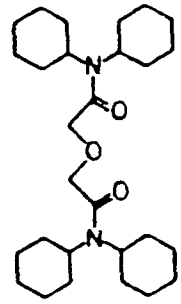

(5)

By the use of (5) together with current membrane technology, selectivities for Ca^{2+} of $10^{7.4}$ and 10^{8} are obtained over Na^{+} and K^{+} respectively. The detection limit of the Ca^{2+} electrode response function in an intracellular ion background is at about 100 pM Ca^{2+}.

There is still a clear need to develop improved lithium and calcium *selective* synthetic ionophores for incorporation into their respective cation sensors. These electrodes incorporate an appropriate selective macrocyclic ionophore embedded into a polymeric membrane. The membrane matrix typically consists of poly(vinylchloride) (PVC) and *o*-nitrophenyl octyl ether (NPOE).[14,16,28] Potentiometric cation selectivity coefficients may be determined using a suitable cell,[14,28,29] for example, the cell represented by (6) may be used to measure lithium selectivity coefficients using the fixed interference method.[21] This method involves measuring the cell potential using solutions with a constant level of interference and with a varying activity of lithium ions.[30]

$$\text{Ag/AgCl/1 M LiCl/PVC membrane/}\overset{\text{sample}}{\underset{\text{solution}}{}}\text{/0.1 M } NH_4NO_3\text{/4 M KCl/AgCl/Ag} \qquad (6)$$

1.1.2 *Medical Applications*

Lipophilic lithium ion carriers have potential pharmocological application because of their predicted ability to enhance uptake of lithium into the brain through biological membranes. The criteria for a species to diffuse passively through the blood-brain barrier are that it should be lipophilic, have a low molecular weight, and preferably possess a zero overall charge.

At present, lithium carbonate is used in the treatment of manic depression and other neurological and psychiatric disorders. It is the

slow penetration of lithium through the blood-brain barrier and across other membranes which delays the onset of drug action necessitating the use of large doses with accompanying undesirable side-effects.[13,19]

1.1.3 *Extraction of Lithium from Sea-water*

The natural abundance of lithium in ores is low and with the expected increasing demand for lithium in the next century, the extraction of lithium from sea-water is under consideration. This predicted rise in demand is due to the probable use of lithium as a blanket material for breeding tritium in thermonuclear reactors and its incorporation into high performance, low density batteries.[31] The extraction of lithium from sea-water may be envisaged by attaching lithium-selective macrocycles onto inert supports. Silica[32] or highly substituted cross-linked polystyrene resins may be considered. In the latter case the binding site may be situated away from the backbone of the polymer by a long alkyl chain.[33] Lithium ions may then diffuse freely to the binding site. A copolymeric resin of styrene and acrylic acid has been used to bring the concentration of lithium ions to thirty times that of sea-water.[34] These polymeric, inert supports are conveniently functionalised with macrocycles using conventional and established methods.[32,33] A stable amide bond may be used to attach the cycle to the support, suggesting the structures represented by (7) and (8).

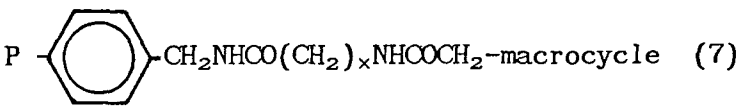

(7)

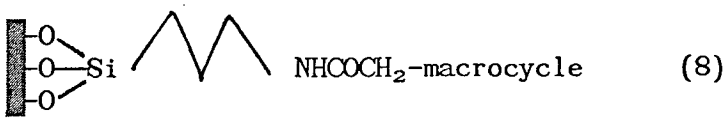

(8)

Lithium ions may be recovered from the support, after its exposure to a lithium-rich solution, by elution with dilute acid.

In direct relation to this work is the extraction of lithium ions from aqueous to organic phases.[35] An extension of this idea, involving lithium ion transport from one aqueous phase through an immiscible organic phase and back into an aqueous phase, may be envisaged.[36] This system has been considered by others as an "artificial membrane" and may be related to lithium transport *in vivo*.[13,19]

1.2 Homo- and Hetero-Dinucleating Ligands Using Functionalised Macrocycles

Mononuclear complexes where a metal cation is surrounded by either inorganic or organic ligands have been studied since the beginning of this century. It is only more recently, within the last seventeen years, that more complex species involving two or more metal centres have emerged. This discussion will limit itself to dinuclear complexes where the incorporation of two chelating sub-units within a ditopic macrocycle should allow the assembling of two cations bound in close proximity.[37-47] Two metal cations adjacent to each other permit the study of various novel properties such as complexation features, cation-cation interactions at short distances, and redox processes. Thus, the study of such complexes may allow greater insight into their potential chemical reactivity as dinuclear catalysts[41,42] and in their significance as models of biological dimetallic sites.[38,48-50] For a more complete discussion of all matters concerning polynuclear species several review articles have been published recently.[51-55]

1.2.1 Topological Characteristics of the Dinucleating Ligands

Dinuclear cryptates of metal cations may be formed by the inclusion of two metal cations within a macrocyclic ligand containing two binding sub-units.[37,41,43,53,56] The nature of the sub-units used as building blocks and the number of connecting bridges used in the construction of these dinucleating ligands give rise to to a variety of macropolycyclic structures.[51-53,57,58] Different possible topologies of the ligands are represented schematically in Figure 1.2, together with their respective derived dinuclear complexes.

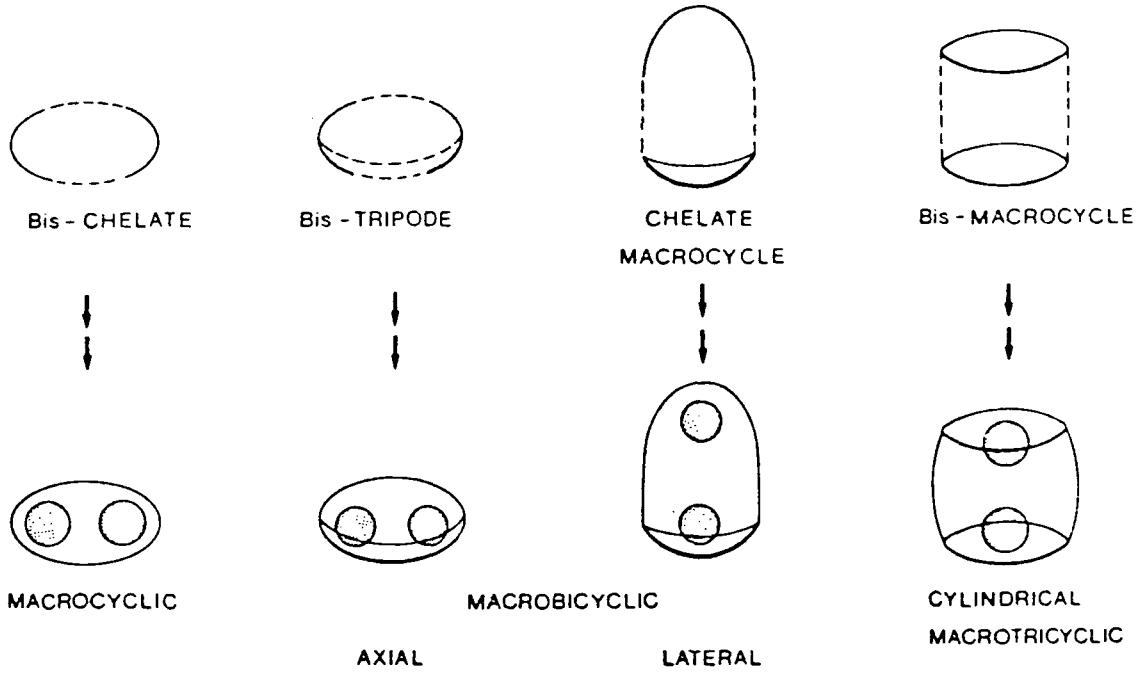

Figure 1.2

Topologies of macropolycyclic cryptands and their corresponding dinuclear cryptates

It is possible to gain control of the properties of these systems by clever design of the ligand. Bridges employed may be either rigid (aromatic groups) or flexible (aliphatic chains). Similarly, the

macrocycles may be saturated crowns (polyoxadiaza or polythiadiaza-derivatives) or unsaturated crowns (porphyrins, tetra-imine macrocycles). Thus, for example, a number of systems can be envisaged for the macrotricycle (Figure 1.3).

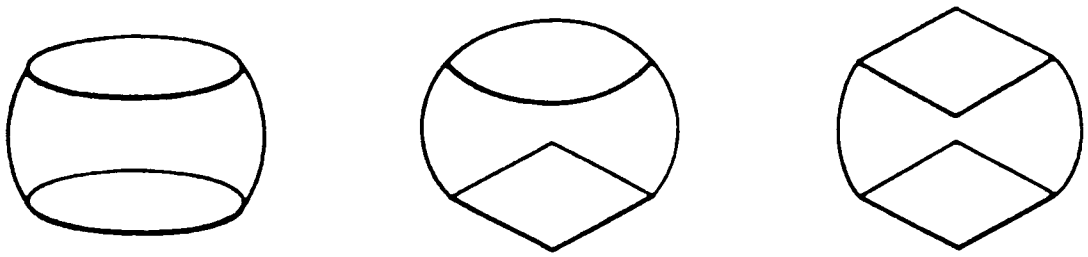

Figure 1.3

Schematic representation of three types of macrotricyclic structure obtained by combining saturated (represented by a circle) and unsaturated (represented by a square) macrocycles

Dinucleating ligands may also be formed by the attachment of one, two, or more functionalised side-arms onto a macrocyclic framework.[40,44,45,59] The topologies of the derived complexes are represented in Figure 1.4.

The nature of the heteroatoms within the binding sub-units will confer on the ligand a degree of selectivity. The length and the geometry of the bridges linking the chelating sub-units define the relative position of the bound cations. Thus, in these complexes the nature of the metal cations and the distance between the cations and their arrangement within the macrocyclic cavity may be controlled by the design of the ligand.[51] The juxtaposition of the two metal centres allows them to behave either independently or co-operatively. The

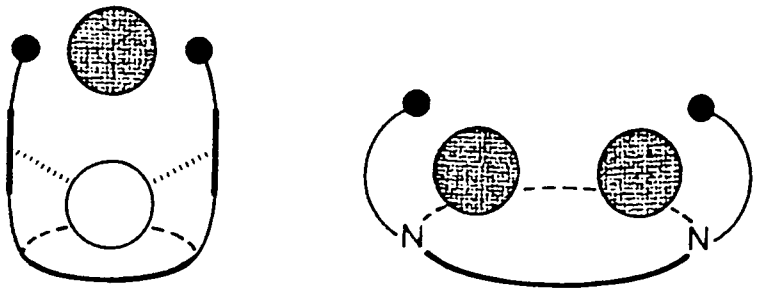

Figure 1.4

Topologies of dinuclear complexes

dinucleating macrocyclic system may exhibit the characteristics of mononuclear complexes[51] (catalysis, recognition, transport) but may also afford an entry into the study of higher forms of molecular behaviour such as co-operativity and regulation.

1.2.2 *Cascade Complexation and Catalysis*

Bis-Chelating macrocyclic ligands may encapsulate two metal cations forming dinuclear cryptates. Where the two binding units are dissimilar, hetero-dinuclear complexes may be formed and where the binding units are identical, homonuclear complexes may be formed. Homonuclear complexes may also be formed where binding units are only slightly dissimilar, in which case the cations will display different characteristics. Bridging of the two metal centres by a substrate molecule may then occur, provided the metal-metal distance is appropriate. The complex formed is denoted a cascade-type complex[37,42,53] and the process is represented schematically in Figure 1.5.

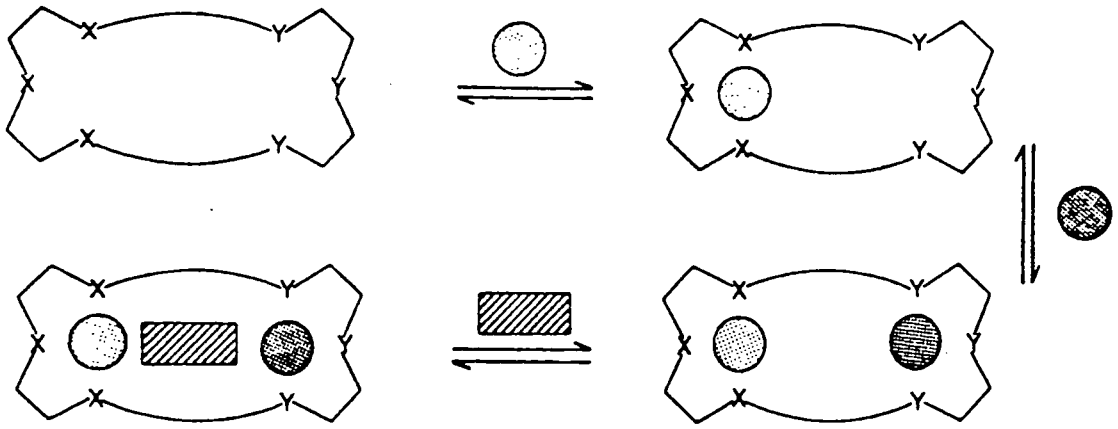

Figure 1.5

Sequential formation of a cascade complex involving complexation of Two different metal cations and a substrate molecule by a dissymmetric macrocyclic ligand

The importance of such complexes lies in their potential ability to bring together two substrate reactant molecules and to activate them to reaction - catalysis. The geometry of the complexes may be controlled by using pre-organised but flexible ligands, pre-organised in terms of size, shape, nature, and arrangement of the binding sites. Thus, the design of the ligand allows control over the assembling process of the complex.

As an example of this behaviour, we can consider the assembly of a cylindrical macrotricycle with two metal cations placed in the lateral cavities. The dimensions of the two face-to-face macrocycles and the lengths of the bridges linking them together will determine the position of the metal cations bound within. Given that the distance between the cations is sufficiently long, a substrate may be inserted into the central cavity to form a cascade complex (Figure 1.6).

The double bridging of two porphyrins (unsaturated cycles) gives

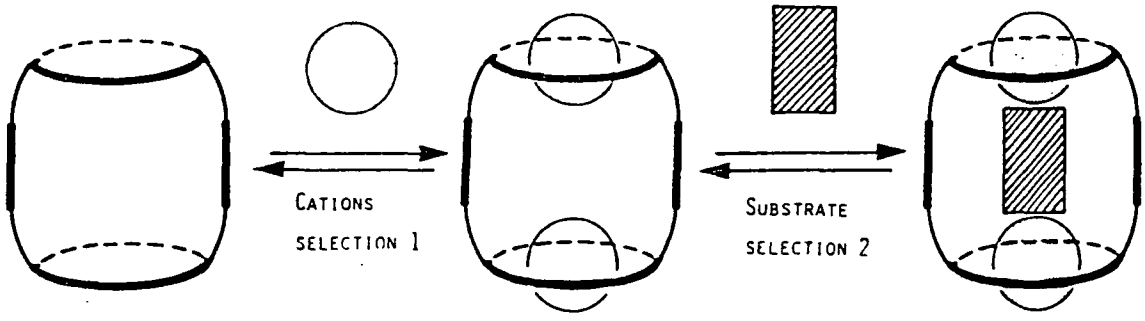

Figure 1.6

Sequential formation of a cascade complex by a macrotricyclic dinucleating cryptand

rise to homoditopic ligands where the distance between the metal centres is sufficiently long that a substrate may be bound between. Both Chang[60-62] and Collman[63-67] have contributed greatly to this area of research. Several of the ligands studied are given in Figure 1.7.

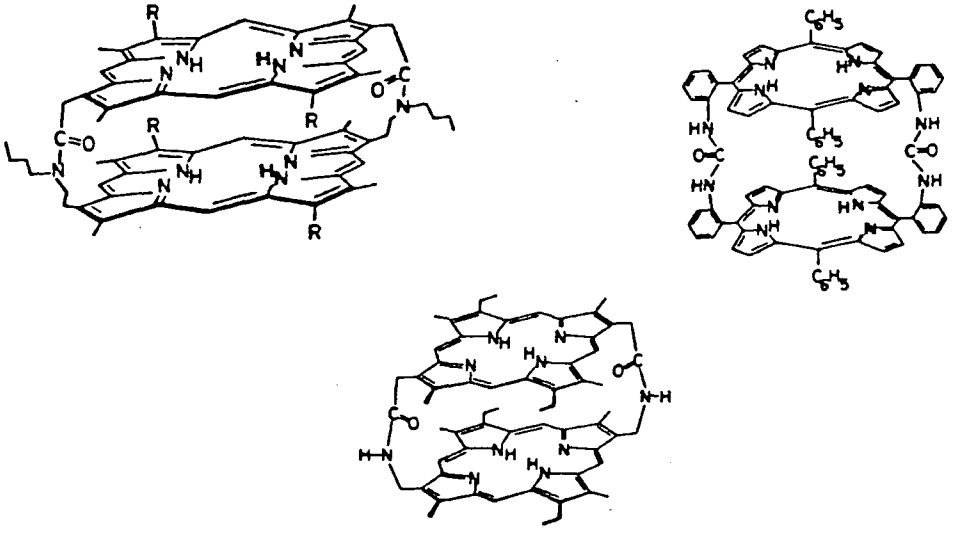

Figure 1.7

Examples of bis-porphyrin homo-ditopic ligands

The catalytic behaviour of these ligands results from their ability to bind small molecules between the cations. The catalytic electroreduction of oxygen to water serves as an example (Figure 1.8).[60,63,64,67]

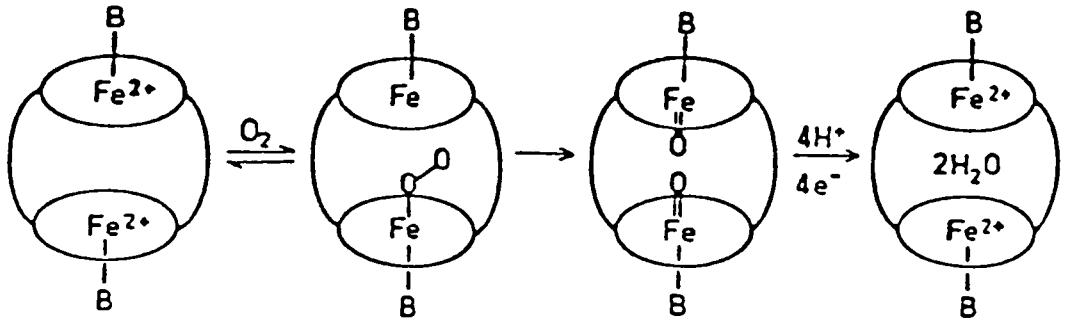

Figure 1.8

Schematic representation of the catalytic reduction of oxygen by a bis-*iron(II) porphyrin complex*[63]

It is interesting to note that the formation of a hetero-dinuclear porphyrin complex relies on the following strategy: bridges between the two porphyrin units are formed between one free porphyrin and one already complexed[66] (see Figure 1.9).

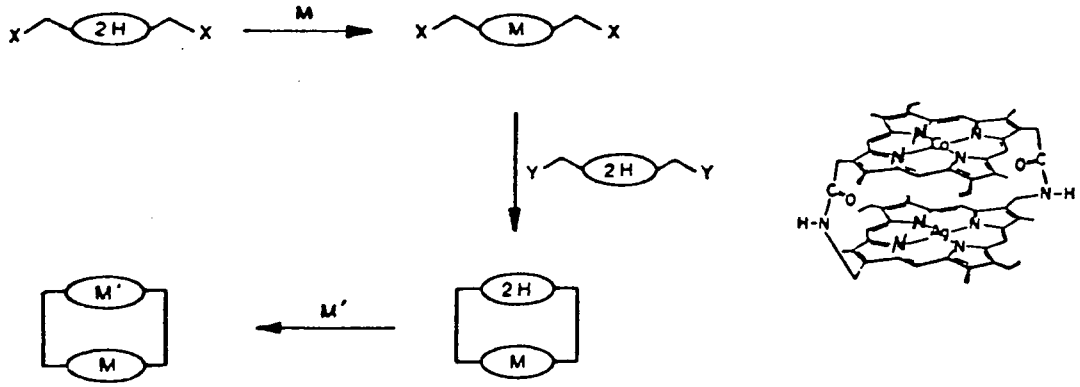

Figure 1.9

Formation of a hetero-dinuclear bis-*porphyrin complex*

1.2.3 *Activation of Substrate Molecules Bound Between Redox and Lewis Acid Metal Centres*

Ligands where one sub-unit bears "soft" binding sites (thia- or phospha-functionality) and one bears "hard" binding sites (aza- or oxa-functionality) will exhibit haptoselectivity: the selective binding of a particular cation at a particular binding sub-unit within the polytopic ligand.[45-47] In particular, a ditopic ligand which combines a sub-unit containing soft sites with one bearing hard sites should form dinuclear complexes displaying respectively a redox and a Lewis acid metal centre.[37] A soft site should bind preferentially to a soft metal, that is, one with a low oxidation state. The metal centre can thus act as a reducing agent and become a redox centre. The hard centre will bind to a metal in a high oxidation state which will accept electrons readily, constituting a Lewis acid centre. There exists potential for co-operative activation of substrates bound between (Figure 1.10).

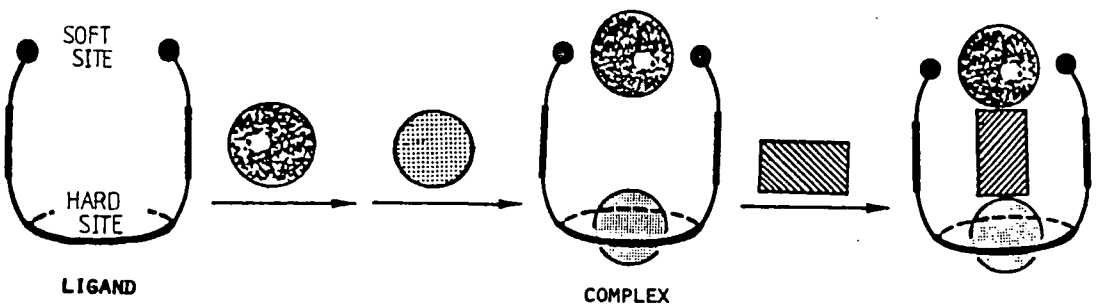

Figure 1.10

Haptoselective formation of a hetero-dimetallic complex

By the attachment of phosphine functionality onto ethylene glycols, Powell *et al.*[68] have prepared ligands which provide both a soft and hard site for metal binding. The phosphorus atoms constitute the soft site and the oxygen atoms on the ether chain the hard site. The binding of soft metals (M = Cr, Mo, W) allows subsequent reaction of an alkyl lithium reagent activating the bound carbon monoxide, so increasing its susceptibility to nucleophilic attack (see Figure 1.11a).

The diphosphine ligand (9) which contains an unusual tripodal O_3N

$$(Ph_2POCH_2)_2NCH_2CH_2OCH_3$$

(9)

unit for complexing lithium has also been reported to activate CO in this manner (Figure 1.11b).[69] The ligand provides the lithium cation with all but one donor atom for a completely satisfactory coordination sphere and the *separation* and *orientation* of the bound metals are appropriate for an M—(RCO)⟶ Li^+ bridge.

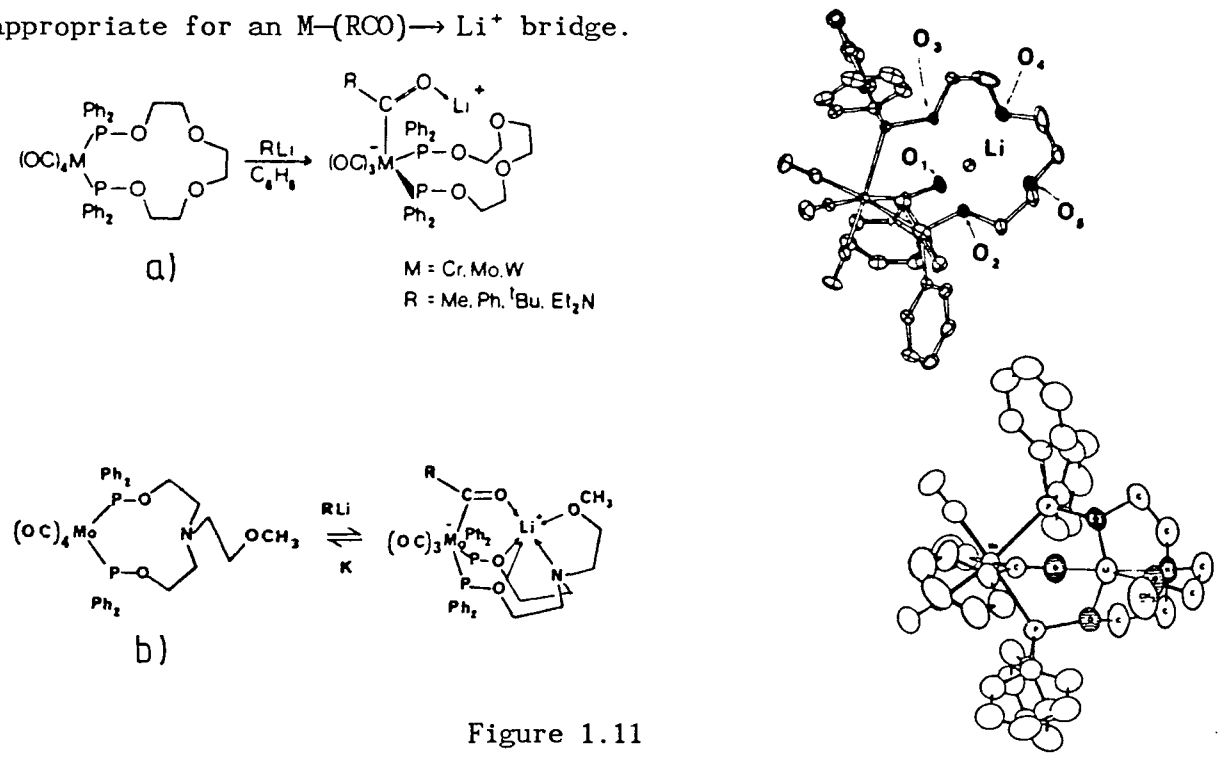

Figure 1.11

Formation and X-ray crystal structures of (a) a hetero-dinuclear Mo-Li complex with a phosphine-functionalised ethylene glycol[68]*, and (b) a hetero-dinuclear Mo-Li complex of* (9)[69]

The incorporation of phosphine functionality onto a side-arm attached to the nitrogen of a macrocycle, enables the ligand to form bimetallic complexes containing different metals in close proximity.[40,44,45,59] Powell[45] has reported dimeric complexes, (10-12) containing two copper(I) atoms situated in the cavity of the macrocycles and a rhodium(I) or iridium(I) atom bound between the phosphine groups. These complexes react reversibly with CO, binding the CO molecule between the two copper atoms.

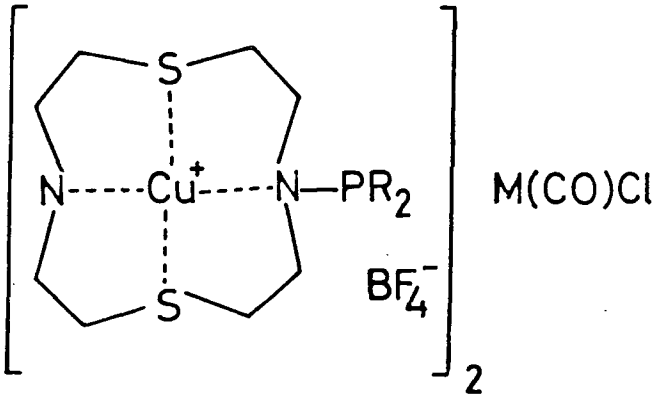

(10) M = Rh, R = Ph

(11) M = Rh, R = Me

(12) M = Ir, R = Ph

The activation of carbon monoxide by a phosphine-functionalised ligand has been reported,[44] where Fe(II) is bound by the soft binding site and sodium is bound by the hard macrocyclic donor atoms and the oxygen of the resulting acylate group (Figure 1.12). The frequency of

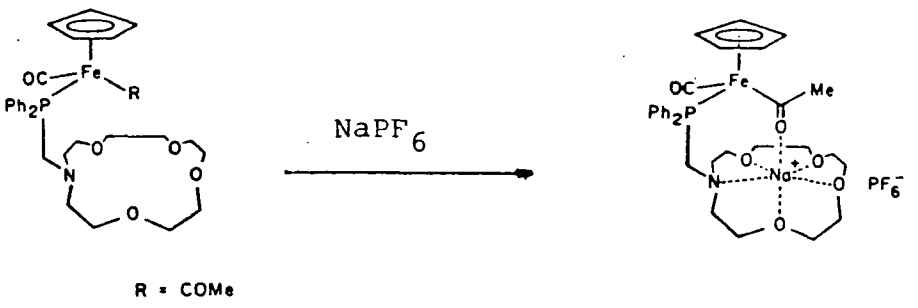

R = COMe

Figure 1.12

Formation of a heteto-dinuclear Fe-Na complex showing activation of the acyl CO[44]

the acyl CO stretch decreases and that of the terminal CO increases, indicative of acyl coordination to a Lewis acid.

Other ligands, for example (15-20), have been prepared where phosphine-functionalised side-arms are attached to the macrocyclic framework *via* a nitrogen atom (see Figure 1.13).[59]

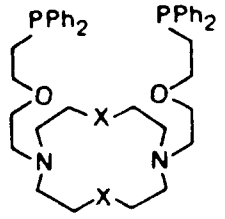

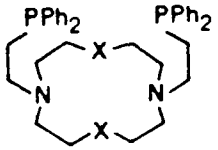

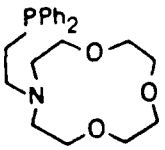

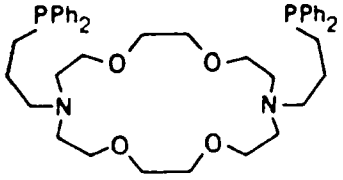

(15) X = O (16) X = S

(17) X = O (18) X = S

(19)

(20)

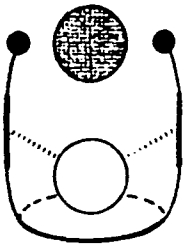

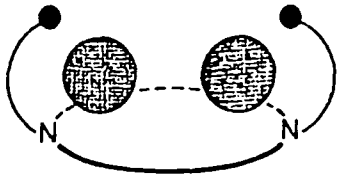

(13) (14)

Figure 1.13

(13) *and* (14) *are representative models of the dinuclear complexes formed by ligands* (15) *to* (20)

Ligands formed by the bridging of a macrocycle by a chelating chain (21-24) have been prepared[70,71] which may also display the properties discussed above. Figure 1.14 depicts a representative model of the

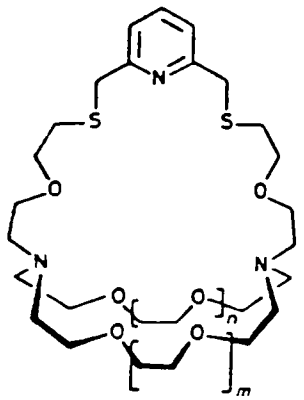

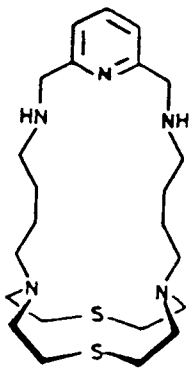

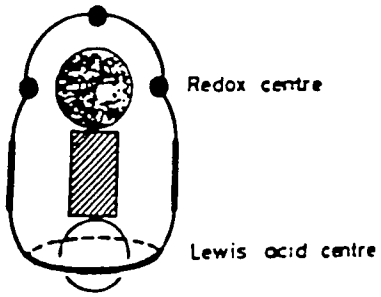

(21) m = n = 0
(22) m = 1, n = 0
(23) m = n = 1

(24)

(25)

Figure 1.14

(25) *is a representative model of the cascade complexes which may be formed by ligands* (21) *to* (24)

dinuclear cryptates which may be formed by ligands (21) to (24). Lippard's macrocyclic phosphands,[72] (26) and (27), combining hard and soft sites within a monocycle have also been synthesised.

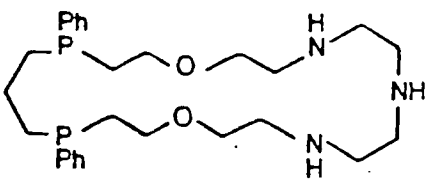

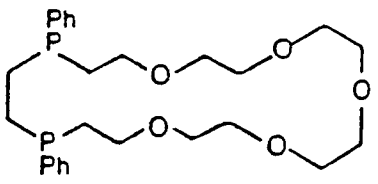

(26)

(27)

The interest in these ligands is stimulated in part by the potential activation of a small substrate molecule such as carbon monoxide or ethene bound between the two metal centres possessing different characteristics. The activation of CO bound in this manner is schematically represented in Figure 1.15 and will be discussed in more detail in Section 3.2.

Figure 1.15

M' Acting as a Lewis acid and enhancing susceptibility of CO to nucleophilic attack

Ligand (25) forms a dinuclear Cu(II) complex with vastly different electrochemical properties for the two cations.[71] Ligands (22-24) form dinuclear complexes with rhodium and various other cations. Rhodium complexes as a $(Rh\text{-}CO)^+$ unit (28) but no activation of the carbonyl occurs on binding of the macrocyclic sub-unit to other cations [Li^+ and Zn^{2+} for (22), Al^{3+}, Ag^+, and La^{3+} for (23), and Ag^+, Cd^{2+}, and Ba^{2+} for (24)]. For a further discussion of these complexes see Section 3.3.

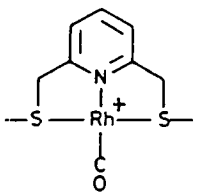

(28)

1.2.4 *The Use of Dinuclear Complexes as Biological Models*

The binding of two metals in close proximity is a characteristic feature of many metalloenzymes.[55] The distance between the two metal centres is usually less than 10 Å and is often less than 5 Å.[73] The metal centres may be homo- or heteronuclear and in many cases the metals share bridging ligands. Where the micro-environment of a metal centre is unknown, speculative models reproducing a physical property of the biomolecule may be synthesised and where the micro-environment is known, corroborative models which are direct analogues of the metallo-centre may be studied.

Lippard's work on the dicopper(II) imidazolate-bridged complex (Figure 1.16),[74,75] serves as an example of a corroborative model for the homo-dinuclear copper site in superoxide dismutase with copper(II) substituted for zinc(II). A series of related imidazolate-bridged

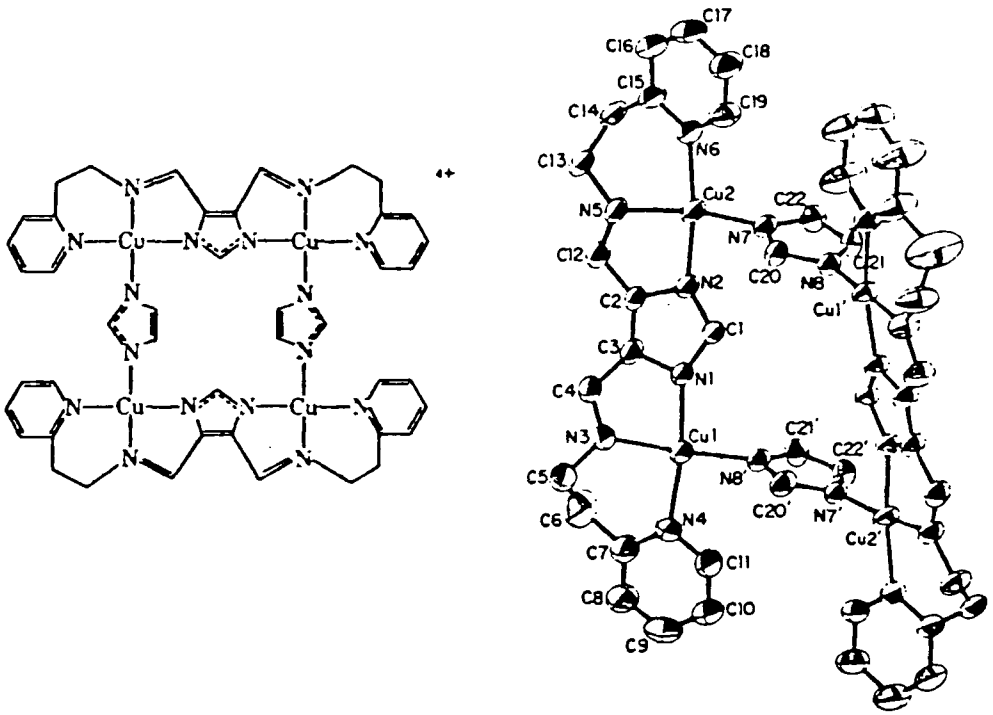

Figure 1.16

Imadazolate-bridged complex of copper(II)

polynuclear copper(II) complexes has been investigated.[76,77] The incorporation of an imidazolate-bridged bimetallic centre within a macrocyclic cavity has also been achieved in (29) and (30)[78-82] which

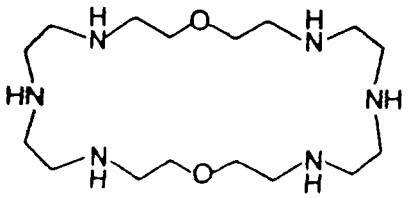

(29)

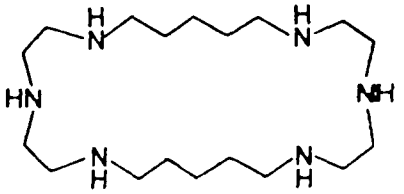

(30)

prevents the metal ions from separating when the bridge is broken [see Figure 1.17 for structure of complex with (29)].

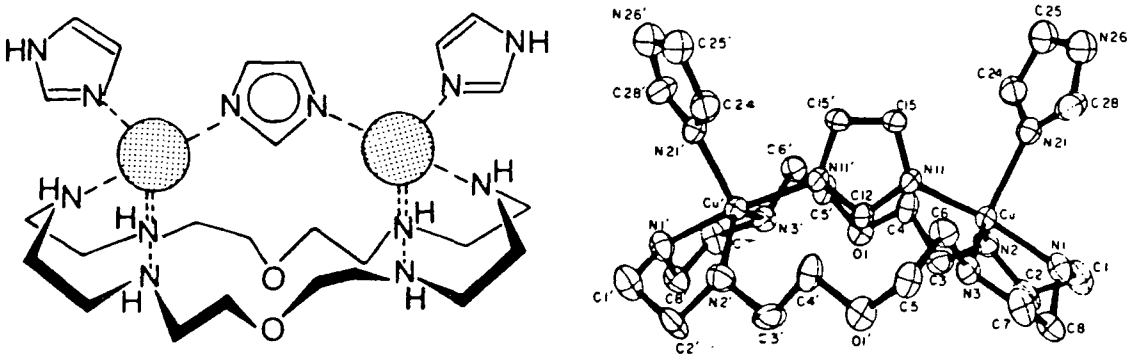

Figure 1.17

X-Ray crystal structure of imadazolate-bridged bis-*copper(II) centre within the macrocyclic cavity of* (29)

These studies confirm the existence of an imidazolate-bridged dicopper(II) centre in a form of bovine erythrocyte superoxide dismutase in which Cu(II) replaces Zn(II) and provide a foundation for the identification of imidazolate-bridged centres in other metallobiomolecules.

A recent review by Lippard and Martin catalogues the important observations on dinuclear copper complexation.[83] A comprehensive treatment of the rôle of dinucleating ligands as biological model systems, which seeks to understand the metal environments in bimetallobiomolecules is given by Fenton.[55]

1.3 The Scope of this Work

The work reported in this thesis is divided into two distinct areas. The first involves the synthesis of a series of *N*-functionalised [12]-membered ring macrocycles which incorporate binding groups on their side-arms. Complexation studies between these ligands and a number of Group IA and IIA metals have been undertaken, primarily using the techniques of Titration Calorimetry and NMR. The second area involves the synthesis of macrocyclic ligands capable of forming hetero-dinuclear and homo-dinuclear complexes. The structural properties of some dinuclear complexes have been studied by multinuclear NMR and X-ray crystallography. The potential activation of a small substrate molecule (CO) bound between two metal centres has been probed.

Chapters Two and Three review the two areas outlined above. Chapter Two includes a discussion on the many properties of macrocycles which influence their binding properties to metal cations and also the

techniques available for measuring stability constants of complexations and selectivities of complexation.

Chapters Four, Five, and Six are devoted to the presentation and discussion of results. Chapter Four is devoted to the synthesis and complexation studies of a series of [12]-ring azamacrocycles. Chapters Five and Six discuss the synthesis and complexation properties of homo- and hetero-dinucleating ligands with a range of transition metal cations.

Chapter Seven is the experimental chapter which includes experimental procedures for the preparation of compounds and also describes briefly the experimental procedures used to determine stabilities and selectivities of complexation.

CHAPTER TWO - FACTORS CONCERNING THE SELECTIVITY OF BINDING IN CYCLIC IONOPHORES

2.1 Introduction

An ionophore may be defined as a receptor molecule which forms stable, lipophilic complexes with charged, hydrophilic cations such as lithium, sodium, calcium, and potassium. Such complexes may be considered as host-guest complexes in which the guest cation resides in the cavity created by the host. The ability of an ionophore to transport an ion into a lipophilic phase across a natural or artificial membrane holds great interest for chemists as expounded in Chapter One. It is the selective transport of particular cations that is sought and this discussion limits itself to the cyclic ionophorous complexes of the alkali and alkaline earth metals. Acyclic ionophores may also act as lipophilic lithium ion carriers.[84]

An ideal ionophore for an alkali metal cation posing as a spherical guest, will provide a cavity of appropriate size, lined with polar groups which can give maximum binding through ion-dipole interactions. Such polar binding groups which more usually consist of electronegative atoms such as nitrogen or oxygen, must be able to bind to the cation in a stepwise fashion, replacing the solvation shell of the cation. A ligand may have a pre-formed cavity whence complexation occurs without major conformational change, or it may (particularly if acyclic) adopt its final conformation having undergone an extensive structural rearrangement, brought about by the complexation. The ligand also requires lipophilic groups which are oriented towards the periphery of the molecule to aid transfer of the entire complex into a non-polar phase.

Valinomycin exemplifies an ionophore exhibiting exceptionally high selectivity, with a 10^4 times greater affinity for potassium ions than

for sodium ions.[4] It is the properties of valinomycin which give rise to this high selectivity that chemists wish to mimic with respect to other alkali and alkaline earth metals. Thus, a mention of the more salient structural features of valinomycin responsible for its ionophorous behaviour is appropriate at this point. Valinomycin is a macrocyclic polypeptide which has six amide and six ester carbonyls. The amide carbonyls are involved in intramolecular hydrogen-bonding and the ester carbonyls co-ordinate to the potassium ion in an almost octahedral fashion, screening the cation from solvent interaction (Figure 2.1). The lipophilic groups are all directed to the periphery of the molecule aiding the lipophilicity of the complex. Space-filling models

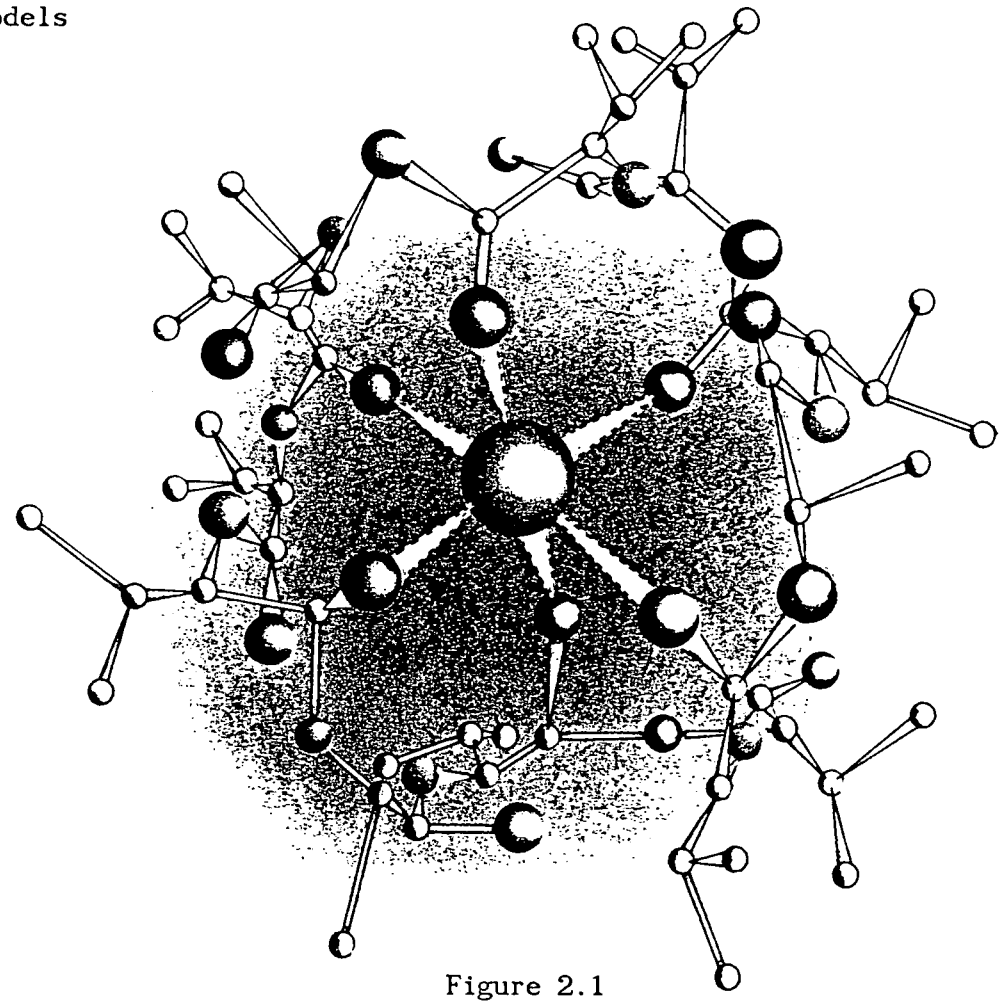

Figure 2.1

X-Ray crystal structure of the K^+ complex of valinomycin

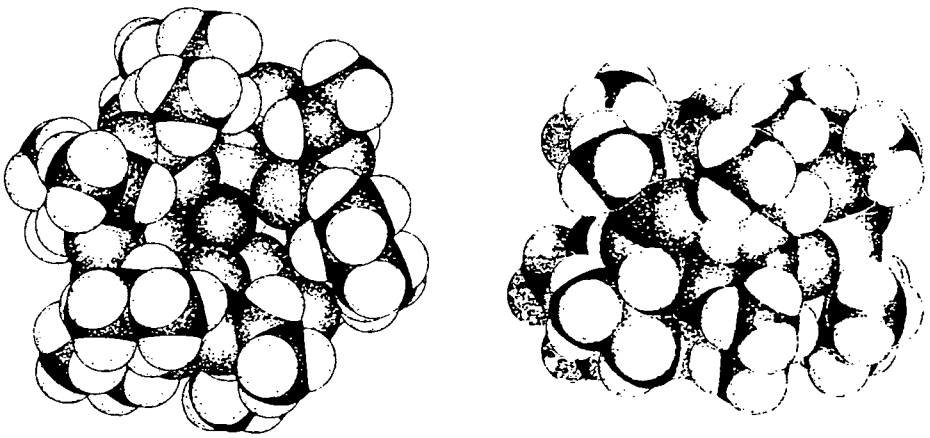

Figure 2.2

Space-filling models of the K^+ complex of valinomycin: a view from above the molecule (left) *demonstrating the optimum fit between host and guest, and a side view* (right) *showing the lipophilic periphery.*

demonstrate that an optimum fit between cavity size and potassium ion is achieved (Figure 2.2). It is the inflexible nature of the ligand, enforced by the intramolecular hydrogen-bonds, that does not allow the cavity to adjust and encapsulate the smaller sodium ions so efficiently. The structure is discussed in much greater detail in the reviews by Hilgenfeld and Saenger[2] and Ivanov.[85]

2.1.1 *Crown Ethers*

The first synthetic ionophores for the Group IA and IIA metals were the macrocyclic polyethers (crown ethers),† for example, (31) and (32) reported by Pedersen.[1] To avoid lengthy IUPAC nomenclature, the crown

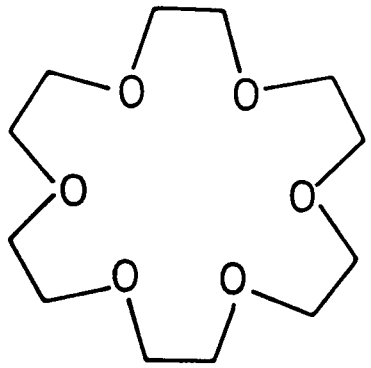

(31)

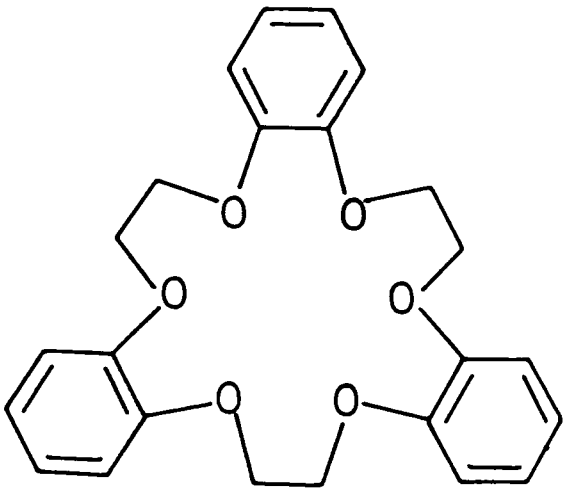

(32)

ethers will be referred to according to the naming system devised by Pedersen.[1] These names derive from the description "crown" given to this class of compounds because of the appearance of their molecular models. The names consist of (1) the number and kind of hydrocarbon rings, (2) the total number of atoms in the polyether ring, (3) the class name, crown, and (4) the number of oxygen atoms in the polyether ring. Thus, 1,4,7,10,13,16-hexaoxacyclooctadecane becomes [18]-crown-6(31) and 2,5,12,15,22,25-hexaoxatetracyclo-[24.4.0.$0^{6,11}$.$0^{16,21}$]triaconta-6,(11),7,9,16(21),17,19,26(1),2,29-nonaene becomes tribenzo[18]crown-6 (32). The brackets may be replaced by hyphens. The positioning of the hydrocarbon rings and the oxygen atoms is as symmetrical as possible in most cases and the exceptions are

---

† Vögtle has suggested that a synthetic ionophore be classified as follows:[87] coronands are macromonocyclic compounds with any heteroatom, the term crown ether specifically refers to coronands with oxygen only as heteroatom. Cryptands are bi- and polymacrocyclic ligands with any heteroatom and podands are acyclic coronand and cryptand analogues. This classification will be used hereafter.

indicated by *asym.*. These ligands bound particular cations selectively and this was explained in terms of a correlation between the cavity size of the host and the spherical size of the guest ion.[86] The crown ethers therefore imitated the ability of the natural ionophores selectively to bind a metal cation in a 1:1 complex. However, in many of the complexes formed, the binding atoms and the metal cation were found to be almost coplanar (Figure 2.3). This structural feature allows that solvent molecules and anions have access to the cationic centre. The cation is not effectively insulated from the solvent (see Section 2.1.2 for an example of solvent access to a cationic centre). The cation/anion pairing (Figure 2.3) is a solid-state effect and is unlikely to occur in solution, particularly in a polar solvent where solvent molecules will separate cations and anions.

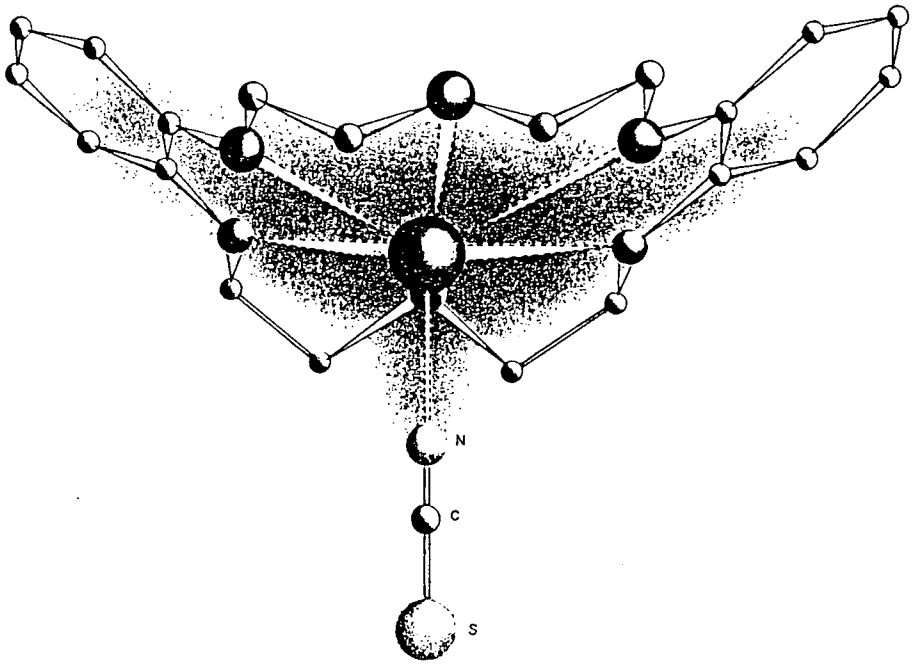

Figure 2.3

X-Ray crystal structure of the Rb(I)SCN complex of dibenzo-18-crown-6[88]

2.1.2 *Cryptands*

Lehn and Sauvage[89-93] synthesised a series of ligands containing two or more macrocycles designed to offer the cation a three-dimensional array of binding sites. The cation is allowed to become inaccessible to the surrounding environment. The cation sits within a cage-like cavity, from which the name "cryptate" given to such complexes comes (Greek κρυπτοσ = cage, Latin *crypta* = cage, cavity). The ligand itself is denoted a "cryptand", [for example, (32) to (38)][51,57] In order to avoid lengthy IUPAC nomenclature, a succinct desciption of the cryptand is given in which the number of heteroatoms in the chains between the bridgehead atoms is given in brackets. Thus, 1,13-diaza-4,7,10,13,16,19,22,27,30-octaoxabicyclo[8.11.11]dotriacontane becomes [3.3.2] (37).

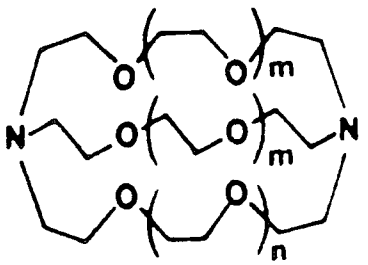

(33) [2.1.1] m = 0, n = 1

(34) [2.2.1] m = 1, n = 0

(35) [2.2.2] m = 1, n = 1

(36) [3.2.2] m = 1, n = 2

(37) [3.3.2] m = 2, n = 1

(38) [3.3.3] m = 2, n = 2

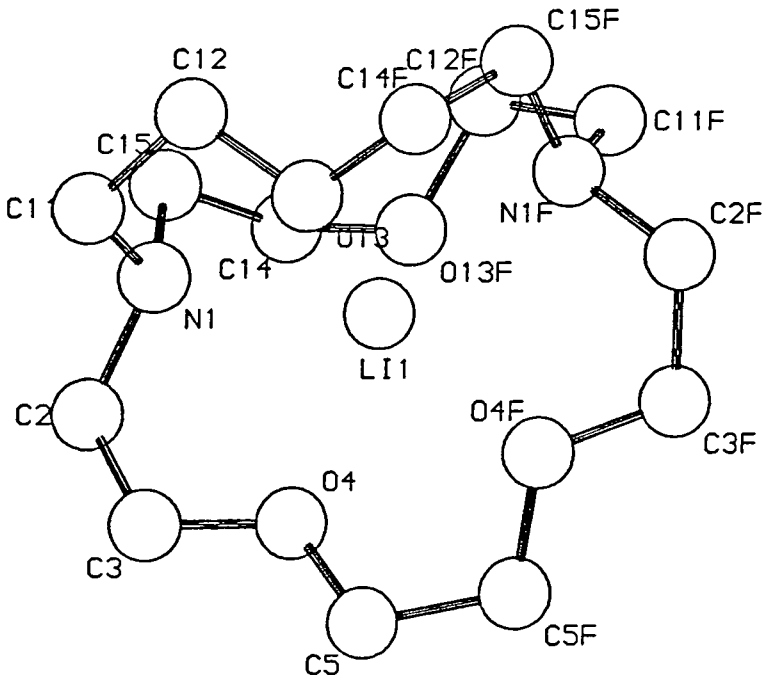

Figure 2.4

X-Ray crystal structure of Li(I) complex of cryptand [2.1.1][94]

The cation guests may become encased within the host (Figure 2.4). The spheroidal cavities of the cryptands should lend themselves very well to the formation of stable, selective complexes with spherical cations, according to the equilibrium represented in Figure 2.5.

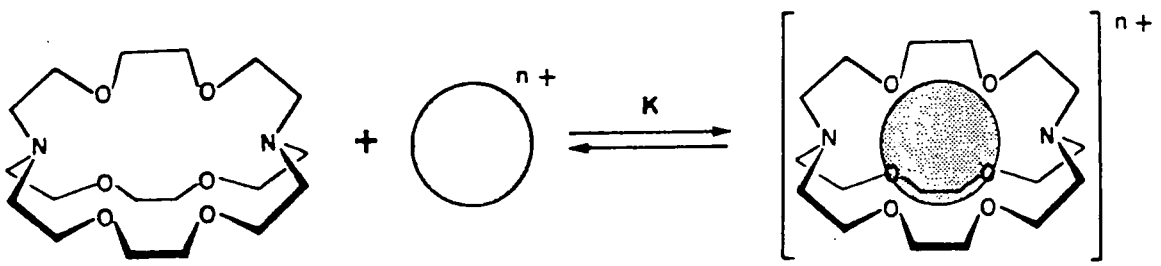

Figure 2.5

Formation equilibrium of a cryptate inclusion complex between cryptand [2.2.2] *and a metal cation* (K *is the stability constant of complexation*)

For example, the potassium complex of cryptand [2.2.2] (35) is more stable by 10^5 times than the potassium complex of the monocyclic species (39) with the same number of heteroatoms.[91] This macrobicyclic cryptate effect is even larger than the related macrocyclic effect which acknowledges that the stability of a macrocyclic complex with an alkali cation will be greater than that for the complex of the same cation with the acyclic counterpart (Figure 2.6).

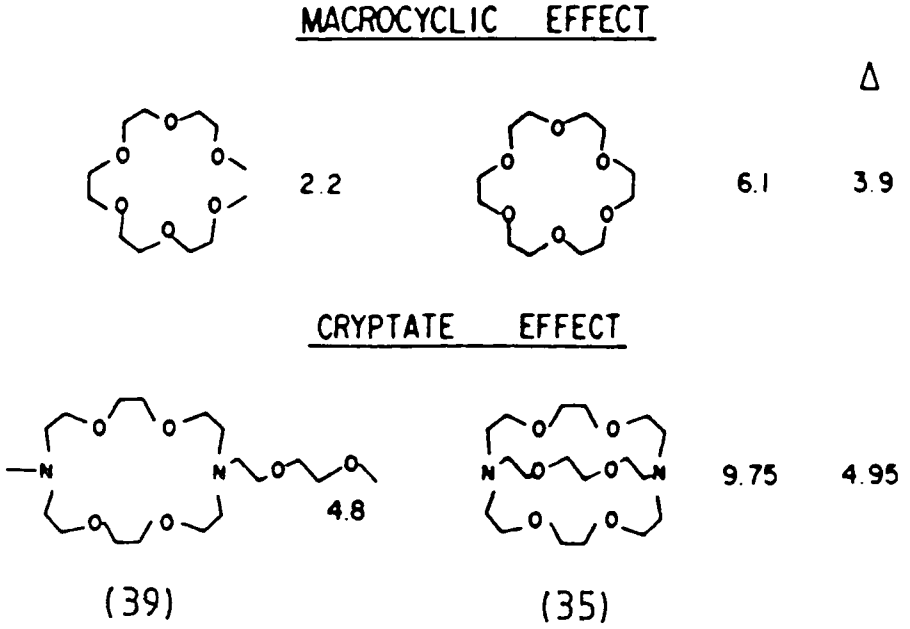

Figure 2.6

The macrocyclic and cryptate effects (Δ) on complex formation. The values given are the stability constants (log K) of the K^+ complex in methanol (top) *and methanol/water* (95:5) (bottom)

Whereas the chelate effect is usually attributed to a large, favourable entropy of complexation ($\Delta S^{\neq}$), cryptate formation is accompanied by large, favourable enthalpies ($\Delta H^{\neq}$) but usually unfavourable entropies.[91,95,96] The large enthalpic term is attributed to the strong interaction between the cations and the weakly solvated macrobicyclic ligands. The enthalpies of complexation show distinct selectivity peaks similar to those found for the stability constants. The cryptands also display high selectivities which tend to agree with a simple cavity size/cation size correlation, the preferred cation being the one whose size most closely matches that of the cavity. Consequently, cryptands [2.1.1], [2.2.1], and [2.2.2] preferentially complex Li^+, Na^+, and K^+ respectively.[91] It is the bicyclic topology of the cryptands which renders them fairly inflexible and which disallows adaption of cavity size to suit a particular cation. The cryptands with longer bridges and thus larger, more flexible cavities possess slightly poorer selective properties.

The discussion has so far mentioned only the inclusive cryptates where the cation is encapsulated within the cryptand cavity and is effectively insulated from the solvent. However, where the ligand cavity is smaller than the size of the metal cation an exclusive cryptate may be formed where the cation is not completely encased within the ligand cavity. For example, the cavity size of cryptand [2.2.2] (35) is smaller than the size of the caesium cation and although X-ray studies have shown that [2.2.2] can accommodate the Cs^+ ion,[97] ^{133}Cs NMR studies reveal that an exclusive complex is also formed.[98-100] The resonance of the cation is solvent dependent and as the temperature of a solution is lowered, the resonance frequencies of Cs^+ in the various solvents approaches the same limiting value. Thus, this behaviour is indicative of an equilibrium between the two forms of the $\{Cs[2.2.2]\}^+$

complex. The temperature dependent equilibrium shifts to the right at

$$\{Cs[2.2.2]\}^{+}\ \text{exclusive} \rightleftharpoons \{Cs[2.2.2]\}^{+}\ \text{inclusive}$$

lower temperatures. A crystallographic study of the $\{K[2.2.1]\}^{+}$ complex,[101] where again the cation size is considerably larger than that of the cavity, shows the cation protruding from the cavity to give an exclusive cryptate, in which the anion (NCS^{-}) is bound directly to the metal.

Both the chorands and the cryptands in the unbound state do not contain cavities because methylene groups turn inwards to fill potential intramolecular voids.[102,103] These inturned methylene groups have to be displaced by alkali cations during complexation, (Figure 2.7). The spherand molecules,[103-108] for example (40), possess superior alkali

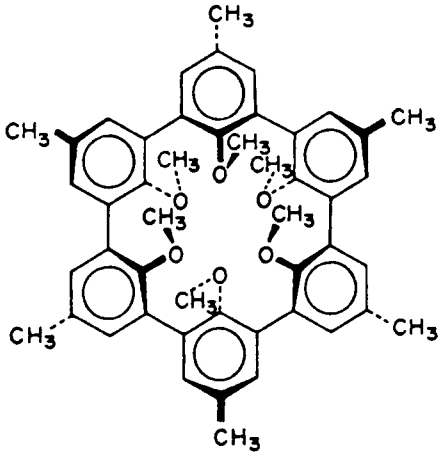

(40)

metal ion binding capabilities and selective powers. This results from the enforced cavities lined with electron pairs already present in the ligand prior to complexation[109,110] (Figure 2.7). The complexation process relieves electron-electron repulsions. For example, spherand (40) has six octahedrally arranged oxygens with their 24 electrons lining a cavity enforced by the rigidity of the benzene rings and by the spatial requirements of the methoxy groups. Spherand (40) binds strongly to lithium and sodium ions with stability constants Ks of

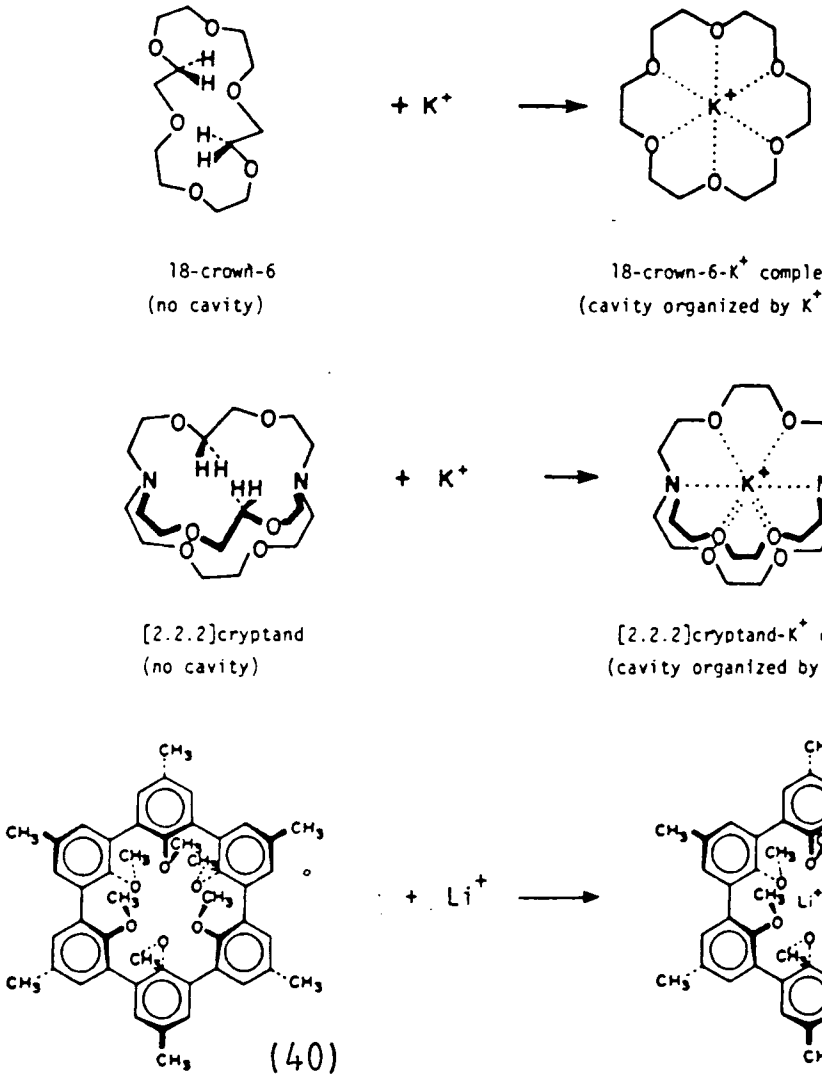

Figure 2.7

Complex formations showing how a crown ether (top) *and a cryptand* (middle) *do not contain cavities in their free state; the free spherand has an enforced cavity*

1.4×10^{14} with sodium and $>5 \times 10^{16}$ with lithium (calculated from the equation $K_s = k_1/k_{-1}$, where k_1 and k_{-1} are the rates of complexation and decomplexation respectively, measured in $CDCl_3$ saturated with D_2O at 25^o).[110] Spherand (40) completely rejects potassium, rubidium, caesium, magnesium and calcium cations.

The synthesis of hemispherands,[111] for example (41), and cryptahemispherands,[112,113] for example (42), offers a blend of rigidity

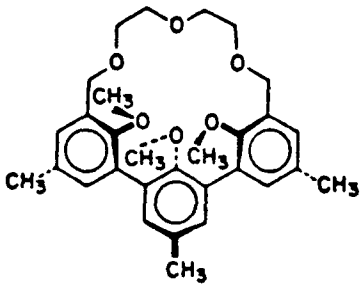

(41)

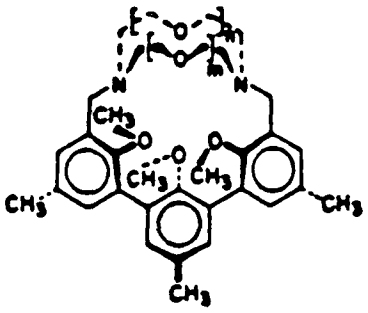

(42)

and flexibility to the incoming cations, maintaining stability and selectivity of complexation but also providing higher rates of complexation and decomplexation than the spherands and cryptands.

The rather inflexible ligands (cryptands and spherands) described in the previous paragraphs show high stabilities of complexation, high selectivities of complexation and succeed in shielding the bound cations from the surrounding environment.[51,103] However, both the rates of complexation and decomplexation of many of these complexes are much slower[105,106,110,114-118] (by several orders of magnitude) than for macrocyclic or antibiotic complexes. For example, for spherand (40)[106] molecular model examinations indicate that to complex or decomplex, a cation must pass through a lipophilic sphere composed of 3 CH_3O groups. At the half-way point the cation can have only one to two ligands

external to the spherand. This structural feature explains why complexation/decomplexation activation energies for these spherand ⟶ metallospherium salt complexations are so high. The dynamic rates of complexation/decomplexation decrease as the stability constant of the complex increases. Thus, whilst the most stable complexes are good cation receptors and release the cation very slowly, it is the less stable compounds which exchange rapidly that may function as effective cation carriers.[51,119]

2.1.3 *Lariat Ethers*

Reports by Lehn[120-122] and Dale[123,124] focussed attention on the macrocyclic ligands referred to as "lariat ethers",[125-138] macrocyclic ligands containing side-chains with additional donor groups. The name derives from the ability of such ether to "rope and tie" cations and the resemblance between a schematic diagram of a one armed lariat ether, for example (44), to a lasso (lariat = lasso) (Figure 2.8). These compounds are distinct from those macrocyclic rings with lipophilic side-arms attached that do not incorporate binding sites.[139-141] The lariat ethers were designed to mimic the naturally occurring antibiotics by providing the cations with a three-dimensional array of binding sites. It was hoped that the stabilities of the complexes formed would be higher than those for the simple crown ethers. The complexes formed might also retain the complexation dynamics characteristic of ionophores like valinomycin, due to the incorporation of binding groups on flexible side-arms.

The formation of lariat ethers by the attachment of side-chains onto the macrocyclic ring at a carbon atom,[127-129] for example (43), generally gave disappointing binding constants. The modest values for

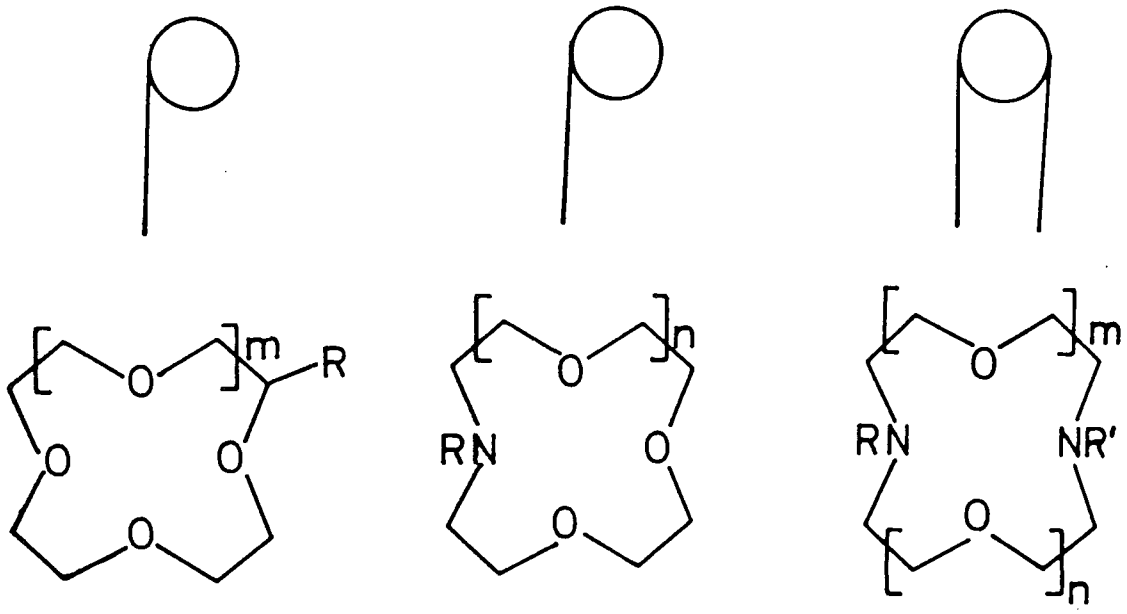

(43) (44) (45)

Figure 2.8

Examples of lariat ether molecules with a schematic representation of their structure

the binding constants were attributed in part to the lack of flexibility of a side-chain attached by a carbon atom. To counteract this, lariat ethers were designed where the side-arm was attached to a nitrogen pivotal atom in the macrocycle.[131] The nitrogen atom is incorporated by replacement of an oxygen atom.

Many factors influence the binding of macrocyclic polyether analogues to the alkali and alkaline earth cations, some of which will now be discussed in detail, with particular reference to the lariat ethers where the side-arm is attached to a nitrogen pivot. It is important to realise that the various factors will contribute to the stability of complexes and selectivity of ligands by varying amounts, depending both on the series of ligands being looked at and on the method being used for the determinations. For example, the degree to which enthalpies and entropies of complexation will contribute to the formation of a complex will be more involved for a two-phase extraction

than for a one-phase determination of stability constant using potentiometric methods or ion-selective electrodes. Thus, valid comparisons may only be made where the same detection methods have been employed and the choice of measuring technique must reflect the use for which the figures are required.

2.2 Factors Arising from the Macrocyclic Ring

2.2.1 *Cavity Size-Cation Size Correlation*

The correlation between cavity size and cation size that has been mentioned in Section 2.1 with respect to the crown ethers, cryptands, and spherands, is not a steadfast rule and must be evaluated separately for each series of ligands under study. It is not a general rule though it is still widely accepted as such.

Gokel[142] *et al.* have determined the stability constants of formation, Ks, (using cation-selective electrodes) for the series of crown ethers, (46) to (50), with cation Na^+, K^+, NH_4^+, and Ca^{2+}, according to the equilibrium represented below:

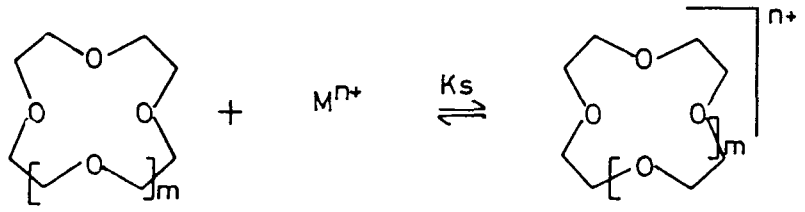

(46), m = 1
(47), m = 2
(48), m = 3
(49), m = 4
(50), m = 5

The results are represented in Figure 2.9 and show quite clearly that the cation diameter/cavity size correlation is contra-indicated. The selectivity of the complexation process can be regarded as ligand selectivity for a cation of a particular size or as cation selectivity for a ligand of a particular size. Neither situation is upheld by this

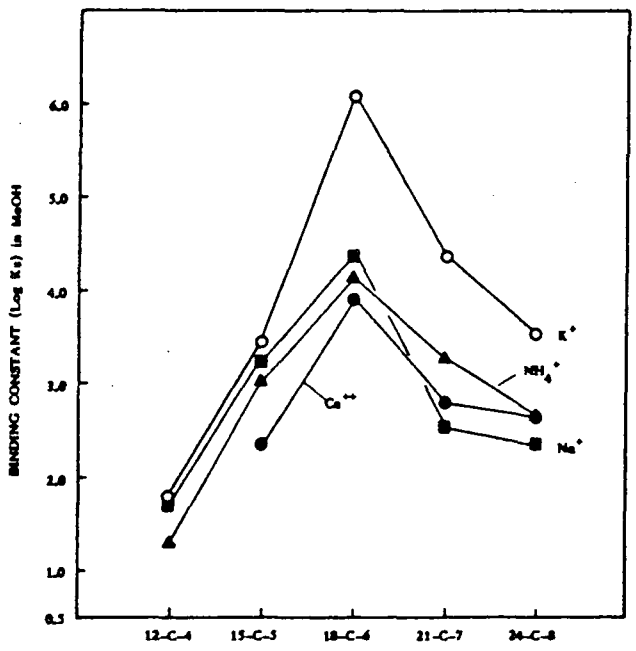

Figure 2.9

Cation binding by simple crown ethers. (log K determined in anhydrous methanol at 25° using cation-selective electrode)

example however. Instead, K^+ is bound more strongly by all the crowns irrespective of hole size and the strongest binding for all the cations occurs with 18-crown-6 irrespective of cation size. These observations confirm the reports by Michaux and Reisse[143] that the enthalpies of binding between Na^+ and K^+ and the 12- to 18-membered crowns do not correlate with hole size. It tends to be the inflexible ligands such as the cryptands and spherands that uphold the size correlation, since the cavity is rigid and cannot adapt itself to suit the optimum binding distances required by smaller or larger cations. In the case of the crown and the lariat ethers, the ligands are flexible and can adopt a conformation suited to binding cations of varying size. Thus, although for these flexible ligands the hole size correlation will make some contribution to the binding of the cations, other factors will dominate.

The cation specificity of a ligand depends on a balance of energies

between ligand-cation interactions and cationic solvation. For example, molecular mechanics calculations[144] show that the most stable Na^+ complex of 18-crown-6 (conformation C_1) is intrinsically more stable than the most stable K^+ complex of 18-crown-6 (conformation D_{3d}). The conformation adopted by the K^+ complex of 18-crown-6 (D_{3d}) is favoured even though the M^+...crown interactions are not of lowest energy, but the conformation also has a very low internal strain energy. For the Na^+ complex, the internal strain energy of the crown is also much lower for the D_{3d} conformation but the cation-crown interaction energy greatly favours the C_i structure overriding the strain energy. The free crown has a C_i conformation[145] and to accommodate the Na^+ion, part of the ring becomes deformed in a highly irregular manner bringing one oxygen into an apical position.

For more detailed accounts of the conformations of the free ligands and the complexated ligands and the differential energy change that occurs on binding see reports by Dale,[146] Wipff,[144] and Boeyens.[147] These preferred conformations calculated on the basis of lowest energy structures are the observed structures.[148] However, the molecular mechanics calculations also show that the sodium cation is more strongly hydrated in aqueous solution than is the potassium cation. The difference between the hydration energies of the Na^+ and K^+ ions is greater than the difference between their total interaction energies with 18-crown-6: thus 18-crown-6 binds more strongly to K^+ (ΔH = -6.21 kcal mol^{-1}; log K = 2.03) than to Na^+ (ΔH = -2.25 kcal mol^{-1}; log K = 0.8) in aqueous solution.[149] The stronger binding of 18-crown-6 to K^+ over Na^+ is also observed in polar solvents such as MeOH, Me_2SO and dimethylformamide. Sodium complexation becomes favoured when weaker solvating (less polar) solvents are used, such as tetrahydrofuran.[150] Thus, it appears that the more favourable binding of potassium cations

by 18-crown-6 in aqueous solution is more a consequence of the differing hydration energies of potassium and sodium ions than of a ring-size or conformational preference. This solvent-dependency of complex-stability has been demonstrated previously by many workers. For example, the complexation stability-constants of the alkali and alkaline earth cryptates are raised by factors of the order of 10^3–10^5 when measured in methanol/water (95:5) or pure methanol solution, compared with measurements in water.[91,95] This effect has been attributed to the increased electrostatic interaction of the cations with the ligand and the decreased interaction with the solvent which has a lower dielectric constant. The balance of energy between ligand-cation interactions and cation solvation discussed above is crucial to the effectiveness of the ligand as a carrier. If the hydration energy of the cation is too large, the cation will never escape its solvation shell. If however the hydration energy of the cation is too small, the cation will have no tendency to re-enter the solution.

The effectiveness of oxygen (and nitrogen) as a donor to metal cations also depends on a delicate balance of two energies: the strain energy induced in the group bearing the oxygen atom and the favourable energy change associated with the inductive efficiency of the oxygen atom. Molecular mechanics calculations by Hancock[151] reveal that the size of the chelate rings formed on complexation play a large rôle in determining the steric strain involved.

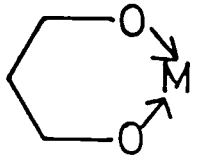

(51) 6-ring chelate

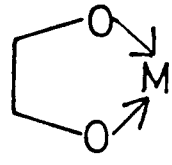

(52) 5-ring chelate

In a six-membered chelate ring, all of the hydrogen atoms are in energetically more favoured staggered conformations when binding to a very small metal cation. As the size of the metal ion is increased the hydrogen atoms are forced to adopt an eclipsed conformation. This is accompanied by an increase in strain energy and a decrease in complex stability. For the five-membered chelates, the favourable staggering of the hydrogens is not possible for complexes of small or large cations and the effect of increasing the metal ion size is much less marked. Thus six-ring chelates should form stable complexes with the smaller cations whereas five-ring chelates may favour larger cations. These observations explain many experimental observations. For example, the substituted crown ether (53) extracts the lithium cation from an aqueous to an organic phase with exceptionally high selectivity over the other alkali metal ions, whereas crown ether (54) with a smaller cavity size shows only small selectivity for lithium.[152] (53) also shows no

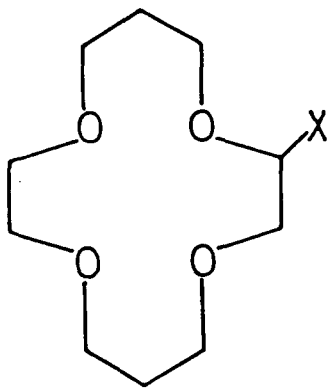

(53)

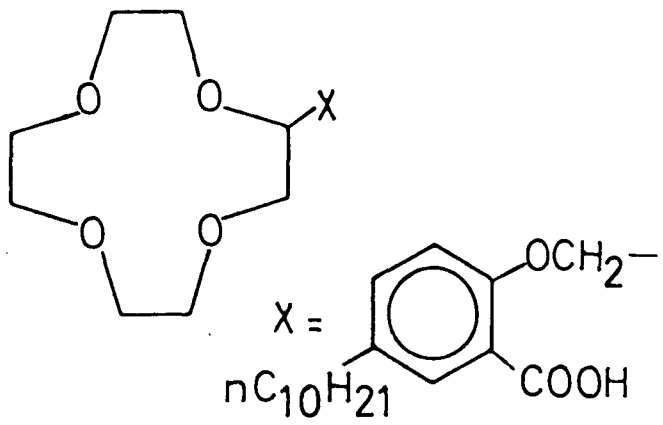

(54)

extraction of the larger Rb^+, Cs^+, and K^+ ions. The effect of enhanced selectivity for smaller cations by increasing the chelate ring size from five- to six-membered may diminish after the inclusion of one or more large chelate rings depending on the series of ligands in question. This is probably due to the extra steric crowding caused by the

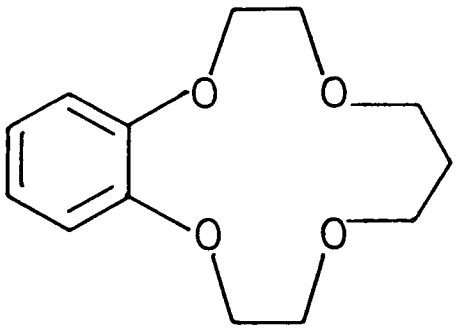

(55)

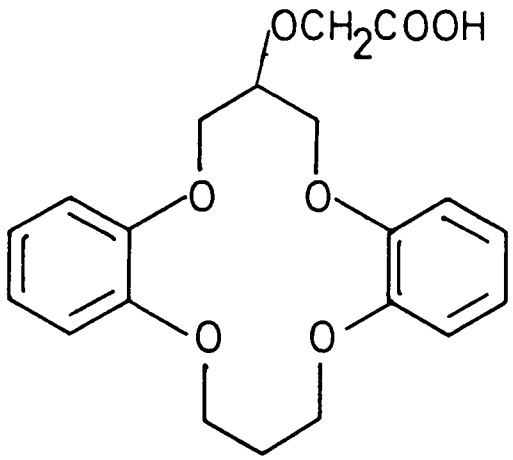

(56)

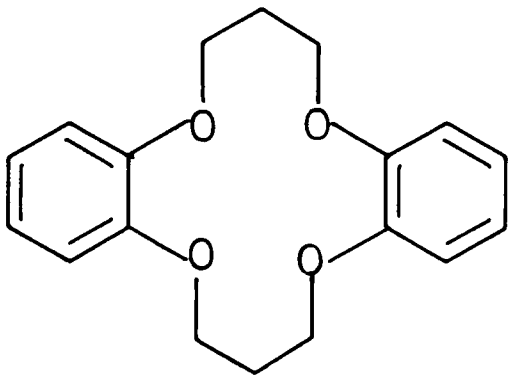

(57)

additional methylene groups surrounding *small* metal cations. Unfavourable energy terms due to this steric crowding may outweigh further energy gains brought about by the staggering of hydrogen atoms.

Effective binding to lithium by crown ethers and their analogues may require penta-coordination as deduced from X-ray analysis of lithium complexes.[153-155] The lithium complexes of ligands (55), (56), and (57) all exhibit penta-coordination with their geometries intermediate between square pyramidal and trigonal bipyramidal. The square pyramidal geometry is preferred. In each case the fifth coordination site is occupied by the anion or, for cycle (56), by a water molecule. The donor atom on the pendant side-arm of (56) is too distant from the apical binding site given the relative inflexibility of the structure and thus, the binding water molecule hydrogen-bonds in a bridging

fashion between both the ethereal oxygen of the side-arm and the carboxyl oxygen. Each of the ligands mentioned has six-membered chelate rings present in their structure. Both 12-crown-4 and 16-crown-4 give penta-coordinated complexes with LiSCN,[156-157] in which Li^+ is bound to the four ether oxygens of the ring and the SCN^- anion giving a square pyramidal coordination geometry.

The complexation of neutral macrocyclic ligands with calcium cations has been studied both in the solid-state[2] and in solution.[123] Calcium requires a higher coordination number than that preferred by lithium cations, usually of six or eight.[2,123] The larger size of the Ca^{2+} ion allows a larger number of coordinating donors without causing crowding which is energetically unfavourable. The larger number of donor atoms also helps to satisfy the charge demands of the doubly charged calcium ion.

2.2.2 *Number of Donor Atoms Available for Binding*

Gokel *et al.*[130] have synthesised the ethers represented by (58), (59), and (60) and used them to demonstrate some interesting trends in the stabilities of the resultant complexes formed with sodium. The binding data for the complexes are represented in Figure 2.10. The data suggest the the ring size-cation size correlation again does not appear to be as significant here as for more rigid crowns. More importantly, the data reflect the number of oxygen donor atoms present in the molecule (both in the ring and on the side-arm) and seem hardly affected by the presence of the nitrogen atom. The highest stability constant in the lariat series is when six donor oxygen atoms are present, lending credence to the possibility that the nitrogen atom has little significance in the stability of the complex. The binding constants

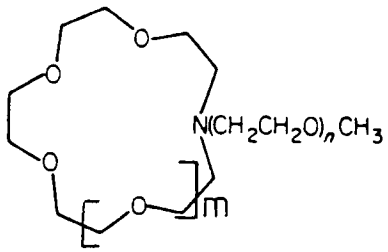

(58) n = 0-5, ≃ 8; m = 1

(59) n = 0-5, ≃ 8; m = 2

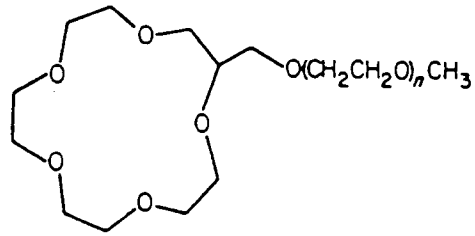

(60) n = 0-2

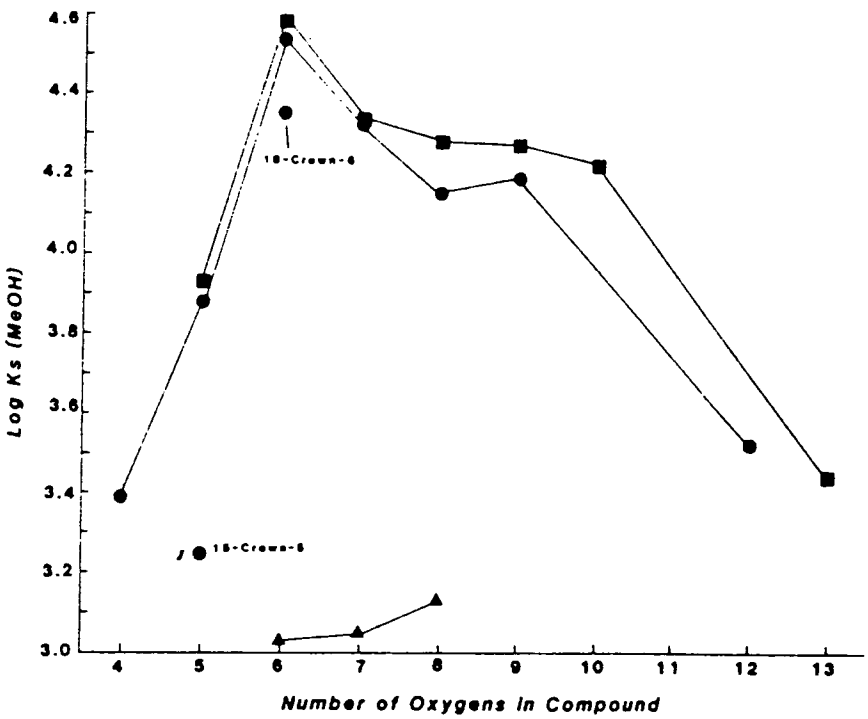

Figure 2.10

Sodium cation binding by 15- *and* 18-*membered N-lariat ethers* (●) 15-*membered N-lariat ethers* (58); (■) 18-*membered N-lariats* (59); (▲) 15-*membered O-lariats* (60).

slump after the peak value at six oxygen donors until, with a long side-arm bearing eight oxygen atoms the stability is roughly equivalent to that exhibited by the corresponding compounds having only a methyl group in the side-arm. The observation of the similarity in binding for compounds having different ring size but equal numbers of oxygens seems to imply that the nitrogen atom itself does not restrict the system conformationally to any large extent and the molecules may modify their conformations to achieve optimum binding orientations making use of the oxygen atoms. The levelling off of the binding may be attributed to the fact that as the side-arms increase in length, the more distant oxygen atoms become inaccessible to the cation. The slump observed in binding constant may be attributed to hydrogen-bonding by the solvent medium, decreasing the flexibility of the arms and their ability to bind to the cation. The side-arm may also coil up limiting the binding ability. This could be due to a hydrophobic effect (lipophilic-lipophilic interaction) or water-bridged hydrogen-bonding between ring and side-arm.

Hancock's[151] molecular mechanics study suggests the formulation of a general rule, with regard to the control of selectivity on the basis of metal size and number of oxygen donors. The increase in the number of oxygen donor atoms incorporated into a macrocyclic structure, on the side-arm or within the macrocylcic ring itself, will increase the selectivity of the ligand for large metal ions relative to small. This is exemplified in Figure 2.11, where the difference in the literature stability constants[158] for 18-aneN_2O_4 (61) and cryptand [2.2.2] (35) with various metal ions is plotted as a function of ionic radius of the cations. It is clear that the larger metal ions show more favourable changes in complex stability than do the smaller ions when groups

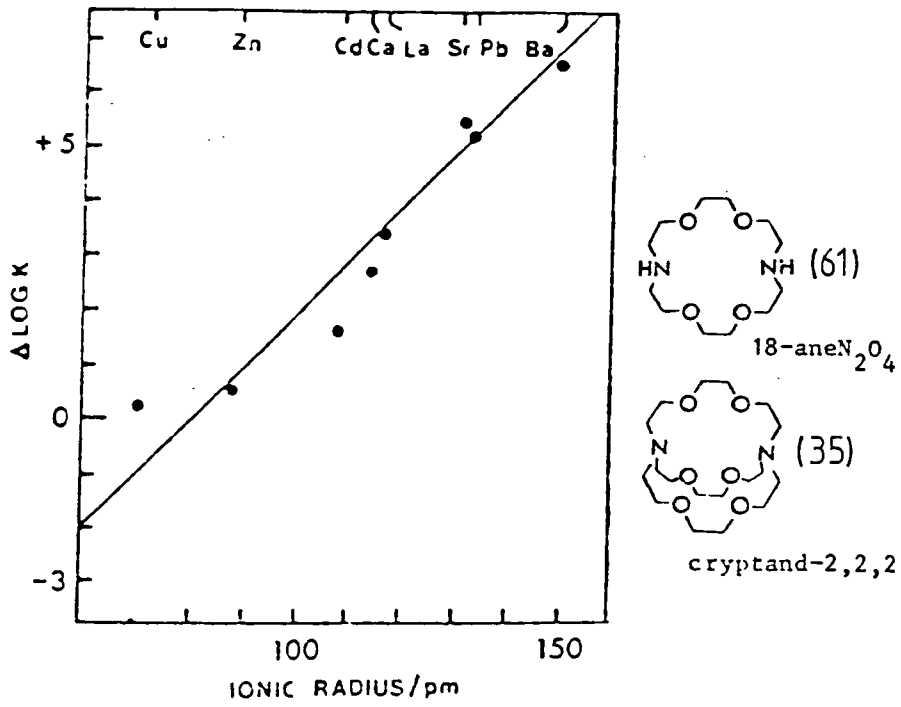

Figure 2.11

Relationship between change in complex stability (Δ log K) and ionic radius for a variety of metal ions. The Δ log K values are for passing from 18-aneN_2O_4 to cryptand [2.2.2].[158]

containing neutral oxygen donors are added to an existing ligand. In effect, the structural difference between (61) and (35) is the addition of a bridge containing two ether groups to (61) to give (35). This behaviour is explained in terms of the steric strain created when the coordination sphere around a small metal cation becomes overcrowded. The effect on complex stability will be the nett balance of the steric and inductive effects produced as the ligand is modified. It appears that steric crowding increases with decreasing metal ion size to the extent that it outweighs the inductive effects, as groups containing neutral donor oxygen atoms are added to ligands. For large metal ions, even though coordination numbers increase, the steric crowding is outweighed by the inductive effects and increases in complex stability

occur. Obviously, entropic effects must also figure in the complex stability.

More recent studies by Gokel and Gandour[159,160] confirm the ability of the metal cation guests to organise their lariat ether hosts to maximise complex stability. The cations organise the available donor groups to provide the most favourable coordination geometry, as long as the ligand is sufficiently flexible.

2.3 Factors Arising from the Addition of a Functionalised Side-Arm to the Macrocyclic Ring

The incorporation of side-arms bearing donating functionalised groups into crown ether structures increases the binding ability of the resulting ligands to metal cations, provided that the side-arm is appropriately oriented and is at a suitable distance from the metal centre. As indicated in Section 2.1.3, the greater flexibility of the side-arm in N-functionalised crowns *versus* C-functionalised analogues leads to enhanced complexation.[128,131] It is the greater flexibility of the ligands and not the complexing ability of nitrogen which leads to the improved binding. The donor group on the side-arm may participate intramolecularly in the cation binding process both in solution[161-163] and in the solid-state.[164-167]

In solution, ^{13}C NMR relaxation times can provide considerable information on ligand structural properties, binding strengths, and binding dynamics,[168-171] as well as giving confirmatory evidence for the participation of side-arms in binding to cations. A study of the changing of ^{13}C relaxation times, T_1, on complexation will allow an

assessment of the change in molecular mobility on complexation. For example, the complexation of sodium perchlorate by 15-crown-5[162] (one molar equivalent Na^+; $MeOH/H_2O$, 90:10), produces a reduction in T_1 for the ring carbon of 42%. The same magnitude of reduction in T_1 on complexation is reported for the 15-crown analogue (62), where the side-arm is attached *via* a carbon atom. This reduction in T_1 reflects the loss of carbon mobility. However, the nitrogen lariats (63) and (64) show a much smaller reduction in ^{13}C T_1 values for the ring

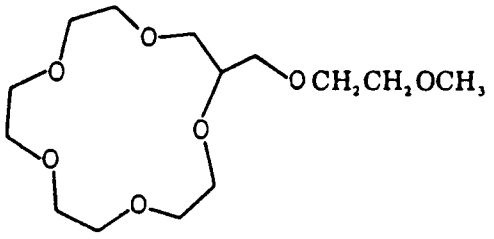

(62)

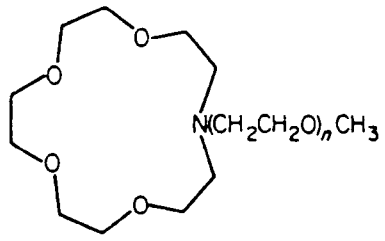

(63) n = 1
(64) n = 2

carbons, indicating a lesser change in carbon mobility, even though the stability constants of complexation for (63) and (64) with sodium ions are high when compared with 15-crown-5 and (62). For (63) and (64) the side-arm carbon atom shows a relative greater loss of mobility than do the ring carbons. This behaviour is explained by the assumption that side-arms capable of binding to the sodium cation may contribute greatly to the complexation process, allowing the ring carbons to retain their mobility, *i.e.* the ring carbons are less strongly involved in the complexation. This explanation is upheld by the fact that the reduction

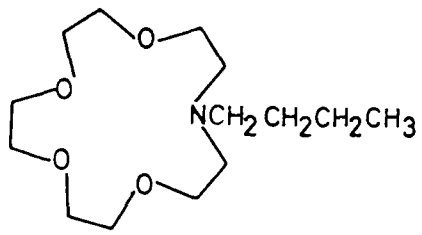

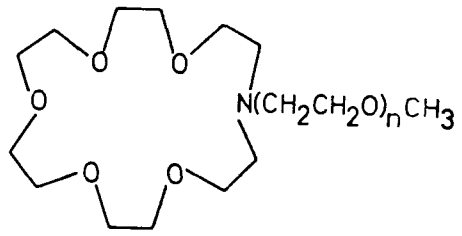

(65) (66) n = 0 - 5, or 8

in T_1 for the ring carbons of (65) on complexation with sodium ions is also quite considerable - (65) binds weakly to sodium ions.

Naturally, a study of binding constants will also give an idea of side-arm contribution to the binding in complexes. For example, the binding constants of 18-membered nitrogen-lariats containing between zero and eight oxygen donors in their side-arms [represented by (66)] have been reported.[161] The binding data reveal that the species with two oxygens in the chain is the most stable complex. The position occupied by the second oxygen atom in the chain is predicted by space-filling molecular models to be the most appropriate for the cation binding.

The rates of complexation and decomplexation of the lariat ether/cation complexes may also be determined using NMR techniques. The dynamics of the complexations are crucial to the use of such ionophores as cation carriers. Cation linewidth measurements in NMR may be determined in appropriate solvents at varying temperatures, for ligands with a 0.5 molar equivalent presence of the cation under determination. Sharp line retention down to lower temperatures indicates rapid cation exchange, whereas broadened lines indicate a slow rate of cation exchange. This method indicates clearly the improved dynamics of

complexation of the lariat ethers with nitrogen side-arm functionality over those with carbon side-arm functionality.

The first example of a lariat ether ionophore to be structurally determined in which an ester carbonyl binds directly to the ring bound cation was reported in 1984.[165] Previously, X-ray crystal structures of complexes with side-arms containing ether, alcohol, carboxamide, and carboxylate side-arms had been determined.[165] It is the ester carbonyl groups in valinomycin that bind so effectively to the potassium cation. However, earlier attempts to incorporate ester linkages on the side-arms of macrocycles attached *via* carbon atoms had revealed that the carbonyl oxygen was oriented outwards and hence was unable to interact with a

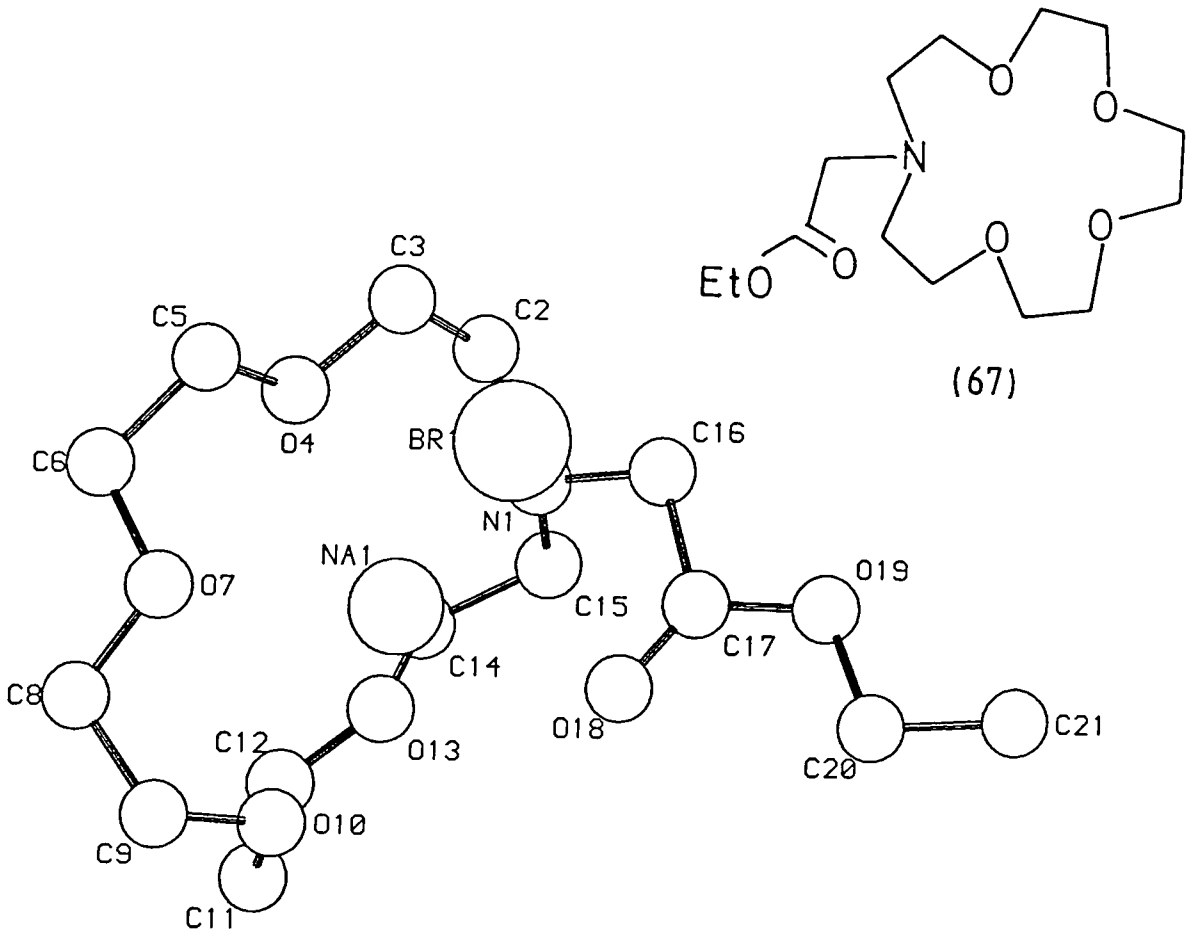

Figure 2.12

X-Ray crystal structure of the sodium complex of ligand (67)

ring-bound cation. The incorporation of an ester group into the N-functionalised crown (67) led to a sodium complex in which the ester carbonyl oxygen lies closer to the metal cations than the ring oxygens (Figure 2.12). The close-lying nature of the carbonyl oxygen to the metal cation indicates that the ester carbonyl oxygen is a strong donor. (67) is indeed better at binding to sodium than the corresponding cycle where the ester linkage is replaced by a methoxy group, (68), [stability constants for (67) and (68) in anhydrous methanol are: log *Ks* = 4.10 and 3.88 respectively]. The ester carbonyl oxygen is a better donor than the ether oxygen which is attributed to the greater σ-donating ability of the ester oxygen or the greater expected electron density on the ester oxygen. The polarity of the binding sites on the side-arms and its relative effects on binding are discussed in Section 2.3.1.

The solid-state structure of the complex of (69) with potassium iodide[164] shows an interesting feature of lariat binding (Figure 2.13). Rather than acting as a flexible cap, whereby the cation is cradled by the macrocyclic ring, the side-arm pushes the metal ion out so that it is not so deeply immersed in the ring. The side-arm oxygen and the iodide anion occupy the two apical binding sites, in the coordination sphere of the cation. While the stability of such complexes may be less than those found for the cryptands, it was thought that the flexibility offered by the side-arm may increase the rates of complexation and decomplexation. However, the accessibility of the potassium cation afforded by the side-arm occupancy of a coordination site pushing the potassium ion out of the ring may be an alternative cause of dynamic rates of complexation.

2.3.1 *Polarity of Side-Arm*

The incorporation of side-arms onto crown ether-type ionophores

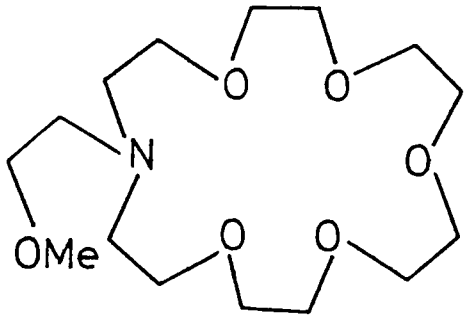

(69)

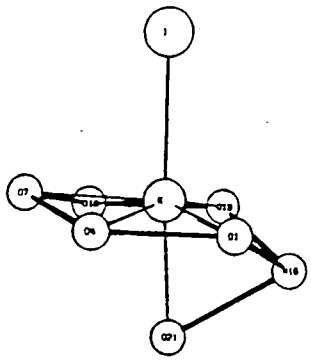

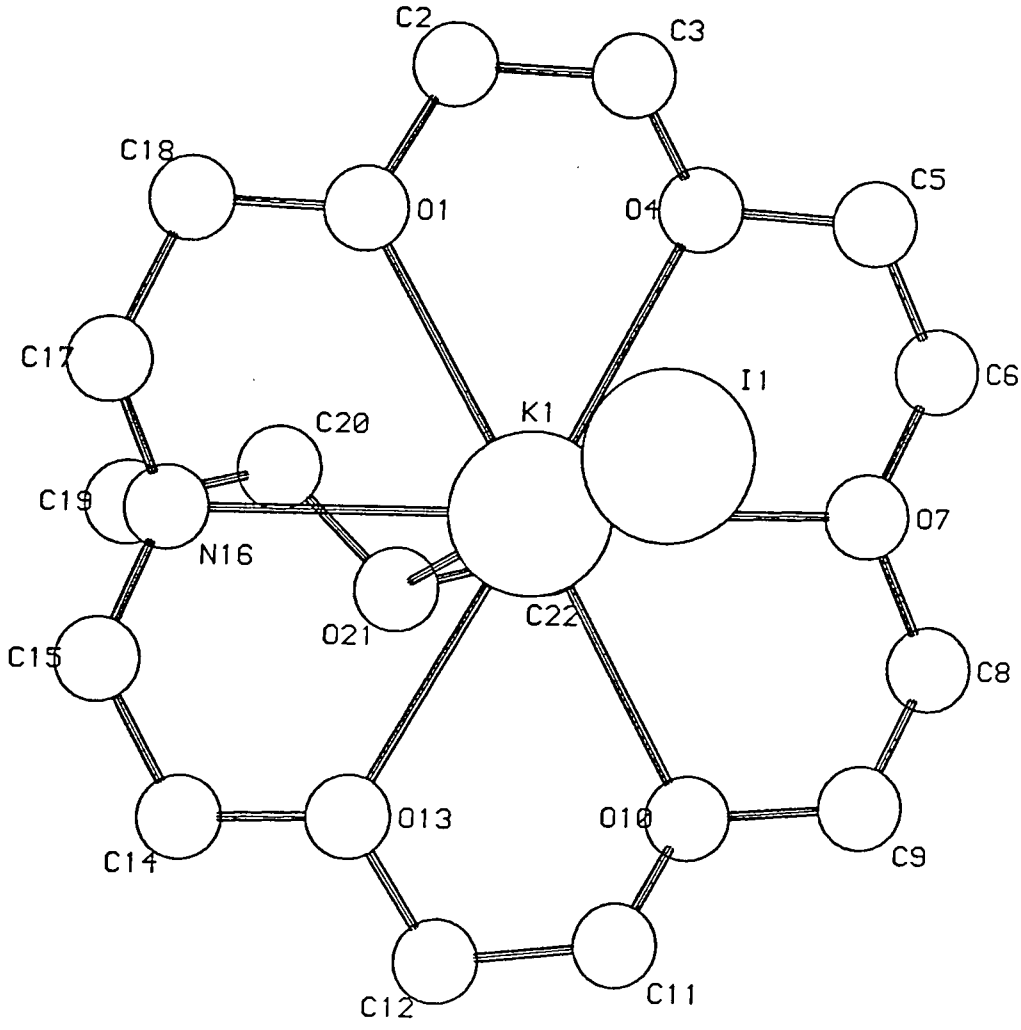

Figure 2.13

X-Ray crystal structure of the potassium complex of ligand (69) *and a schematic representation of the coordination sphere about potassium.*

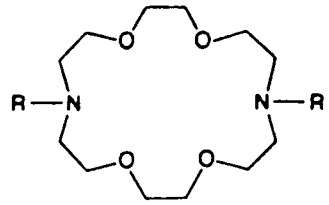

(70) R = H

(71) R = CH_2CH_2OMe

(72) R = CH_2CH_2OH

(73) R = CH_2COOEt

(74) R = CH_2COOH

leads to the possibility of altering the nature of the binding groups on those side-arms to enhance complex stability. Given that the orientation and distance from the metal cation of an oxygen donor atom on a side-arm is appropriate for complexation, the amount of electron density on the oxygen atom will greatly influence its σ-donating ability to the metal cation.

A study by Gokel[172] looked at a series of neutral two-armed lariat ethers [(71) to (74)] with secondary donor groups two carbon atoms removed from the ring based on the parent compound (70). Gokel has suggested that the polarity of the donor groups may be assessed by considering the side-arm as a whole molecule (addition of H *e.g.* CH_2COOEt = ethyl acetate) and looking at the dielectric constants of the resulting solvents. It was suggested that the polarity increases from (71)(methyl ethyl ether) to (72)(ethanol) to (73)(ethyl acetate). Whilst the order of the expected polarities is correct,[165] the correlation between polarity and dielectric constant is incorrect: the dielectric constant of ethanol greatly exceeds that of ethyl acetate. The rationale that the electron density on the oxygen of the ethyl acetate carbonyl is greater than that on the ethanol oxygen holds (see Section 4.1). This indicates that the ester carbonyl will have greater

ligand	R	log Ks Na^+	Ca^{2+}	K^+
(70)	H	≃ 1.5	na	≃ 1.8
(71)	CH_2CH_2OMe	4.75	4.48	5.46
(72)	CH_2CH_2OH	4.87	6.02	5.08
(73)	CH_2COOEt	5.51	6.78	5.78
(74)	CH_2COOH	na	na	≃ 1.8

Table 2.1

Stability constants for ligands (70) - (74) *measured in methanol at* 25° *using ion-selective electrodes.*

σ-donating power than will the alcohol oxygen.

The binding data are represented in Table 2.1. Of obvious interest is the fact that the presence of donor groups on the side-arms enhances binding for all of the cations studied. It is also clear that as the polarity of the side-arm increases the binding constants for the sodium and calcium complexes increase. Moreover, the increase in stability for the calcium complexes is larger than for the sodium complexes. Calcium cation binding when the ether function in compound (71) is replaced by an ester carbonyl (73) increases more than two orders of magnitude, but the increase in sodium binding between the same compounds is less than one order of magnitude. This behaviour is a reflection of the fact that the calcium cation has a higher effective charge density than the sodium cation. Indeed for compound (71) (methyl ethyl ether) with low polarity on the side-arm, the stability constant for the sodium complex is greater than that for the calcium complex. This order of complex stability is not upheld by the complexes with potassium cations. The potassium cation however will have a low charge density and thus will not drastically favour binding by highly polar ligands. This rationale should enable the design of ligands which favour binding to calcium cations over sodium and potassium ions. The low stability constants of complexation reported for the compound with a carboxylic group on the side-arm (74) may be explained by postulating

the presence of the zwitterionic form of the bis-amino acid. The protonation of the nitrogens in the ring will greatly diminish binding capability.

2.3.2 *Ionisable Groups on the Side-Arms*

The presence of ionisable groups such as COOH on the side-arms of N-functionalised macrocycles has been referred to as disadvantageous for the complexation ability of the said cycles with alkali and alkaline earth cations. This is due to the probable formation of the zwitterionic form of the ligand under neutral conditions. Protonation of the ring nitrogen will reduce complex stability. However, C-functionalised crown ethers with pendant ionisable groups[173] are effective reagents for the solvent extraction and transport of alkali metal cations across bulk liquid and liquid surfactant (emulsion) membranes.[174-181] Ionisable crown ethers have the positive advantage that transport of the metal cation from the aqueous phase into an organic medium does not require concomitant transfer of the anion. This allows the use of anions such as chloride, nitrate, and sulphate which are hard hydrophilic entities, distributing poorly to an organic medium.

The presence of a carboxylic acid group on a crown ether has been demonstrated to aid extraction of a lithium cation from an aqueous to an organic phase with exceptionally high selectivity over the other alkali metal ions under alkaline conditions. Competitive solvent extractions (discussed in Section 2.4.3) of aqueous solutions of lithium, sodium, potassium, rubidium, and caesium chlorides with solutions of lipophilic crown-ether carboxylic acids (75) and (53) have given lithium:sodium ratios of 19:1 and 20:1 respectively in the organic phase:[152] only lithium and sodium are extracted into the organic phase, with no

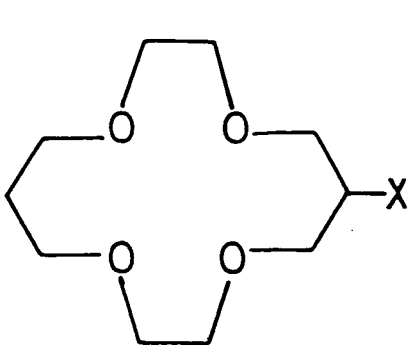

(75)

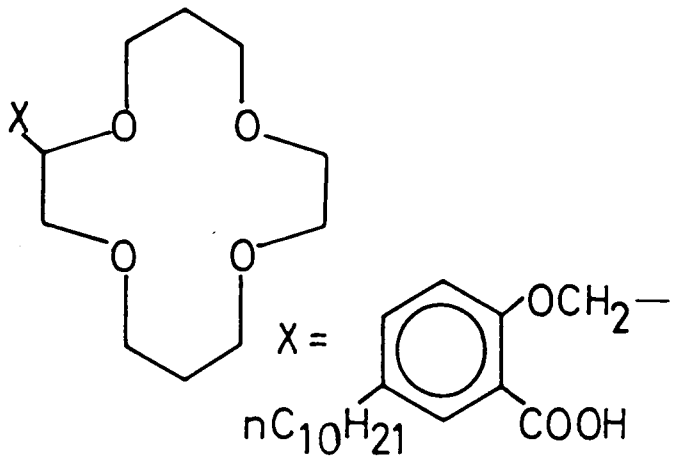

(53)

detection of the other cations. Bartsch ascribed the high selectivity to a simple ring size function but Hancock[151] has indicated a preference for six-ring chelates when binding to small metal cations such as lithium. The conformation adopted by the C_3 chains permits the staggering of the hydrogen atoms (see Section 2.2.1 for a full discussion).

Comparison of extraction results[182] for ligands (76) and (77) are represented in Figure 2.14. The only structural differences between the two ligands is the nature of the ionisable group: ligand (76) has a carboxylic acid group whereas ligand (77) has a phosphonic acid monoalkyl ester. Ligand (77) extracts metal cations into the organic phase even when the aqueous phase is highly acidic. Ligand (76) requires the aqueous phase to be neutral or basic before appreciable extraction occurs. Since the ionised form of the ligand is required for extraction, this difference is explained by the anticipation of a greater acidity of the phosphoric acid monoethyl ester than for the carboxylic acid. Sodium ions are extracted preferentially by both ligands, although the selectivity ratio of sodium:lithium is much greater for ligand (76) than for (77), with no appreciable extraction of lithium observed for ligand (76). These data demonstrate clearly that

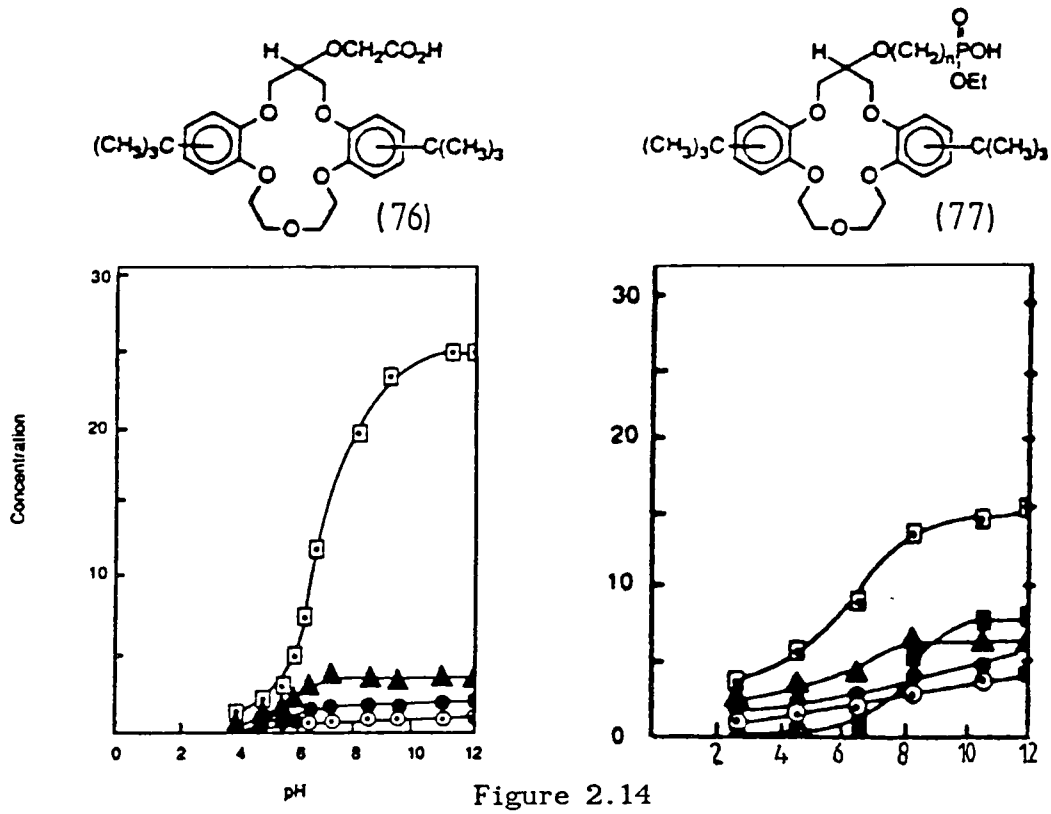

Figure 2.14

Concentrations of alkali metal cations (x 10^3) *in a chloroform phase* vs. *pH of the aqueous phase for competitive solvent extractions of* 0.25 M *alkali cations by* 0.05 M (76) (left) *and* (77) (right): (■) *Li*, (□) *Na*, (▲) *K*, (●) *Rb*, (o) Cs.

the identity of the ionisable groups does influence the selectivity and efficiency of alkali-metal cation solvent-extraction.

The use of chromogenic nitrophenol and azophenol ionisable groups allow of spectrophotometric determination of cation extractability into organic solvents. Kimura and Shono[183] have incorporated such groups into 14-crown-4 structures and reported selectivity ratios of between 45 and 240 for lithium to sodium extraction. These results were obtained using single solution techniques and are not based on competitive metal ion extractions.

Of interest is the difference in lithium extractability exhibited by ligands (78) and (79) where the only difference in ligand structure is the position of the phenoxy group. Ligand (79) where the phenoxy

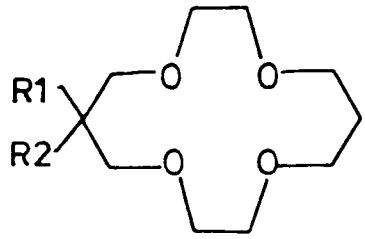

(78) R1 = 2-DNP; 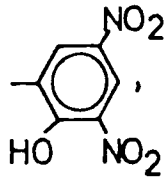 R2 = $C_{12}H_{25}$

(79) R1 = 4-DNP; 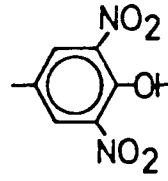 R2 = $C_{12}H_{25}$

group is situated further from the probable metal centre, extracts lithium very poorly: no extraction is detectable. The inability of the anion to interact favourably with the small, highly-charged lithium cation is reflected in the poor Li^+ extractability. Ligand (78) has a Li/Na extractability ratio of 87, thus providing further evidence for the favourable interaction of proton-dissociable groups with metal cations, aiding their extraction into organic media. Also of note is the fact that loss of the lipophilic group causes a loss of selectivity for lithium. (Loss of efficiency of extraction for all cations will be caused by loss of lipophilicity.) This may be attributed to the bulky groups geminal to the chromophores projecting the phenoxide anion over the crown ring, allowing easy intramolecular interaction of the phenoxide anion and the lithium ion.

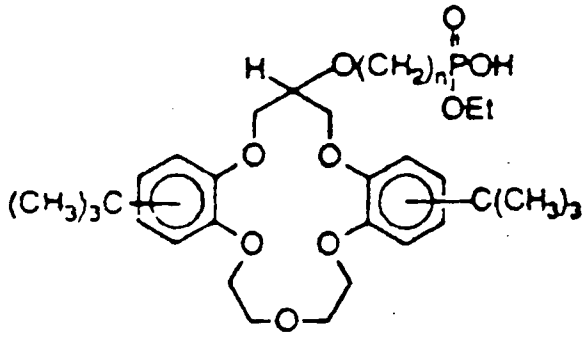

(77) n = 1

(80) n = 2

(81) n = 3

(82) n = 4

A further study by Bartsch[182] has looked at the effect of side-arm length upon competitive alkali metal solvent extraction. Synthetic constraints necessitated looking at the series of lipophilic crown phosphonic acid monoalkyl esters, (77) and (80)-(82). The attachment of lipophilic *t*-butyl groups is necessary to retain the acids in the organic phase during extraction. The ligands (77), and (80)-(82) represent a series of ligands in which the number of carbon atoms between the polyether ring and the phosphonic acid group is varied from one to four. The series enables the effects of side-arm length on selectivity and efficiency of metal ion complexation to be gauged. The selectivity of sodium over lithium is observed for ligands (77) and (80) but lithium is preferentially extracted over sodium by ligands (81) and (82). The cavity size of these ligands is more appropriate for the sodium cation,[175] and lithium selectivity over the other alkali metal cations has been observed for lipophilic phosphonic acid monoethyl esters which do not have polyether rings.[184] The extraction data may be explained by suggesting that the metal cation is bound within the ring for ligands (77) and (80) but is bound primarily by the side-arm for ligands (81) and (82). Space-filling models confirm that in ligands (81) and (82) the side-arms are too long to coordinate to the metal simultaneously with the crown ether ring. Ligand (80) however has a side-arm of appropriate length to sit directly over the ether ring and it is for this ligand that a very large selectivity for sodium over lithium is observed. The ligand with the shortest arm, (77), appears to be too short to enhance the binding by the ring. This is supported by the crystal structure[154] of the complex between ligand (56) and Li^+ where the lithium is coordinated within the ring and a water molecule bridges the gap between lithium and the ionised group (Figure 2.15, discussed further in Section 2.2.1).

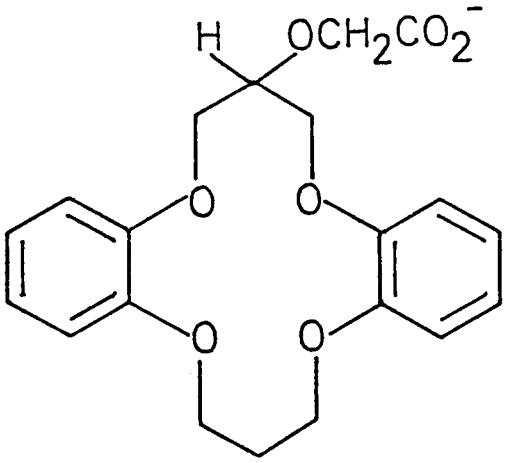

(56)

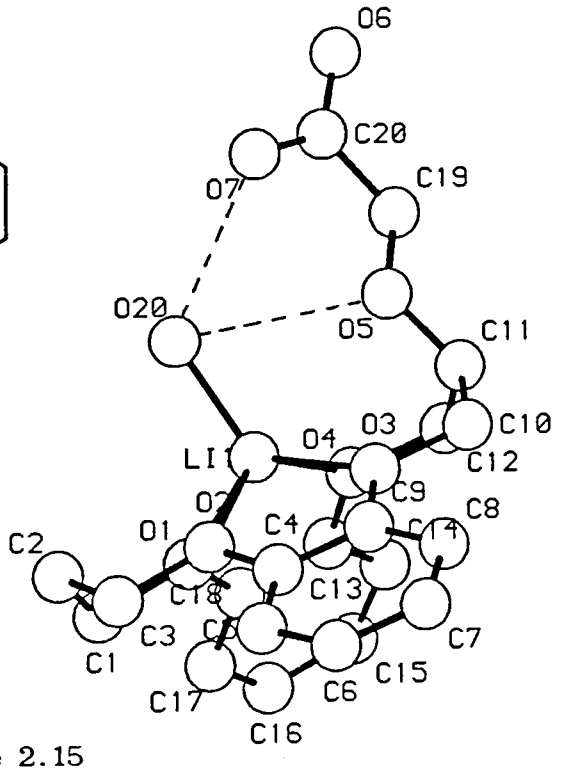

Figure 2.15

X-Ray crystal structure of the lithium complex of ligand (56)

2.4 Methods for the Determination of the Stability and Selectivity of Complexation by Ligands

The stability constant of complexation is usually referred to as the $\log_{10} K$ value, where K is determined according to the following equations:

$$M + L \underset{\longleftarrow}{\overset{K}{\longrightarrow}} ML$$

$$K = \frac{[ML]}{[M][L]}$$

where M is the metal cation, L is the ligand, and ML the complex and the brackets denote concentration. Obviously this equation represents the formation of a 1:1 complex. The formation of 2:1 complexes requires the determination of two complexation constants, log K_1 and log K_2:

$$M + L \overset{K_1}{\rightleftharpoons} ML$$

$$ML + L \overset{K_2}{\rightleftharpoons} ML_2$$

Many workers relate the selectivity of complexation, the preference of a particular ligand to bind to a particular cation over and above other cations, directly to the stability of the complexes formed. Thus selectivity constants are given as direct ratios of the K values determined. A selectivity constant, S, for the preference of a ligand for lithium over sodium will be given as:

$$S = K_{Li}/K_{Na}$$

where K_{Li} and K_{Na} refer to the following equations:

$$L + Li \overset{K_{Li}}{\rightleftharpoons} LLi$$

$$L + Na \overset{K_{Na}}{\rightleftharpoons} LNa$$

In fact this is not a *true* selctivity value, for high stability of complexation does not necessarily imply high selectivity. It is the *dynamics* of the complexation which are more relevant for cation selectivity. The rate of formation, k_f, and the rate of dissociation, k_d, are related to the stability constant in the following way:

$$M + L \underset{k_d}{\overset{k_f}{\rightleftharpoons}} ML$$

$$K = k_f/k_d$$

Cox and Schneider[185] showed for the alkali metal cryptates that the pronounced selectivities observed were reflected entirely in their dissociation rates and not in their formation rates. The formation rates increase monotonically with increasing cation size for a particular cryptand. Such data suggest that the specific size-dependent interactions between a cryptand and a cation occur subsequent to the formation of the transition state (in the formation reaction). This comment may be related to an observation made by Bartsch[182] that both the efficiencies and *selectivity orders* observed for the competitive

solvent extraction of alkali metal cations by crown ether carboxylic acids were often quite different from those expected, based upon the results of single-ion extractions.[174,175] The single-ion extractions determine the percentage of a particular cation extracted from aqueous solution into an organic solvent (by a particular ligand)(see Section 2.4.3). Competitive solvent extractions determine the percentage extracted for several different cations which are competing for a limited amount of ligand. Justifiable comparisons of the extraction experiment data require that the counter-ion is unchanged and the same solvent system is studied. Anion solvation must be a constant factor. In effect, the stability constants of complex formation over two-phase systems do not predict the selectivity order of complexation when all cations are present at the same time, competing for the ligand.

A futher *caveat* to be considered when discussing the selectivities of ligands for particular cations requires that the method of determination is the same for each ligand. Whilst it might be thought that different methods will provide the same order of selectivity, though requiring calibration, this is not the case. Different methods induce different selectivities. For example, Kimura *et al.*[139] have reported benzo-13-crown-4 (83) to be more selective for sodium than for lithium using the mixed-solution potentiometric method, whereas Olsher and Grodzinski[186] report the same macrocycle to be lithium-selective using extraction techniques.

It is clear that the measurement technique employed must reflect the use for which the potentially selective macrocycles are intended. In the proceeding paragraphs, some of the techniques used for measuring stability constants and selctivities will be examined, primarily those used in relation to our own work.

2.4.1 *NMR Methods*

NMR experiments permit the determination of the stoichiometry of a complex, a qualitative indication of the strengths of the complex and a measure of the dynamics of the complexation. For example, the titration of a deuterated methanol solution of a macrocyclic ligand with solid alkali salt with spectra recorded after each titre may reveal the above-mentioned information by monitoring the shift of the ^{13}C NMR resonance signals. If no complexation between ligand and metal cation occurs, the spectra are identical. However, if complexation does occur, two possible situations arise. Firstly, if the rates of complexation and decomplexation are fast on the time-scale of the NMR experiment at room temperature, an averaged signal for the carbon atoms in the free ligand and the corresponding carbon atoms in the ligand bound to the metal cation will be observed. A curve may be plotted representing the ^{13}C NMR chemical shift displacement ($\Delta\delta$) for a particular carbon atom in the ligand on successive addition of a solid alkali salt (Figure 2.16). The stoichiometry of complexation may be derived from the position of the curve bend and a qualitative idea of the strength of the complex may

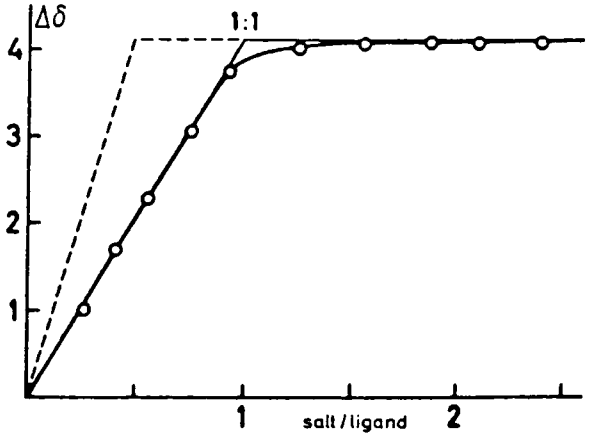

Figure 2.16

Example of curve-shape observed when monitoring complexation by ^{13}C NMR

be gained from the deviation from a sharp bend. The theoretical curve in Figure 2.16 represents a relatively strong complex with a 1:1 stoichiometry. When the stoichiometry of complexation is estimable, the stability constants of the complex formation may also be calculated. For example, a suitable method involves detailed analysis of the shift of a specific ^{13}C NMR resonance signal.[187,188] Consider the complex formation equilibria between ligand, L, and metal ion, M:

$$M + L \rightleftharpoons ML \qquad K_1 = \frac{[M][L]}{[ML]} \quad .. \quad .. \quad .. \quad 2.1$$

$$ML + L \rightleftharpoons ML_2 \qquad K_2 = \frac{[ML][L]}{[ML_2]} \quad .. \quad .. \quad .. \quad 2.2$$

where K_1 and K_2 are dissociation constants (stability constants have the reciprocal value of dissociation constants), brackets denote concentration of species.

The observed shift, δ, is given by the expression:

$$\delta = \frac{[ML]\cdot\delta_1}{L_T} + \frac{2[ML_2]\cdot\delta_2}{L_T} \quad .. \quad .. \quad .. \quad 2.3$$

where δ_1, δ_2 are the chemical shifts of the ML and ML_2 species respectively. This can be re-arranged to give:

$$\frac{[ML]}{L_T\cdot\delta} = \frac{1}{\delta_1} - \frac{2[ML_2].\delta_2}{L_T\cdot\delta\ \delta_1} \quad .. \quad .. \quad .. \quad 2.4$$

The total concentrations of ligand and metal ion, denoted by L_T and M_T respectively, are known and are defined thus:

$$L_T = [L] + [ML] + 2[ML_2] \quad .. \quad .. \quad .. \quad 2.5$$

$$M_T = [M] + [ML] + [ML_2] \quad .. \quad .. \quad .. \quad 2.6$$

Combining equations 2.1, 2.2, 2.5, and 2.6 gives the following expression:

$$[L]^3 + (K_2 + 2M_T - L_T)[L]^2 + K_2(K_1 + M_T - L_T)[L] - K_1K_2L_T = 0$$

derived thus:

from (2.1), $[ML] = \frac{[M][L]}{K_1}$

from (2.2), $ML_2 = \frac{[ML][L]}{K_2} = \frac{[M][L]^2}{K_1K_2}$.

Substituting these in equation (2.5) gives:

$$L_T = [L] + \frac{[M][L]}{K_1} + \frac{2[M][L]^2}{K_1K_2} \quad \ldots\ \ldots\ \ldots \quad (2.7)$$

Similarly, substituting in (2.6) gives:

$$M_T = [M] + \frac{[M][L]}{K_1} + \frac{[M][L]^2}{K_1K_2}$$

$$= [M].\left[\frac{[L]}{K_1} + 1 + \frac{[L]^2}{K_1K_2}\right]$$

which implies $[M] = \frac{M_T}{\phi}$, where $\phi = \left[\frac{[L]}{K_1} + 1 + \frac{[L]^2}{K_1K_2}\right]$.

Substituting for [M] in (2.7) gives:

$$L_T = [L] + \frac{[M_T]}{\phi}.\frac{[L]}{K_1} + \frac{2[M_T][L]^2}{\phi K_1K_2}$$

multiply through by ϕ:

$$\phi.L_T = \phi.[L] + \frac{M_T[L]}{K_1} + \frac{2M_T[L]^2}{K_1K_2}$$

substitute for ϕ:

$$\left[1 + \frac{[L]}{K_1} + \frac{[L]^2}{K_1K_2}\right].L_T = \left[1 + \frac{[L]}{K_1} + \frac{[L]^2}{K_1K_2}\right].[L] + \frac{M_T[L]}{K_1} + \frac{2M_T[L]^2}{K_1K_2}$$

$$L_T + \frac{L_T[L]}{K_1} + \frac{L_T[L]^2}{K_1K_2} = [L] + \frac{[L]^2}{K_1} + \frac{[L]^3}{K_1K_2} + \frac{M_T[L]}{K_1} + \frac{2M_T[L]^2}{K_1K_2}$$

Rearranging gives:

$$\frac{[L]^3}{K_1K_2} + \left[\frac{1}{K_1} + \frac{2M_T}{K_1K_2} - \frac{L_T}{K_1K_2}\right].[L]^2 + \left[1 + \frac{M_T}{K_1} - \frac{L_T}{K_1}\right].[L] - L_T = 0$$

Multiply by K_1K_2:

$$[L]^3 + (K_2 + 2M_T - L_T).[L]^2 + K_2.(K_1 + M_T - L_T).[L] - K_1K_2L_T = 0$$

This expression may be solved iteratively for [L] using the Newton-Raphson method,[188] with estimated values of K_1 and K_2.

Given [L], the equilibrium concentrations of the other species can be calculated with ease:

$$[M] = \frac{M_T}{(1 + [L]/K_1 + [L]^2/K_1K_2)}$$

$$[ML] = [M][L]/K_1$$

$$[ML_2] = [M][L]^2/K_1K_2$$

Thus, K_1 and K_2 are initially estimated and equilibrium concetrations evaluated for all species for each set of M_T and L_T values. These figures are used with equation (2.6) to obtain values for δ_1 and δ_2. Finally, using equation (2.5), values of the expected chemical shift are calculated and compared with the observed values. K_1 and K_2 are varied over a wide range until a standard deviation of less than 5% is obtained. The values of K_1 and K_2 corresponding to this minimum may be considered to be reasonably realistic.

For the situation when K_2 is zero, the expression to determine the equilibrium concentration of ligand is much simpler:

$$[L]^2 + (M_T + K_1 - L_T)\cdot[L] - L_TK_1 = 0$$

For criteria of reliability the discussion by Lenkinski[187] may be considered. Stability constants are reliable only for the weaker complexes with, say, $\log K < 3$.

The second situation arises if the rate of complexations and decomplexations are slow on the time-scale of the NMR experiment (relative to the rates observed in the first situation) at the temperature of the experiment. Here, two discrete signals will be observed for each carbon atom of the ligand: one for the carbon atom in the free ligand and one for the corresponding carbon atom in the ligand bound to the metal cation. An estimate of the stoichiometry of the complex may be obtained from the mole ratio of metal cations added to the ligand at the point where the resonance lines for the carbon atoms in the free ligand disappear. A further guide to the strength of complexation may be obtained from the maximum shift differences observed for each of the carbon atoms. It is reasonable to assume that the

stronger the binding of a particular heteroatom within a ligand to a cation, the greater the contribution to the observed shift difference for the resonance signals of the surrounding carbon atoms in the ligand. However, this presumption must be treated with caution, for the same phenomenon may arise when large conformational changes occur within the ligand on complexation. In the same way, the strength of binding of the individual heteroatoms to a metal cation within a particular ligand may be estimated from the relative maximum shifts of their surrounding carbon atoms. The importance of conformational changes that may take place on complexation which may also contribute to the relative shift must not be overlooked.

The above discussion is best illustrated by examples. Dale[123] has used the technique discussed in the preceeding paragraphs to study ligands (84) and (85). The addition of increasing amounts of lithium and sodium perchlorate to (84) and (85) was monitored using ^{13}C NMR. Ligand (84) showed only very small shift differences with these salts with the complexation constants, log K, estimated to be less than unity. The shift differences recorded for the addition of lithium perchlorate to ligand (85) are represented in Figure 2.17. The relative shift values for the ring carbon atoms only are shown, although all the resonance signals were shifted to lower frequency. The shift displacements are also larger for the ring carbons than for the side-arm carbons and this may indicate a change of the ring conformation on complex formation.[146,189] The sharpness of the curve bend indicates a fairly strong complex and the position of the curve bend suggests the dominance of a 1:1 complex. The complexation constants were derived by analysis of these titration curves using an iterative least squares procedure.[190,191] The constants determined are listed in Table 2.2,

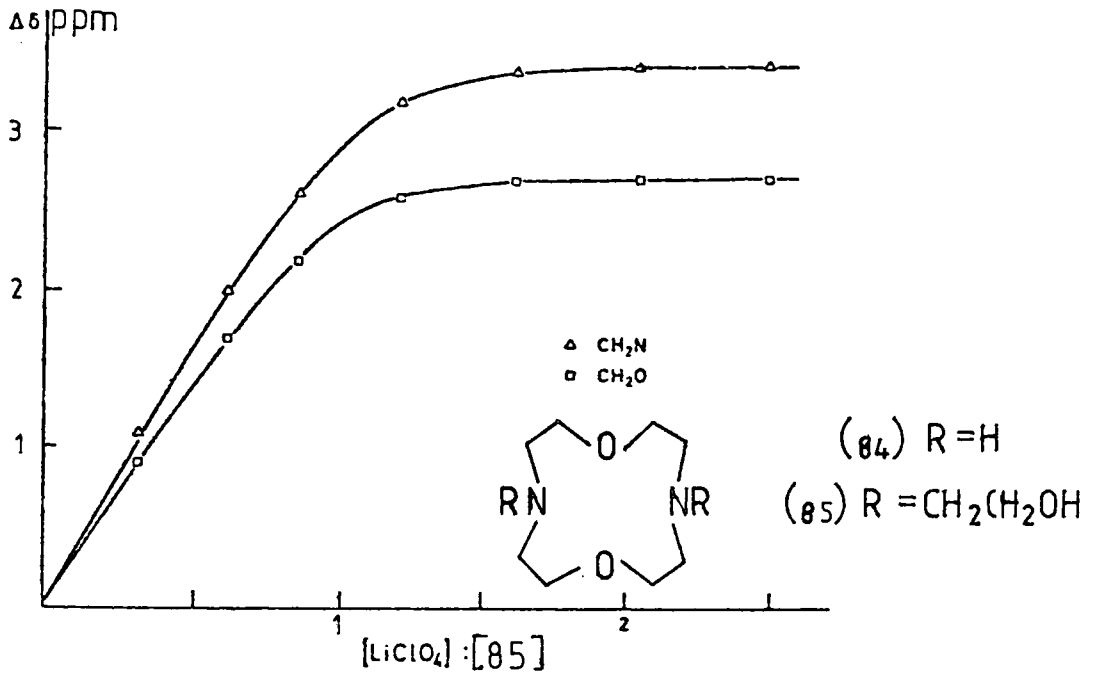

Figure 2.17

^{13}C *NMR chemical shift displacement* ($\Delta\delta$) *for the ring carbon atoms of ligand* (85) *vs. relative lithium perchlorate concentration.*

together with those determined by an alternative method using potentiometry. This comparison is necessary since large errors in the stability constants may be induced using the least squares programme for analysis of the NMR curves, especially where the complexation constant is greater than three. The data confirm that the addition of the

Salt	Resonance	log *K*
$LiClO_4$	CH_2O	2.8 (2.4)
	CH_2N	2.5
$NaClO_4$	CH_2O	3.4 (3.6)
	CH_2N	3.2

Table 2.2

Complexation constants for ligand (85) *from analysis of* ^{13}C *NMR titration curves with, in parentheses, the values determined by potentiometric methods*

hydroxyethyl side-arms enhance metal binding relative to the unsubstituted amine, (84). This enhanced binding is most likely due to the additional binding sites available to the cations. The decreased solubility of the tertiary amine function when compared with the secondary amine function in the free ligand may also contribute to increased binding. Dale and many other workers estimate then the selectivity of a ligand for a particular cation by evaluating the direct ratio of the respective stability constants. This does not represent a competitive selectivity determination however where cations compete for a limited amount of ligand. The selectivity of (85) for calcium over sodium measured in this fashion is 2000. Cryptand [2.1.1] which has the same number of donor atoms as ligand (85) is reported to have a *sodium preference of* 55[91] *over calcium*. At the time of reporting, the stability of the complex between (85) amd calcium ions was the highest known for a neutral macrocyclic ligand. This fact stimulated our interest and has led to the synthesis of a series of similar ligands as discussed in Chapter Four. In deference to the discussion concerning the effect of greater polarity of the side-arms, the hydroxy groups on the side-arms have been replaced with amide groups which are anticipated to be better σ-donors.

Dale[124] also used this NMR technique to study the behaviour of ligands (86) and (87) on complexation with Li^+, Na^+, and K^+ in methanol solution. (87) contains a side-arm incorporating a binding group whereas (86) does not. The experimental observations are represented in Figure 2.18. The curves were interpreted in the following manner. Ligand (86) gives a weak 1:1 complex with lithium and slightly stronger, 2:1 (sandwich) complexes with sodium and potassium cations as was found for 12-crown-4 (46). The sodium complex is the strongest of the three

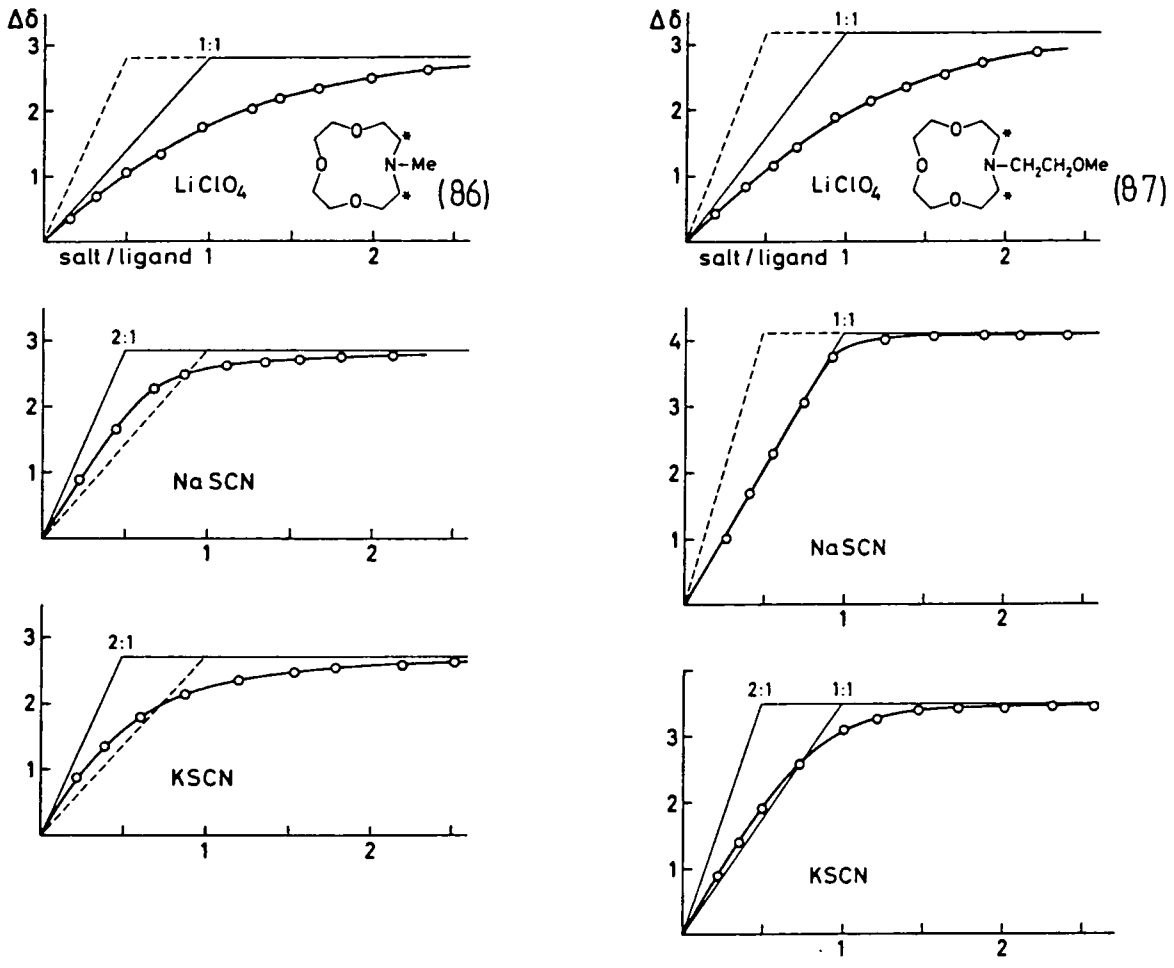

Figure 2.18

^{13}C NMR chemical shift displacement ($\Delta\delta$) for the ring NCH_2 carbon of ligand (86) (left) and ligand (87) (right) in methanol solution relative to the salt concentration (lithium perchlorate, sodium thiocyanate, and potassium thiocyanate): molar ratio as abscissa. The limiting chemical shift is fitted visually to the experimental curve.

complexes in both cases though replacement of an oxygen donor in 12-crown-4 by a nitrogen atom in (86) results in weaker binding as expected. The assignment of 2:1 complex formation for the Na^+ and K^+ complexes relies also on a consideration of realistic possible stoichiometries, given the geometry of the 12-membered rings. Strictly speaking, interpretation of the curves is ambiguous and may also suggest mixtures of weak complexes with various stoichiometries. The Na^+ curve however is best interpreted on the basis of a dominating 2:1

stoichiometry and the less well-defined K^+ curve is likely to indicate the same stoichiometry. Ligand (87) forms a weak 1:1 complex with Li^+ but a very strong 1:1 complex with Na^+. The strength of the Li complex is virtually unchanged when compared qualitatively with the N-methyl derivative, suggesting the side-arm is not used in co-ordination to Li^+. The formation of the strong 1:1 complex between (87) and Na^+ when compared with the weaker 2:1 complex formed between (86) and Na^+ demonstrates clearly that the presence of a side-arm bearing a donating group can suppress the formation of sandwich (2:1) complexes. It is most likely that the fifth binding group situated on the side-arm of (87) is correctly positioned to bind to the cation and this binding is more advantageous than that by the four heteroatoms of a second cycle. This preference may be aided by a re-establishment of ion-pairing of the salt, since sandwich binding completely separates the cation from the anion.

The titration curve for ligand (87) with K^+ is more complex. The observation that when one equivalent of K^+ ions has been added a constant chemical shift is quickly reached suggests the formation of a relatively strong complex. The stoichiometry cannot be 2:1 however since the curve at low salt concentration is not equally closely followed. Thus, it seems likely that the stoichiometry of the strong complex is 1:1, but at low salt concentrations a 2:1 complex forms which is present only when there is an excess of ligand. These data have led to our interest in the same 12-ring structure with one functionalised side-arm containing ester or amide functionality.

Olsher and Grodzinski's[186] work on benzo-13-crown-4 (83) also shows changes in the chemical shifts of the protons of benzo-13-crown-4 in nitromethane due to changes in the ratio of $LiClO_4$:ligand, as depicted in Figure 2.19. The curve shows a deflection at a Li^+:(83) ratio of $\simeq$

0.5:1 suggesting the formation of a sandwich complex. Similar behaviour is noted with dichloromethane as solvent but only a 1:1 complex is formed in acetonitrile solution. The stability constants were determined according to the methods of Reuben,[187,188] as outlined previously and seem to indicate that when the donating ability of a solvent is poor the formation of a 2:1 complex at low salt concentrations readily occurs.

Whether the titration experiment gives an average signal or discrete signals depends on the dynamics of the complexation process at that temperature. However, it may be reasonably assumed that a slow

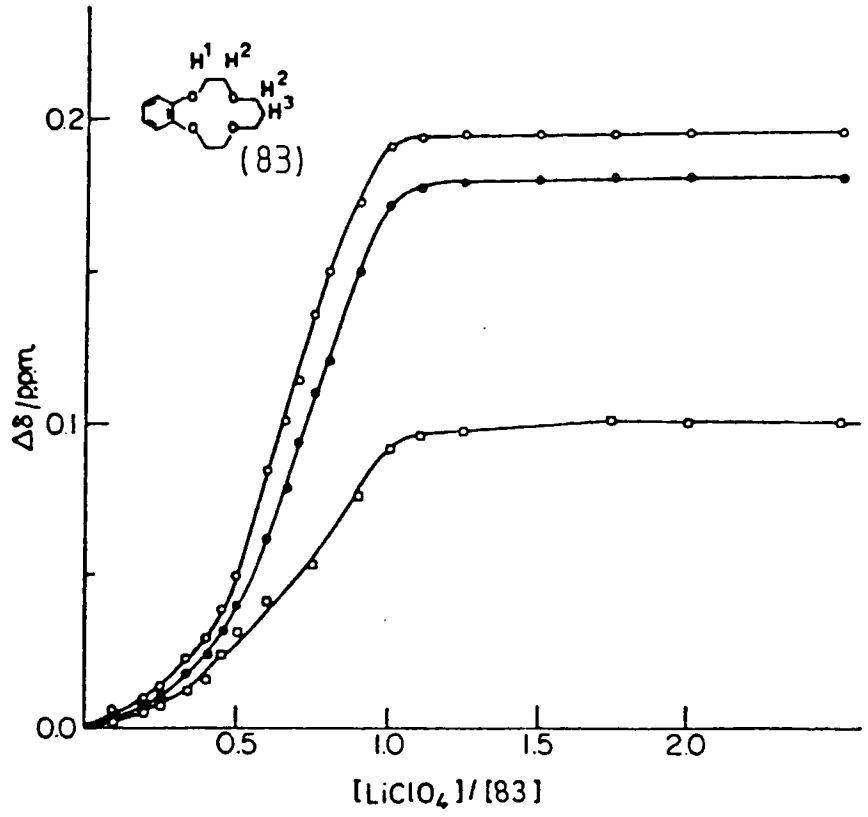

Figure 2.19

^{1}H NMR chemical shift displacements ($\Delta\delta$) of ligand (83) in nitromethane relative to lithium perchlorate concentration. H^1 (o), H^2 (•), *and* H^3 (□).

dynamic situation results from the formation of a strong complex. Where the binding of a metal cation by a ligand is strong the ligand will not want to release the cation to the solvent. Conversely, formation of a weak complex generally should result in fast reaction dynamics. It may be assumed that a high dissociation barrier parallels strong complexation.

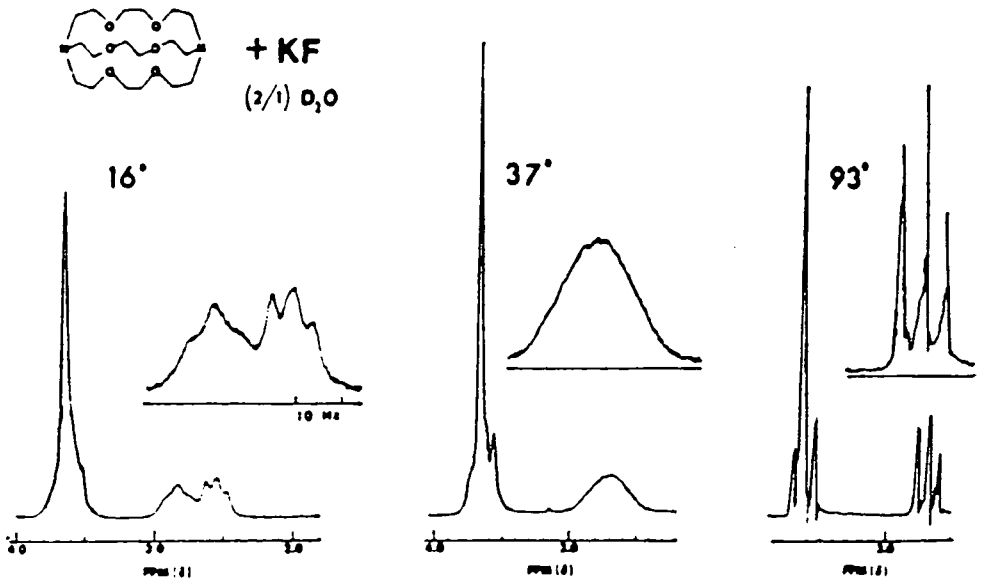

Figure 2.20

Temperature dependence of the 60 MHz ^1H NMR spectra of a D_2O solution containing cryptand [2.2.2] (35) *and the* [(35), K^+] F^- *cryptate in equal amounts*

A variable temperature NMR study[114,192,193] (^1H, ^{13}C, or alkali metal cation nucleus) may reveal that the exchange process is temperature dependent. For example, Lehn and Sauvage[114] have reported the ^1H NMR spectra at various temperatures for the cryptand [2.2.2] (35) with several cations. Reproduced in Figure 2.20 are the spectra for the complex with KF at three temperatures. The quantity of KF added is such that the solution contains equimolar quantities of [2.2.2] and the

corresponding potassium ion cryptate, [2.2.2].KF. At 310 K, a broad unresolved signal is obtained for the CH_2N protons. When the solution (in D_2O) is cooled to 289 K, the CH_2N signal splits into two triplets at 2.83 and 2.55 ppm. These signals correspond to the signal for the free cryptand and the signal for the potassium cryptate respectively. On heating of the solution to 366 K a sharp, single triplet is observed at 2.67 ppm. From these data, the free energy of activation, $\Delta G_c^{\neq}$, and the exchange rate, k_c, at the particular coalescence temperature observed may be calculated. The general equations are given below and derive from the Eyring equation:[194]

$$k_c = \pi\delta\upsilon/\sqrt{2}$$

$$\Delta G_c^{\neq} = RT_c[22.96 + \ln(T_c/\delta\upsilon)]$$

where $\delta\upsilon$ is the frequency separation of the inital, sharp signals (Hz), and T_c is the coalescence temperature (K).

The mechanism of exchange may be a bimolecular process which is represented by the equation below:

$$L + ML^* \underset{k_{-1}}{\overset{k_1}{\rightleftharpoons}} ML + L^*$$

This process is particularly likely for stable complexes where the complex is far more stable than the dissociated ligand (*i.e.* where $\log K > 10^3$, $k_1 > 10^3\ k_{-1}$). The mechanism of exchange may also follow the dissociation-association process represented below:

$$[L]_{solvent} + [M,m(solvent)] \underset{k_d}{\overset{k_f}{\rightleftharpoons}} [L.M]_{solvent} + m(solvent)$$

The exchange rate, k_c, and the free energy of activation, $\Delta G_c^{\neq}$, relate to the dissociation rate of the metal cation leaving a complex. It is noteworthy that the k_c and $\Delta G_c^{\neq}$ values tend to reflect the reverse order of the stability constant of complex formation: exchange becomes slower if the stability of the complex increases.

2.4.2 *Fast-Atom Bombardment Mass Spectroscopy (FAB MS) Techniques*

Fast-atom bombardment mass spectroscopy[195-197] is a relatively new technique first introduced in 1981.[198] The experiment requires bombardment of the chemical sample by a beam of relatively high energy fast atoms, usually xenon or argon. The chemical species is usually introduced to the probe in a high-boiling solvent, for example in glycerol or in 2,2'-thiodiethanol. In solution, the chemical species is mobile and may continually migrate to the surface of the solution, replenishing the number of surface molecules of the compound available for ionisation by the neutral beam. FAB MS permits the acquisition of stable, relatively long-lived and intense signals, representative of the molecular masses of the species being investigated. A wide range of chemical compounds may be examined notably organometallic and inorganic species. This wide applicability stems from the fact that FAB MS yields ions from involatile species without the need to apply heat to the sample. Thus, spectra may be observed for thermally fragile materials, a feature which may be applied to metal-containing species advantageously.

Complex formation between macrocyclic ligands and metal cation have been observed by FAB MS,[199] and the selectivity of the ligand for the various cations can be determined. The method requires that the cations compete with each other for a deficiency of the ligand, thus constituting a direct observation of selectivity. Johnstone and Rose[199] have reported the observation of complex formation between alkali metal cations, Li^+, Na^+, K^+, Rb^+, and Cs^+ and several macrocyclic ligands including 12-crown-4, 15-crown-5, 18-crown-6, and cryptand [2.2.2]. They observe that the abundances of gas-phase ions at *m/e* values corresponding to ligand-metal cation complexes reflecting closely the calculated concentrations of these complexes in solutions at normal

temperatures. Thus, FAB MS allows the determination of the selectivity of a particular ligand for the various alkali metal ions.

Analytical solutions were prepared by mixing equal volumes of two solutions, one containing the iodides of Li^+, Na^+, K^+, Rb^+, and Cs^+ each of a concentration of 5 mM in 2:1 glycerol-water and tetra-*n*-butyl-ammonium chloride at a concentration of 60 μM as an internal standard which does *not* interact with the ligand, and the other also in 2:1 glycerol-water, containing the macrocyclic ligand at a concentration of 5 mM. Thus, the analytical solution contains ligand and cations in equimolar concentrations, forcing the metal cations to compete for a limited amount of the ligand. The FAB probe is coated with a thin layer of the analytical solution and positive ion FAB MS performed. For a full account of the actual FAB experiment the report by Johnstone and Rose[199] may be consulted. The abundance of ions at each *m/e* value corresponding to [ligand-metal cation] complexes were measured relative to the abundance of the internal standard tetra-n-butylammonium ion at *m/e* 242. For comparative purposes, the concentration of complexes expected have been calculated using the stability constants of complexation in aqueous solution (no data exist for glycerol solutions). The data are given in Table 2.3.

No peaks are observed for 12-crown-4 with any of the metal cations which corresponds well with the low K values cited for this ligand in aqueous solution. The low binding constants for all the ligands discussed with lithium ions is also in keeping with the fact that no signals for $[Li\text{-ligand}]^+$ complexes were observed. Similarly, the binding constant of cryptand [2.2.2] with Cs^+ is extremely low and no peak corresponding to cryptand [2.2.2] plus Cs^+ was observed. Generally for the other ligands the variation in abundance of ions corresponding

Ligand	Li^+	Na^+	K^+	Rb^+	Cs^+
12-crown-4	not observed	not observed	not observed	not observed	not observed
15-crown-5	not observed	21.1	10.0 (12.4)	5.3 (9.6)	1.7 (14.2)
18-crown-6	not observed	2.9	183.4 (123)	114.5 (50.8)	23.3 (14.8)
[2.2.2]	not observed	28.0	464.6 (385)	152.3 (113)	not observed (0.6)

Table 2.3

Abundances of [ligand + metal]$^+$ ions relative to the tetra-n-butyl-ammonium ion as internal standard. The abundances were determined by assigning the internal standard an arbitrary peak height of 10 units for each spectrum. Values in parentheses are concentrations of the complexes in aqueous solution containing three ions (K^+,Rb^+, and Cs^+) calculated by an iterative procedure from stability constants determined in aqueous solution.

to the [metal cation-ligand]$^+$ complexes closely parallels that expected from the stability constant data. Thus, FAB MS may be used to examine the simultaneous complex formation of various metal cations with macrocyclic ligands in solution. It is the close similarity of FAB ion abundances to the concentrations of cation-ligand complex calculated to be present that suggests the stability constant of complex formation does not alter much in aqueous glycerol solution compared with aqueous solution.

A further study looked at the FAB spectrum of N,N,N',N'-tetra-i-butylcyclohexane-1,2-dicarboxamide (1), discussed in the introduction as a compound exhibiting strong lithium selectivity, introduced by W. Simon for incorporation into solvent-polymeric membrane electrodes. It was found that analysis of (1) in PEG solution gave cleaner spectra than alternative solvents: that is, matrix suppression was superior in PEG

solution. Addition of dilute HCl to the solution was also found to enhance sensitivity. This work reported selectivity constants, S, according to the equation:

$$S = \log \left[\frac{I(L + Li)^+}{I(L + C)^+} \right]$$

where $I(L + Li)^+$ is the signal intensity for [ligand + Li]$^+$, and $I(L + C)^+$ is the signal intensity for [ligand + alkali metal cation]$^+$. The selectivity factors may be represented graphically (see Fig. 2.21). Thus, the lithium selectivity of ligand (1) was observed using FAB MS.

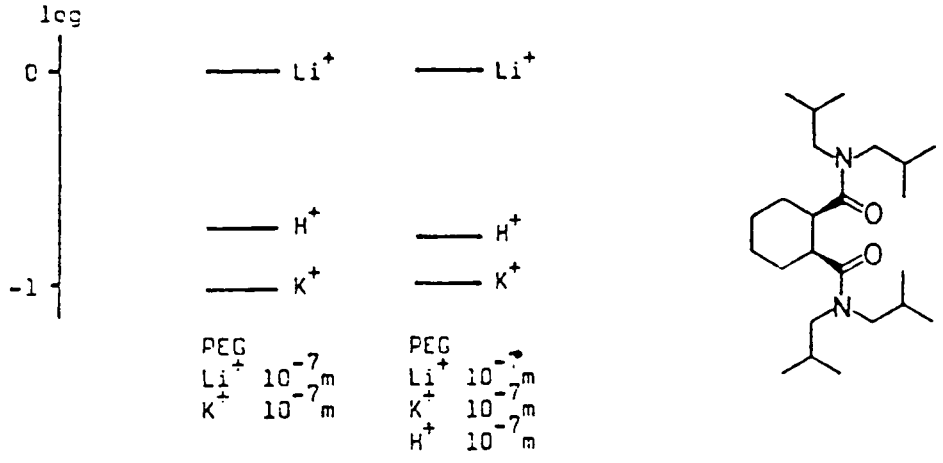

Figure 2.21

Lithium selectivity of (1)

2.4.3 *Extraction Techniques*

Extraction techniques have been used by many workers to gauge the selectivity of a particular macrocyclic ligand for the various Group IA and IIA metal cations. The experiment consists of extracting cations from an aqueous phase into an organic phase. As has already been discussed, both single-ion extractions and competitive extractions may be investigated. However, it has been demonstrated[174,175] that both the efficiencies and selectivity orders found for competitive extractions are not what one would expect on the basis of single-ion extraction

results. Thus, for a *true* selectivity ratio, competitive extractions must be undertaken.

The process of extraction for those macrocyclic ligands with pendant ionisable groups is very different from that for neutral macrocycles without the pendant proton-dissociable group. Macrocycles with ionisable groups on their side-arms have the distinct advantage that transport of the metal cation from the aqueous phase to the organic phase does not require simultaneous transfer of the aqueous phase anion into the organic medium. This means that the use of chloride, nitrate, and sulphate anions is permitted. For comparisons of the selectivity of different ligands determined in this way, however, the anion and solvent must be the same in each case.

A typical experiment[152,182,183] consists of shaking thoroughly together an aqueous solution and an organic solution. The aqueous solution may contain several alkali metal chlorides in equal concentrations and hydroxide compounds for pH adjustment. The organic solution, for example with chloroform as solvent, may contain the complexing ligand in the same concentration. Thus, if four different cations are present the total cation concentration will be four times greater than the ligand concentration. After thorough mixing the two immiscible layers are allowed to separate and the organic phase is analysed for its cation concentrations. This may be done using methods such as ion chromatography and atomic absorption spectrophotometry.

For the neutral macrocycles, transport of the aqueous phase anion is required, which precludes the use of hard, hydrophilic anions such as chloride, nitrate, and sulphate. These anions distribute very poorly to the organic phase. Picric acid is eminently suitable for providing an anion which transfers to an organic phase concomitantly with a metal cation. The picrate anion has the added benefit that it is chromophoric

and thus the extraction may be monitored spectophotometrically. It is found[201] that if an aqueous solution which contains an alkali metal hydroxide or salt, and a low concentration of picrate anion is shaken with an equal volume of an immiscible organic solvent the organic phase remains effectively colourless with all the picrate remaining in the organic medium. In fact, distribution constants, (K_d) have been determined[202] for some picrate salts between water and chloroform according to the following equation:

$$[M^+]_{H_2O} + [picrate^-]_{H_2O} \xrightleftharpoons{K_d} [M^+.picrate^-]_{CDCl_3}$$

The values of K_d and corresponding concentrations of picrate anion were so small that the final salt concentration in the water layer lay within the error limits of the initial concentration. If, however, a macrocyclic ligand is added to the organic solution, the picrate anion transfers to the organic phase accompanying the bound cation. The extent of picrate transfer will depend on the effectiveness of the ligand as a complexing agent for the cation. If the macrocycle is ineffective, the organic phase will remain virtually colourless whereas if the extraction of the cation is high, the organic phase will become highly coloured (bright yellow). These two situations represent the extremes of behaviour and usually the extent of complexation will lie between them. The extraction result is conveniently expressed as a "percentage of cation extracted". The stoichiometry of the extracted species is 1:1 with respect to alkali cation and picrate anion, thus the concentration of the metal cation extracted is determined by measuring the concentration of its ion partner, the picrate anion. This may be done as has already been suggested using UV/vis techniques or by NMR methods. The maximum extraction is limited by the component present in the lowest concentration, thus, "percentage extracted" always refers to the percentage of the extractable maximum. A typical experiment[201-206]

for a neutral macrocycle consists of thoroughly mixing equal volumes of two immiscible phases at a given temperature. An aqueous phase may contain a known concentration of a metal cation together with a known concentration of picrate anions. The organic phase contains the neutral macrocyclic ligand at a known concentration. On separation of the phases, the organic phase may be analysed for its cation concentration.

2.4.4 *Potentiometric Methods*

The stability constants of formation for complexes between basic ligands and metal cations may be determined using potentiometric methods. Analysis of pH-metric titration curves allows the calculation of stability constants. The pH curves are obtained following titration of a solution of the protonated ligand with tetramethylammonium hydroxide solution in the presence and absence of metal cations and are plotted as the pH of the solution against the volume of base added to the solution.[91,207-209] Tetramethylammonium hydroxide is used since the cation is sufficiently large that it is unlikely to interact with the relatively small macrocyclic cavity. The ligands are basic by character and will alter the pH of the solution on complex formation. Consider the equilibrium between the basic ligand, L, and a proton, represented below:

$$L + H^+ \rightleftharpoons LH^+$$

The addition of metal cations to the equilibrium mixture which may result in the binding of the cation to the ligand will force the equilibrium to the left and thereby decrease the pH of the solution. In effect, bound metal cations cause deprotonation of the ligands, increasing the free concentration of protons.

Many computer programs exist and are widely used for the calculation of formation constants of species in solution equilibria

from the data obtained by potentiometric titration. For example, superquad,[210,211] micmac,[212] SCOGS,[213] and BEST[214] are all well-established programs.

The efficient determination of the complete set of successive protonation constants of a multi-dentate ligand or a poly-functional base is required for the characterisation of the complexation properties of the compounds under investigation. The above-mentioned programs for the determination of metal-ligand formation constants may also be employed for the determiantion of the successive overlapping protonation constants, $K_1 \ldots K_x$, represented in the equations below:

$$L + H^+ \underset{\longleftarrow}{\xrightarrow{K_1}} LH^+; \quad K_1 = \frac{[LH^+]}{[L][H^+]}$$

$$LH^+ + H^+ \underset{\longleftarrow}{\xrightarrow{K_2}} LH_2^{2+}; \quad K_2 = \frac{[LH^{2+}]}{[LH^+][H^+]}$$

$$LH_2^{2+} + H^+ \underset{\longleftarrow}{\xrightarrow{K_3}} LH_3^{3+}; \quad K_3 = \frac{[LH^{3+}]}{[LH^{2+}][H^+]}$$

$$\ldots \quad \ldots \quad \ldots \quad \ldots \quad \ldots \quad \ldots \quad \ldots \quad \ldots \quad \ldots \quad \ldots \quad \ldots$$

$$LH_{x-1}^{(x-1)+} + H^+ \underset{\longleftarrow}{\xrightarrow{K_x}} LH_x^{x+}; \quad K_x = \frac{[LH_x^{x+}]}{[LH_{x-1}^{(x-1)}][H^+]}$$

However, PKAS[215] developed by Motekaitis and Martell is a program which is specifically designed to determine the protonation constants by an iterative process. They maintain that these constants are important enough to warrant separate and accurate determination. The report by Motekaitis and Martell details the programme and its advantages over alternative methods. Here follows an outline only of the mathematical procedure, intended only to highlight *how* such constants may be found.

The two following mass balance equations must be satisfied at every volume addition point in a potentiometric equilibrium curve:

$$T_L = [L]A_1 \quad \ldots \quad 2.8$$

where T_L is the analytical concentration of ligand, and

$$T_H = [L]A_2 + B \quad \ldots \quad 2.9$$

where T_H is the analytical concentration of ionizable hydrogen, B is $[H^+] - [HO^-]$ + [titrant added] + other corrections, and L is the symbol for the most deprotonated form of the ligand, H_xL.

$$A_1 = 1 + K_1[H^+] + K_1K_2[H^+]^2 + \ldots + K_1\ldots K_x[H^+]^x \quad .. \quad .. \quad 2.10$$

$$A_2 = K_1[H^+] + 2K_1K_2[H^+]^2 + \ldots + XK_1\ldots K_x[H^+]^x \quad .. \quad .. \quad 2.11$$

For a general equilibrium point:

$$K_i = \frac{[K_iL]}{[H^+][H_{i-1}L]} \quad .. \quad .. \quad 2.12$$

i.e. for $LH_{i-1} + H^+ \rightleftharpoons LH_i^{i+}$.

2.9 divided by 2.8 gives:

$$(T_H - B)/T_L = A_2/A_1 \quad .. \quad .. \quad 2.13$$

Given a set of protonation constants, K_i's, this simple equation of order X+1 in $[H^+]$, is most efficiently solved for $[H^+]$ at any degree of neutralisation by the Newton-Raphson method with the use of the following techniques. Define a function, F, from 2.13 when the correct solution to equation 2.13 in $[H^+]$ is determined, *i.e.* $F = (T_H-B)/T_L - A_2/A_1$ (2.14). The iterative method involves the determination of the derivative $\delta F/\delta[H^+]$ at an initially estimated value of $[H^+]$.

By the quotient rule for the determination of derivative functions, letting $A_2/A_1 = u/v$:

$$\delta F/\delta[H^+] = 0 + (v\cdot\delta u/\delta x - u\cdot\delta v/\delta x)/v^2 \quad \text{N.B. } T_H \text{ and } T_L \text{ are known constants}$$

$$= -1/T_L\cdot(\delta B/\delta[H^+]) - 1/A_1\cdot(\delta A_2/\delta[H^+]) + A_2/A_1^2\cdot(\delta A_1/\delta[H^+]) \quad .. \quad 2.15$$

We also have:

$$\delta B/\delta[H^+] = 1 - \frac{\delta(K_W/[H^+])}{\delta[H^+]} \text{ given } K_W = [HO^-][H^+]$$

$$= 1 - K_W(-1/[H^+]^2) = 1 = K_W/[H^+]^2$$

and $\delta A_1/\delta[H^+]$ and $\delta A_2/\delta[H^+]$ may be obtained directly from 2.10 and 2.11 by differentiation.

Using the Newton-Raphson method, the equation for the j^{th} iteration

gives:

$$[H^+]_j = [H^+]_{j-1} - F/F' \quad .. \quad .. \quad .. \quad 2.16$$

When $[H^+]$ is found, the refinement is terminated and the next experimental point is considered.

The strategy employed involves formulating an initial tentative value of each log K_i and calculating a potentiometric equilibrium curve using the mathematical algorithm, 2.16 given above. A calculation of the standard deviation in pH residuals for the entire curve is a measure of the closeness of fit and is a criterion for deciding when to stop adjusting the protonation constants.

The fundamental differences between this algorithm and others are: (1) the parameter computed at each titration volume is the pH and the parameter minimised is the mean sum of the squares of the deviation between the calculated and observed pH values; (2) the final refinement of the protonation constants is based on a weighted algebraic mean of the deviations of each interval in which that protonation equilibrium is considered to dominate the reaction.

The program BEST[214] may then be used to determine the formation constants corresponding to the equations below from the potentiometric data obtained in the presence of metal cations and the already calculated protonation constants.

$$L + M^+ \underset{\longleftarrow}{\xrightarrow{K^1}} LM^+$$

$$LM^+ + M^+ \underset{\longleftarrow}{\xrightarrow{K^2}} L_2M^{2+}$$

$$L_2M^+ + L \underset{\longleftarrow}{\xrightarrow{K^3}} L_3M^+$$

$$L + M^+ + H^+ \underset{\longleftarrow}{\xrightarrow{K^4}} LMH^+ \quad etc.$$

BEST also computes the equilibrium pH value at each equilibrium point and refines the chosen equilibrium constant accordingly. The discrepancy between the calculated and experimentally determined pH

value is minimised. The analytical mass balance equations usually employed are replaced by a general form which simply states that the analytical concentration of a given component is always balanced by its distribution in all the equilibrating species. BEST thus computes also the complete species distribution consistent with the current data base.

At this junction it is appropriate to mention the use of cation-selective glass electrodes which allow direct measurement of metal cation concentrations.[91,216,217] The emf of the electrode is directly proportional to the free cation concentration and thus, $E = E_0 + k \log[M^+]$, where the coefficient k is a constant which may be determined by appropriate calibration solutions and $[M^+]$ is the concentration of the *free* metal cation at equilibrium. Given the values of $[M^+]$, the stability constants for the formation of 1:1 complexes may easily be calculated. This ion-selective electrode technique for determining log K values was originally developed by Frensdorff.[218] Values for ΔH and ΔS of complexation may be determined by examination of a plot of $\ln K_s$ vs. $1/T$. The gradient of the line is equal to $-\Delta H/R$ and the intercept value is equal to $\Delta S/R$. Unfortunately, this method precludes the direct calculation of stability constants of ligands with calcium cations in organic solvents such as methanol, since the commercially available calcium ion-selective electrodes will not tolerate organic solvents to any extent. A competitive technique[142] utilising the sodium-selective glass electrode however, does enable the determination of the stability constants for calcium.

The selectivites of ion-selective, liquid-membrane electrodes may be determined both by single-solution and mixed-solution methods.[18,21,219,220] For example, to determine selectivity potentiometrically using the single-solution method, membranes containing the macrocyclic ligand are incorporated into electrode

modules with internal reference electrodes. Electrode potentials are measured on suitable cell systems and have been found to fit the expressions below, where the equations represent a determination of cation selectivity relative to lithium ion:

$$E_1 = E_o - 2.303\frac{RT}{F} \log A_{Li^+} \quad .. \quad .. \quad .. \quad 2.17$$

where E_1 is the electrode potential with a sample solution containing lithium ions only and A_{Li^+} is the activity of lithium ion.

$$E_2 = E_o - 2.303\frac{RT}{F} \log K.A_{M^{x+}}^{1/x} \quad .. \quad .. \quad .. \quad 2.18$$

where E_2 is the electrode potential with a sample solution containing M^{x+} ions only, $A_{M^{x+}}$ is the activity of M^{x+}, x is the charge on M, and K is the selectivity coefficient of M relative to lithium (K is unity for lithium and a value of K of less than one means lower selectivity). Activities may be calculated from the Debye-Hückel equation.

Combining equations 2.17 and 2.18 gives:

$$\log K = \frac{(E_2 - E_1)F}{2.303RT} - \log A_{M_{x+}}^{1/x} + \log A_{Li^+}$$

The mixed-solution method consists of measuring the electrode potentials for sample solutions containing both lithium ions and other alkali ions, M^{x+}, where the electrode potentials are given by:

$$E = E_o - 2.303\frac{RT}{F} \log (A_{Li^+} + K.A_{M^{x+}}^{1/x})$$

Combining this with equation 2.17 gives:

$$E_1 - E = 2.303\frac{RT}{F} \log \left[\frac{A_{Li^+} + K.A_{M^{x+}}^{1/x}}{A_{Li^+}}\right]$$

and re-arranging gives an explicit expression for K:

$$K = \frac{A_{Li^+} \cdot 10^{\left[\frac{(E_1-E)F}{2.303RT}\right]} - A_{Li^+}}{A_{M^{x+}}^{1/x}}$$

Thus, selectivity coefficients may be evaluated by measuring the potentials of a solution containing lithium ion only and of a mixed

solution containing equal concentrations of lithium ion and other alkali ion.

2.4.5 *Calorimetric Methods*

Log K values and reaction enthalpies may be determined by titration calorimetry[221] provided that the log K value is less than 5.5 and that the reaction enthalpy is non-zero. Ligand solutions may be titrated against metal ion solutions and usually the equilibrium shown in the equation below adequately describes the reaction in the calorimeter.

$$M^{x+} + L \rightleftharpoons ML^{x+}; \quad \beta_1 = K_1 = \frac{[ML^{x+}]}{[M^{x+}][L]}$$

Where the above equilbrium does not satisfactorily fit the data the equilibrium below may be considered:

$$M^{x+} + 2L \rightleftharpoons ML_2^{x+}; \quad \beta_2 = K_1K_2 = \frac{[ML_2^{x+}]}{[M^{x+}][L]^2}$$

A thermogram of the reaction is a plot of the heat produced in the reaction *versus* time, from which K and ΔH values may be obtained. It is found that the heat produced during the reaction, Q, is related to the reaction enthalpy, ΔH, by $Q_t = \Delta H \times \Delta_{nt}$, where Δ_{nt} is the number of moles of product formed at time t (heat of dilution corrections are made by titrating solutions of the ligand or metal ion into the solvent). It follows that Δ_{nt} is dependent on the stability constant of the reaction. However, if the temperature increase during the titration is small, the stability constant is effectively unchanged. The reaction enthalpy and stability constant may be determined from the titration data. For a simple 1:1 complex formation, the following equations indicate how such results may be obtained.

Consider equations 2.19 to 2.22:

$$Q_t = \Delta H \cdot [ML]_t \cdot V_t \quad .. \quad .. \quad .. \quad .. \quad 2.19$$

$$K = \frac{[ML]_t \cdot \gamma_{ML_t}}{[M] \cdot \gamma_{M_t} \cdot [L] \cdot \gamma_{L_t}}$$

$$= \frac{[ML]_t}{[M]_t [L]_t \cdot \Gamma_t} \quad .. \quad .. \quad .. \quad .. \quad 2.20$$

$$[M_{Total}]_t = [M]_t + [ML]_t \quad .. \quad .. \quad 2.21$$

$$[L_{Total}]_t = [L]_t + [AB]_t \quad .. \quad .. \quad 2.22$$

where Q is the heat produced in the calorimeter by chemical reaction,

V is the volume of solution in the calorimeter,

γ is the activity coefficient of the sub-scripted species,

Γ is the product of the activity coefficients of the products, and

t denotes at time t on the thermogram.

Combining 2.19, 2.20, 2.21, and 2.22 gives 2.23:

$$\frac{\Delta H}{K} = \frac{V_t \cdot [L_{total}]_t \cdot [M_{total}]_t \cdot \Gamma_t}{Q_t} \cdot (\Delta H)^2$$

$$- ([L_{Total}]_t + [M_{Total}]_t) \cdot \Gamma_t \cdot \Delta H + \frac{\Gamma_t Q_t}{V_t} \quad .. \quad .. \quad 2.23$$

If Γ_t is assumed to be known, there are only two unknowns, ΔH and K, and:

$$\Delta H/K = X(\Delta H)^2 + Y\Delta H + Z \quad .. \quad .. \quad .. \quad 2.24$$

where X, Y, and Z are the appropriate constants from 2.23.

Since K is a thermodynamic equilibrium constant, the quantity $\Delta H/K$ has the same value at any point on the thermogram provided that ΔH is independent of the ionic strength over the range of the titration.

Thus, 2.24 may be solved by combining any two points on the curve:

$$(D_2 - D_1)(\Delta H)^2 + (E_2 - E_1)\Delta H + (F_2 - F_1) = 0 \quad .. \quad .. \quad .. \quad 2.25$$

K can be calculated from equation 2.24 and ΔS° obtained from equations 2.26 and 2.27.

$$\Delta G^\circ = -RT \ln K_p \quad .. \quad .. \quad .. \quad 2.26$$

$$\Delta S^\circ = (\Delta H^\circ - \Delta G^\circ)/T \quad .. \quad .. \quad 2.27$$

The use of titration calorimetry for the determination of log K and

ΔH values for macrocyclic ligands with metal cations is well documented in the literature.[222-228]

CHAPTER THREE - HOMO- AND HETERO-DINUCULEATING SYSTEMS AND THE POTENTIAL ACTIVATION OF CARBON MONOXIDE MOLECULES BOUND BETWEEN TWO METAL CENTRES

The synthesis of macrocyclic ligands which may form homo-dinuclear or hetero-dinuclear complexes requires that *two* similar or dissimilar binding sites are incorporated into the ligand structure. As indicated in the introduction, the formation of dinuclear complexes may lead to many exciting areas of chemistry. At the outset of this work there existed a clear requirement for the development of dinuclear systems where the following criteria are met: a versatile ligand synthesis is available such that the ligand product is formed in multigram quantities; the hetero-dinucleating systems have *clearly* dissimilar binding sites; second and third row transition elements may be complexed; the chemical reactivity of the *isolated* complexes may be explored.

Reinhoudt *et al.*[229,230] have recently reported the synthesis and complexation of macrocyclic ligands (88) and (89) with two very different cavities combined within one molecule. The polyether cavity

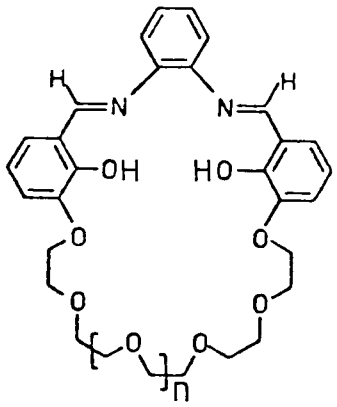

(88) n = 1

(89) n = 3

may bind hard cations and the *N,N'*-ethylenebis(salicylideneaminato) unit may bind softer cations such as Ni^{2+}, Cu^{2+}, and Co^{2+}. Reinhoudt[229] has isolated the hetero-dinuclear $Ni.Ba(ClO_4)_2$ complex of ligand (88). The X-ray structure determination[230] of the complex of (89) with the uranyl cation (UO_2^{2+}) bound to the Schiff base cavity and a urea molecule bound

to the polyether chain shows also that the urea is coordinated to the uranyl cation within the structure. The bond forms between a lone pair of electrons on the carbonyl oxygen and the uranium atom (C=O•••U). This work shows the potential of electrophilic centres present in macrocyclic cavities to aid the complexation of neutral molecules.

3.1 Homo- and Hetero-Dinucleating Ligand Systems

Ligands (15),[40] (90),[43] and (91) exemplify systems having clearly defined different hetero-dinuclear binding sites whereas ligand (92)[41] has two identical binding sites capable of forming homo-dinuclear complexes. Ligands (15), (90), and (92) have been shown to form

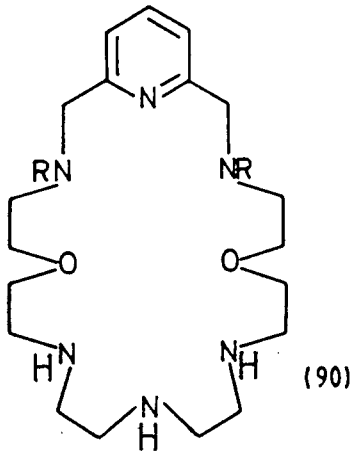

(90)

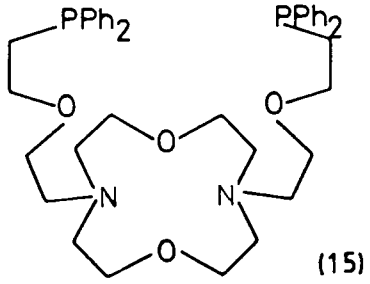

(15)

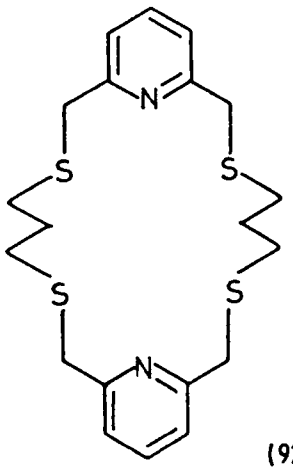

(92)

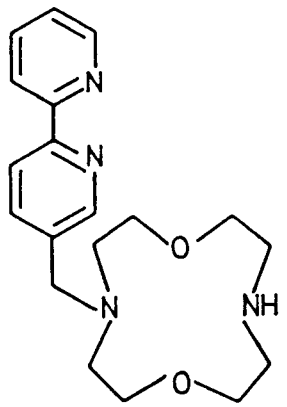

(91)

well-defined homo- or hetero-dinuclear complexes. In particular, the prior coordination of a hard cation to the hard binding site of (15) may be responsible for regulating the ligand structure and facilitating the subsequent complexations of a soft metal ion to the generated *cis*-diphosphine site.

The synthesis of (91) has been achieved (see Chapter Five) and a preliminary study of the binding properties has been undertaken. Clearly the ligand offers two dissimilar binding sites for complexation which may allow site selectivity. The bipyridine group may bind to a whole series of transition metal ions and the ring system is capable of binding to several metal cations such as Ag^{+}, Cu^{2+}, Ni^{2+}, and Na^{+}. Of particular interest is the potential study of electron transfer between the two metal cations and an exploration of possible *dinuclear* catalytic reactions. For example, ligand (91) should be capable of forming a mixed palladium(II)-copper(II) complex. Reaction of (91) with $PdCl_2(MeCN)_2$ may generate the $PdCl_2$(bipy) complex and subsequent addition of Cu^{2+} cations to the isolated palladium complex may generate the hetero-dinuclear compound. Electron transfer within the complex may be studied by cyclic voltammetry in the presence of halide anions or other potentially bridging ligands. Reaction of (91) with a rhodium species such as $Rh_2Cl_2(hexadiene)_2$ may give the corresponding rhodium(diene)(bipy) complex. This may be an active hydrogenation catalyst for ketone reduction.[231] The addition of lithium salts may alter the rates of hydrogenation and cooperative dinuclear effects may arise which can be detected by altering the conditions of the experiment, for example, by varying the acidity of the solvent.

The complexation chemistry of ligand (92) (see Chapter Six, Section 6.5) has been elaborated by studying the homo-dinuclear complex

formation with metals such as Ag, Pd, and Pt.

3.2 Dimetallic Activation of Small Substrate Molecules Bound between Two Metal Centres Held in Close Proximity

The activation of small substrate molecules may occur when they are bound between two metal centres within a single complex in which the two metal centres are held at a fixed distance apart. Such a system has the potential of displaying catalytic activity. In particular, the activation of a carbon monoxide molecule may occur which is discussed further in the proceeding paragraphs. The bond between the carbon of a carbon monoxide molecule and the metal atom within metal carbonyl complexes is characterised by two synergic effects:

(1) σ-donation from a σ-orbital of the carbon monoxide molecule to the metal centre; and

(2) π-donation from a π-orbital of the metal cation to a vacant π^*-orbital on the CO molecule (π back-bonding).

These effects are represented schematically below:

(1)

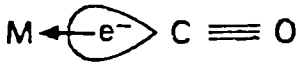

(2)

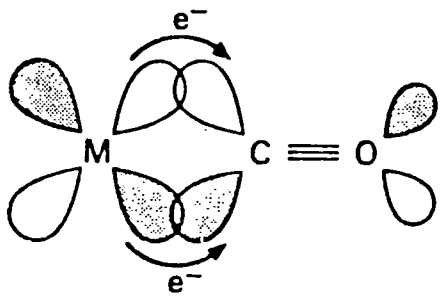

For neutral or cationic complexes, σ-donation may be the dominant bonding force which renders the CO molecule vulnerable to nucleophilic attack (Nuc^-) at the carbon atom, $Nuc^- \rightarrow M \overset{\delta-}{=} C^{\delta+} \equiv O$. If the metal centre is electron rich the dominating mode of bonding will be the π back-donation. The high charge density on the metal is delocalised towards the carbon monoxide molecule, $^{\delta+}M=C=O^{\delta-} \rightarrow E^+$. This electron density shift will be accompanied by a decrease in the bond-order between the carbon and oxygen atoms, that is, an increase in the CO bond length and a decrease in the vibrational frequency of absorption υ(CO) in the infrared. Such carbonyls are then susceptible to electrophilic attack at the oxygen atom by electrophiles, E^+.

Thus, metal carbonyl complexes have a bifunctional activation process. They may be activated to reaction at the carbon centre or at the oxygen centre. In particular, the polarity of the bound carbon monoxide molecule may be increased by the addition of an electron acceptor (*e.g.* M^+) which binds to the oxygen of the carbon monoxide molecule to enhance the susceptibility of the carbon atom to nucleophilic attack.

$$M{-}C^{\delta+} \equiv O^{\delta-} \cdots\cdots M^+$$

The presence of the electrophilic group attached to the oxygen will have the effect of lowering the HOMO(σ) and LUMO(π^*) molecular orbital energies of the carbon monoxide molecule (see Figure 3.1).

The σ-donating contribution to the metal-carbon bond may become weaker but the CO molecule may become better able to accept π-electron density. A strong displacement of charge density onto the oxygen atom from the carbon of the carbon monoxide may thus occur, rendering the carbon atom very susceptible to nucleophilic attack.

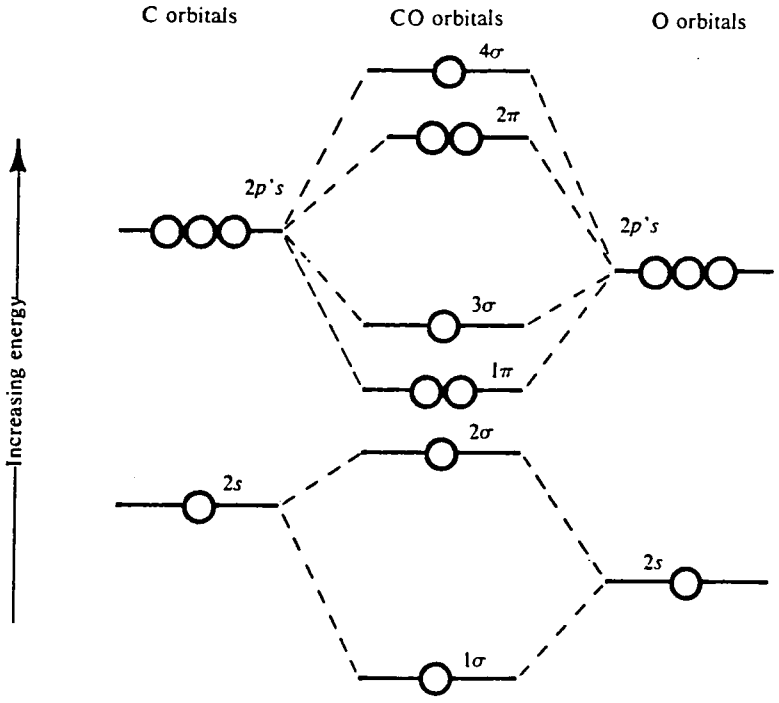

Figure 3.1

Relative orbital energies in carbon monoxide.[232] *The electronic configuration is* $(1\sigma)^2(2\sigma)^2(1\pi)^4(3\sigma)^2$

The effects of coordination of an electrophile to the oxygen of a bound carbonyl group may be summarised briefly: the delocalisation of charge density from the carbon to the oxygen centre is favoured; the energy of the vacant π^*-orbital of the carbon monoxide ligand is lowered which grants easier formation of a transition state; the bond-order of the CO entity is also weakened which brings it closer to the bond-orders of likely reaction products, for example, CH_3OH or H_2CO.

The types of reactions which may be catalysed by these interactions are nucleophilic attack at the carbon atom, insertion of the CO group by migration, and a breaking of the carbon-oxygen bond. Activation of a CO ligand is generally accepted to be demonstrated when the vibrational frequency υ(CO) is considerably lowered (approximately 100-200 cm^{-1}).

3.3 Examples of Dimetallic Activation of Carbon Monoxide

Many studies have indicated that the insertion of a carbon monoxide ligand between a metal atom (M) and an alkyl group (R) may occur accompanied by the addition of another ligand (L'). Such a reaction is represented below:

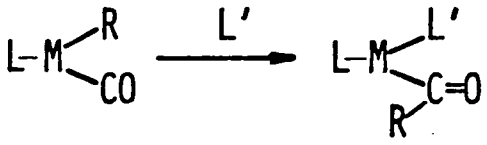

It was first reported by Collman[233] that such a reaction could be greatly enhanced by electrophilic attack on the oxygen of the carbon monoxide. The presence of small cations such as lithium or sodium enhances the migration of carbon monoxide in the complex $Fe(CO)_4R^-$. Lithium ions enhance the reaction rate more than do the sodium ions. Moreover, the addition to the reaction mixture of a ligand which binds to the alkali cation (for example, a crown ether) suppresses this increase in reaction rate. Other complexes of the same type [$Na^+ Mn(CO)_5^-$, $Na^+ Mn(CO)_4PPh_3^-$, and $Na^+ HFe(CO)_4^-$] were shown to have significantly lower frequencies of vibration for the CO ligand bound to the metal cation than those for the same complexes with crown ethers added.[234]

However, the activation of a carbon monoxide ligand bound to a metal cation may be increased further by an attack on the oxygen atom by a strong Lewis acid such as an aluminium trihalide. Insertion of a CO molecule occurs very quickly and occurs without the acompanying addition of an extra ligand,[235] as outlined in the following equation:

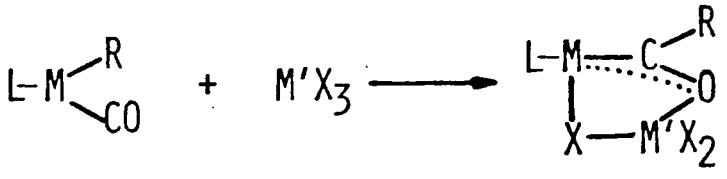

The strong Lewis acid fulfils three rôles: it increases the rate of insertion of the CO molecule, helps to stabilise the acyl group, and it replaces the extra ligand required for reaction when a weak Lewis acid is utilised. The binding of the aluminium atom to the carbonyl oxygen has been clearly demonstrated by the isolation and crystal structure determination of the intermediate formed in the reaction between $Mn(CH_3)(CO)_5$ with $AlBr_3$.[235] (see Figure 3.2).

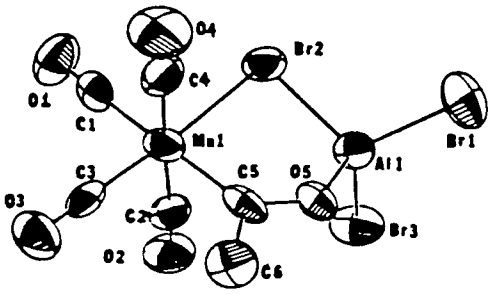

Figure 3.2

X-Ray crystal structure of a Mn-Al(III) hetero-dinuclear complex

Other metals such as zirconium[236] and titanium[237] have also been used to activate carbon monoxide. For eample, reaction of $(\eta^5\text{-}C_5H_5)_2Zr(IV)Me_2$ with $(\eta^5\text{-}C_5H_5)Mo(II)(CO)_3H$[236] yields methane and the hetero-dinuclear complex $(\eta^5\text{-}C_5H_5)_2ZrMeMo(CO)_3(\eta^5\text{-}C_5H_5)$. (Figure 3.3).

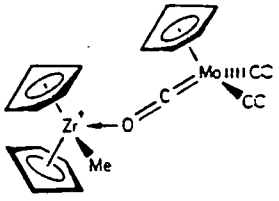

Figure 3.3

Schematic representation of the hetero-dinuclear complex $(\eta_5\text{-}C_5H_5)_2ZrMeMo(CO)_3(\eta_5\text{-}C_5H_5)$ *in which a carbonyl is bound through the carbon and oxygen sites.*

In the infrared, the two terminal carbonyls absorb at 1948 and 1863 cm^{-1} whereas the third carbonyl which bridges between the two metal centres absorbs at 1545 cm^{-1}. The analogous titanium/molybdenum complex[237] has a bridging carbonyl which has a stretching frequency of 1623 cm^{-1}. The structure of both complexes has been determined using X-ray crystallography.

During the course of our studies, Lehn[70] reported the synthesis of a series of ligands (21) to (23) which incorporate both a soft, redox-active, binding site (NS_2 chelate) and a hard Lewis acid centre (azaoxamacrocycle). The ligands were reacted with $Rh_2Cl_2(CO)_4$ in

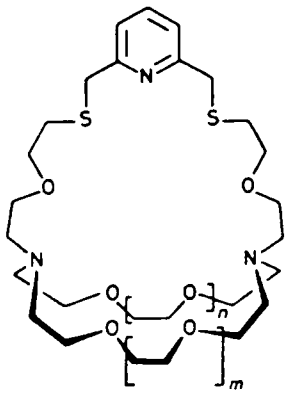

(21) m = n = 0

(22) m = 1, n = 0

(23) m = n = 1

methanol solution to give haptoselective, 1:1 complexes containing the $(Rh(CO))^+$ unit bound to the *soft* NS_2 sub-unit in a square-planar coordination. The expected orientation of the carbonyl group towards the *hard* macrocyclic sub-unit suggests the possible activation of the carbonyl ligand by the formation of appropriate hetero-dinuclear cryptates. The additions of Li^+ and Zn^{2+} to (21), Ag^+, La^{3+}, and Al^{3+} to (22), and Ag^+, Ba^{2+}, and Cd^{2+} to (23) were investigated by ^{13}C NMR and by IR. The shifts of the CH_2 NMR signals were consistent with the formation of hetero-dinuclear complexes as represented by (93). The ^{13}C

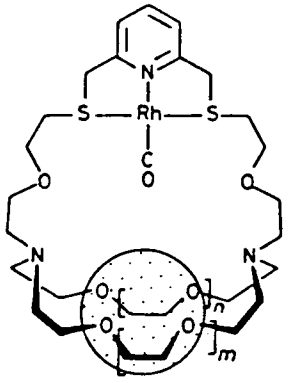

(93)

NMR parameters of the ^{13}CO groups were little affected by the binding of the second cation and the vibrational frequency $\nu(CO)$ was unchanged. This suggests little activation of the CO group. It is likely that either the metal-metal distance is too great for activation of substrates bound to the one metal centre or the orientation of the CO group is not appropriate for interaction with the second metal cation as anticipated by Lehn. This work was published during our study of the reaction of ligands (94) to (96) and related compounds with $Rh_2Cl_2(CO)_4$.

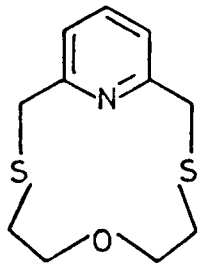

(94)

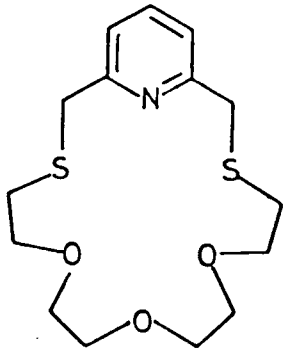

(95)

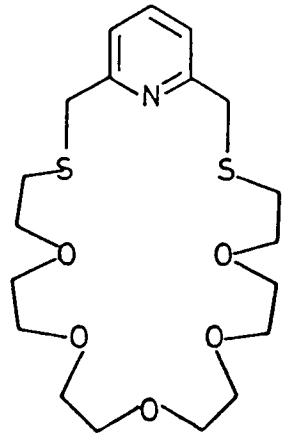

(96)

It was hoped to activate a carbon monoxide molecule bound to rhodium by the addition of Li^+ to (95) and K^+ to (96). The distance between the metal centres should be less than in Lehn's cryptands (see Chapter Six).

CHAPTER FOUR - SYNTHESIS AND COMPLEXING STUDIES OF MACROCYCLIC LIGANDS WITH THE ALKALI AND ALKALINE EARTH METAL CATIONS

4.1 Introduction

As has been indicated in the previous chapters, this work on the synthesis and cation complexing properties of a series of macrocyclic ligands has been in part stimulated by the work of Dale.[123,124] The stability of the calcium complex of ligand (85)[123] in methanol-water (9:1) is very high (log K = 6.9; pH-metric titration) and when reported, the complex was the most stable calcium complex known for an uncharged monocyclic ligand. Further, the ratio of the stability constants of the calcium and sodium complexes was 2000, promising a selectivity for calcium ions over sodium ions. The tetraaza-12-crown-4 analogue with four 2-hydroxyethyl side-arms (97)[238] also forms strong 1:1 complexes with calcium ions. The complexation properties of ligand (97) were

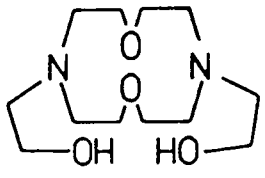

(85)

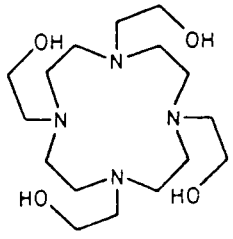

(97)

studied in DMF solution by titration with dry calcium *bis*(toluene-4-sulphonate), monitored by ^{13}C spectroscopy. The slow-exchange spectrum at 298 K of a 1:1 mixture of the complexed and free ligand indicated strong complexation. The signals did not coalesce even at 399 K implying a decomplexation barrier higher than 84 kJ mol^{-1}. The rate of exchange will of course be crucially dependent upon the solvent in which

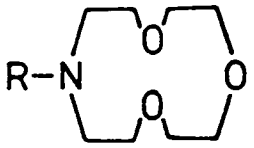

(100) R = H

(101) R = Me

(102) R = CH_2Ph

(103) R = CH_2CH_2OMe

(104) R = CH_2CONH_2

(105) R = Ph

(106) R = CH_2CH_2OH

(107) R = CH_2COOEt

the complex is dissolved. Dale[124] also reported the cation complexing properties of a series of macrocycles (101) to (107) derived from the monoaza-12-crown-4 compound (100)(discussed in Section 2.4.1). Compounds (102) to (107) were conveniently prepared by condensing the appropriate primary amine with the diiodo-compound 1,11-diiodo-3,6,9-trioxaundecane (99) in acetonitrile solution containing dispersed sodium carbonate, according to the equation below:

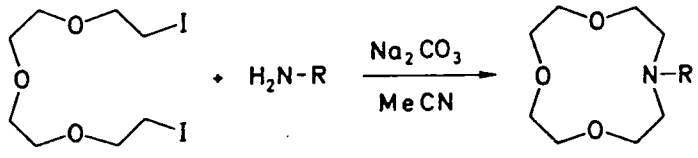

(99) (102) to (107)

The unsubstituted compound (100) and the *N*-methyl derivative (101) were obtained from the *N*-benzyl derivative (102) since the volatility of ammonia and methylamine precluded their use in the reaction represented above.

This work set out to synthesise and study the complexation of ligands (106) to (116). The series of macrocycles examined by Dale has

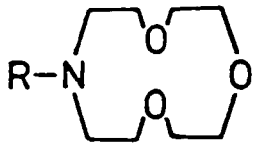

(106) R = CH_2CH_2OH
(107) R = CH_2COOEt
(108) R = CH_2COOH
(109) R = CH_2CH_2COOMe
(110) R = CH_2CH_2COOH
(111) R = CH_2CONMe_2

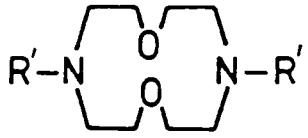

(112) R' = H
(113) R' = CH_2CH_2OH
(114) R' = CH_2CONMe_2
(115) R' = $CH_2CH_2CONMe_2$

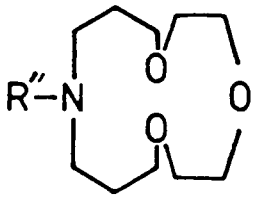

(116) R'' = CH_2CH_2COOMe

thereby been extended. Ligands (106) to (111) are *N*-substituted derivatives of monoaza-12-crown-4 each containing an additional binding group on the side-arm. Ligands (113) to (115) are also 12-membered ring structures containing two side-arms attached to the ring *via* nitrogen atoms, with one additional binding group on each arm. These ligands thus have six potential binding sites. Ligand (116) is a 14-membered ring containing just one side-arm incorporating a binding site. The intention was to examine the effect of an increase in polarity of the donor groups on the side-arms, in particular by the incorporation of amide groups. The amide carbonyl is anticipated to have greater electron density located on the oxygen than an ester carbonyl oxygen or an alcohol oxygen and thus to be a stronger σ-donor, capable of binding more strongly to cations with high charge density (*e.g.* Li^+, Ca^{2+}). The electrostatic interaction energy between a donor atom and a cation is determined by ion-dipole, ion-quadrupole and ion-induced dipole interactions.[239] Thus a consideration of the dipole moments of simple

carbonyl species will give a measure of the contribution of the interaction between cation and carbonyl donor to the stability of the complex (all other factors being equal). Relevant gas-phase dipole moments (D): DMF (3.82), HCO_2Me (1.77), HOMe (1.70), HCO_2H (1.41), and $HCONH_2$ (3.73) indicate that the amide carbonyl has the highest charge density on oxygen. A preference for amide donors to Na^+ has also been demonstrated.[240] The series of cycles studied also allows an examination of the effect of the length of the side-arm on complexation: one carbon in the alkyl chain attached to the nitrogens of the two-armed amides generates 5-ring chelates upon metal complexation, and two carbons in the chain generates the less entropically favoured 6-ring chelates. The number of side-arms and thus the number of potential donor atoms (five or six) and the size of the macrocyclic ring may also be examined.

4.2 Synthesis of the Ligands

Those ligands (106), (107), (112), and (113) previously studied by Dale[123,124] were made according to his methods but were purified using different techniques. For completeness, the synthesis of all the ligands used in this study (106) to (116) are described hereafter and the various purification techniques applied are discussed.

The *N*-substituted derivatives of monoaza-12-crown-4 (106), (107), and (109) were prepared by the reaction of the diiodide, 1,11-diiodo-3,6,9-trioxaundecane (99) with the appropriate primary amine in dilute acetonitrile solution containing suspended sodium carbonate powder (Scheme 4.1). The diiodide (99) was prepared from the corresponding dichloride of tetraethylene glycol (98) by heating under reflux in acetone in the presence of NaI and was used as the crude

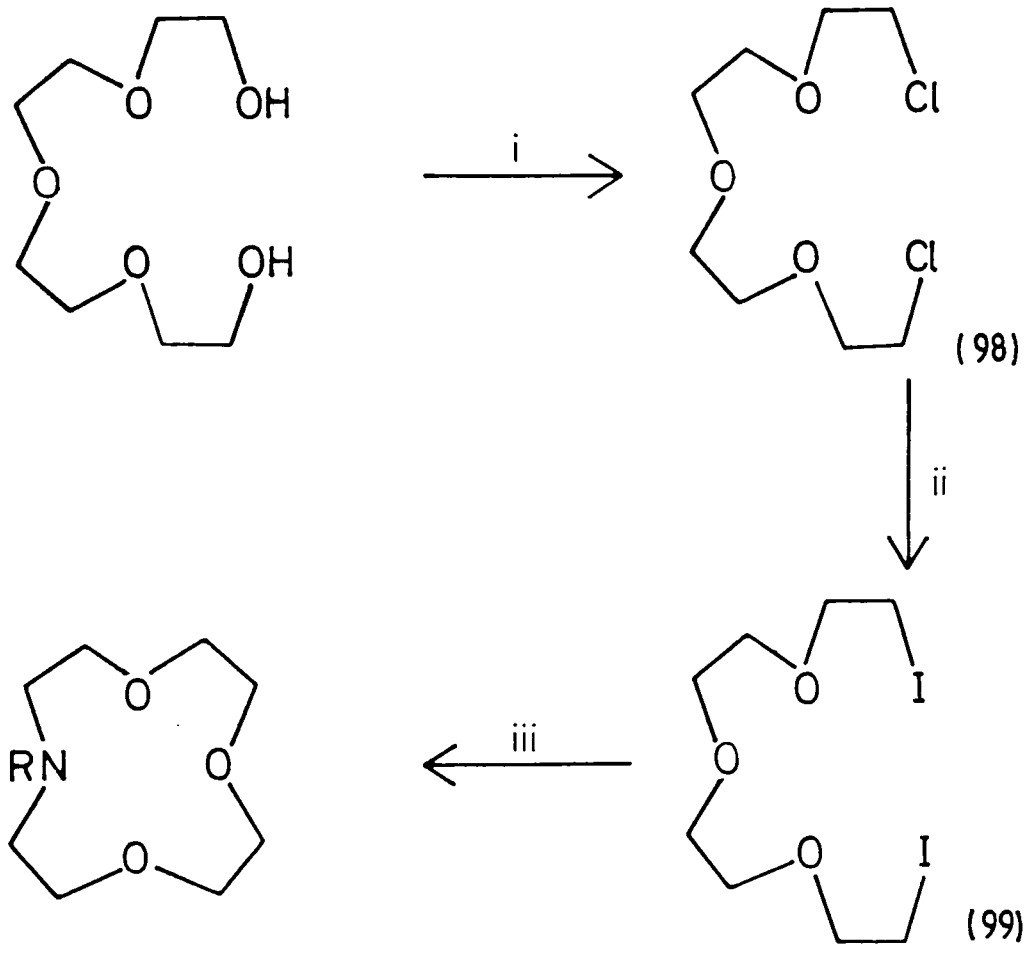

(106) R = CH_2CH_2OH

(107) R = CH_2COOEt †

(109) R = CH_2CH_2COOMe †

Scheme 4.1

i, $SOCl_2$, pyridine; *ii*, NaI, acetone; *iii*, RNH_2, Na_2CO_3, MeCN.

†Substrate used as hydrochloride.

product. The dichloride (98) was prepared from tetraethylene glycol by reaction with sulphonyl chloride at 0^o and was purified by distillation (Scheme 4.1). Purification of the ligands (106) and (107) was effected by chromatography on alumina in contrast to the method of Dale who purified them by distillation. Ligand (109) was crystallised from cold propan-2-ol as the hydrochloride salt and was washed thoroughly with

cold propan-2-ol. The free ligand was obtained by treatment of the salt with tetramethylammonium hydroxide in dichloromethane solution and was purified by passage through alumina. The carboxylic acids (108) and (110) were obtained by heating the corresponding esters under reflux in concentrated hydrochloric acid (Scheme 4.2).

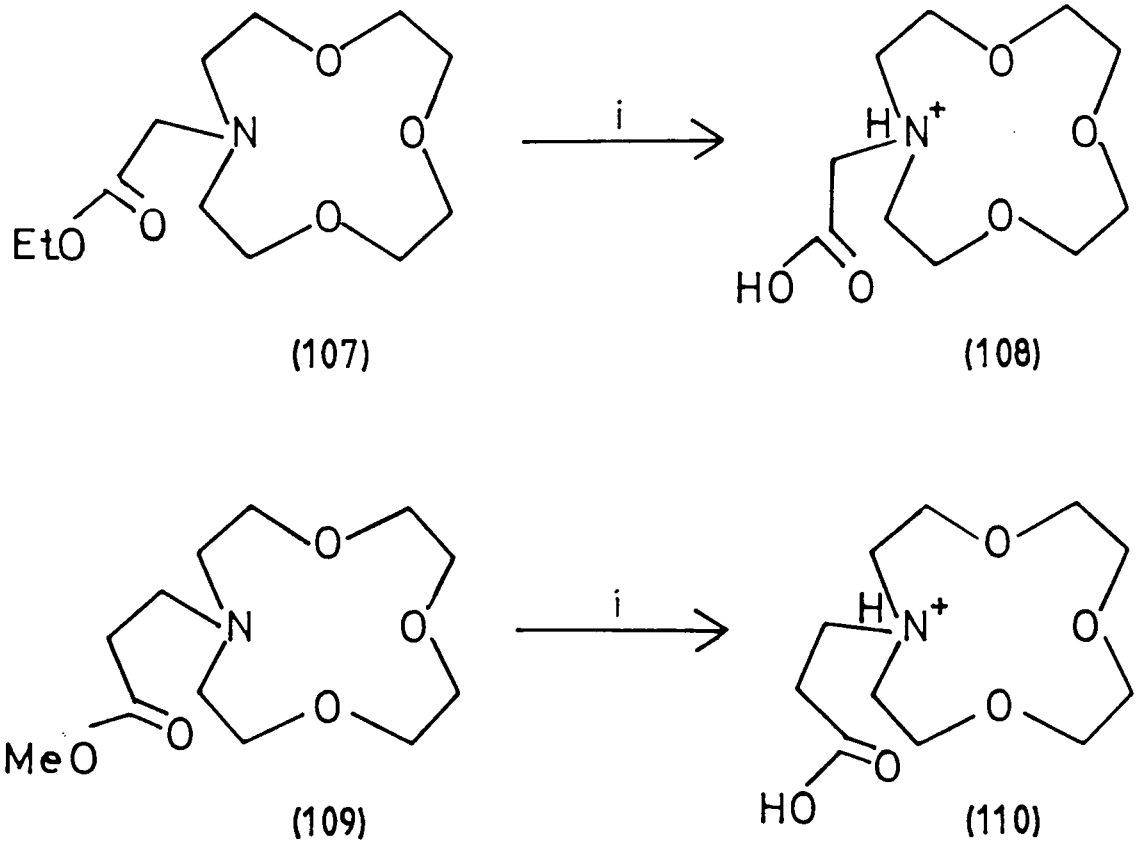

Scheme 4.2

i, Conc. HCl, Δ.

The use of benzylamine as the primary amine in the reaction with the diiodo compound (99), resulted in the formation of 10-benzyl-1,4,7-trioxa-10-azacyclododecane (102).[124] The *N*-benzylmonoaza-12-crown-4 derivative may be purified by distillation[124] or by passage through alumina to give a colourless oil. The pure *N*-benzyl derivative may then be converted into the parent azacrown (100) by hydrogenolysis in acetic acid containing 10% palladium on activated carbon catalyst. This hydrogenolysis proved very difficult to accomplish and it was found that the reaction proceeded only when Analar acetic acid-distilled water (1:1) was used as solvent. Unfortunately, this reaction proved to be difficult to reproduce. The reaction conditions were varied starting from the conditions stipulated by Dale[124] (60^{o}, 3 atmospheres of hydrogen, 15 h) and thereafter examining the effect of increasing the temperature or increasing the pressure of hydrogen, lengthening the reaction time, or varying the solvent composition. The desired product from the hydrogenolysis reaction may be heated under reflux with *N*,*N*-dimethylbromoacetamide in acetonitrile in the presence of anhydrous sodium carbonate to form the monoaza- macrocycle with amide functionality on the side-arm (111). Ligand (111) was also purified by chromatography on basic alumina. This reaction sequence is represented in Scheme 4.3.

The 14-membered ring analogue (116) of the methyl ester compound (109) was prepared using analogous reaction conditions. Dale's condensation reaction with the primary amine hydrochloride, 3-aminomethylpropanoate hydrochloride and the diiodide compound, 1,13-diiodo-4,7,10-trioxatridecane (119) using sodium carbonate as a template in acetonitrile solution yielded the 14-membered macrocycle as an orange oil which was purified by passage through basic alumina.

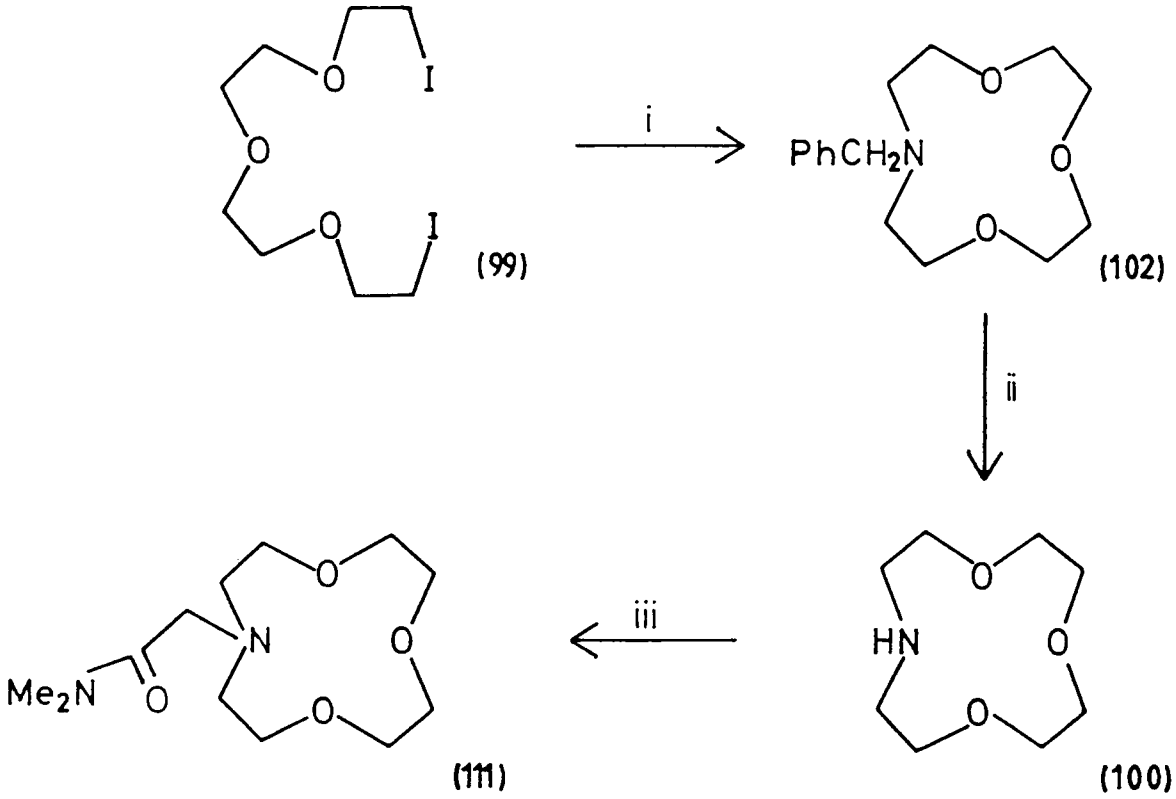

Scheme 4.3

i, $PhCH_2NH_2$, Na_2CO_3, MeCN; *ii*, H_2, 10% Pd, AcOH-H_2O; *iii*, *N*,*N*-dimethyl-bromoacetamide, Na_2CO_3, MeCN.

Compound (119) was prepared from the corresponding dichloride compound (118) by heating under reflux in acetone in the presence of NaI. The dichloride (118) was in turn prepared from the corresponding diol (117) which was formed from propan-1,3-diol. Sodium metal was added to an excess of propan-1,3-diol to form the mono-alkoxide and diethyleneglycol ditosylate was added to this solution. The resulting mixture was heated at 110^{o} for 18 h. It was important that the temperature did not exceed 110^{o} otherwise oligomeric products formed giving rise to a dark tar-like material. The reaction sequence for the formation of the 14-membered macrocycle is given in Scheme 4.4.

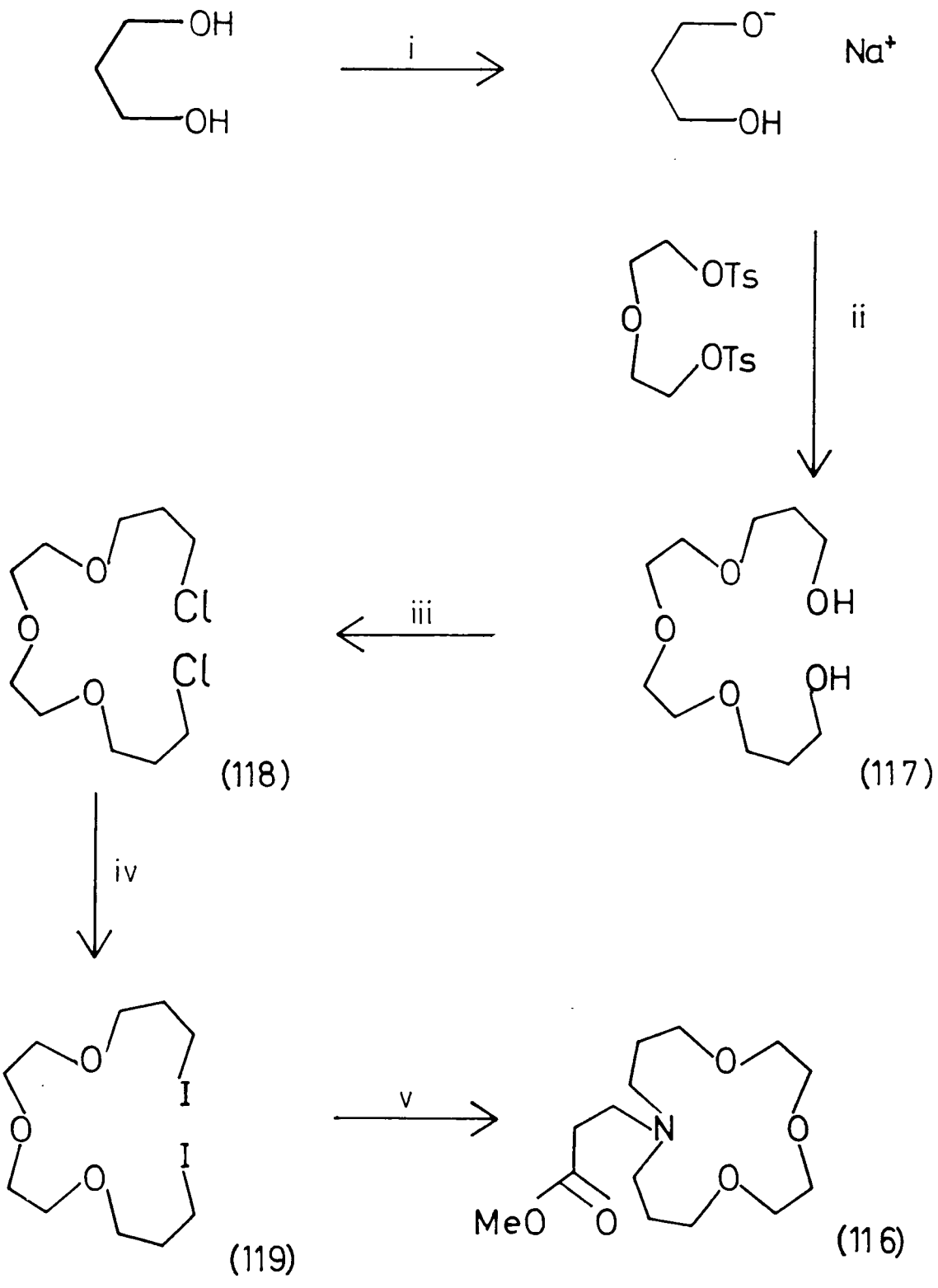

Scheme 4.4

i, Na, N_2, Δ; *ii*, N_2, 18 h, Δ; *iii*, $SOCl_2$, pyridine; *iv*, NaI, acetone; *v*, $MeOOCCH_2CH_2NH_3^+$ Cl^-, Na_2CO_3, MeCN.

The diaza 12-membered ring structures containing two side-arms (113) to (115) were obtained from the same precursor, (112) [≡ (84)]. Compound (112) was formed using a series of well-established reactions,[123] represented in Scheme 4.5. The disodium salt of *N,N'*-ditosyl-2,2'-diaminodiethyl ether (122) and diethylene glycol ditosylate (123) were condensed in DMF to give 4,10-di-4-toluene-sulphonyl-1,7-dioxa-4,10-diazacyclodecane (124). Acid hydrolysis removed the tosyl protecting groups and the secondary amine (112) was isolated by passage through an anion-exchange column. The residual orange gum was crystallised from a hot toluene-hexane mixture. Diethyleneglycol ditosylate (123) was formed from diethyleneglycol and tosyl chloride in pyridine at 0^{o}. The disodium salt of *N,N'*-ditosyl-2,2'-diaminodiethyl ether (122) was formed from the dichloride of diethylene glycol in three stages. Reaction with potassium phthalimide in DMF gave the 2,2'-(diphthalimido)ethyl ether (120). This was treated with hydrazine hydrate in ethanol at 20^{o} followed by the addition of concentrated hydrochloric acid at 0^{o} which gave the bis-ammonium salt (121). The final step involved the addition of tosyl chloride to (121) in a mixture of sodium hydroxide solution and ether. Vigorous agitation ensured complete reaction. The crude bis-aminotosylate was isolated and crystallised from toluene-chloroform (1:1) mixtures before being converted into the required sodium salt (122). This step was performed immediately before the cyclisation reaction.

Ligands (113) to (115) were formed from the unsubstituted diazamacrocycle (112) in one-stage reactions (Scheme 4.6). Hydroxyethylation with ethylene oxide in aqueous methanol at 0^{o} gave the dihydroxy species (113), synthesised in accordance with the method of Dale.[123] The two-armed amide compound with the shorter side-arms,

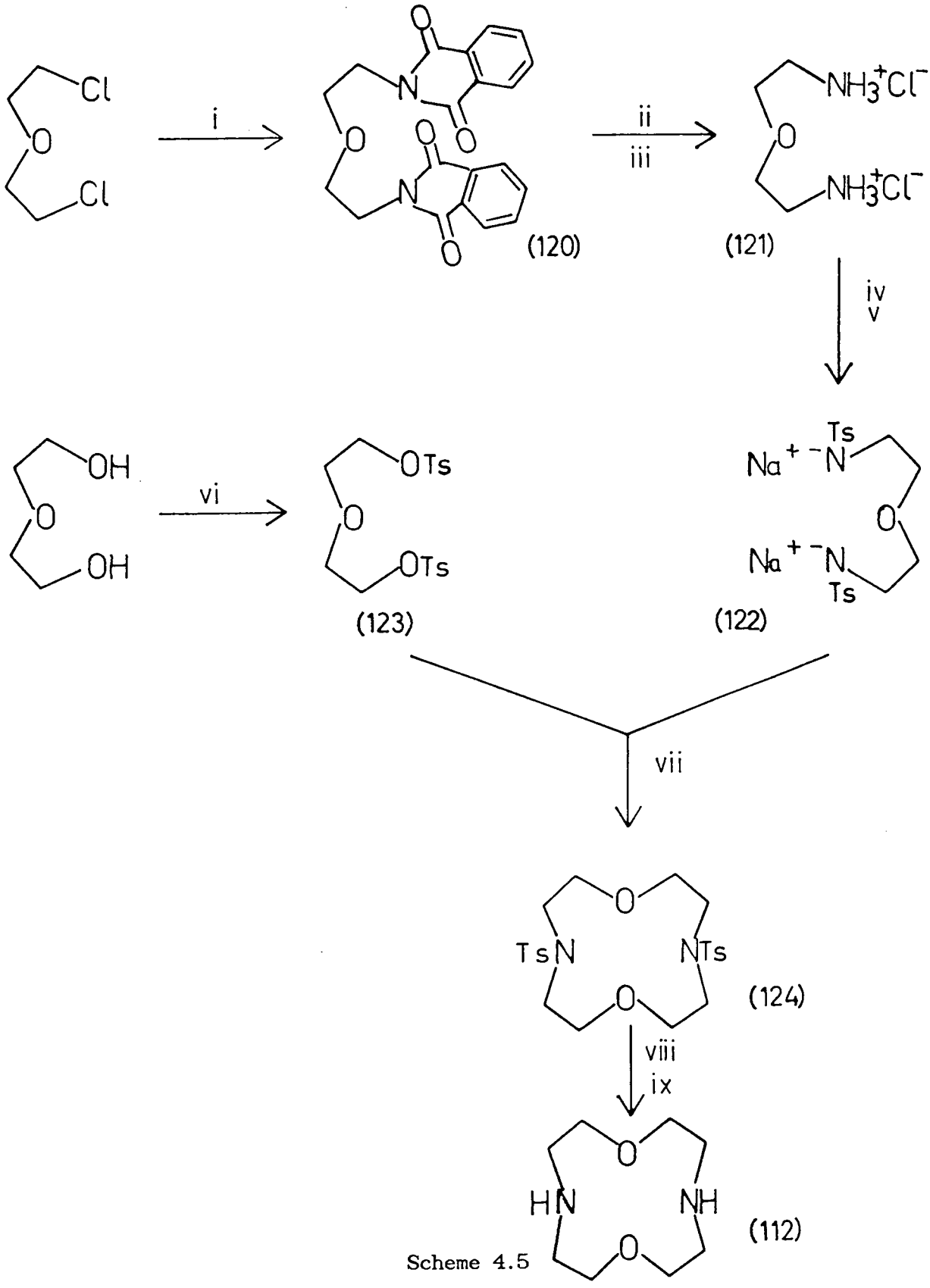

Scheme 4.5

i, potassium phthalimide, DMF, Δ; *ii*, N_2H_4, EtOH; *iii*, HCl, H_2O; *iv*, TsCl, NaOH; *v*, Na, MeOH; *vi*, TsCl, pyridine, 0^o; *vii*, DMF, 80^o; *viii*, HBr, AcOH, PhOH; *ix*, ion-exchange.

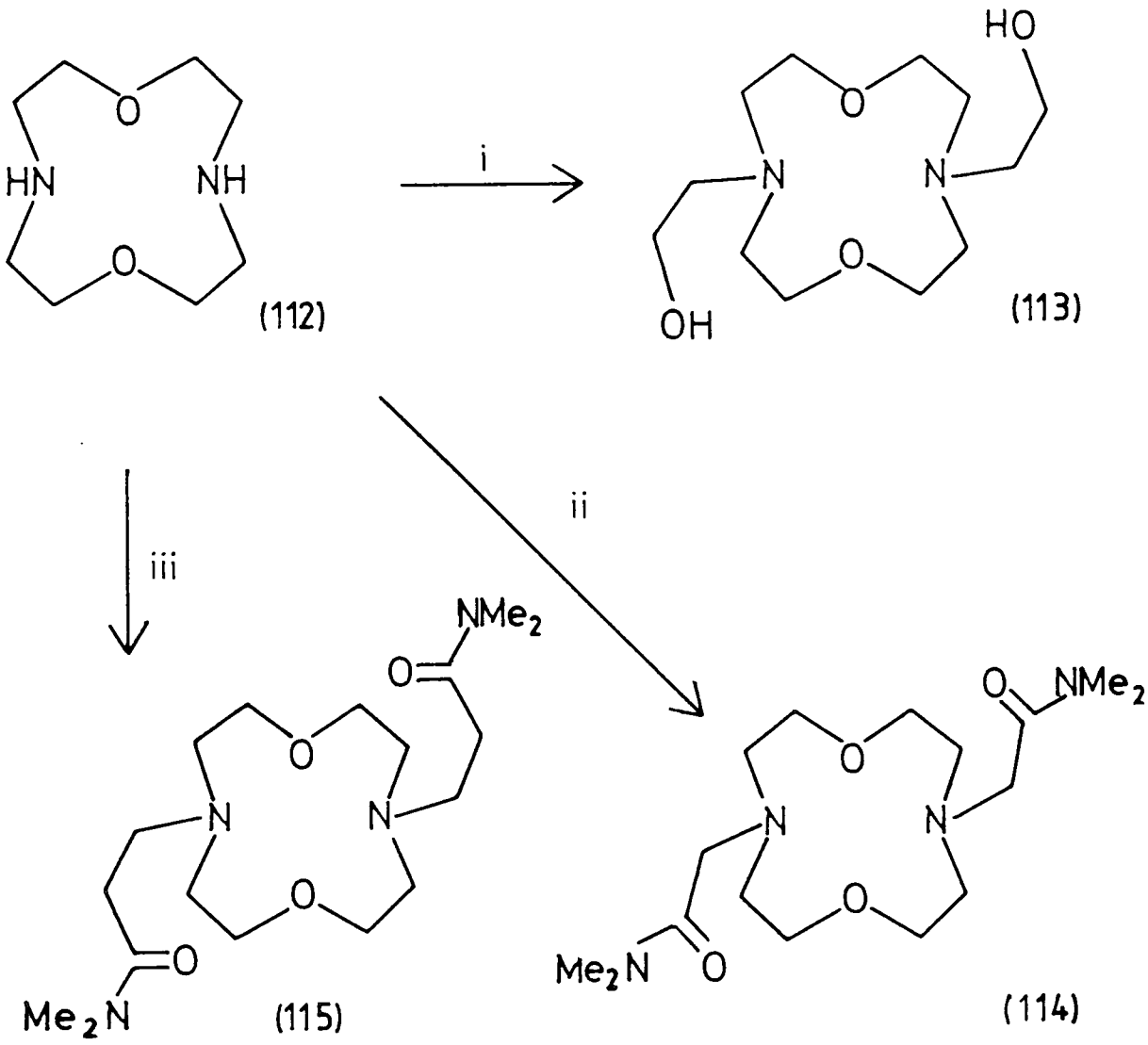

Scheme 4.6

i, ethylene oxide, methanol, 0°; *ii*, *N*,*N*-dimethylbromoacetamide, Na_2CO_3, MeCN; *iii*, *N*,*N*-dimethylpropenamide, MeOH, Δ.

4,10-bis(*N*,*N*-dimethylethanamide)-1,7-dioxa-4,10-diazacyclododecane (114) was prepared by reaction of (112) with *N*,*N*-dimethylbromoacetamide in acetonitrile solution in the presence of anhydrous sodium carbonate powder. *N*,*N*-Dimethylbromoacetamide[241] was prepared by the gradual addition of bromoacetylbromide to a solution of dimethylamine hydrochloride in an aqueous sodium hydroxide (20% *w*/*v*)-ethylene

dichloride (2:3) mixture. The reaction mixture was maintained at -10^{o}. Less rigorous reaction conditions led to problems such as the amination of the alkyl group by S_N2 displacement of the bromine atom. The macrocyclic diamide (114) was purified by chromatography on alumina and washed with acid and base. The two-armed amide compound with the longer side-arms, 4,10-*bis*- (*N*,*N*-dimethylpropanamide)-1,7-dioxa-4,10-diaza-cyclododecane (115) was prepared by the conjugate addition of *N*,*N*-dimethylpropenamide to (112) in methanol: heating under reflux for 2 h ensured complete reaction. The residue was purified by passage through an alumina column to give a pale yellow oil which was crystallised from hot toluene with a trace of ether present to give colourless plate crystals of the required compound (115). The molecular structure of the ligand is shown in Figure 4.1 and the pertinent crystal data are given in Chapter Seven.

The crystal structure determination revealed that the ligand has a centre of inversion and that the hydrogens on the *N*-methyl C(13) [and therefore on C(13^{*})] are disordered over two sites with 0.5 occupancies. The twelve-membered diamine macrocycle adopts a predictable and well-defined 'square' [3333] conformation,[146,147] with 'corners' at C(2), C(5), C(2^{*}) and C(5^{*}) (Figure 4.2): corners are identified using the rules for corner definition adumbrated by Boeyens and Dobson.[147] Stereochemical descriptions of all macrocycles in the remainder of this work are based on this classification scheme. The substituents on the amino nitrogens predispose the ligand into this *endo-endo* conformation as required for rapid metal complexation with a minimal conformational change in the ligand: the lone pairs of electrons on the nitrogens are appropriately oriented for binding to a cation sitting on top of the [12]-ring cycle. The two side-arms sit over and beneath the macrocyclic ring as

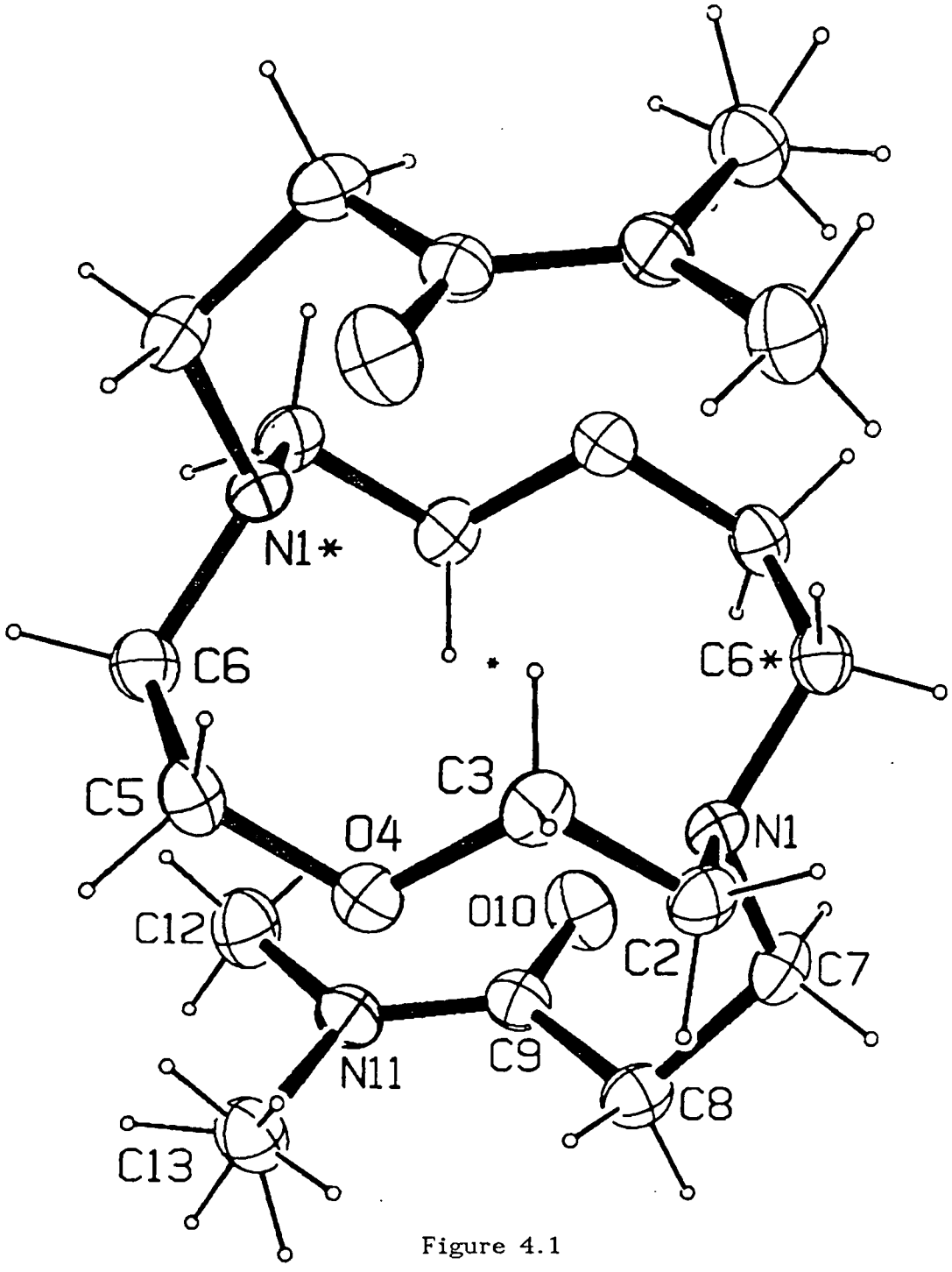

Figure 4.1

ORTEP drawing of molecular structure of ligand (115)

Selected bond lengths (Å) and angles (°): N(1)-C(2) 1.457(3), N(1)-C(6*) 1.461(3), N(1)-C(7) 1.455(3), C(2)-C(3) 1.503(3), C(3)-O(4) 1.416(3), O(4)-C(5) 1.421(3), C(5)-C(6) 1.503(4); C(2)-N(1)-C(6*) 1.457(3), C(2)-N(1)-C(7) 1.457(3), C(6*)-N(1)-C(7) 1.457(3), N(1)-C(2)-C(3) 1.457(3), C(2)-C(3)-O(4) 1.457(3), C(3)-O(4)-C(5) 1.457(3), O(4)-C(5)-C(6) 1.457(3).

The * refers to the atom at equivalent position -x, -y, -z.

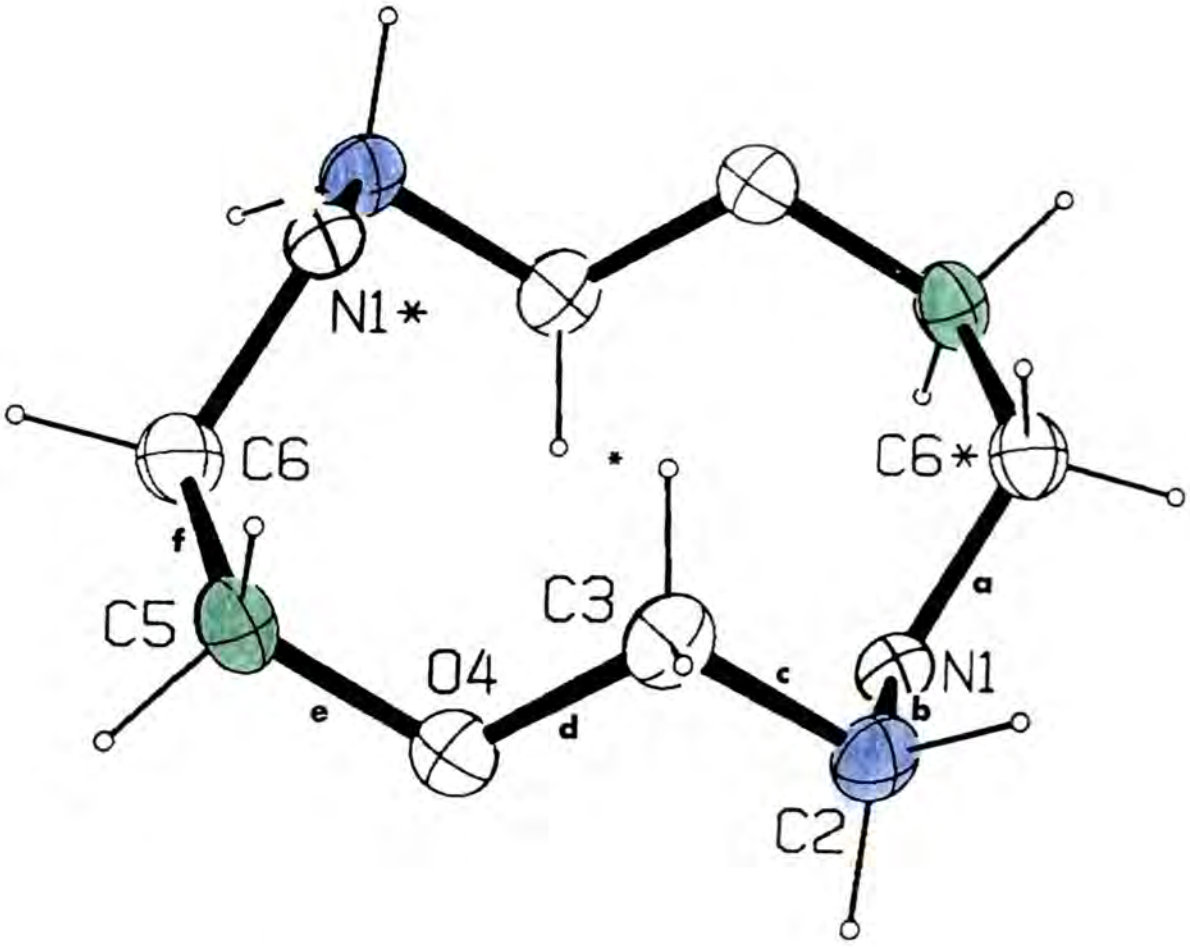

a, -147.4; *b*, 86.0; *c*, 76.6; *d*, -165.5; *e*, 93.8; *f*, -76.3.

Figure 4.2

Torsion angles (°) *for ligand* (115) *showing Dale-type corners* (shown in blue) *as well as the additional corners defined by Boeyens and Dobson* (shown in green).[147]

anticipated, enabling the carbonyl oxygen atoms O10 and O10* to participate in binding to complexed metal cations.

4.3 NMR Experiments

The complexing properties in d_4-methanol solution of some of the mono- or di-substituted azacyclododecanes (109)-(111), (114) and (115) and the mono-substituted azacyclotetradecane (116) were studied by

titration with solid alkali salts (LiCl and $CaCl_2$). Complexation was monitored by examining the ^{13}C NMR shift of the ligand resonances. In most cases an averaged resonance signal was observed (fast exchange), though for ligands (114) and (115) with $CaCl_2$ discrete lines for the free ligand and the complexed ligand were found (slow exchange). An estimate of the stoichiometry of the complexes formed may be gauged from the position of the curve bend (origin of curve detailed in Section 2.4.1). In addition the deviation from a sharp bend may give a qualitative idea of the *strength* of the complex formed, assuming that the limiting chemical shift is the same in 1:1 as in 2:1 complexes of the same cation. The addition of increasing amounts of LiCl to solutions of (109) and (116) in methanol showed only very small shift differences (Figure 4.3). Ligand (110) showed no detectable shift differences in any of the ^{13}C resonance signals. The complexation constant for ligand (116) with LiCl is therefore likely to be very low ($\log K \simeq 1$) and the complexation constant for ligand (109) with LiCl is unlikely to be much greater ($\log K < 3$). The complexation of ligand (116) with LiCl is clearly significantly weaker than that observed for ligand (109) with LiCl. The complex between ligand (116) and LiCl will involve two six-ring chelates which should be favourable for binding a small lithium cation. The hydrogen atoms in the trimethylene chains should be able to adopt the energetically more favoured staggered conformation.[151] However, the two six-ring chelates are adjacent to one another which may increase steric crowding in the metal's coordination sphere due to the extra methylene groups. The extra van der Waals repulsions induced between the methylene chains of the ligand may override the favourable energy changes caused by the hydrogens being able to adopt staggered conformations.[151]

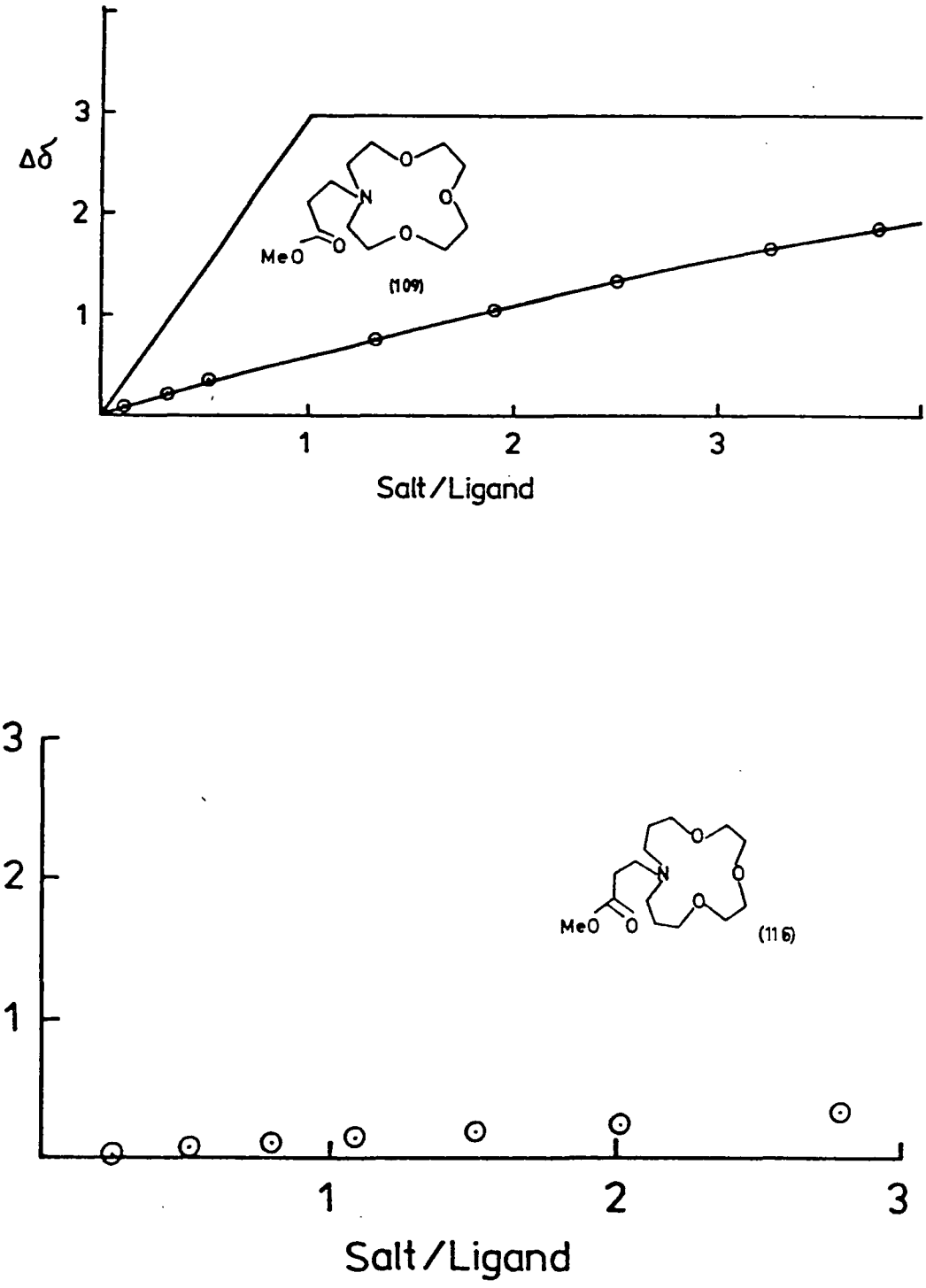

Figure 4.3

^{13}C NMR chemical shift displacement ($\Delta\delta$) for the ring OCH_2 carbon of ligand (109) (top), *and for the ring OCH_2 carbon of ligand* (116) (bottom) *in methanol solution relative to salt concentration (LiCl): molar ratio as abscissa. The limiting chemical shift is fitted visually to the experimental curve.*

The errors induced in the plotting of these curves may originate from two sources. The error in $\Delta\delta$ is unlikely to be significant because the value is a "difference" and thus any inherent frequency shift in the NMR spectrometer will be compensated for. The error in the mole ratio of salt:ligand may be greater however. The ligands used are unlikely to be 100% pure [but are greater than 98% (by ^{1}H NMR at 250 MHz)], thus the true molarity of the ligand present may be slightly less than that used in the calculation and thus increase the salt:ligand ratio. The molecular weights of the alkali salts used to plot the curves have been determined by a prior determination of the *effective* relative molecular mass using atomic absorption spectrophotometry. Incomplete transfer of the solid alkali salt to the NMR tube may also be a cause of error however. The two discrepancies will tend to cancel one another out, thus it is very difficult to put a numerical value to the error. Error bars have therefore been omitted from the graphs. Since only qualitative effects are being construed from the results it is necessary only to bear in mind the potential error which should not affect the qualitative interpretations.

It is now appropriate to consider the titration curves for the one- and two-armed amide compounds (111), (114), and (115) on successive additions of solid LiCl. The results are shown in Figure 4.4. In each case, the signals for each of the carbons in the ligand respond in a similar manner to a greater or lesser extent. This is demonstrated graphically in Figure 4.5 for ligand (115). For clarity, however, the signal for the carbon which underwent the greatest displacement (to higher or to lower frequency) was selected for plotting of the other curves.

The curve shape observed for ligands (114) and (115) (Figure 4.4 *b*

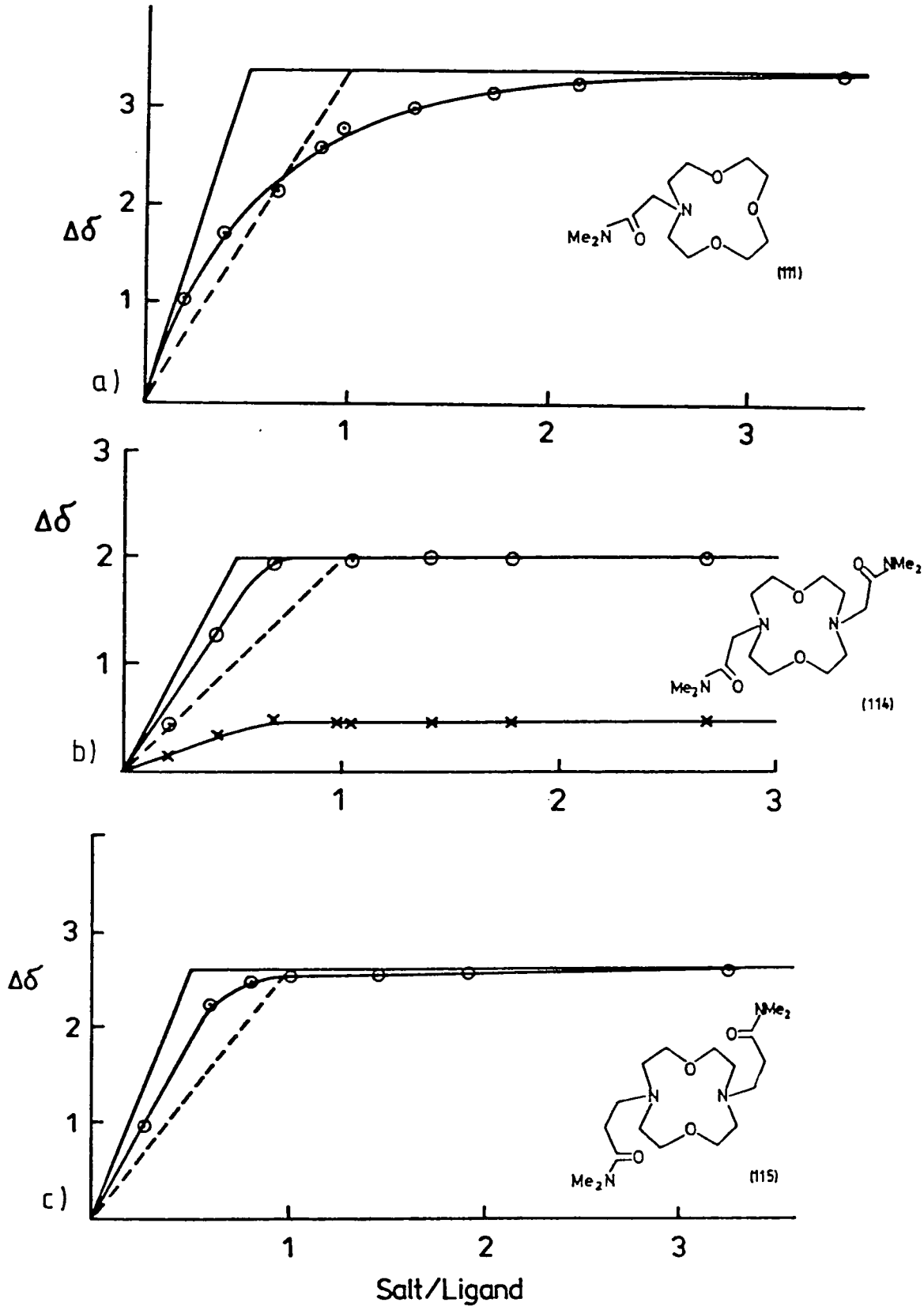

Figure 4.4

^{13}C NMR chemical shift displacement ($\Delta\delta$) for the ring OCH_2 carbon of ligand (111) (top), for the ring OCH_2 carbon of ligand (114) (middle), and for the ring NCH_2 carbon of ligand (115) in methanol solution relative to salt concentration (LiCl): molar ratio as abscissa. The limiting chemical shift is fitted visually to the experimental curve.

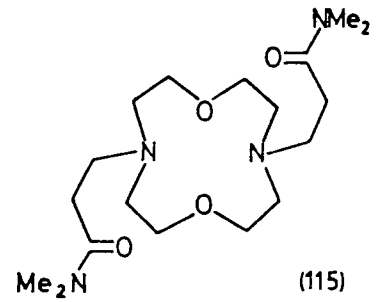

(115)

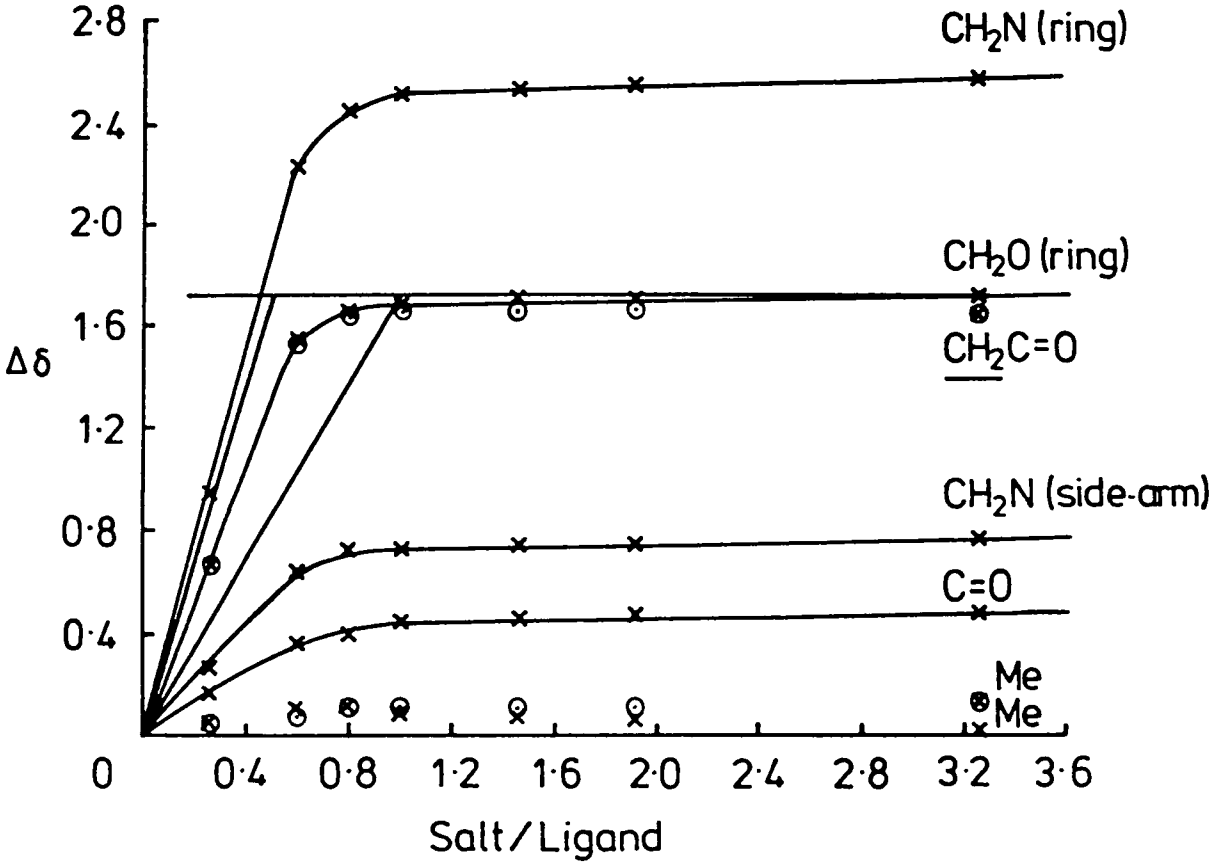

Figure 4.5

^{13}C NMR chemical shift displacement ($\Delta\delta$) for all the carbon resonances of ligand (115) in methanol solution relative to salt concentration (LiCl): molar ratio as abscissa. The limiting chemical shift for the ring OCH_2 carbon is fitted visually to the experimental curve.

and c) indicates that a strong complex is formed at high salt concentrations since a constant chemical shift is quickly reached after the addition of one equivalent of LiCl. However, at low salt concentrations the curve is not closely followed. The most probable explanation is that the stoichiometry of the strong complex is 1:1 and that for lower salt concentrations a weaker 2:1 complex is present. The 2:1 complex would only be present while the salt concentration remained low with an accompanying excess of ligand. At higher salt concentrations, the 2:1 complex would disappear. The formation of a 2:1 complex is somewhat surprising considering the low coordination number preferred by lithium ions.[153-157,238] However, the curve shapes do seem to indicate a strong 1:1 complex and a weaker 2:1 complex.[124,242] This interpretation is shared by Dale.[243] Thus, it seems that these ligands do not completely suppress the formation of 2:1 complexation as was found for ligand (111) [≡ (85)](Figure 2.17) by Dale.[123] The presence of two ligating side-arms containing hydroxyl groups completely suppresses the formation of a 2:1 complex with $LiClO_4$: the presence of two ligating side-arms containing amide carbonyls (both one and two carbons in the alkyl chains of the side-arms) apparently does not. The curve-shape observed for ligand (111) (Figure 4.4α) suggests the formation of a relatively weak 2:1 complex at both low and high salt concentrations. This adds credence to the interpretation placed on the titration curves observed for ligands (114) and (115) since again, the presence of a 2:1 complex was *not* expected. It must be noted however that this latter interpretation relies also on a consideration of "realistic possible stoichiometries". Strictly speaking, the curve could also represent a mixture of weak complexes of varying stoichiometry.

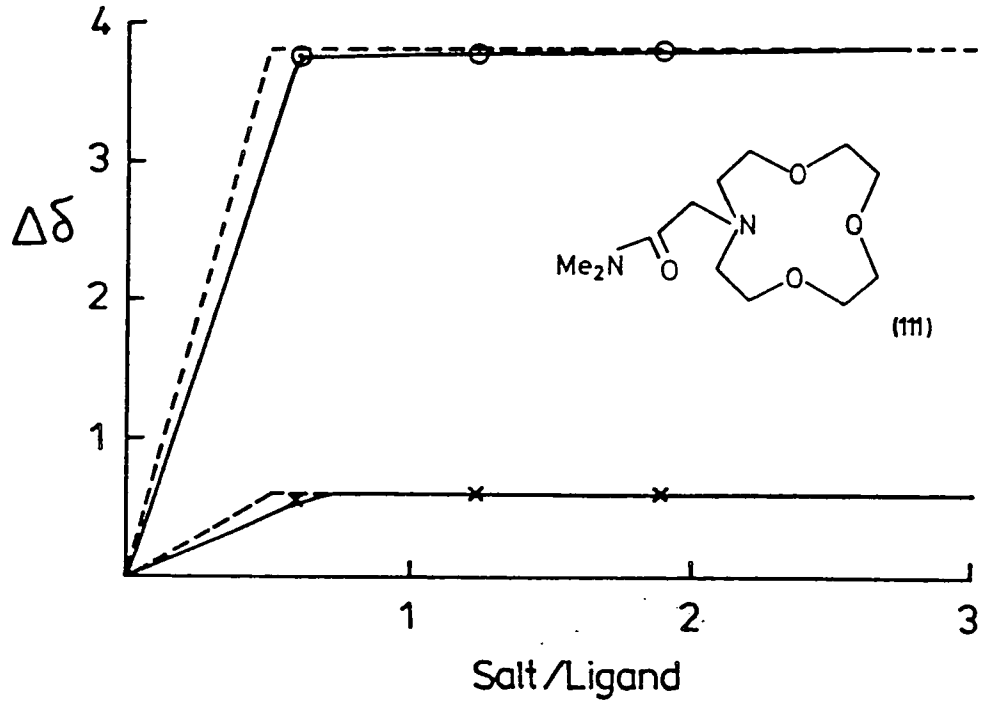

Figure 4.6

^{13}C NMR chemical shift displacement ($\Delta\delta$) for the ring OCH_2 carbon (o) and one CH_3 carbon (x) of ligand (111) in methanol solution relative to salt concentration ($CaCl_2$): molar ratio as abscissa. The limiting chemical shifts are fitted visually to the experimental curve.

The curve shape observed for the calcium complex of ligand (111) (Figure 4.6) seems to indicate a relatively strong 2:1 complex. Given the larger size of the calcium cation relative to that of the lithium cation and the preference of the calcium cation for higher coordination numbers (six to eight),[2] this result ties in well with that found for the lithium complex of the same ligand.

Complexation was again monitored by examination of the ^{13}C NMR shift of the ligand resonances when solutions of ligands (114) and (115)

were titrated with solid $CaCl_2$. The results obtained are represented in Figures 4.7 and 4.8. These ligands have six donor atoms available for binding to the calcium cation and could therefore potentially satisfy the primary coordination sphere around the calcium ion (although a coordination of eight is preferred by calcium in the solid state).[2,244] Figures 4.7 and 4.8 reveal that for the complexes formed, on the time-scale of the NMR experiment, cation exchange is slow and discrete signals are seen for the free ligand and for the ligand bound to calcium ions at each titre. Figure 4.7 shows the chemical shifts for the carbonyl (C=O) carbon of ligand (115) in methanol solution on successive additions of solid $CaCl_2$. The same shift phenomenon to a greater or lesser extent occurs for each of the carbon resonance signals of the ligand but for clarity only the carbonyl resonance is depicted. Figure 4.8 shows the chemical shifts for the CH_2O, CH_2N (ring) and CH_2N (side-arm) carbons of ligand (114) in methanol solution, also on successive additions of solid $CaCl_2$. It is interesting to note that the carbonyl resonance for ligand (115) shifts to higher frequency whereas the CH_2O and CH_2N signals for ligand (114) shift to lower frequency. It is difficult however to attribute the direction and magnitude of the observed shifts for each carbon atom within a ligand to a particular factor. The effects on the shifts may be caused by the degree of binding to a cation but it is more likely that they are caused by conformational changes within the ligand.[146]

It is clear from Figures 4.7 and 4.8 that for both ligands (114) and (115) relatively strong complexes are formed with calcium. On addition of calcium ions, discrete resonances appear for the ligand bound to calcium, in addition to those resonances present due to the free ligand. This situation is indicative of slow dynamic cation

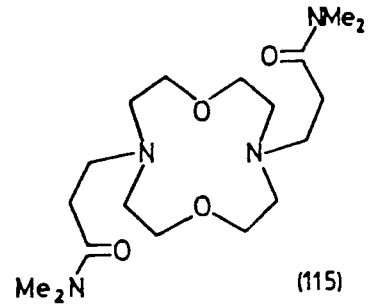

(115)

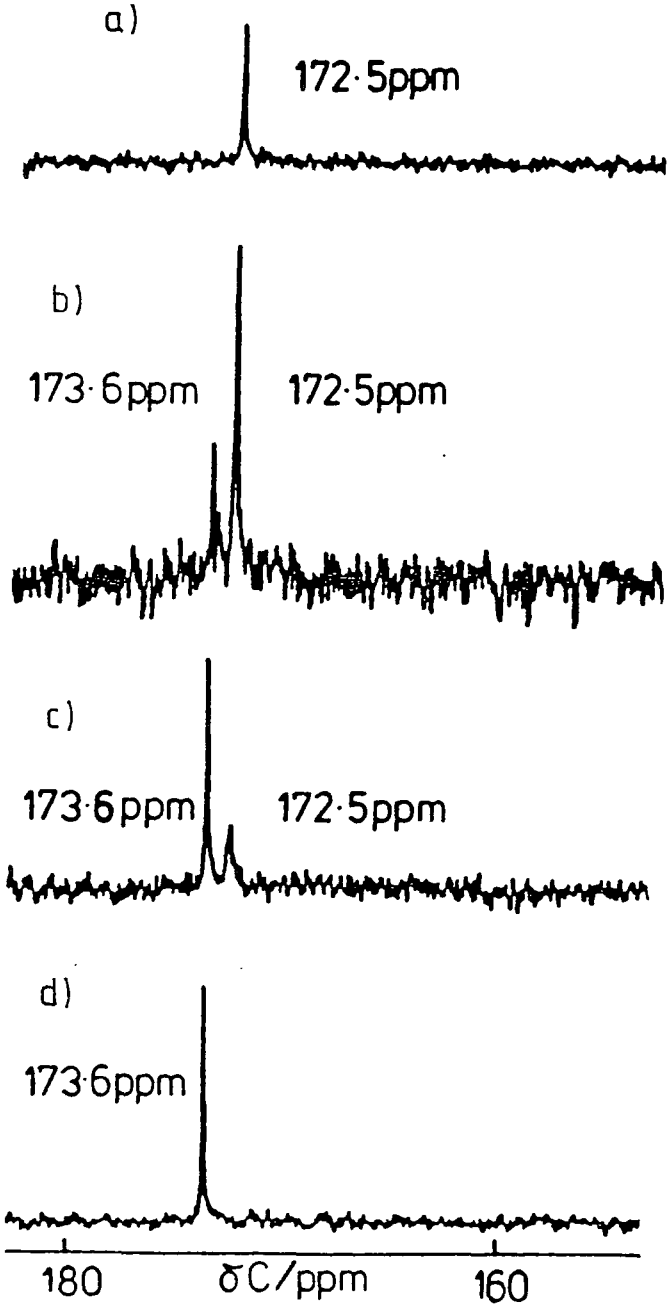

Figure 4.7

^{13}C NMR chemical shifts for the carbonyl carbon of ligand (115) *in methanol solution on successive additions of solid calcium chloride: ratio of salt to ligand* (*a*) 0:1; (*b*) 0.15:1; (*c*) 0.46:1; (*d*) 0.99:1.

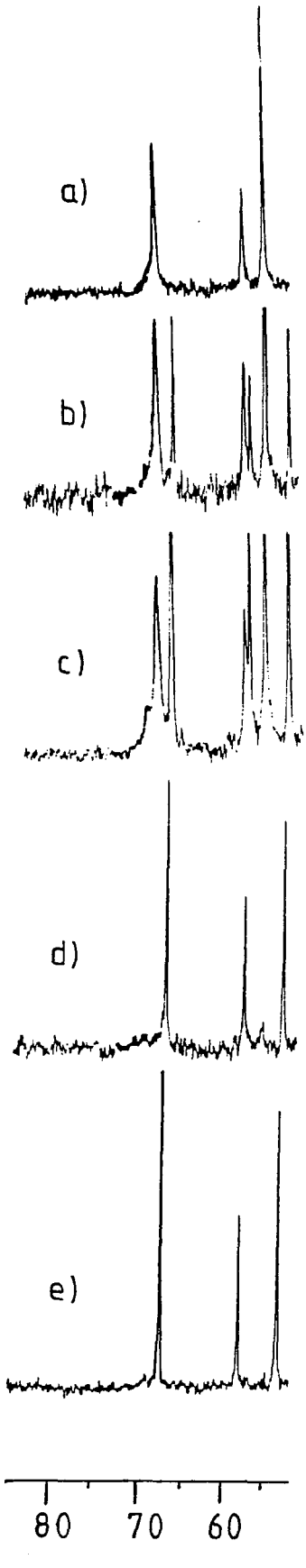

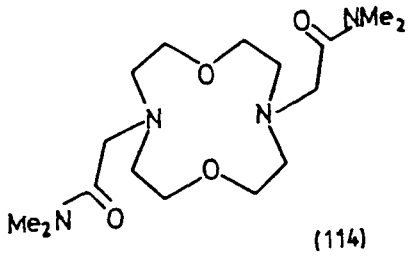

(114)

Figure 4.8

^{13}C *NMR chemical shifts for the ring* OCH_2, *ring* NCH_2, *and side-arm* NCH_2 *carbons of ligand* (114) *in methanol solution on successive additions of solid calcium chloride: ratio of salt to ligand* (*a*) 0:1; (*b*) 0.25:1; (*c*) 0.53:1; (*d*) 0.92:1; (*e*) 1.39:1..

exchange on the time-scale of the NMR experiment. As more calcium ions are added to the systems, the lines due to the free ligands gradually disappear and those due to the bound ligand intensify. When one molar equivalent of calcium ions has been added to each system, the free ligand signals completely disappear. This indicates that the ratio of binding may be 1:1. Most importantly, these results clearly indicate that the complexes formed when amide functionality is present are strong. The lack of dynamic exchange implies that the ligands are bound tightly to the calcium cations and are unwilling to release them to the solvent at the temperature of the experiment (25^{o}) and in this solvent system (methanol). The shift observed for the carbonyl oxygen of ligand (115) suggests that both of the side-arms participate in binding. These interpretations must be treated with caution however, since major conformational changes within the ligands could have similar effects on the chemical shift displacements to those observed.

The relative rates of dissociation of the complexes formed between ligands (114) and (115) and calcium ions have been further assessed by a study of the ligand exchange kinetics evaluated by dynamic ^{13}C NMR spectroscopy using a ratio of ligand to salt of 2:1. For ligand (115) the signals had not coalesced at 55^{o} with methanol as solvent which implies a decomplexation barrier of greater than 62.7 kJ mol^{-1}. Complex stability may be expected to be lower with water rather than methanol as solvent by up to three orders of magnitude[91] and exchange may be expected to be faster. For the calcium complex of ligand (115) in D_2O, the dissociation barrier ($\Delta G^{\neq}$) was found to be 53.7 $\pm$ 0.4 kJ mol^{-1} whereas for the calcium complex of ligand (114) in the same solvent $\Delta G^{\neq}$ was 65.1 $\pm$ 0.4 kJ mol^{-1}. Assuming that a high dissociation barrier parallels strong complexation, the results imply that the calcium

complex with ligand (114) is the stronger complex.

4.4 Fast-Atom Bombardment Mass Spectroscopy (FAB MS) Experiments

FAB mass spectroscopy has been used to determine the selectivity of ligands (114) and (115) for the alkali metal ions Li^+, Na^+, K^+, and Ca^{2+}, using a procedure adapted from that reported by Johnstone and Rose[199] and Meili and Seibl.[200]

An aqueous solution of the chlorides of lithium, sodium, potassium, and calcium was prepared with each cation being present at a concentration of 2.5×10^{-2} M. Methanol solutions of the ligands (114) and (115) were also prepared at a concentration of 2.5×10^{-2} M. Analytical solutions were prepared by mixing an equal volume of the cation solution with each of the ligand solutions together with an equal volume of glycerol. Thus, all components were present in equal concentrations in a methanol-water-glycerol (1:1:1) solvent mixture which allowed the metal cations to compete for a limited amount of the ligand. The stainless steel tip of a FAB probe was coated with a thin layer of the analytical solution and positive ion FAB mass spectroscopy was performed (see Chapter Seven).

Cation selectivity has been evaluated by using the expression:

$$S = \log \left[\frac{I(L + Li)^+}{I(L + C)^+} \right]$$

where S is the selectivity factor, $I(L + Li)^+$ is the signal intensity for [ligand + $Li]^+$, and $I(L + C)^+$ is the signal intensity for [ligand + alkali metal cation]$^+$. The selectivity factors are calculated with respect to the lithium cation and a low value indicates a poor selectivity for lithium over that cation. The selectivity factors are

	Selectivity Factor, S					
Ligand	H^+	Li^+	Na^+	K^+	Ca^{2+}	$(CaCl)^+$
(114)	1.10	0	0.57	0.84	—	0.37
(114)	—	0	0.52	0.69	—	0.35
Average	—	0	0.55	0.77	—	0.36
(115)	0.52	0	1.06	1.87	—	1.65

Table 4.1

Lithium selectivity of ligands (114) *and* (115)

given in Table 4.1. The selectivity factors are also represented graphically in Figure 4.9.

In conclusion, the data seem to indicate that both ligands (114) and (115) preferentially bind lithium, with ligand (115) showing the greater selectivity for lithium. However, there are several features of this method which warrant further discussion.

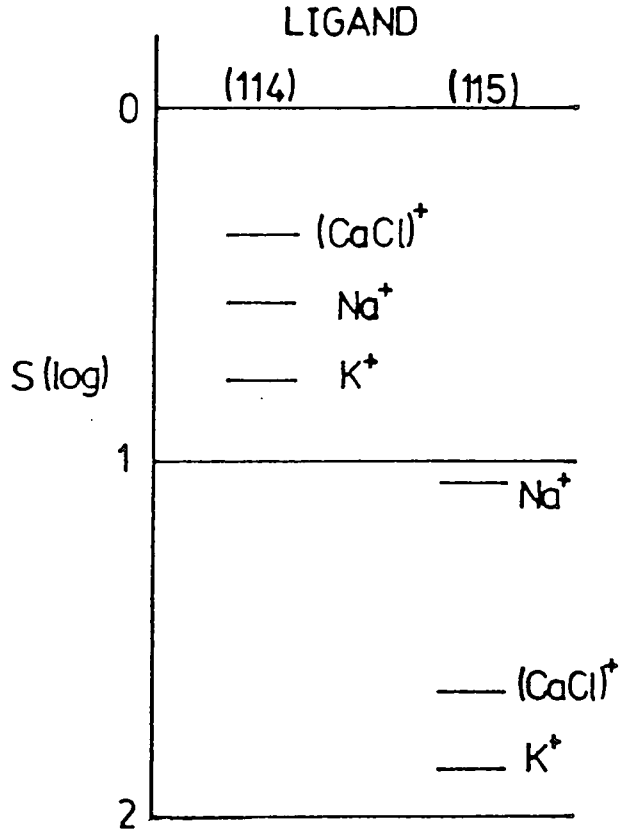

Figure 4.9

Lithium selectivity of ligands (114) *and* (115)

The calcium complexes formed *in situ* have an associated chloride ion and thus the complex is dissimilar to those formed with the lithium, sodium, and potassium cations. Thus, a direct comparison of the selectivity of the ligand for calcium ions with the other cations is not justified. It is also important to point out that weak peaks were observed in some cases for [ligand + cation + H]$^+$ complexes. This suggests that protonation of some complexes occurs: protonation of a ring nitrogen would negate nitrogen binding in cation complexation. This interference will affect the reported results and may distort the conclusions.

Thus, while the NMR experiments suggested that these ligands formed the strongest complexes with calcium cations, competitive FAB experiments have suggested that these ligands are lithium selective. It must be remembered that these experiments are:

(1) mixed solution experiments;

(2) carried out in a methanol/water/glycerol solvent medium;

(3) competitive experiments implying that the rate of formation of the complex may be the determining factor;

and (4) that a different complex was formed for the divalent calcium cation belying a direct comparison with the other alkali metal complexes.

There are only a few reports of macrocyclic ligand selectivities determined by FAB MS. Thus, all the problems and methods are perhaps not yet fully understood. However, the results reported were reproducible. We have also examined the selectivity of ligands (107) and (109) by FAB MS: we found that in PEG400 solution the selectivities for lithium over sodium cations were small and there was no indication of 1:1 complex formation with either calcium or potassium cations. It

is likely that the calcium and potassium cations may prefer to bind to the solvent molecules.

4.5 Potentiometric Experiments

Preliminary potentiometirc experiments only have been carried out for ligand (106) with lithium and calcium cations and for ligand (109) with lithium and sodium cations. The procedure outlined by Lehn and Simon[207] was followed (see Chapter Seven) for the determination of the stability constants of complexation as defined by the equations below:

$$L + M^+ \underset{}{\overset{K}{\rightleftharpoons}} LM^+$$

$$K = \frac{[LM^+]}{[L][M^+]}$$

where [L], [M^+], and [LM^+] are respectively the concentrations of the ligand, the cation and of the 1:1 complex. Computer analysis (see Chapter Seven) of the pH-metric titration curves in the absence and presence of cations allows the determination of K, since ligands (106) and (109) are basic amines and complex formation changes the pH of the solution. For each experiment, three titrations were performed: of the free ligand and of the ligand in the presence of two different concentrations of salt. In each case, one protonation equilibrium may be considered and one complexation to give a 1:1 complex. Protonation of the nitrogen site participating in the complexation is expected to destabilise the complex sufficiently that the corresponding equilibrium may be ignored.

The pK value for ligand protonation for ligand (106) is 9.8 $\pm$ 0.2 in methanol-water (9:1) solution. The stability constant obtained for the complex of ligand (106) with calcium cations is 4.0 $\pm$ 0.3. The titration curve found for ligand (106) with lithium cations indicates

that lithium cations bind more strongly to the solvent than they do to the ligand: the pH at each titre in the presence of lithium is higher than that found in the absence of lithium (Figure 4.10). With ligand (109), the titration curve found for lithium cations again indicates that lithium cations are interacting preferentially with the solvent. The titration curve observed for the interaction of (109) with sodium cations was consistent with very weak complexation.

The experiments with ligand (109) pin-pointed many experimental difficulties associated with this procedure:

(1) the use of an electronic pipette to introduce microlitre volumes of solution was probably insufficiently accurate and the use of an automatic titration apparatus would be preferable;

(2) the determination of salt solution concentrations by ion-chromatography or by titration would probably be more accurate than by atomic absorption spectrometry;

(3) for weak complexations the use of a computer program that takes solvolysis of the cation into account may be preferable.

(The program BEST[214] takes cation solvolysis into account. At present our version of BEST needs to be translated into standard FORTRAN to be compatible with our computer system.)

The problems outlined above need to be corrected before great account may be taken of the results obtained from potentiometric titrations. Thus, whilst seeking to perfect the potentiometric method we turned to the method of titration calorimetry for the determination of stability constants of complexation.

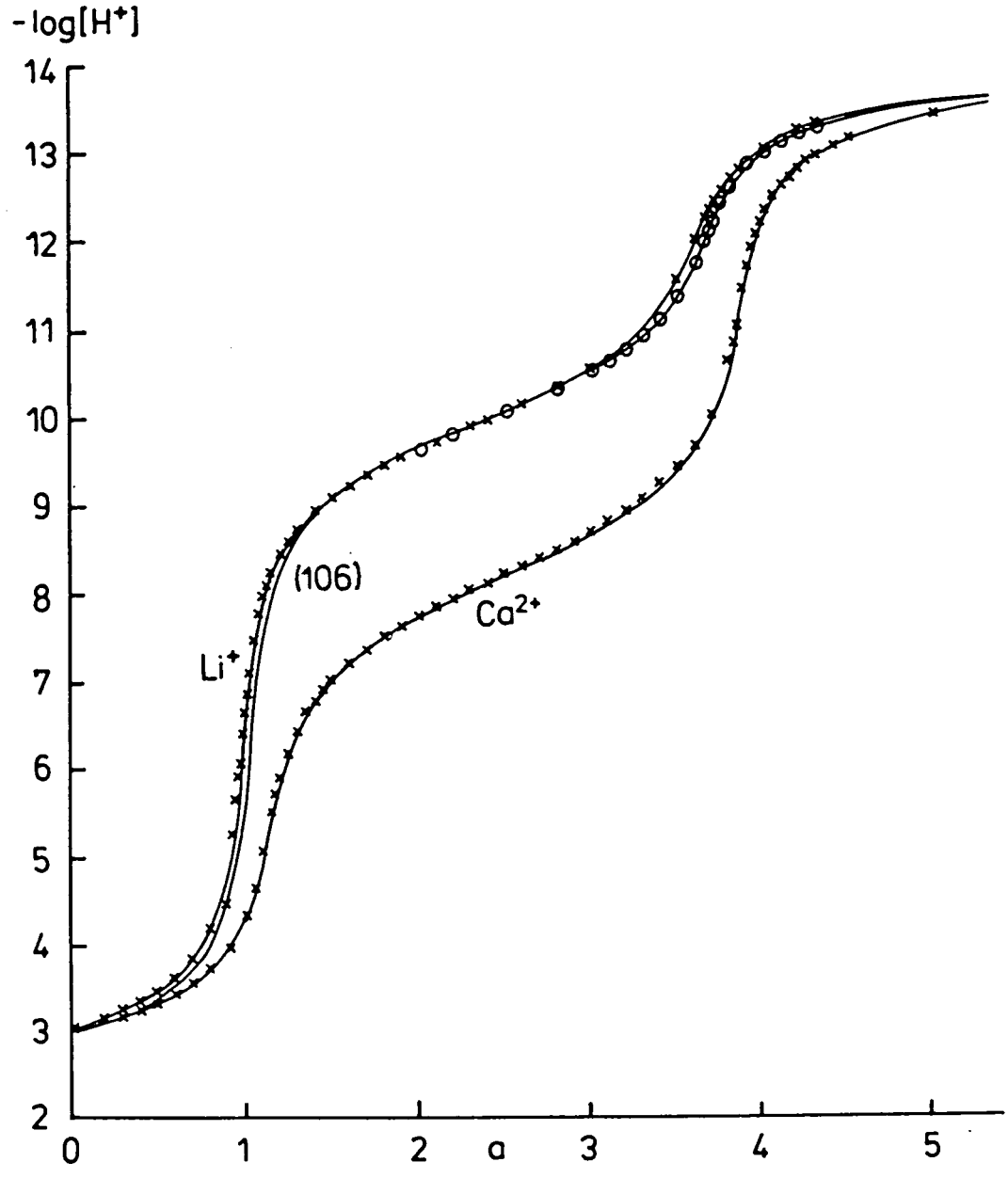

Figure 4.10

Potentiometric equilibrium titration curves for ligand (106) *and ligand* (106)-Li^+ *and ligand* (106)-Ca^{2+} *systems at* 298 K. *a is the volume* (ml) *of* NMe_4OH *solution added.*

4.6 Calorimetric Experiments

The importance of thermodynamic measurements coupled with the equilibrium cation binding stability constant data (log K values) is now widely recognised in the understanding of cation complexation by macrocycles. A recent review by Izatt and Christensen *et al.*[245] has tabulated the known thermodynamic data for cation-macrocyclic interactions. Enthalpic and entropic contributions to the stability constant values may be discussed separately: a recent review by Buschmann[239] has addressed the relative importance of entropic and enthalpic contributions to the macrocyclic and cryptate effects. Stability constant (log K) and thermodynamic values (ΔH and $T\Delta S$) for the interaction of ligands (109), (114), and (115) with Li^+, Na^+, K^+, Rb^+, Ca^{2+}, Sr^{2+}, Ba^{2+}, and Ag^+ have been measured in methanol solutions by titration calorimetry. The data are given in Table 4.2 and are compared with the reported values with the unsubstituted diaza ligand (112)[227] and the two-armed dihydroxy compound (113)[123] [ligand (113) forms five-ring chelates on side-arm complexation].

The substitution of the protons of the diaza-unsubstituted ligand (112) by the relatively bulky side-arms in ligands (114) and (115) leads to an increase in the measured reaction enthalpies of complexation. Thus complexation with cations Li^+, Na^+, K^+, Rb^+, Ca^{2+}, and Sr^{2+} may be observed. Contributions to this favourable reaction enthalpy may come from several sources. The diaza ligands may adopt different conformational forms (Figure 4.11). With bulky side-arms, the ligand prefers the *endo-endo* conformation [solid-state structure of (115) is *endo-endo*, Figure 4.11]. This conformation is most appropriate for cation binding. A free ligand which adopts the *exo-exo* conformation

Ligand		Li^+	Na^+	K^+	Rb^+	Ca^{2+}	Sr^{2+}	Ba^{2+}	Ag^+
	log *K*	2.71	—	—	—	2.72	—	—	—
(109)	$-\Delta H$	3.00	20.8	13.1	—	6.8	11.9	19.1	49.9
	$T\Delta S$	12.4	—	—	—	8.7	—	—	—
	log *K*							2.34	6.5
(112)	$-\Delta H$							13.3	31.9
	$T\Delta S$							-4.4	5.1
	log *K*	2.4	3.6	2.0	—	6.9			
(113)[a]	log *K*	(2.8,2.5)	(3.4,3.2)						
	log *K*	5.38	4.72	3.85	3.08	> 5	≥ 5	4.94	—
(114)	$-\Delta H$	12.7	26.0	25.7	22.7	46.6	35.8	33.0	59.1
	$T\Delta S$	17.9	0.8	-3.8	-5.2	—	—	-4.9	—
	log *K*	2.99	3.01	3.03	3.08	4.10	4.36	3.30	> 5
(115)	$-\Delta H$	23.8	37.6	30.6	11.0	45.9	19.9	44.5	82.5
	$T\Delta S$	-6.8	-20.5	-13.4	6.5	-22.6	4.9	-25.7	—

[a]Data from ref. 123 determined potentiometrically in methanol-water 9:1. Values in parentheses obtained from analysis of ^{13}C NMR titration curves in methanol at 298 K.

Table 4.2

Stability constants and thermodynamic values for the reaction of (109), *and* (112) *to* (115) *with various cations. Titrations were effected in anhydrous methanol at* 298 K (*see Chapter Seven*); *log* K (± 0.1), ΔH (*kJ* mol^{-1}) (± 1), $T\Delta S$ (*kJ* mol^{-1}).

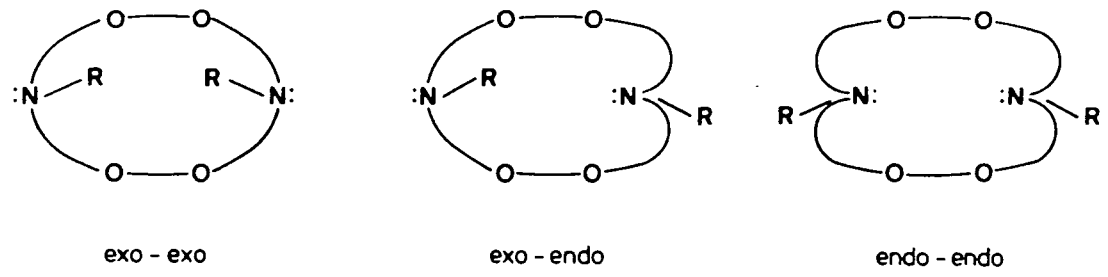

Figure 4.11

Different conformational forms of uncomplexed diaza-crown ethers.

[*e.g.* (112)] must undergo a conformational change during complexation and therefore the reaction enthalpies are reduced. This reduction may be associated with the energy necessary to invert the nitrogen atoms. The reaction enthalpy will also be favourably affected by the additional interactions occurring between the cation and the side-arm donor groups.

Changes in the ligand internal entropy because of orientational, rigidificational, and conformational changes may also occur on complexation. In the final complexed state some of the ligand flexibility is lost resulting in a negative (unfavourable) term for the reaction entropy. For the ligands (114) and (115) with mobile side-arms the loss of flexibility will be considerably greater than for ligand (112) causing a large negative contribution to the reaction entropy. This may be demonstrated by comparing the values of the reaction entropies for the complexations of Li^+, Na^+, and K^+ with the ligands (114) and (115). The longer, more flexible arms of ligand (115) result in a greater loss of mobility on complexation than for ligand (114), resulting in a much less favourable entropy term. The most important contribution to the reaction entropy however is the translational

entropy of the liberated solvent molecules. This factor results in higher values for ΔS for the more strongly solvated small cations. This may be demonstrated by comparing the value of the reaction entropy for the complexation of Li^+ with the ligand (114) with the values reported for the reaction entropies of the other cations with that ligand. The differential solvation interactions with cation and with ligand are also important: for example, the repulsion between solvent molecules constituting the solvation shell around a small cation with a high charge density will favour ring binding. Similar arguments obviously apply to ligand (109) when compared with the monoaza-unsubstituted compound.

Ligand (115) does not show any discrimination in binding alkali metal cations as gauged by log K measurements but clearly prefers calcium and strontium over IA cations. This invariance masks strong differences in the enthalpic and entropic contributions which tend to compensate for each other in the overall free energy change (and hence log K). The strong complex formed between calcium ions and (115) is due to a highly favourable complexation enthalpy. Indeed the entropy term is less favourable than that found for the complexation reactions with lithium, sodium, potassium, or rubidium. The enthalpic energy *may* be related to the intermediate size of the calcium cation and its possible ability to interact more strongly with all the donor atoms of the ligand, causing perhaps less ligand deformation than for the other cations. Cations which are either too small or too large to bind to the focussed lone-pairs of the ligand may require a more dramatic ligand conformational change in order to optimise binding interactions. The calcium cation also has a dipositive charge which will further enhance the ligand-cation interactions, particularly with the amide donors (see Section 4.1). However, an unfavourable entropy term (-22.6 kJ mol^{-1})

offsets the increase in reaction enthalpy. The calcium complex is a factor of ten more stable than the lithium, sodium, potassium, and rubidium complexes of the same ligand.

Ligand (114) which has shorter side-arms than those in ligand (115) exhibits markedly different behaviour. The lithium complex of (114) is more stable than the lithium complex of (115) by a factor of more than 100. Despite the decrease in reaction enthalpy, there is a much more favourable reaction entropy. This may be related to a better pre-disposition of the less flexible side-arms. The same phenomenon to a slightly lesser extent is observed for the complexes with sodium and potassium. For the complex of rubidium with ligand (114) however, compared with the complex with ligand (115), it is the reaction enthalpy which is favoured and the reaction entropy which is disfavoured: the two terms compensate for each other entirely, yielding a value of log K of 3.08 for rubidium ions with both ligands. The less favourable enthalpy terms observed for the lithium, sodium, and potassium complexes of (114) may be related to a pre-disposition of the amide oxygen lone-pairs in the less flexible side-arms of (114) away from the cation which sits on the [12]-ring.

The log K values for the complexes of (114) with calcium and strontium are unobtainable by this method but are at least 5.5 and may be estimated to be ≥ 8 for calcium.[†] An alternative method of analysis is required using either a competitive calorimetric titration, a competitive cation-selective electrode experiment or a potentiometric titration experiment. Such experiments are in progress.

In conclusion, complexes with ligand (114) are more stable than

---

[†]For log K $\geq$ 8.2, TΔS must approximate to zero. The order of calcium complex stability for ligands (114) and (115) is in accord with that predicted by dynamic ^{13}C NMR studies.

those with ligand (115) and this enhanced stability is primarily associated with more favourable reaction entropies, particularly for those cations with a high charge density. Ligand (114) exhibits a selectivity for Li^+ over other IA cations and is dramatically selective for Ca^{2+}.

Ligand (109) complexes significantly to lithium and calcium cations giving almost identical stability constants. In each case the stability constant is only slightly less than that determined for ligand (115). This is due to a vast decrease in reaction enthalpy which is partially compensated for by an increase in reaction entropy. This suggests that the interaction between donor atoms and cation is very weak yielding a poor complexation enthalpy, although the ligand internal entropy changes are favourable.

4.7 X-Ray Structures of some Cu(II) Complexes of 12-Membered Aza-substituted Macrocyles

Attempts have been made to grow crystals suitable for X-ray crystal structure analysis of the complexes of the 12-membered diaza- and monoaza-substituted ligands with lithium, calcium, and copper(II) cations. To date, structural determinations for the copper(II) complexes of ligands (113),[166] (106), and (109) have been completed. Whilst our primary interest was in the alkali and alkaline earth metal complexes of these ligands, it has proved far more difficult to grow suitable crystals of such complexes. The complexes with copper(II) cations may not be directly compared with the complexes expected with lithium and calcium ions: copper(II) is a transition metal cation (d^9)

and is thus a directional cation with highly favoured coordination geometries within its complexes [Jahn-Teller effects have a profound effect on Cu(II) stereochemistry if placed in an environment of octahedral or tetrahedral symmetry]. The [12]-ring *usually* adopts a [2424] conformation[146,147] in its complexes with six-coordinate copper. This conformation is favoured in order to accommodate the folding of the macrocycle to provide two vacant *cis* positions for other ligands. The ring may be too small to embrace all four equatorial ligand positions, but can easily connect two equatorial and both apical positions. The copper complex of ligand (106) adopts this conformation, however, the copper complex of (113) adopts the 'square' [3333] conformation. The [12]-ring may be expected to adopt this well-defined 'square' [3333] conformation in its complexes with the IA and IIA metal cations.[238,246,247] However,

(1) the copper(II) complexes are interesting *per se*;

(2) insight into the possible stoichiometries of complexation may be gleaned from these complexes;

(3) the complexes furnish information on the binding capabilitites of donor groups on the side-arm.

The properties of the copper(II) complexes of ligands (113),[166] (106), and (109) are discussed in the proceeding section and structures of the cations are given as determined by X-ray analysis.

4.7.1 *Cu(II) Complex of Ligand* (113)

Reaction of (113) with a one molar excess of copper(II) perchlorate in aqueous ethanol led to the slow formation of a green crystalline solid (125) (λ_{max} 273 nm, ϵ 9.7 x 10^3 dm^3 mol^{-1} cm^{-1}; 720, 120) whose positive ion FAB mass spectrum in a glycerol matrix gave peaks centred at *m/e* 811 and 711 corresponding to $[(113)_2\text{-}Cu_3ClO_4]^+$ and

$[(113)_2\text{-}Cu_3]^{\bullet+}$. Needles of the complex (125)[166] as the hexafluorophosphate salt, having composition $[(113)_2\text{-}Cu_3][PF_6]_2$ were grown from cold propan-2-ol. The structure of the complex cation is shown in Figure 4.12 and the pertinent crystal data are given in Chapter Seven.

The two hydroxyl groups of (113) have lost their protons during complex formation. The central copper atom lies on an inversion centre and has square planar geometry. The Cu(2) atom [and Cu(2*)] is six-coordinate with distorted octahedral geometry and the macrocyclic ring adopts a [3333] conformation (see Figure 4.13). Atoms Cu(2), O(1), O(2), N(1), and N(2) are essentially coplanar, with O(3) and O(4) above and below this plane.

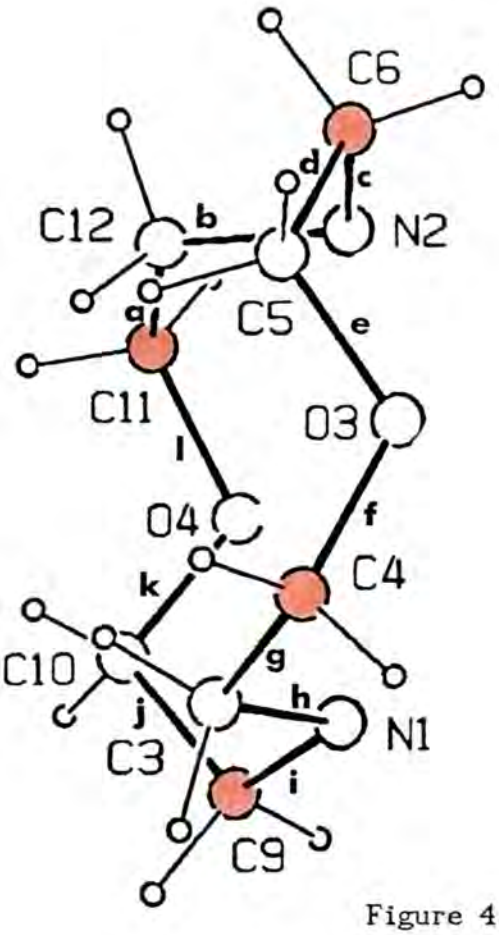

a	-50.2
b	176.3
c	-77.0
d	-58.3
e	150.9
f	-91.0
g	-45.5
h	168.1
i	-76.8
j	-61.1
k	148.7
l	-85.7

Figure 4.13

Torsion angles (^{o}) *for the ligand in complex* (125) *showing Boeyens and Dobson-type corners* (shown in red).[147]

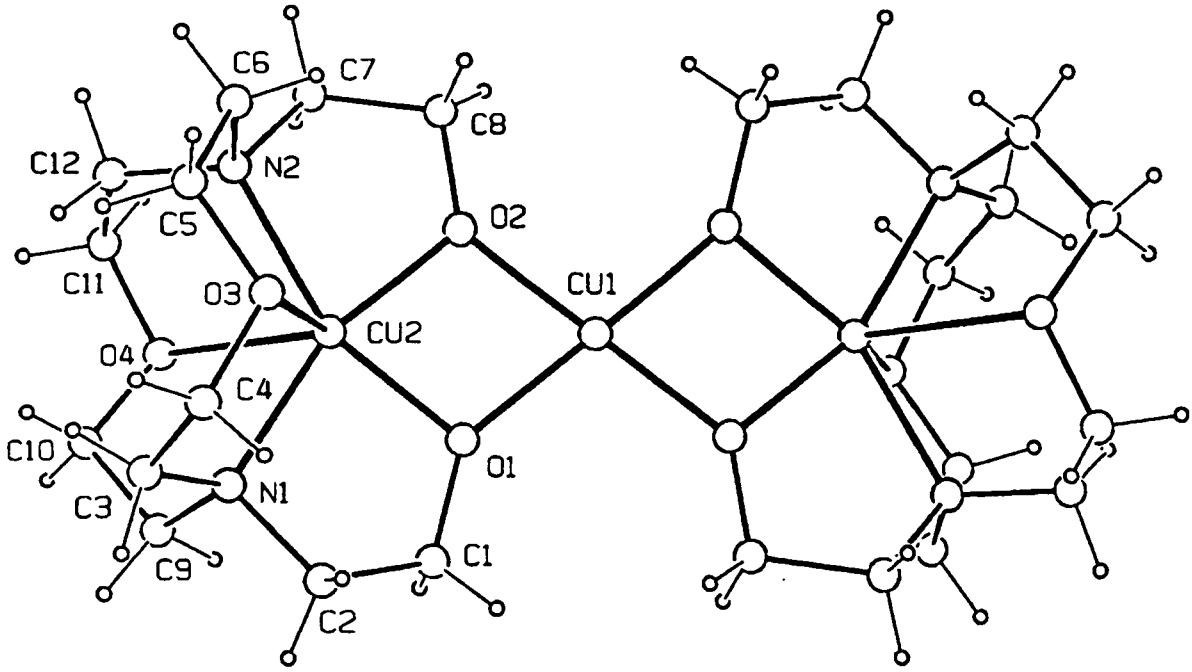

Figure 4.12

A view of the tri-copper complex cation (125) *showing the crystallographic numbering scheme.*

Main dimensions are Cu(1)-O(1) 1.918(4), Cu(1)-O(2) 1.902(5), Cu(2)-O(1) 1.918(4), Cu(2)-O(2) 1.904(5), Cu(2)-O(3) 2.444(4), Cu(2)-O(4) 2.681(5), Cu(2)-N(1) 2.086(5), Cu(2)-N(2) 2.101(5) Å; O(1)-Cu(1)-O(2) 77.6(2), O(1)-Cu(2)-O(2) 77.6(2), O(3)-Cu(2)-O(4) 118.8(2), N(1)-Cu(2)-N(2) 116.8(2)°.

The complex has a magnetic moment at 295 K of 1.1 μ_B (per copper atom) suggesting that there are strong antiferromagnetic interactions operating within each Cu_2O_2 ring, and that the spin doublet (S = 1/2) state is the ground state at room temperature.[248,249] The powder ESR spectrum is of the axial type with $g_{\parallel}$ = 2.23 and $g_{\perp}$ = 2.04, and a normal $A_{\parallel}$ hyperfine splitting was observed (0.015 cm^{-1}). The electrochemical behaviour of (125) has been studied in H_2O (μ = 0.1 M; $NBu^n_4ClO_4$) on a glassy carbon electrode by cyclic voltammetry. Two quasi-reversible peaks were observed at +0.23 and -0.04 V (relative to the standard calomel electrode), as indicated by $i_a/i_c \simeq 1$ and by the observation that the peak separation ΔE remains constant for scan rates between 10 and 100 mV s^{-1}. Coulometric reductions indicate that two Faradays per mole of complex are exchanged at +0.23 V and that the redox process at -0.04 V is a one-electron process. Similar two electron reduction waves have been observed at +0.28 V for dinuclear copper(II) cryptates which possess two [12]-N_2O_2 or [12]-N_2S_2 macrocyclic rings.[250-253] Complex (125) may therefore be regarded as a [2 + 1] three electron receptor.

In conclusion, the X-ray structure analysis of the complex has confirmed that both side-arm oxygens may bind to copper. The trinuclear complex is antiferromagnetic and may be regarded as a trielectronic receptor complex. It also clearly suggests that in the calcium complex of this ligand, both hydroxyethyl side-arms will participate in binding. In addition, the X-ray structure lends support to the premise that in hetero-dinuclear complexes of (15)[40] coordination of a hard cation regulates the ligand structure.

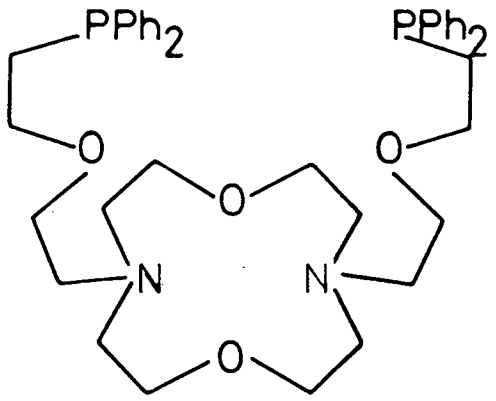

(15)

4.7.2 *Copper(II) Complex of Ligand* (106)

Reaction of (106) with a two molar excess of copper(II) perchlorate hexahydrate in methanol gave immediate formation of a pale green precipitate. Needles of the complex (126) as the perchlorate salt with composition $[(106)_2\text{-}Cu_2][ClO_4]_2$ were grown from methanol. The structure of the complex cation is shown in Figure 4.14 and the pertinent crystal data are given in Chapter Seven.

The two hydroxyl groups (one per ligand) have again lost their protons during complex formation. The cation structure has a centre of inversion and each copper atom is six-coordinate with Cu, O(1), O(3), N and O(1*) essentially coplanar, with O(2) and O(4) above and below this plane in a distorted, tetrahedral array. The conformation of the macrocyclic ring is [2424] (see Figure 4.15). The macrocyclic ring folds such that atoms O(2) and O(4) occupy the apical sites and atoms N and O(3) occupy two equatorial sites leaving two *cis*-equatorial sites vacant. These latter sites are occupied by the oxygens of the side-arms, O(1) and O(1*).

The positive ion FAB bombardment mass spectrum of complex (126)

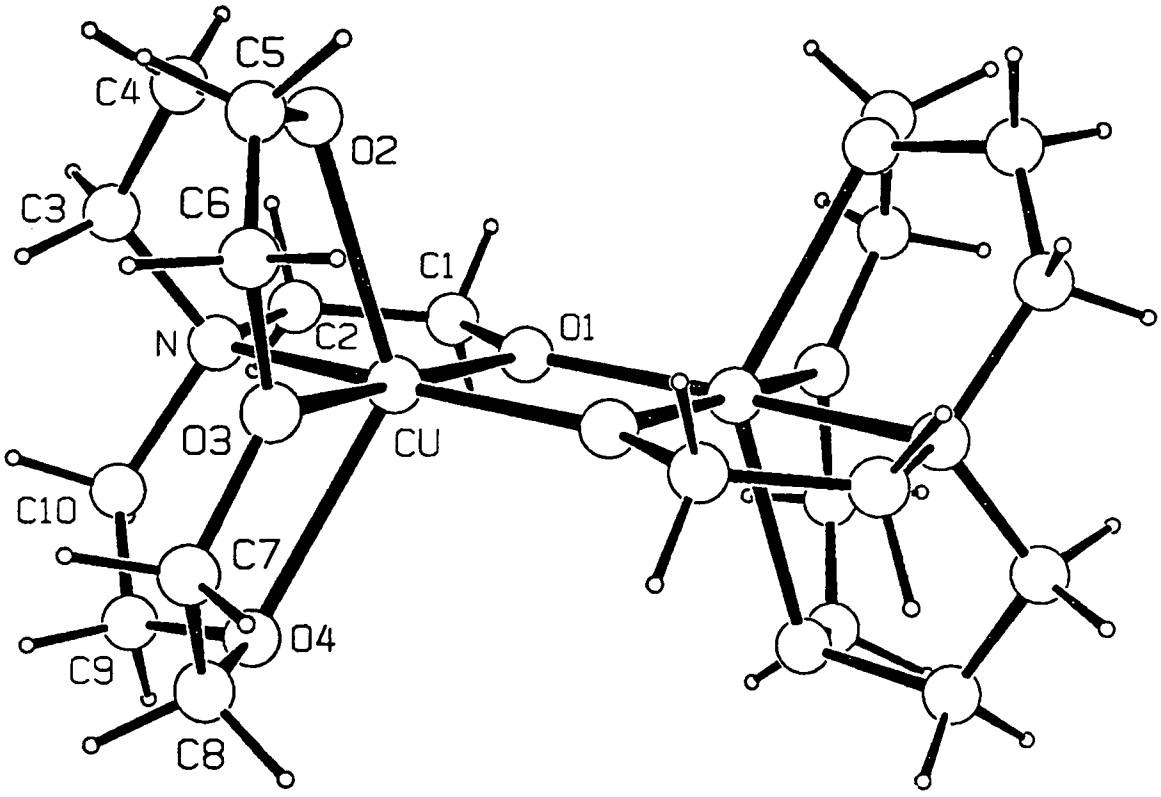

Figure 4.14

A view of the dimeric copper complex cation (126) *showing the crystallographic numbering scheme.*

Main dimensions are Cu-O(1) 1.881(12), Cu-O(1^{*}) 1.886(12), Cu-O(2) 2.322(13), Cu-O(4) 2.345(12), Cu-O(3) 2.164(12), Cu-N 2.012(13) Å; O(1^{*})-Cu-O(1) 79.2(5), O(3)-Cu-N 106.0(5), O(2)-Cu-O(4) 129.9(5)°. The * refers to the atom whose coordinates are obtained by applying the symmetry transformation -x, -y, 1-z.

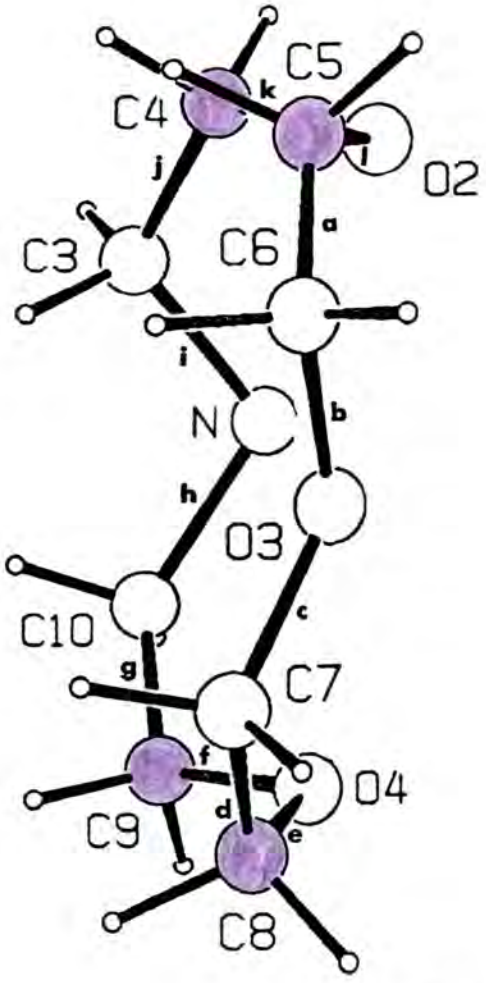

a	-8.1
b	-150.7
c	169.1
d	-16.7
e	-99.8
f	120.8
g	5.1
h	-123.1
i	148.4
j	-34.4
k	-101.1
l	108.4

Figure 4.15

Torsion angles (^{o}) *for the ligand in complex* (126) *showing Boeyens and Dobson-type corners* (shown in purple).[147]

gave peaks centred at *m/e* 282 and 220 corresponding to $[(106)-Cu]^{+}$ and $[(106)-H]^{+}$ respectively. The electrochemical behaviour of the complex (126) has been studied in acetonitrile solution (μ = 0.07 M); $NBu^{n}_{4}ClO_{4}$) on a platinum electrode by cyclic voltammetry. A quasi-reversible peak at 0.36 V (relative to the standard calomel electrode) was observed.

Both this copper dimer and the tri-nuclear complex of ligand (113) promise to have interesting magnetic chemistry. The predominance of ferromagnetic or antiferromagnetic interactions within Cu_2X_2 rings (X = Cl, OH, O^{-}) may be predicted by a consideration of the relative orientations of the magnetic orbitals[254-256] for values of θ (θ =

$\hat{CuOCu}$): molecular orbital calculations may provide a quantitative evaluation of the effect of the effect of variation of θ. To illustrate this concept, the molecular orbital analysis of the model planar system, $Cl_2Cu(OH)(OH)CuCl_2$[255] may be highlighted. Each Cu(II) (d^9) has a square

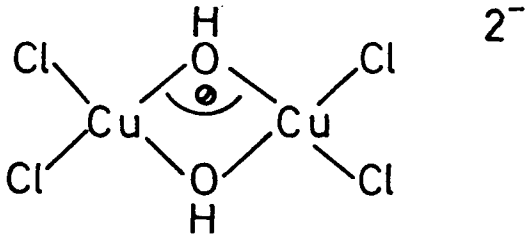

planar geometry and each unpaired electron [one per Cu(II)] occupies an x^2-y^2 orbital oriented along the bond axes. The highest occupied orbitals of the dimer are the symmetric (ϕ_S) and antisymmetric (ϕ_A) combinations of the monomer x^2-y^2 orbitals, represented in Figure 4.16,

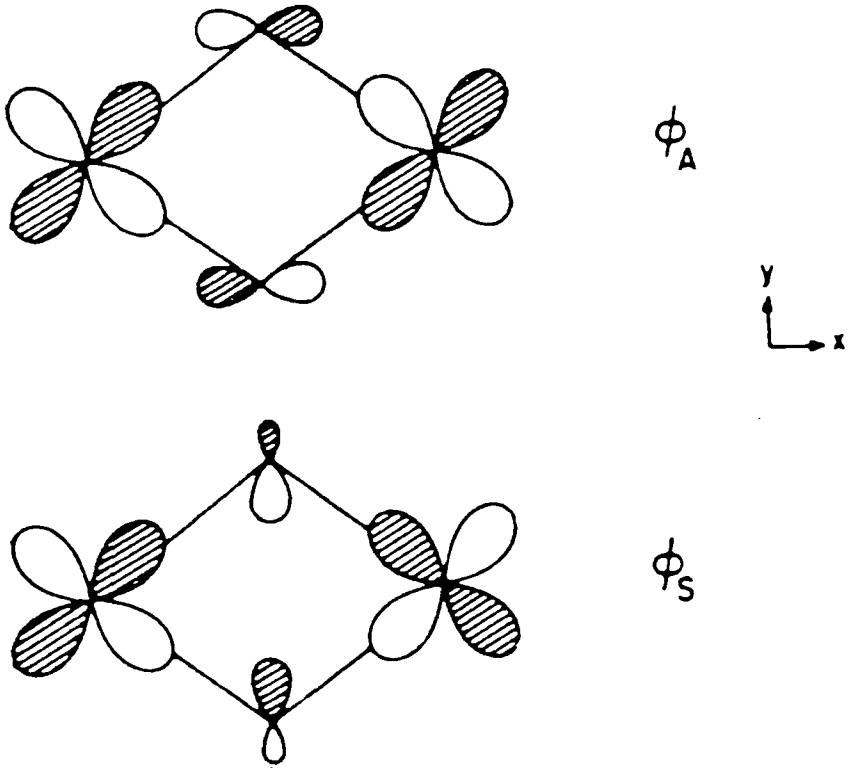

Figure 4.16

Schematic representation of the two highest molecular orbitals of the Cu-X-Cu bridging unit: ϕ_S *(symmetric) and* ϕ_A *(anti-symmetric).*

together with the lower-lying filled 2p orbitals of the bridging ligands (oxygen) which may interact with the d-orbitals. The relative order of the energies (ϵ_S and ϵ_A) of the two orbitals (ϕ_S and ϕ_A) as a function of θ are determined by the metal-bridging ligand overlap, especially with the 2p orbitals since thay lie much higher in energy than the 2s orbitals (for simplicity the unimportant admixture of $4p_z$ component into the metal orbitals and the 2s bridging orbitals are ignored in this discussion). At a certain value of θ ($\simeq 90^o$) one may expect that the orbitals ϕ_A and ϕ_S will be degenerate ($\epsilon_A = \epsilon_S$), since orbital overlap is equal. Ferromagnetic coupling may thus occur with the triplet spin system ($\uparrow\uparrow$)(parallel spins) as the ground state. As θ increases, overlap (antibonding character) within ϕ_A increases and overlap within ϕ_S decreases. This leads to a corresponding increase in ϵ_A and a decrease in ϵ_S. Thus for high θ, an antiferromagnetic coupling is expected, with the singlet spin system ($\uparrow\downarrow$) (paired spins) as the ground state. Calculation of the angle (the cross-over point) which allows the equation of ϵ_S and ϵ_A gives $\theta \simeq 107^o$. Consideration of the 2s orbitals of the bridging oxygens which have an antibonding interaction with ϕ_S displaces the crossing point to $\theta \simeq 96^o$.

Our complex dimer (126) has both copper atoms six-coordinate, each with a distorted octahedral geometry. The tri-nuclear comlex (125) has the central copper atom exhibiting square planar geometry with the two remaining coppers six-coordinate with distorted octahedral geometries. For complex (126) the geometry around the coppers is approaching square planar with the long Cu-O(2) and Cu-O(4) bonds (2.322 and 2.345 Å respectively) oriented in the z plane. The lone electrons are therefore likely to occupy the $d_{x^2-y^2}$ orbitals and overlap between the magnetic orbitals may occur. For a certain range of θ, also dependent on the

electronegativity and type of the terminal and bridging ligands, antiferromagnetic interactions may dominate, as was found for complex (125).

4.7.3 *Copper(II) Complex of Ligand* (109)

Reaction of (109) with a one molar excess of copper(II) perchlorate hexahydrate in methanol solution led to the immediate formation of a blue precipitate (127) [υ_{max} (FT)(KBr) 1606 $\pm$ 1 cm^{-1} (C=O stretch)] whose powder ESR spectrum is of the axial type with $g_{||}$ = 2.21 and $g_{\perp}$ = 2.09. Brilliant blue cubic crystals of the complex (127) as the hexafluorophosphate salt, having composition $[(109)_4\text{-}Cu_4]^{4+}[PF_6]^-_4$ were grown from a methanol solution containing a small volume of ethyl acetate. Determination of the complex cationic structure by X-ray crystallographic analysis at ambient temperature gave a highly disordered structure. Figure 4.17 shows one of the two models which together give the disordered structure and we are now awaiting a low temperature study (the current R factor is 9.1%). The complex is a tetramer with two-fold symmetry. The complex has crystallographic 222 point symmetry because of the space group symmetry demands which lead to the disorder observed. The carboxyl groups show disorder over two sites with 0.5 occupancy (Figure 4.18). During the course of complexation the ester groups have hydrolysed to generate the uninegative carboxylates. The four PF_6 anions (one per copper atom) are disordered over three sites. Clearly the copper cations are sitting well out of the macrocyclic cavities and one oxygen O(7) of the ring does not participate in binding to the copper. The copper atoms are instead bound by two oxygen atoms from two different bridging carboxylate groups. The copper coordination sphere thus consists of three donors from the macrocyclic ring and two oxygens of two different carboxylate

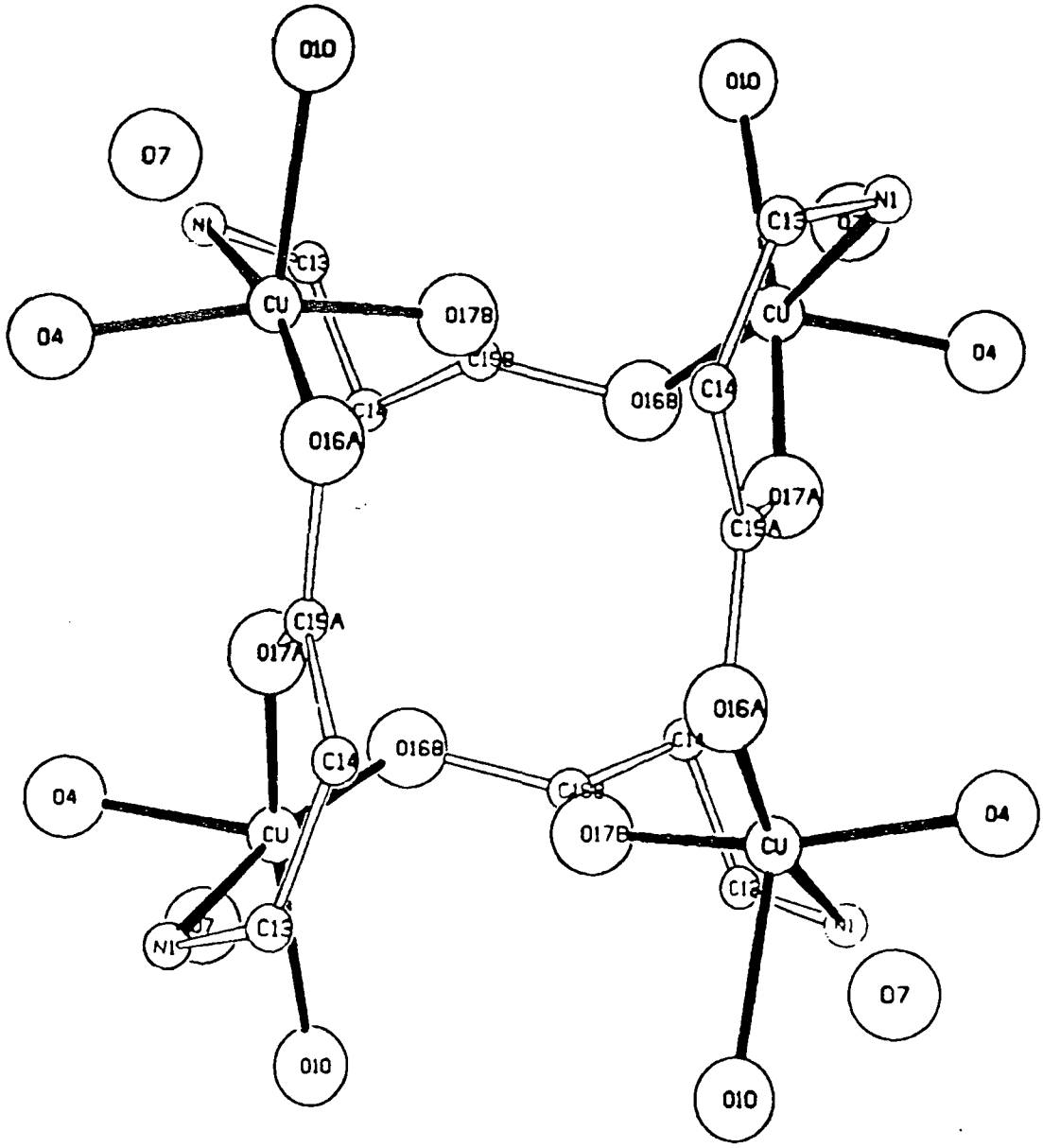

Figure 4.17

One of the two models which together give the disordered structure of the complex cation (127) *showing the environment of the copper centres.*

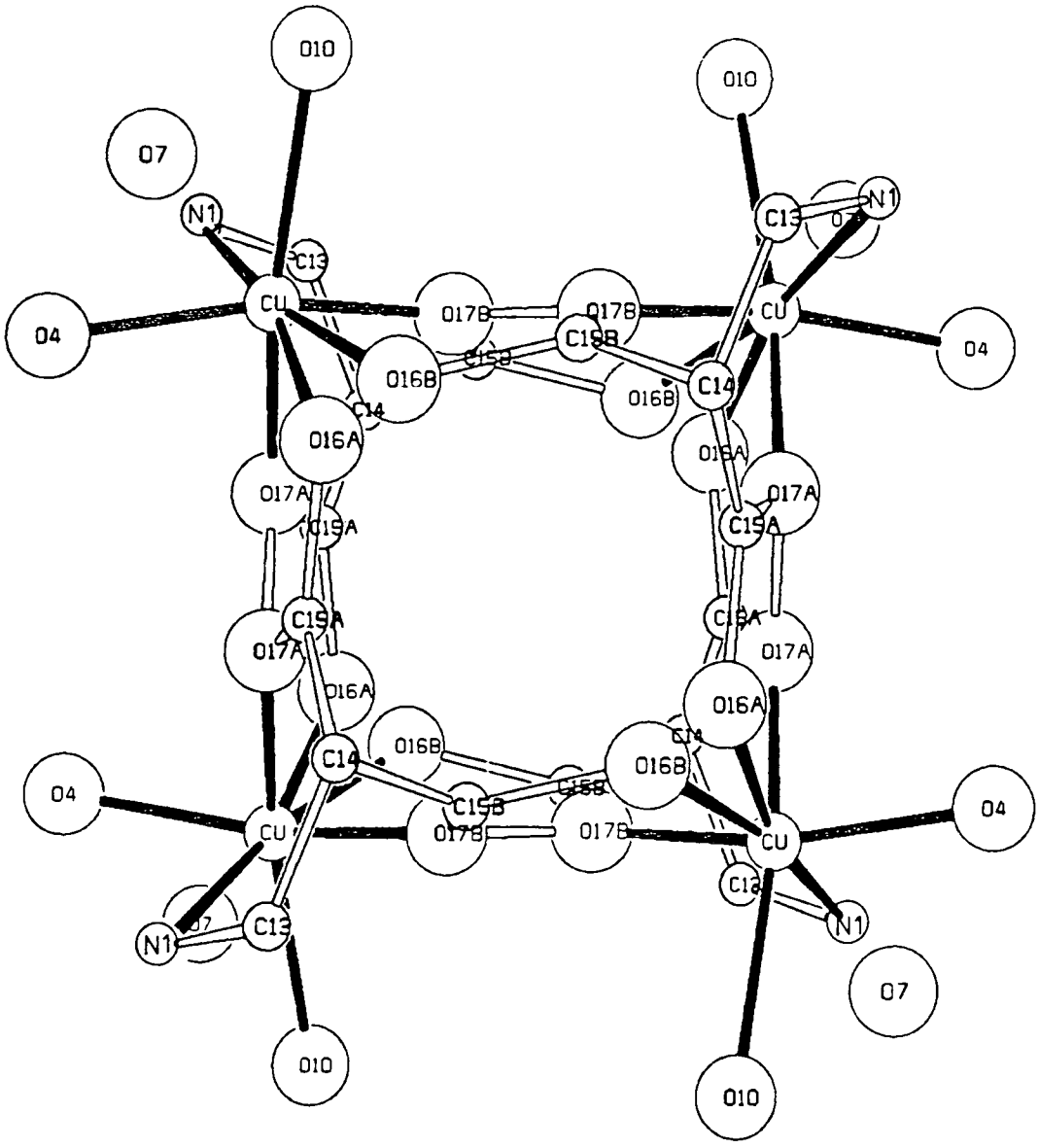

Figure 4.18

Disordered structure of the complex cation (127)

groups. The coppers are five-coordinate and the coordination geometry appears to be distorted square planar pyramidal in one disordered sub-structure and trigonal pyramidal in the other.

4.7.4 *Copper(II) Complex of Ligand* (114)

Reaction of (114) with a 1.25 molar excess of copper(II) perchlorate as a solution in methanol led to the formation of a turquoise solid (128) [υ_{max} (FT)(KBr) 1627 $\pm$ 1 cm^{-1} (C=O stretch)] whose positive ion FAB mass spectrum in a glycerol matrix gave peaks at *m/e* 407, 409 and 506,508 corresponding to $[(114)\text{-}Cu]^+$ and $[(114)\text{-}Cu(ClO_4)]^+$. Analysis was consistent with the formation of a complex with 1:1 stoichiometry. The lowering of the amide carbonyl stretching frequency from 1641 cm^{-1} in the free ligand to 1627 cm^{-1} in the complex suggests that *both* amide carbonyls are participating in the complexation. The data clearly suggest that in the calcium complex of this ligand, both amide carbonyls may participate in binding to give a complex with a 1:1 stoichiometry.

4.8 Conclusions

In summary, the results presented in this chapter have demonstrated that amide groups are excellent selective donors to cations of high charge density and are preferred over ester or ether donors. The data also suggest that stronger complexation to the smaller group IA and IIA metals occurs when five-membered as opposed to the less entropically favoured six-membered ring chelates are generated upon complexation.

CHAPTER FIVE - SYNTHESIS AND COMPLEXING PROPERTIES OF A HETERO-DINUCLEATING LIGAND 4-(2,2'-BIPYRIDINE-5-METHYL)-1,7-DIOXA-4,10-DIAZACYCLODODECANE (142)

5.1 Introduction

The isolation of hetero-dinuclear complexes requires the prior synthesis of a ligand with clearly dissimilar binding sites, as stipulated in Chapter Three. The bipyridine ligand which functions as a π-acid favours binding to transition metal cations.[257] The N_2O_2-twelve-membered ring discussed in Chapter Four, preferentially binds to hard metal cations. At the outset of this work it was thought that the combination of these two binding centres within one ligand might permit the formation of dinuclear complexes. The conformationally mobile ligand (142) was synthesised with the N_2O_2-ring attached at the 5-position of the bipyridine ligand. This enables the study of potential interaction between two bound metal centres.

5.2 Synthesis of the Ligand (142)

The hetero-dinucleating ligand (142) was prepared using an adaption of Dale's reaction[124] between 1,11-diiodo-3,6,9-trioxaundecane and a primary amine (discussed in detail in Chapter Four) to give *N*-substituted derivatives of monoaza-12-crown-4.[124] The reaction of the diiodide 4-toluenesulphonyl-*N*,*N*-di(iodo-1-oxa-3-pentane)amide (135) with the primary amine (140) in dilute acetonitrile solution containing suspended sodium carbonate powder gave the hetero-dinucleating ligand (141), the tosylated derivative of (142). Detosylation of ligand (141) (S_N2 substitution at the sulphur atom) by bromide in hydrogen bromide in acetic acid (45%) in the presence of phenol gave the protonated form of the required ligand (142) as an orange gum. This protonated residue was

treated with tetramethylammonium hydroxide in dichloromethane to give the free ligand (142) as a brown oil. This was crystallised from boiling toluene to give ligand (142) as a white powder (Scheme 5.1).

The diiodide (135) was prepared from the corresponding dichloride (134) by heating under reflux in acetone in the presence of NaI and was used as the crude product. The dichloride (134) was prepared from the corresponding diol (133) by reaction with sulphonyl chloride at 0^{o} with dichloromethane as solvent containing pyridine and was used as the crude product. The diol (133) was prepared from the corresponding diacid (132) by reduction with diborane. The diacid had previously been prepared[104] by D. Parker in a series of stages represented in Scheme 5.2.

The hydrochloride salt of the primary amine (140) was prepared in a series of reactions represented in Scheme 5.3. 2-Acetyl pyridine and iodine in pyridine were heated under reflux for 3 h. The black crystals which formed were recrystallised from ethanol to give shiny silvery crystals of pyridacyl pyridinium iodide (136). Treatment of (136) with methacrolein in dry formamide in the presence of ammonium acetate gave 5-methyl-2,2'-bipyridine (137) on gentle warming. Compound (137) was purified by passage through alumina to give a pale yellow oil.

Compounds (136) and (137) were prepared according to the methods of Kröhnke.[258] Reaction of the methyl-bipyridine compound (137) with freshly recrystallised *N*-bromosuccinimide in dry carbon tetrachloride with heating under reflux gave the bromomethyl-bipyridine derivative (138) as an intermediate compound which was used directly in the next stage. The intermediate compound was treated with potassium phthalimide in dry dimethylformamide and the mixture was warmed to 80^{o}. The product 5-phthalimidomethyl-2,2'-bipyridine (139) was isolated as a pale orange

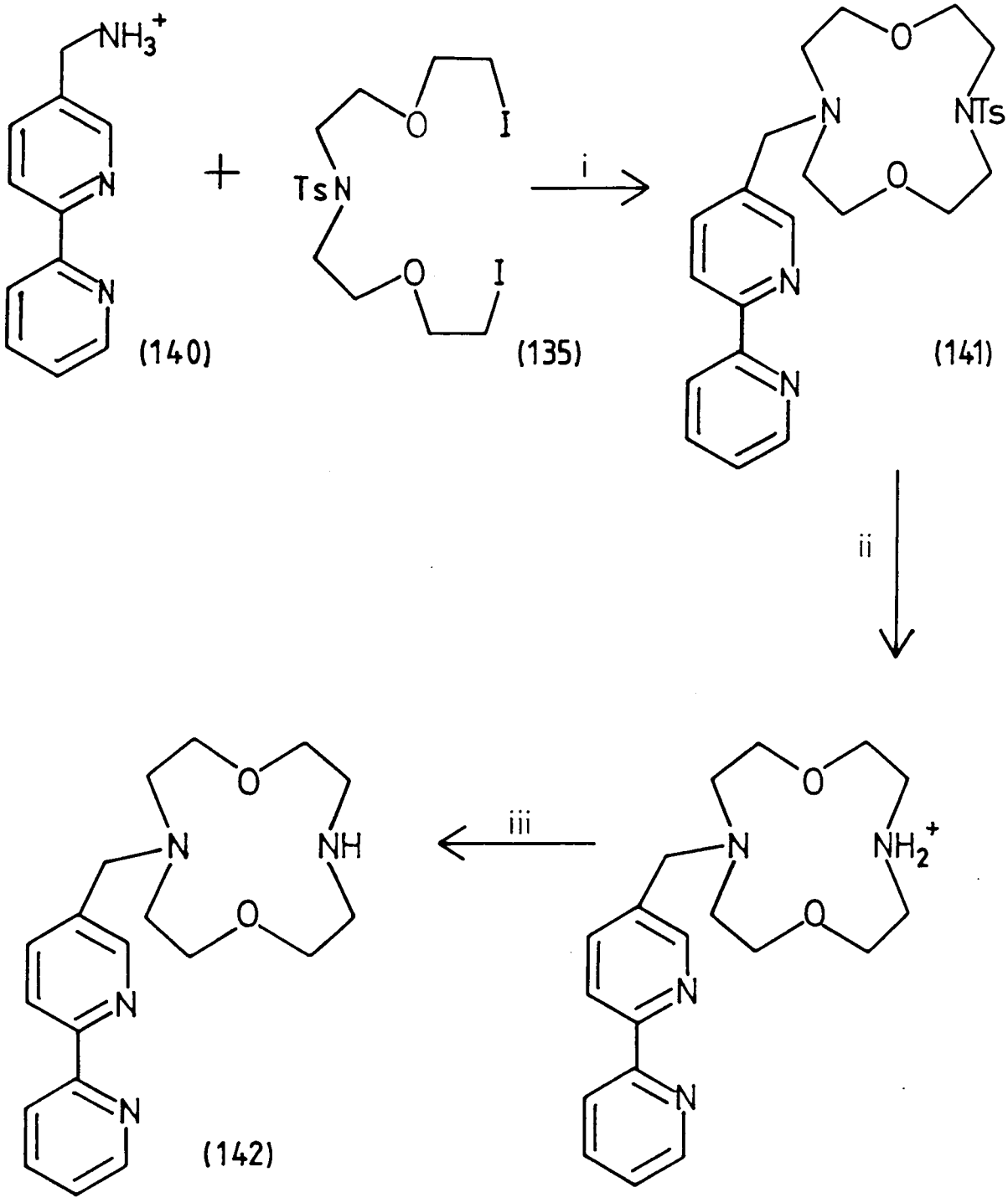

Scheme 5.1

i, Na_2CO_3, MeCN, Δ; *ii*, HBr, AcOH, PhOH, Δ; *iii*, NMe_4OH, CH_2Cl_2.

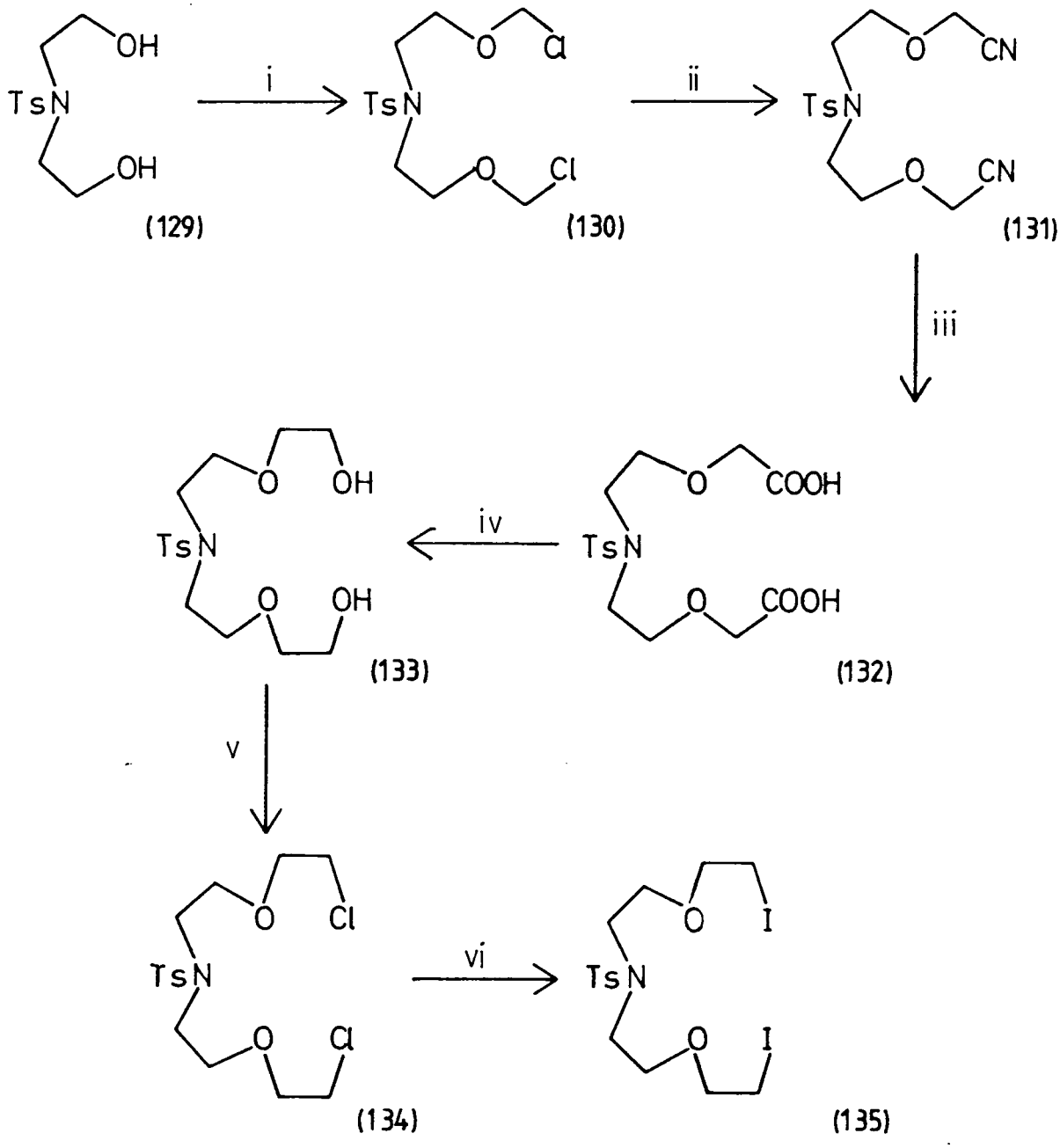

Scheme 5.2

i, CH_2O, HCl, $CHCl_3$, 0^o; *ii*, NaCN, DMF, 0^o; *iii*, $Ba(OH)_2$; *iv*, BH_3.DMS, THF, 0^o; *v*, $SOCl_2$, CH_2Cl_2, pyridine, 0^o; *vi*, NaI, acetone, Δ.

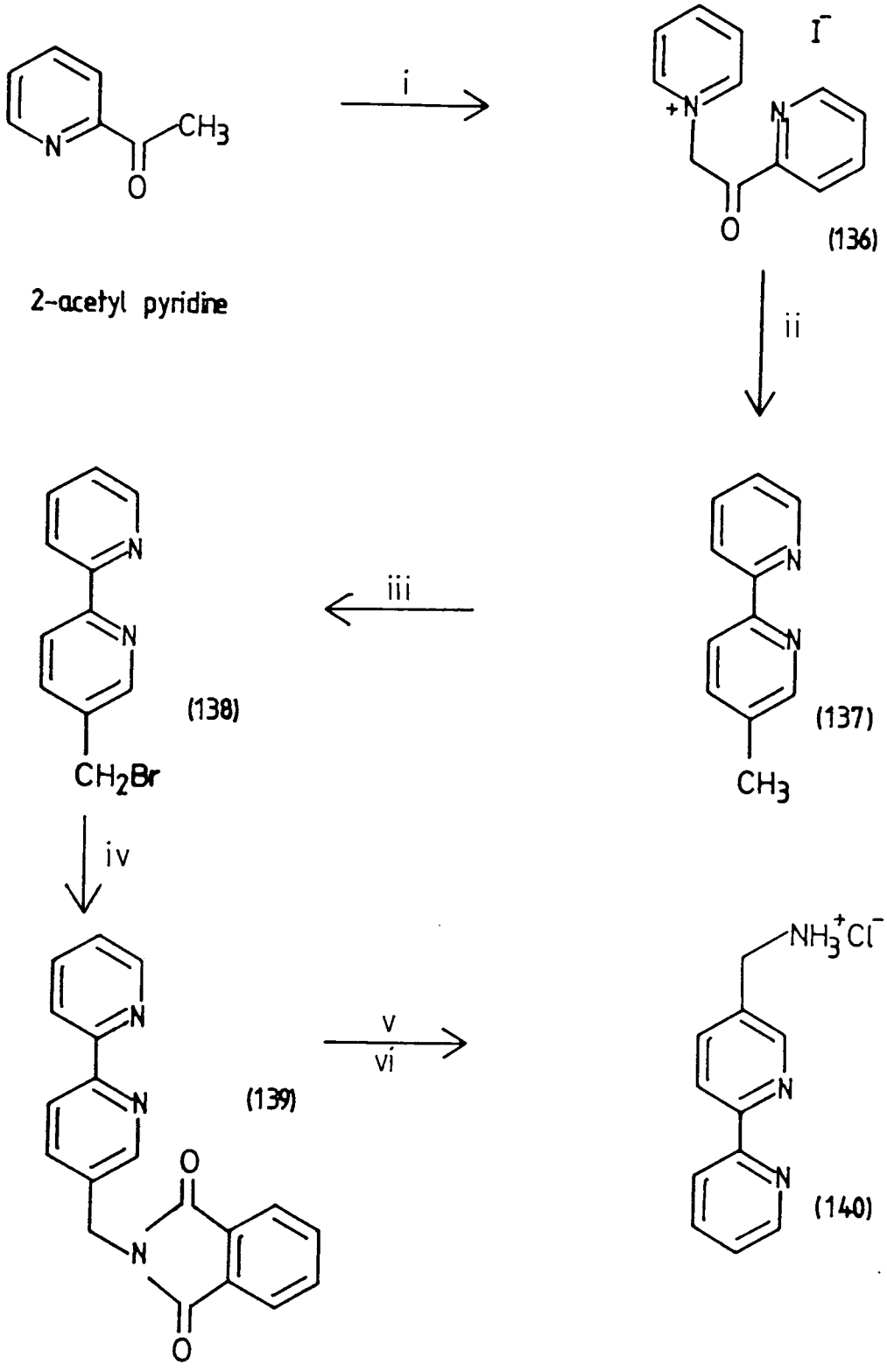

Scheme 5.3

i, I_2, pyridine; *ii*, NH_4^+ AcO^-, pyridine, methacrolein; *iii*, NBS, CCl_4, azo-bis-butyronitrile; *iv*, potassium phthalimide, DMF, Δ; *v*, NH_2NH_2, EtOH; *vi*, 6 M HCl.

solid. The final stage involved the treatment of the phthalimide (139) with hydrazine monohydrate in ethanol followed by the addition of hydrochloric acid. Orange needles of the required primary amine (140) were obtained on crystallisation of the residue from ethanol.

5.3 Complexing Properties of Ligand (142)

5.3.1 *Reaction with Iron(II)*

Complexation with Fe(II) was studied since the formation of a *stable* Fe^{2+}/Fe^{3+} M(bipyridine)$_3^{2+}$ couple was expected.[259] Electron transfer between iron and a proximate redox active cation [*e.g.* Cu(I)[252]] bound by the N_2O_2 ring was considered feasible and could be examined by cyclic voltammetry and related methods.

Reaction of (142) with ferrous sulphate[260] in aqueous solution gave an immediate blood-red solution. The addition of ammonium hexafluorophosphate as a solution in water led to the precipitation of a maroon solid after heating of the mixture under reflux for 15 min. Alternatively, a solid cationic complex (143) could be obtained by heating of the blood-red solution under reflux for 3 h in the presence of sodium tetrafluoroborate. In the complex obtained from the latter method, sodium ions were bound to the [12]-N_2O_2 ring and the sodium proved difficult to remove completely.

The positive ion FAB mass spectrum in a glycerol matrix gave ligand signals only. The electrochemical behaviour of (143) was studied in acetonitrile solution (μ = 0.1; $NBu^n_4ClO_4$) at a platinum electrode by cyclic voltammetry. A cyclic voltammogram was obtained which was consistent with the formation of a *tris*-(bipyridine) Fe(II) complex,[259] $[(142)_3Fe]^{2+}$. A quasi-reversible peak was observed at +1.17 V (relative to the standard calomel electrode) for the one-electron Fe(II)/Fe(III)

oxidation/reduction.

The spectrophotometric data (λ_{max} 522 nm with a shoulder at $\simeq$ 495 nm) were also consistent with the formation of a *tris*-bipyridine Fe(II) complex. Ligand (142) is an unsymmetrical bidentate ligand, and may be represented by AB. Thus, the octahedral complex $[(142)_3\text{-Fe}]^{2+}$ exists as two geometrical diastereoisomers, *meridial* and *facial*, each of which is chiral. The facial isomer has C_3 symmetry and any atom coordinate on one ligand within that isomer is related to an identical position on the two remaining ligands by 120^o rotations. The meridial isomer lacks any C_n axes and thus the three ligands are distinguishable. The ^1H NMR spectrum in D_2O is broadened which may be a consequence of sodium ion contamination. Attempts to isolate the analytically pure complex were unsuccessful.

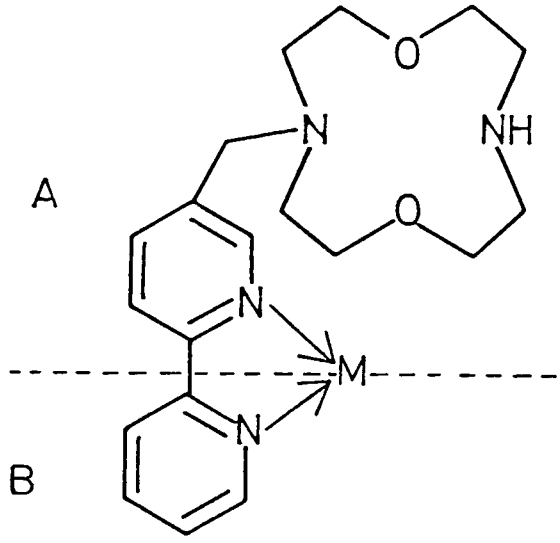

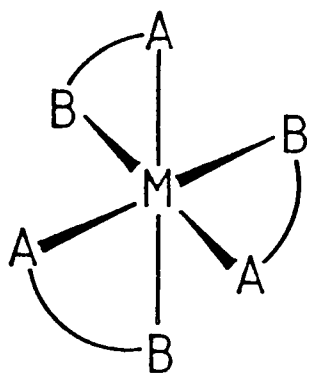

fac

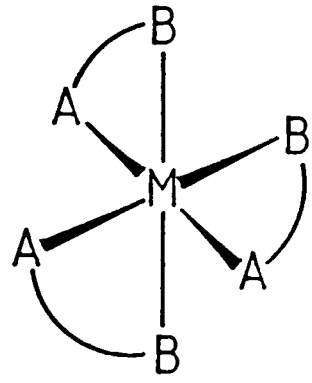

mer

5.3.2 *Reaction with Copper(II) and Palladium(II)*

Reaction with Cu(II) and with Pd(II) was undertaken in order to model, simplistically, the dinuclear site in the Wacker system of alkene oxidation. A dinuclear Pd/Cu system may probe electron transfer between palladium(II) in a low oxidation state, stabilised by the bipyridine π-acid and copper(II) which acts as an oxidant.

Reaction of (142) with copper(II) perchlorate hexahydrate[261] in ethyl acetate resulted in the formation of a pale blue-green solid (144). The positive ion FAB mass spectrum of this complex in a glycerol matrix gave peaks at *m/e* 405 and 407, and 505 and 507 corresponding to $[(142)Cu]^{2+}$ and $[(142)\text{-}Cu(ClO_4)]^{+}$. Bright blue crystals of complex (144) were grown from a methanolic solution. Analytical data are consistent with the formation of a 1:1 ligand:copper complex.

Reaction of ligand (142) with *bis*-(benzonitrile)dichloro-

palladium(II)[41] in dichloromethane gave a pale yellow microcrystalline solid (145). The analysis data are not consistent with either a mono- or a dinuclear palladium complex. The insolubility of species (145) in most common solvents (water, alcohols, dimethylsulphoxide, acetone, chlorinated solvents) precluding solution analysis indicates that the presence of an oligomeric species must be considered.

CHAPTER SIX - COMPLEXATION STUDIES OF LIGANDS WITH TWO SIMILAR OR DISSIMILAR BINDING UNITS WITH TRANSITION METAL CATIONS [NOTABLY RH(I), PD(II), AND PT(II)]

6.1 Introduction

As has been expounded in Chapter Three, ligands (92), and (94)-(96) have been synthesised and their complexing properties with various metal cations studied. Ligands (95) and (96) combine a *soft* pyridyl-dithio (PyS_2) binding unit with a *harder* polyether binding unit. These ligands with two clearly dissimilar binding units may exhibit haptosectivity.[70] In particular, the rhodium(I) complexes of ligands (94) to (96) have been isolated in which the $(Rh\text{-}CO)^+$ unit binds to the *soft* NS_2 sub-unit. At the outset of this work, it was anticipated that the carbonyl group could be oriented towards the crown ether chain.

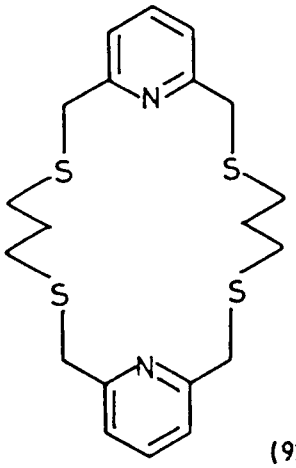

(92)

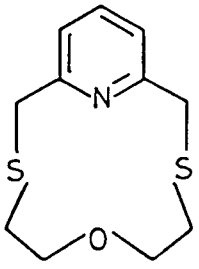

(94)

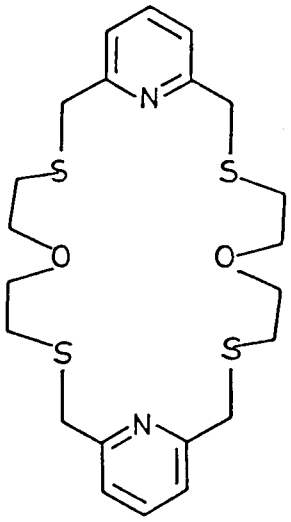

(94a)

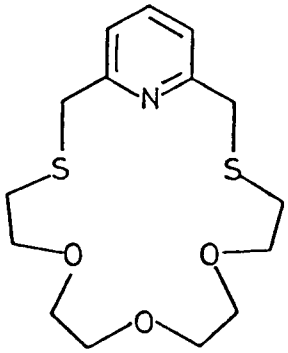

(95)

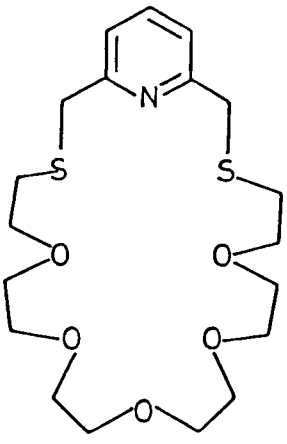

(96)

It was intended to investigate the formation of hetero-dinuclear complexes, and examine the potential activation of the CO substrate towards nucleophilic reactions at the carbon centre. The cationic complexes with other noble metals (palladium and platinum) have also been examined.

Ligand (92)[41] combines two pyridyl-dithio (PyS_2) binding units and may be expected to form homo-dinuclear or mononuclear complexes (the latter utilising the S_4 binding site). The complexation chemistry of ligand (92) has been further investigated.

6.2 Synthesis of the Ligands

Sulphur-containing macrocycles are accessible in particular by cyclisation reactions involving the formation of two carbon-sulphur bonds. Condensation of propane-1,3-dithiol with 2,6-dibromomethyl-pyridine (146) in butan-1-ol yielded a mixture of compounds from which the tricyclic ligand (92) and its bicyclic counterpart (92a) could be isolated.[41] Ligands (92) and (92a) were separated by chromatography on

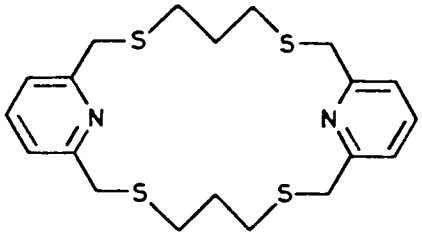

(92)

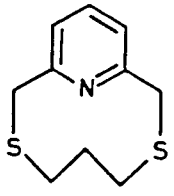

(92a)

alumina. Colourless crystals of ligand (92) were grown from methanol and an X-ray crystallographic analysis was performed. The molecular structure of the ligand is shown in Figure 6.1. The structure is disordered and a low temperature analysis is awaited (the current R factor is 9.7%: the central C_3 chains are clearly disordered). However, it is evident from the diagram that the molecular structure of the ligand has an effective mirror plane. The crystal structure determination also revealed that the sulphur heteroatoms are oriented away from the macrocyclic cavity, adopting an *exodentate* conformation. This fairly common orientation of sulphur atoms has been attributed to the preference of C-S linkages to adopt a *gauche* placement.[262]

gauche *anti*

The preference of C-S bonds for a *gauche* placement contrasts with the antipathy of C-O bonds for such an arrangement. The substantial difference in C-S and C-O bond lengths has a marked effect on the stabilising and destabilising 1,4 interactions encountered in *gauche* C-C-E-C and E-C-C-E (E = O,S) units, as shown in Figure 6.2. Whereas the *gauche* placement of a C-C-O-C fragment results in repulsion between the terminal hydrogen atoms, the *gauche* C-S linkages suffer little or no repulsion. Furthermore, the *gauche* placement of an S-C-C-S unit is disfavoured relative to the O-C-C-O unit as shown in Figure 6.3. The greater size of the sulhpur atoms causes electron-electron repulsions which destabilise such a *gauche* placement. In a cyclic thioether structure some bonds must adopt a *gauche* placement. It is the C-S bonds that are more likely to do so, predisposing the sulphur to an

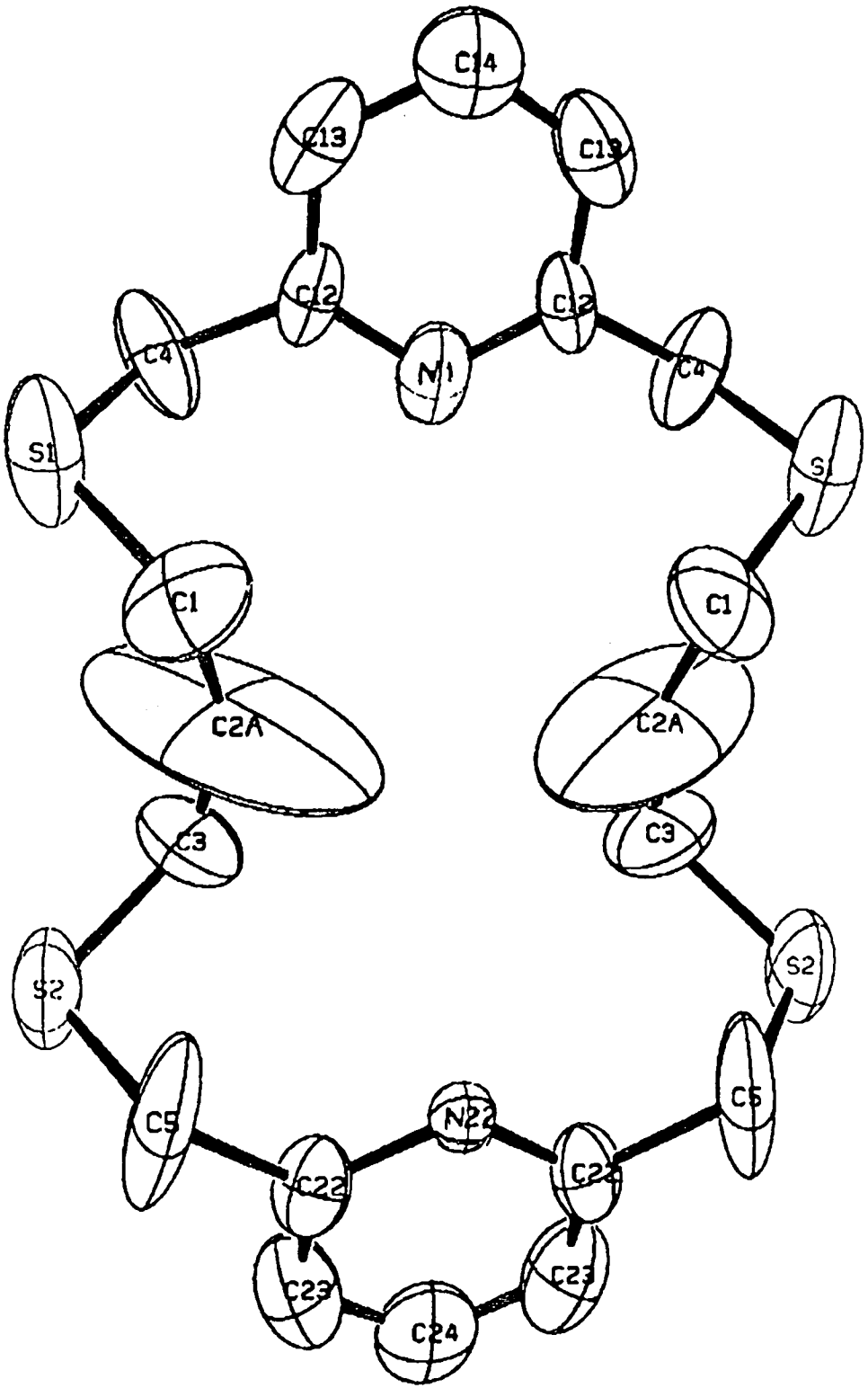

Figure 6.1

X-Ray crystal structure of ligand (92)

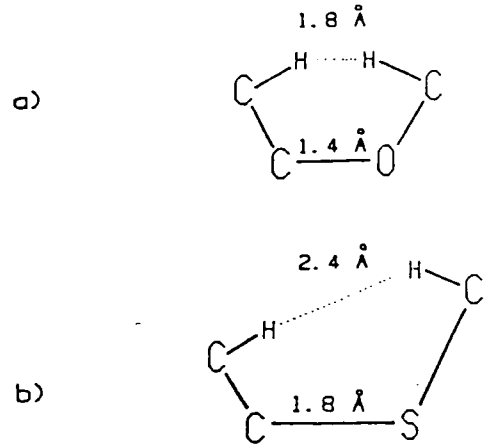

Figure 6.2

Schematic representation of 1,4-*interactions in* gauche $CH_2CH_2ECH_2$ *linkages*: (a) E = O; (b) E = S.

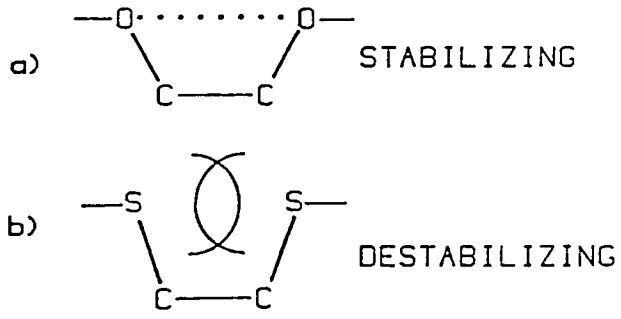

Figure 6.3

Schematic representation of 1,4-*interactions in* gauche ECH_2CH_2E *linkages*: (a) E = O; (b) E = S.

exo-conformation.

The unusual *exodentate* conformation adopted by many thioethers has important ramifications for coordination chemistry: the ligand must undergo conformational change in order to form a complex where the

cation is bound within the macrocyclic cavity. Indeed, niobium pentachloride reacts with the symmetrical tetrathia-14-crown-4 ligand[263] to give an adduct in which two $NbCl_5$ fragments are bridged by two sulphur atoms of the macrocycle. The macrocycle takes up an *exo*-conformation, in a similar manner to the free ligand itself.[264] Ligand (95) however adopts diverse conformations within its complexes. In the barium complex of ligand (95)[265] both sulphurs are *endocyclic*, as shown in Figure 6.4 and the alkaline earth cation is held in the centre of the cavity by interactions with all six heteroatoms of the macrocycle. In the copper(II) complex of ligand (95)[265] also shown in Figure 6.4, in which only the N and two S atoms of the pyridyl-dithio unit of the ligand are bound to the copper, both sulphur atoms adopt *exocyclic* conformations. Two chlorine atoms complete the coordination sphere of the copper atom. The polyether chain is folded away from the metal centre. In the Ag(I) complex of ligand (95) (crystals grown by A.S. Craig)[266] the dimeric cationic structure (Figure 6.5) revealed two vastly different coordination spheres for the two silver atoms. One silver is bound by three oxygens of a polyether chain, the nitrogen of a pyridine ring and an *endocyclic* sulphur atom of the same ligand. The remaining sulphur atom adopts an *exodentate* conformation, that is, the chelating pair of electrons are oriented away from the macrocyclic cavity, and binds to the second silver atom. The coordination sphere of this second silver atom is completed by binding to the nitrogen atom, one oxygen atom, and both *endodentate* sulphur atoms of the second ligand. Thus, the second silver atom is bound by three sulphur atoms in total. The dimeric $[(95)_2\text{-}Ag_2]^{2+}$ cation thereby constitutes an interesting example of a complex in which a ligand exhibits simultaneous *exodentate* S-binding to one cation and *endodentate* S-binding to

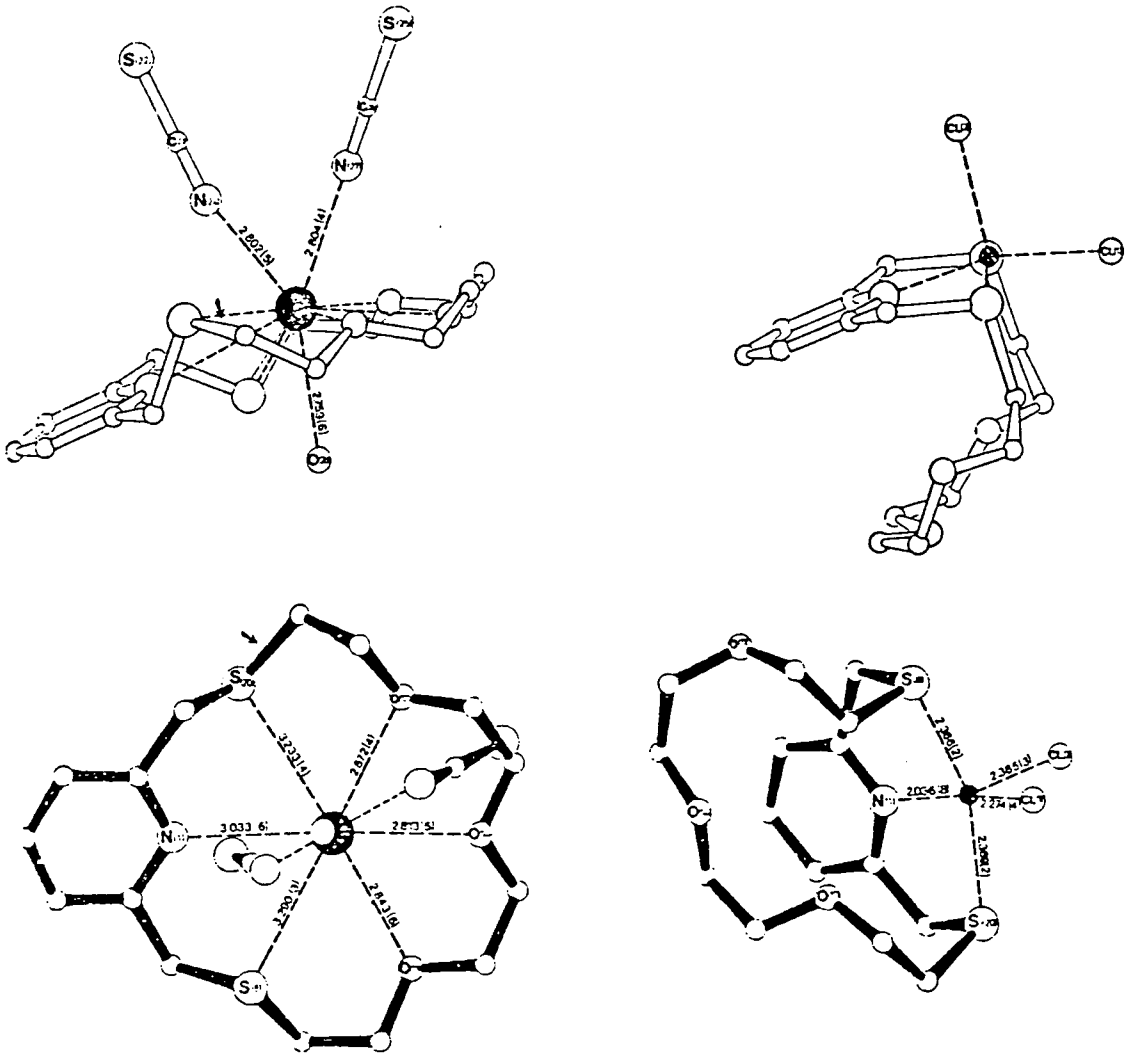

Figure 6.4

Perspective views of the barium complex of ligand (95) (left) *and of the copper(II) complex* (right)

another.

Ligands (94) and (94a) were prepared by the condensation of 2-mercaptoethylether with 2,6-dibromomethylpyridine (146) in butan-1-ol. The ligands (94) and (94a) were also separated by chromatography on

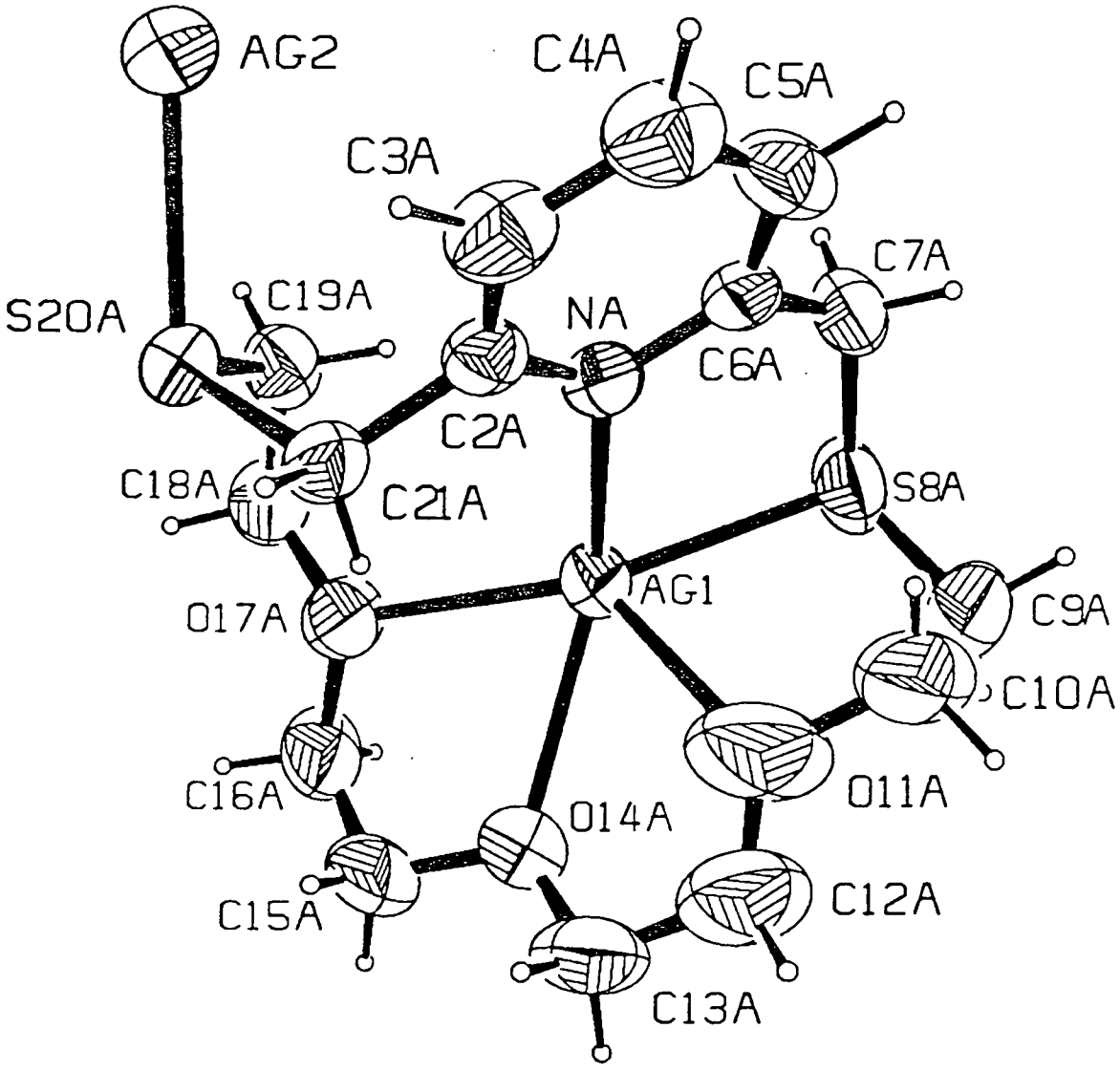

Figure 6.5

X-Ray crystal structure of the silver(I) dimeric complex of ligand (95)

(a) *The ORTEP diagram showing the coordination sphere of one silver atom,* Ag(1)

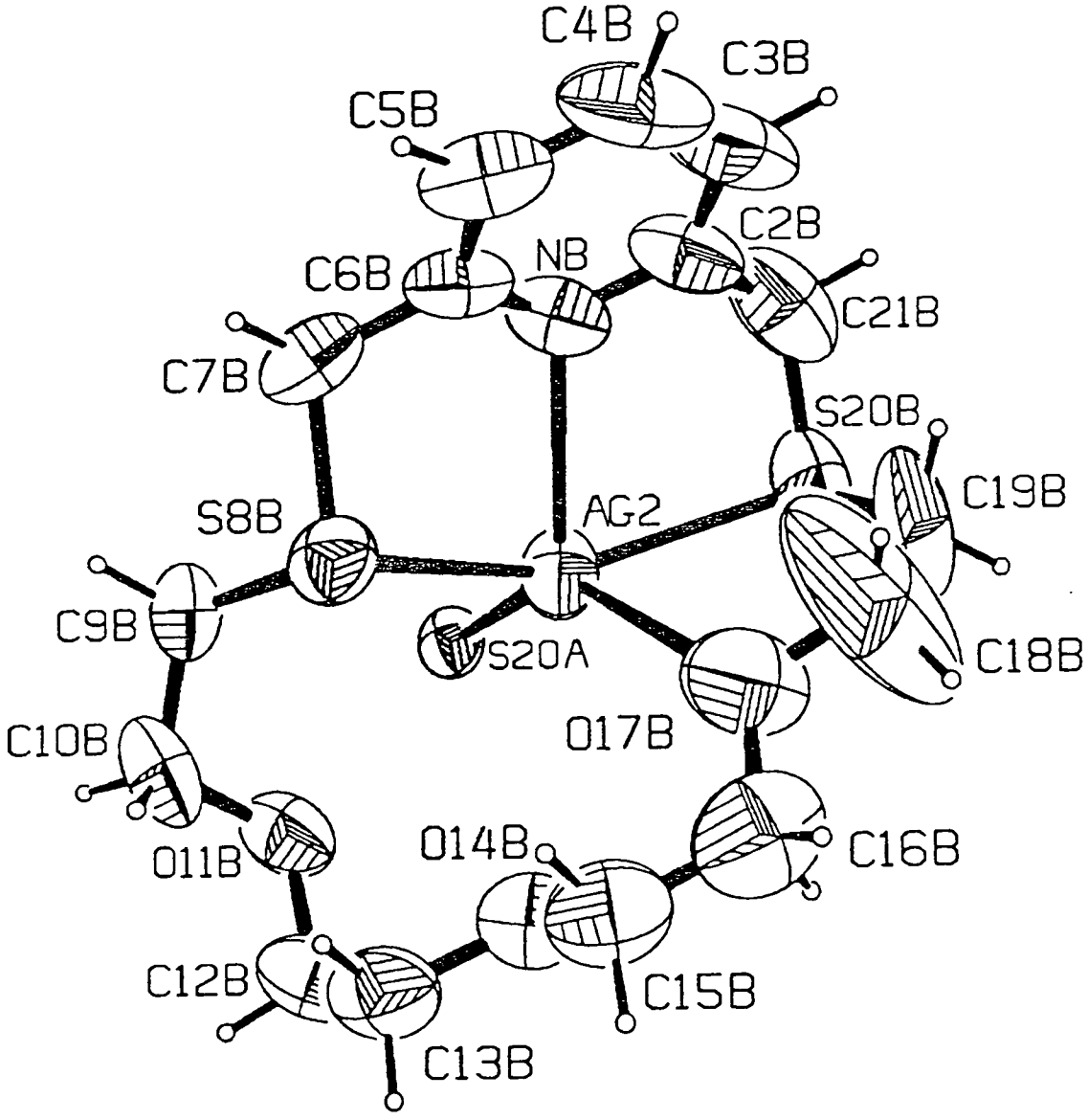

(b) *The ORTEP diagram showing the coordination sphere of silver atom,* Ag(2)

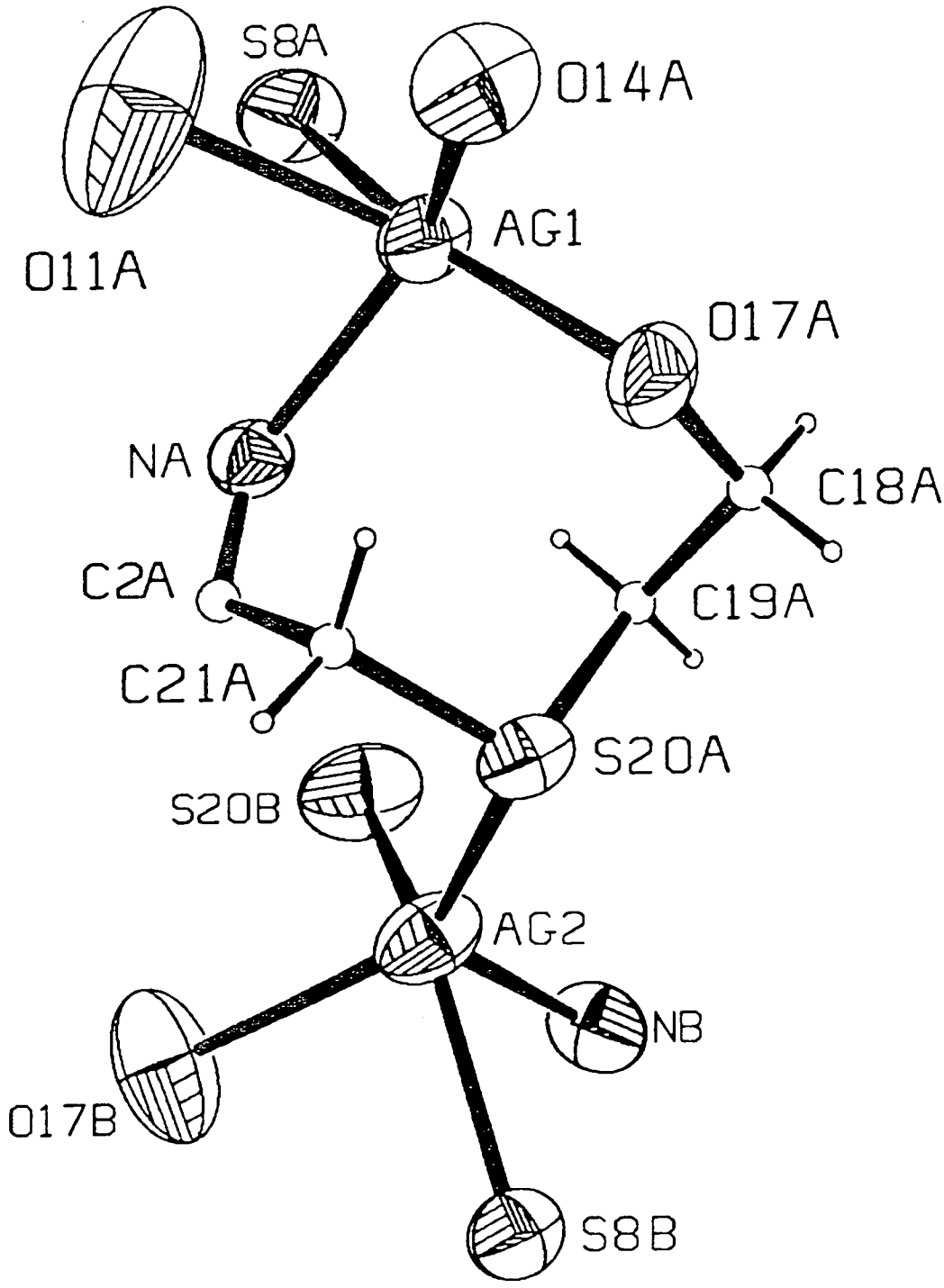

(c) *The ORTEP diagram showing the link between the two silver monomeric units*

alumina.

Ligand (95) was prepared by the reaction of the disodium salt of 2,6-dithiomethylpyridinde with the diiodo compound 1,11-diiodo-3,6,9-trioxaundecane (99) in butan-1-ol. Purification of (95) was effected by chromatography on alumina to give a colourless oil which was crystallised from hexane. The disodium salt of 2,6-dithiomethypyridine was prepared from 2,6-dihydroxypyridine using established procedures.[54,267] The reaction scheme for the synthesis of ligand (95) is given in Scheme 6.1. Ligands (94) and (95) have previously been described in the literature but were prepared by a different synthetic route.[265,268]

Ligand (96) was prepared by the reaction of the disodium salt of 2,6-dithiomethylpyridine (148) with hexaethylene glycol ditosylate (150) in butan-1-ol. Purification of (96) was effected by chromatography on alumina followed by extraction with hexane to give a colourless oil. Hexaethylene glycol ditosylate (150) was prepared from hexaethylene glycol (149) which was in turn synthesised from diethylene glycol using literature procedures.[269] The reaction sequence for the synthesis of ligand (96) is given in Scheme 6.2.

6.3 Rhodium Complexes

6.3.1 *Rhodium Complex of Ligand* (95), PyS_2O_3

Reaction of (95) with $[Rh_2Cl_2(CO)_4]$ in methanol was accompanied by a brisk evolution of carbon monoxide and the addition of an excess of ammonium hexafluorophosphate as a solution in methanol led to the slow formation of a red micro-crystalline solid (151). On standing of the

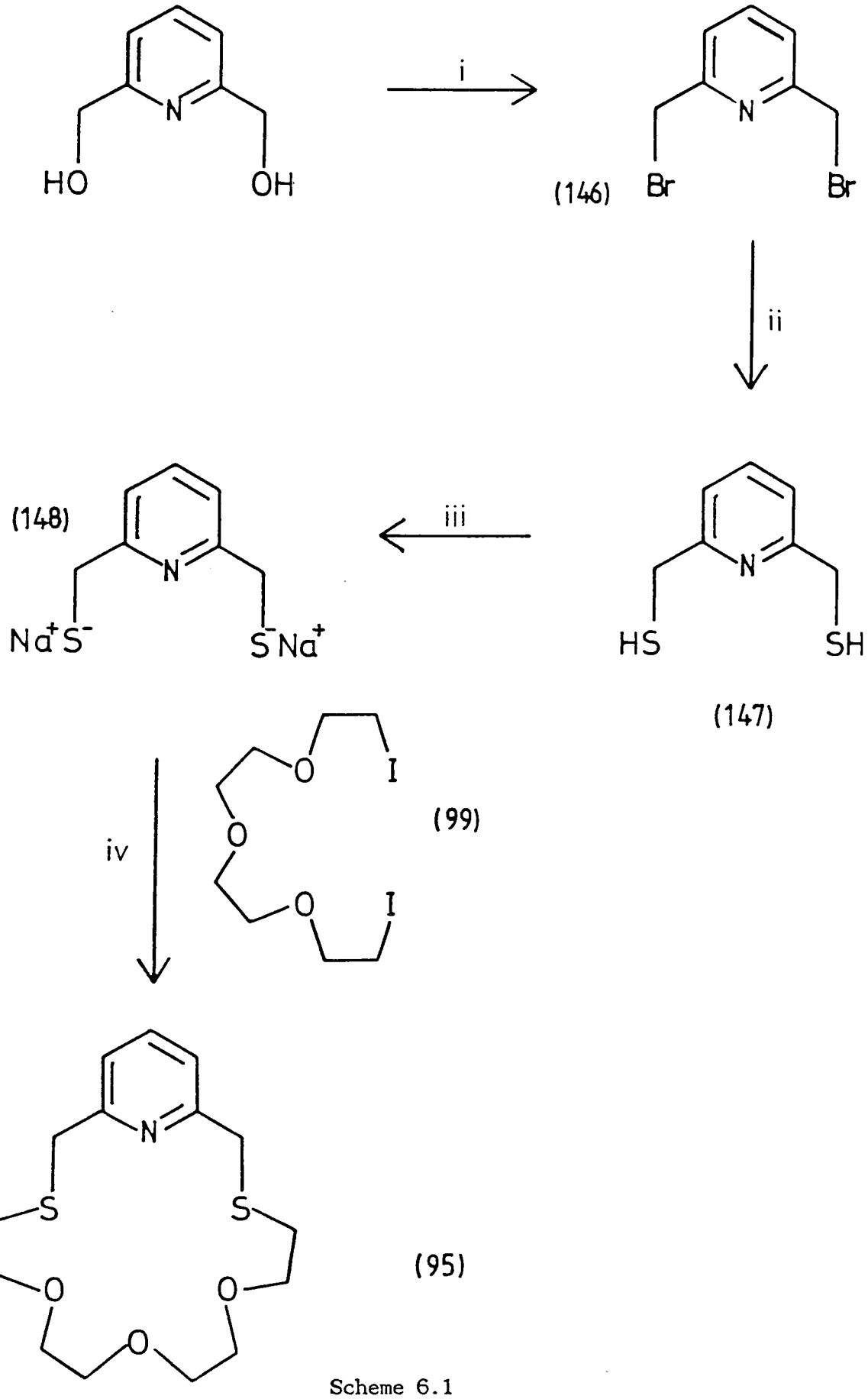

Scheme 6.1

i, HBr, AcOH; *ii*, thiourea, EtOH, Δ; *iii*, NaOH; *iv*, butan-1-ol, Δ.

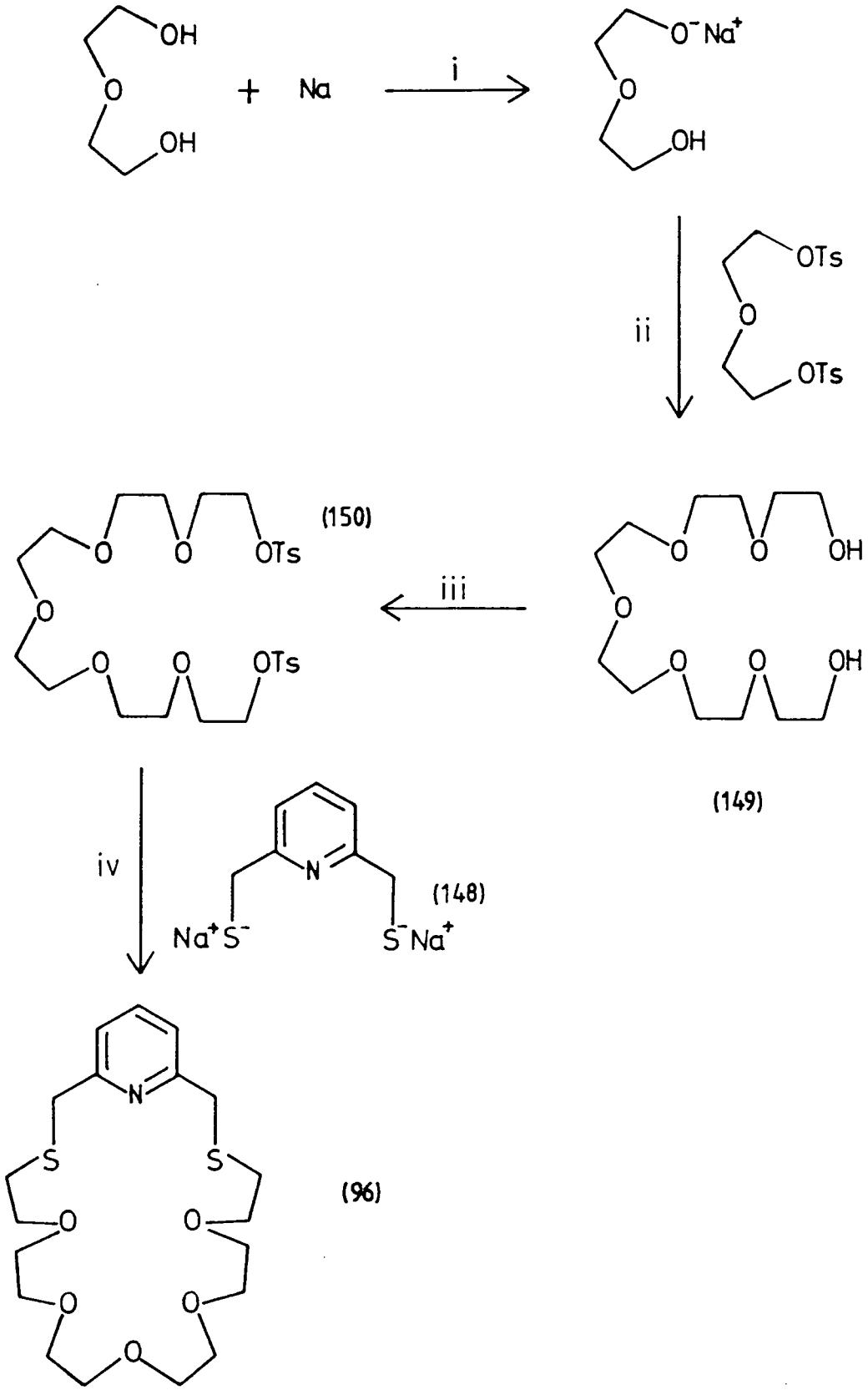

Scheme 6.2

i, N_2, 20°; *ii*, Δ; *iii*, TsCl, pyridine, -20°; *iv*, butan-1-ol, Δ.

supernatant, ruby-red diamond-shaped crystals of the complex were formed. The FAB mass spectrum in a glycerol matrix gave a peak centred at *m/e* 460 corresponding to $[(95)\text{-}Rh(CO)]^+$. The infrared carbonyl stretch occurred at 2020 cm^{-1}, consistent with a terminal rhodium carbonyl.[40,41,43,70] The ^1H NMR spectrum (see Figure 6.6) (298 K; CD_2Cl_2 as solvent) revealed that the benzylic methylene protons were diastereotopic (δ 4.79 and 5.07 ppm), consistent with stereogenic sulphur centres with a stable configuration. The data were consistent with the formation of a haptoselective complex (151) in which an $(Rh\text{-}CO)^+$ group is bound to the soft pyridyl-dithio PyS_2 unit of (95), in a square planar coordination geometry. Such species have been reported

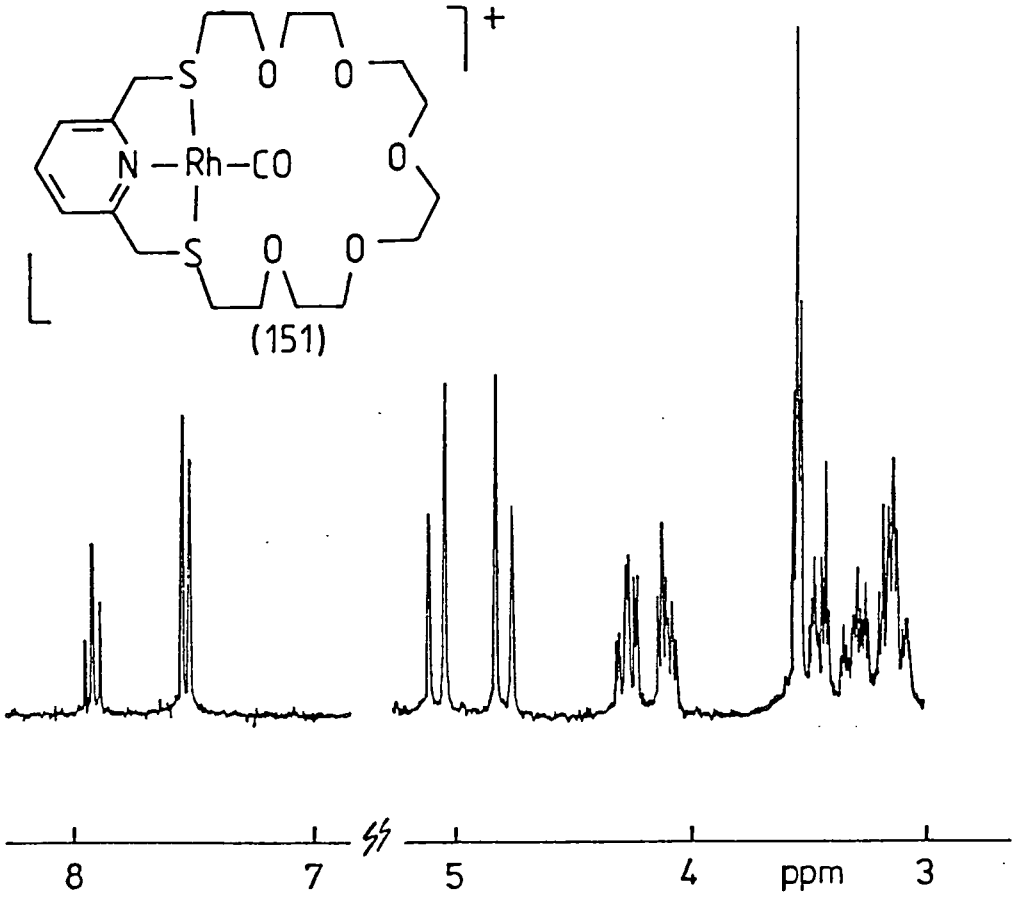

(151)

Figure 6.6

250 MHz ^1H NMR spectrum of complex (151)

with other ligands incorporating the PyS_2 binding unit.[41,70] Since it was anticipated that in (151) the carbonyl group may have been oriented towards the polyether chain, it was of interest to investigate the formation of Rh-Li hetero-dinuclear complexes. In particular, the activation of the carbonyl group was sought involving interaction between the oxygen lone-pair of the rhodium-bound carbonyl group and the proximate Lewis acidic centre (see Chapters 1 and 3). However the infrared carbonyl stretching frequency of complex (151) was not perturbed by the addition of $LiClO_4.H_2O$ to a solution of the complex in dichloromethane, acetone, or tetrahydrofuran. Reaction of complex (151) in dry dichloromethane with phenyl lithium in cyclohexane:ether solution[68] also gave no perturbation of the infrared carbonyl stretching frequency. There was no evidence therefore for the formation of a metal-acyl or for binding of a IA cation to the bound CO..

The crystal structure analysis of the complex cation (151)[270] offers an explanation for the observed behaviour. The structure of the cation is shown in Figure 6.7 and the pertinent crystal data are given in Chapter Seven. The crystal structure of (151) revealed that the complex was dimeric with a weak rhodium-rhodium interaction [Rh-Rh = 3.3320(6) Å]. In solution, dissociation occurs readily - particularly in coordinating solvents such as acetonitrile and acetone - to give yellow solutions. Similar weak rhodium-rhodium bonds have been observed in other dicationic systems.[271-273] The coordination about each rhodium may be regarded as a distorted square pyramid in which the principle distortion arises from the obtuse S(8)-Rh-S(20) bond angle of 169.8°. This is because of the intrinsically small bite angles of the two adjacent five-ring chelates.

The crystal structure also reveals that the Rh-CO vector is

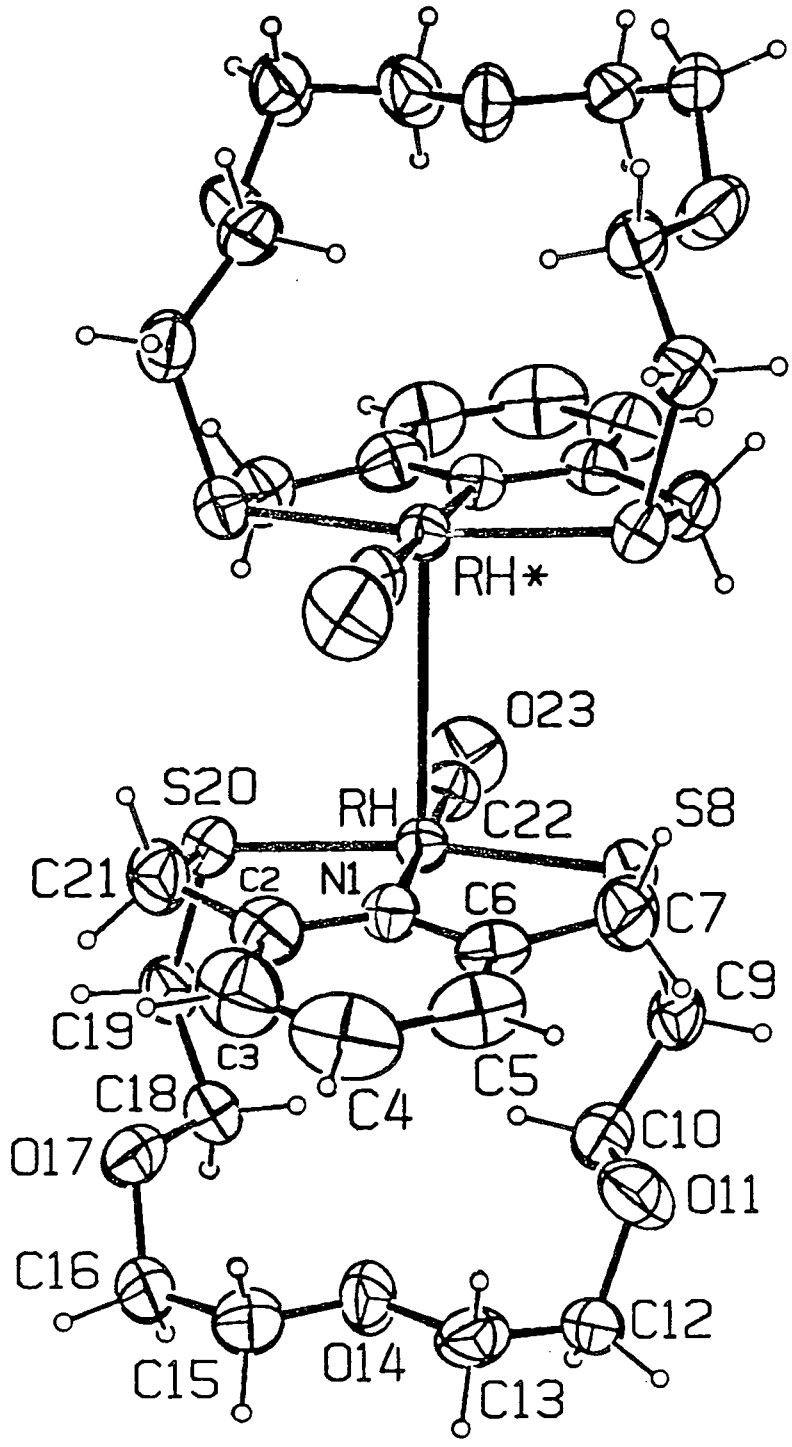

Figure 6.7

Perspective ORTEP drawing of the di-rhodium complex cation (151).

Main dimensions are: Rh-S(8) 2.295(2), Rh-S(20) 2.298(2), Rh-N(1) 2.060(4), Rh-C(22) 1.833(6), Rh-Rh 3.3320(6) Å; N(1)-Rh-S(8) 85.1, N(1)-Rh-S(20) 85.7, N(1)-Rh-C(22) 179.2, S(20)-Rh-S(8) 169.8, C(22)-Rh-S(8) 94.2°.

directed *away* from the polyether chain which itself folds back to sit over the electron-poor pyridinium ring. Similarly, stabilizing interactions between macrocyclic polyethers and pyridinium cations have been defined recently.[274-277] Thus, the tendency of the rhodium centres to interact, and the weakly stabilising effect of the pyridinium ring intramolecularly associating with the polyether chain disfavour the interaction between the oxygen lone-pair of the rhodium-bound carbonyl and any bound lithium atom.

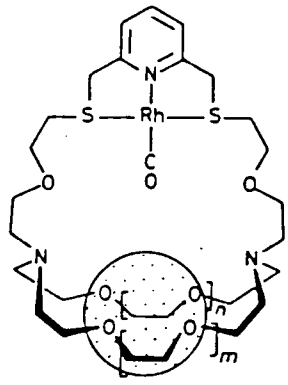

This same alignment is therfore probably disfavoured in other recently reported macrocyclic ligands incorporating the same 2,6-dithiomethylpyridine sub-unit.[†] [70]

[†]Similar arguments explain the lack of magnetic coupling observed between a copper(II) cation bound to a pyridine [NS_2] ligand and a proximate iron-porphyrin as the copper $d_{x^2-y^2}$ orbital will be oriented *away* from the iron d_{z^2} orbital.[278]

6.3.2 *Rhodium Complexes of Ligands* (94), PyS_2O *and* (94a), $Py_2S_4O_2$

Reaction of (94) with $[Rh_2Cl_2(CO)_4]$ in methanol was accompanied by a brisk evolution of carbon monoxide and a darkening of the solution to a deep blue. Ammonium hexafluorophosphate was added as a solution in methanol and an indigo crystalline complex (152) formed immediately. The carbonyl stretch in the infrared occurred at 1740 cm^{-1}, consistent with the presence of bridging carbonyl groups.[41,42] The ^1H NMR spectrum (298 K; CD_3CN as solvent) revealed that the benzylic methylene protons were diastereotopic, suggesting that the pyridine ring and both the sulphur atoms were bound to the rhodium. The complex was soluble only in polar solvents (DMF, CH_3CN) and rapidly decomposed. Elemental analysis was consistent with the formation of a cationic rhodium carbonyl complex with a ratio of carbonyl to rhodium of 1:1, $[(94)_x(RhCO)_x].x(PF_6)$. The bridging carbonyl groups enforce a Rh-Rh interaction which may be associated with the deep indigo colour of the complex. A description of the electronic structures of systems with weak metal-metal bonds between square planar systems has received attention.[279-281] It is now well established that a principal electronic spectroscopic feature of dinuclear rhodium(I) isocyanide complexes is a prominent low-lying absorption band attributable to $^1A_{1_g} \longrightarrow {}^1A_{2_u}$. The transition involves axially directed donor and acceptor orbitals and the energy of the transition should be a sensitive function of the metal-metal interaction.

Reaction between $[Rh_2Cl_2(CO)_4]$ and the ligand with an equivalent length of alkyl chain between the sulphurs (94b) (*i.e.* replacement of the oxygen atoms in the ligand by CH_2) was reported to give a violet crystalline complex (153)[41] with a terminally bound CO ligand, and the ^1H NMR gave an AB pattern for the benzylic methylene protons. The

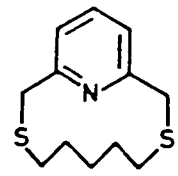

(94b)

violet colour of the solid is suggestive of a rhodium-rhodium interaction in the solid-state.

A similar weak interation between Rh atoms may occur in the deep red dirhodium complex (154) formed on reaction of $[Rh_2Cl_2(CO)_4]$ with ligand (92).[41] The rhodium atoms may be constrained to interact by the ring topology: complex (154) is soluble only in polar solvents (DMSO, CH_3CN) and gives red solutions.

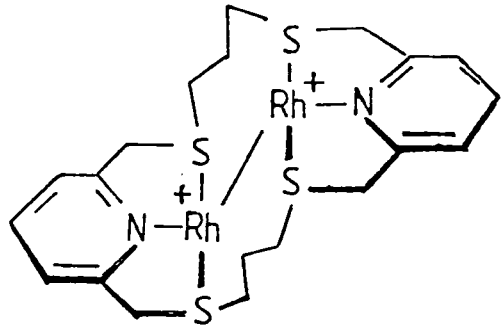

(154)

Reaction of (94a) with $[Rh_2Cl_2(CO)_4]$ in methanol followed by the addition of ammonium hexafluorophosphate gave a brilliant red precipitate (155). Complex (155) was also isolated as tiny red crystals. The spectroscopic properties observed for (155) indicated the formation of a dinuclear complex with two terminal carbonyl groups (one per rhodium atom)[υ_{max} (C=O) 2044, 1993 cm^{-1}].[41] The two carbonyl siganls may be related to the formation of two diastereoisomers. These may be considered as those formed when the configurations of the sulphur atoms are either [RSRS] or [SRRS]. It seems likely that the structure of (155) resembles that of (154) in the solid-state, but dissociation of any weak rhodium-rhodium bond would occur readily in solution.

The photochemical properties of these systems may be examined in the future, particularly for those systems in which the rhodiums are constrained to interact.

6.3.3 *Rhodium Complexes of Ligand* (96) PyS_2O_5

Reaction of (96) with $[Rh_2Cl_2(CO)_4]$ in methanol followed by the addition of an excess of ammonium hexafluorophosphate as a solution in methanol gave a red microcrystalline solid (156). Transformation to a bright yellow solid occurs readily when the complex is wet and exposed to air. It may be the case that the red form of the complex is the analogous dimeric species to (151) and the yellow form is the analogous monomeric species. The FAB mass spectrum of (156) revealed peaks centred at *m/e* 548 and 520 corresponding to $[(96)-Rh(CO)]^+$ and $[(96)-Rh]^+$ respectively. The carbonyl stretching frequency in the infrared occurred at 2020 cm^{-1} consistent with a terminal rhodium carbonyl.[40,41,43,70] The complex gave an exchange-broadened ^1H NMR spectrum (298 K; CD_2Cl_2 as solvent). On cooling of the solution to 260 K the signals sharpened and revealed a simple AB pattern for the

benzylic protons, (δ 4.91 and 5.05 ppm). The inversion at sulphur ($\Delta G^{\neq}$ = 64 kJ mol^{-1}) may be attributable to a ring *skip* of the flexible polyether chain over the Rh-CO vector. The carbonyl stretching frequency was not perturbed by the addition of metal salts (neither $LiClO_4$ nor KPF_6) to a solution of the complex in CD_2Cl_2. Colourless cubic crystals (157) however, were grown from a methanolic solution containing ligand (96) and potassium chloride. The FAB mass spectrum of this complex in a glycerol matrix gave a peak centred at *m/e* 456 corresponding to $[(96)\text{-}K]^+$. The ^{13}C NMR spectrum of complex (157) gave resonance values for the carbons in the polyether chain (CH_2O's) which had shifted ($\Delta\delta$ = 0.45 - 0.76 ppm) relative to the same resonances in the free ligand. This behaviour is indicative of binding of the potassium cation to the polyether chain. It is likely that the orientation of the carbonyl group is again away from the polyether chain and is inappropriate for CO activation.

Reaction of the ditopic macrocycle (96) with rhodium trichloride in boiling methanol followed by the addition of ammonium hexafluorophosphate yielded an orange crystalline complex (158), whose FAB mass spectrum in a glycerol matrix revealed peaks at *m/e* 608, 573, 555, and 520 corresponding to $[(96)\text{-}RhCl_2(H_2O)]^+$, $[(96)\text{-}RhCl(H_2O)]^+$, $[(96)\text{-}RhCl]^+$, and $[(96)\text{-}Rh]^+$ respectively. The same complex was also formed by aerial oxidation of the cationic rhodium(I) carbonyl complex, (156), in chloride saturated methanol. The ^1H NMR spectrum (298 K; CD_2Cl_2 as solvent) revealed that the benzylic methylene protons were diastereotopic (δ 4.92 and 4.70 ppm) consistent with stereogenic sulphur centres with a stable configuration. The crystal structure of (158)[282] (Figure 6.8) showed an octahedral coordination for the Rh(III) centre in which the main distortion arises from the S(8)-Rh-S(26) bond angle of

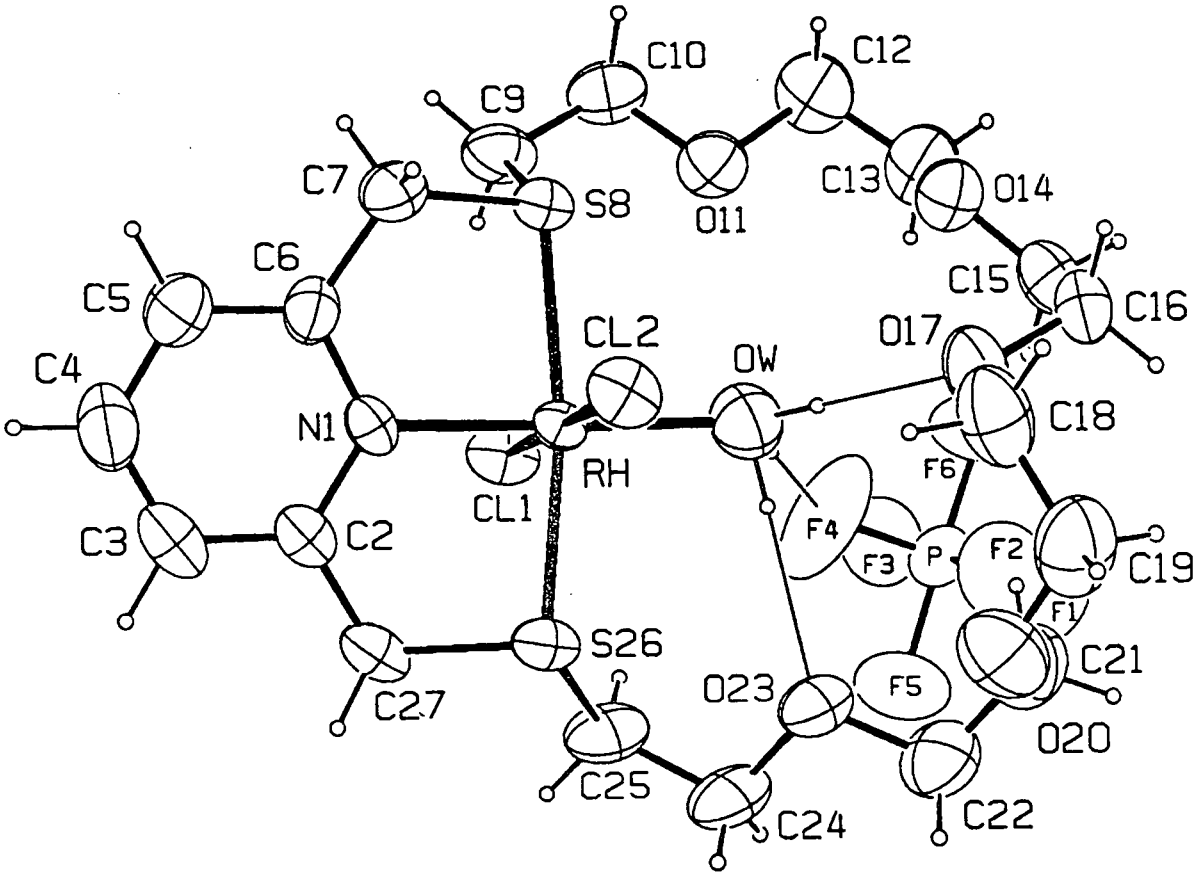

Figure 6.8

X-Ray crystal structure of complex (158).

Main dimensions: Rh-N(1) 2.025(4), Rh-O(W) 2.070(4), Rh-Cl(1) 2.332(1), Rh-Cl(2) 2.330(1), Rh-S(8) 2.329(1), Rh-S(26) 2.327(1), O(W)...F(4) 3.133(6), O(W)...O(17) 2.986(6), O(W)...O(23) 3.128(6)Å; S(8)-Rh-S(26) 166.76(5), O(W)-Rh-N(1) 178.2(2), Cl(1)-Rh-Cl(2) 179.50(5)°.

166.76(5)°. Once again this is associated with the intrinsically small bite angles of the two five-ring chelates. The coordinated water molecule is strongly bound to the Rh(III) centre[283] [Rh-O(W) = 2.070(4) Å) increasing the polarisation of the OH bonds which are directed towards the polyether chain. The bound water molecule is stabilised by intramolecular hydrogen-bonding to the polyether chain. Electron density difference maps at R = 0.025 showed that the water hydrogens are disordered over three sites (occupancies from peak densities are 0.72, 0.80, and 0.48) and form three bonds. Two of these are intramolecular bonds to O(17) and O(23) and the third is to a fluorine atom of the PF_6 counter-ion. This secondary binding is a consequence of the enhanced acidity of the coordinated water molecule. Although this binding of a neutral ligand (H_2O) to the metal centre (Rh) within a macrocyclic complex is a common feature of the coordination chemistry of macrocyclic systems, there are very few examples[284,285] in which the complex is further stabilised by secondary binding of the neutral ligand to the receptor molecule. Stoddart[284] *et al.* reported the dirhodium diammine *bis*(1,5-cyclooctadiene) complex of diaza-18-crown-6, in which the rhodium is bound by simultaneous first and second sphere coordination, the latter through the neutral ammonia molecule, as shown in Figure 6.9. Alcock and Brown[285] have characterised an acyclic phosphine complex in which the rhodium atom is complexed by a water molecule which is simultaneously bound to a polyether chain (Figure 6.10).

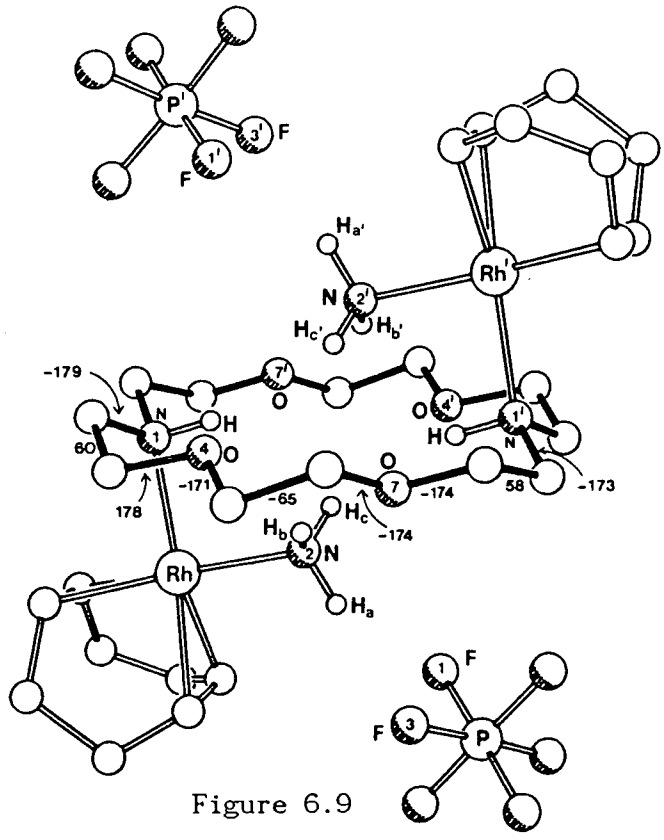

Figure 6.9

X-Ray crystal structure of the dirhodium diammine bis(1,5-cyclooctadiene) complex of diaza-18-crown-6

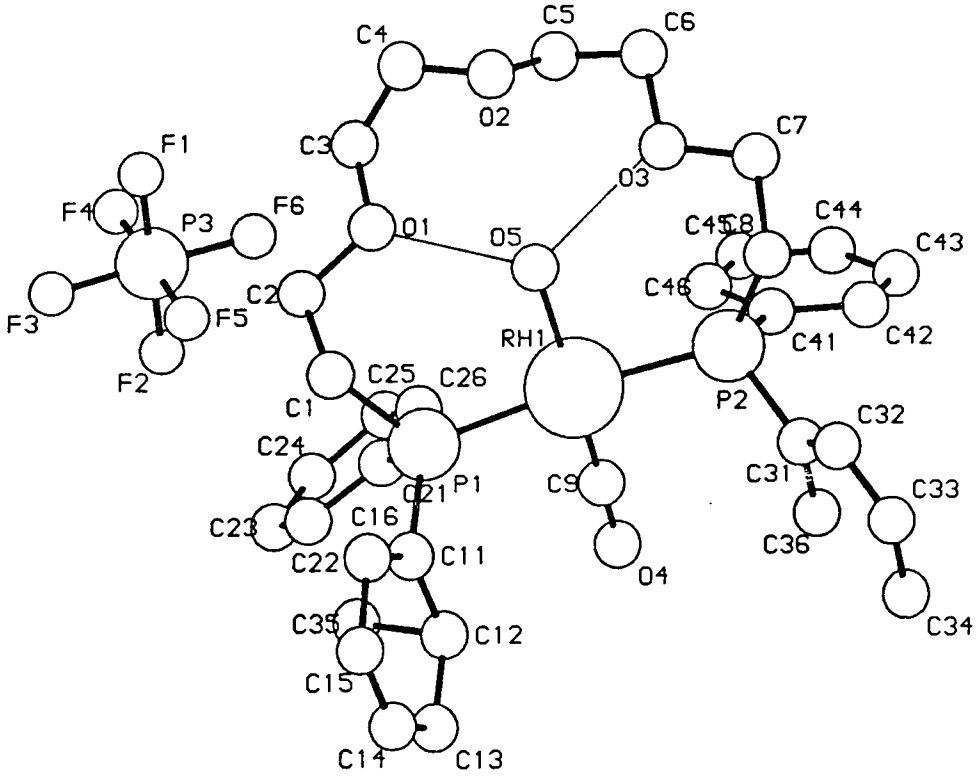

Figure 6.10

X-Ray crystal structure of the phosphine complex

6.4 Palladium and Platinum Complexes

Ligands (95) and (96) also form monocationic complexes with other noble metals such as palladium and platinum.

6.4.1 *Ligand* (95), PyS_2O_3

Reaction of one equivalent of $[PdCl_2(PhCN)_2]$ with (95) in boiling dichloromethane yielded the bright yellow compound $[(95)\text{-}PdCl]^+ Cl^-$ (159) which is soluble in water. The ^1H NMR spectrum revealed an AB quartet for the benzylic protons (δ 4.96 and 5.12 ppm) and a simple doublet and triplet for the aromatic ring protons, as shown in Figure 6.11. The positive ion FAB mass spectrum of complex (159) in a glycerol matrix revealed peaks at 470 and 435 with the expected palladium isotope patterns, corresponding to $[(95)\text{-}PdCl]^+$ and $[(95)\text{-}Pd]^{2+}$. The spectroscopic data are consistent with the expected structure

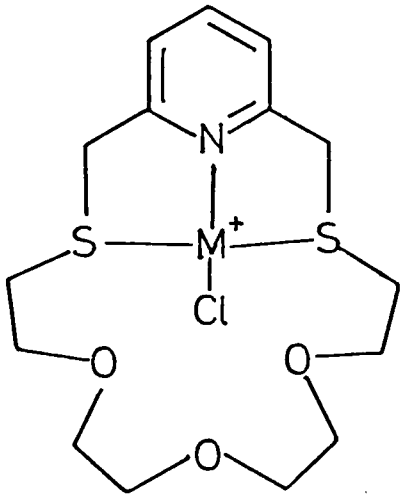

(159) M = Pd

(160) M = Pt

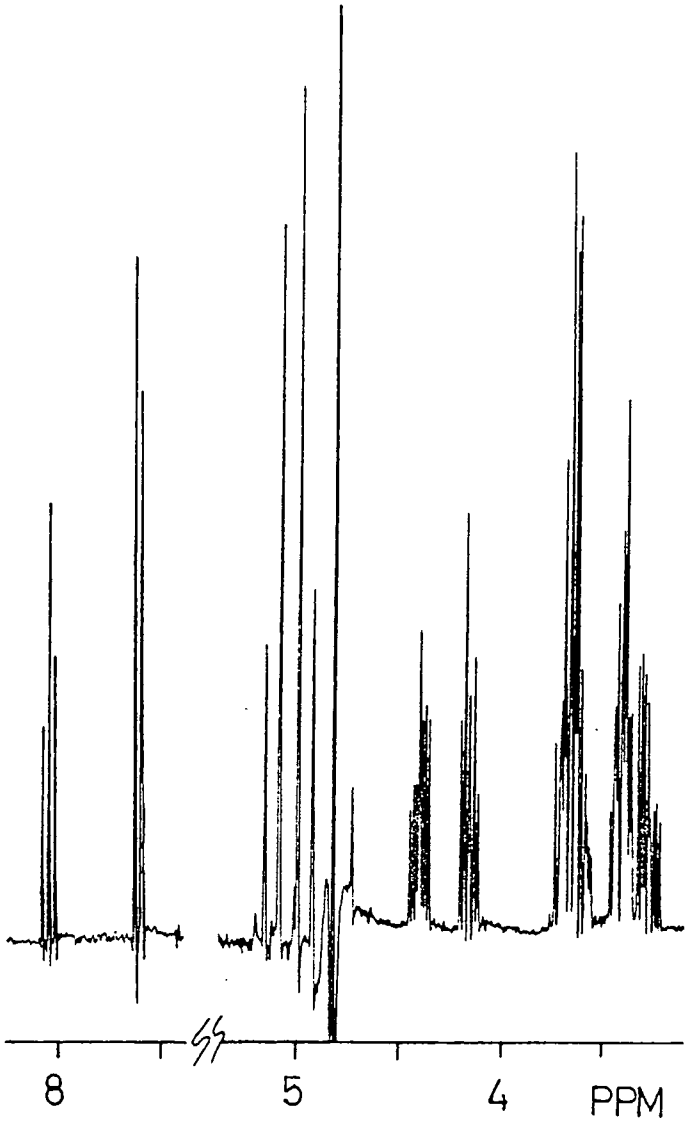

Figure 6.11

250 MHz ^1H NMR spectrum of complex (159)

represented by (159), in which the palladium is coordinated to the pyridyl-dithio (PyS_2) binding unit in a similar fashion to the analogous Rh-CO complex (151). The polyether chain is probably folded back over the electron-poor pyridinium ring in the solid-state.[270]

Reaction of one equivalent of $[Pt(t\text{-}BuCN)_2Cl_2]$ with ligand (95) in refluxing dichloromethane gave a white solid $[(95)\text{-}PtCl]^+ Cl^-$ (160), which is also soluble in water. The ^1H NMR spectrum yielded an AB quartet for the benzylic protons (δ 5.05 and 5.30 ppm) and a simple doublet and triplet for the aromatic ring protons. The positive ion FAB

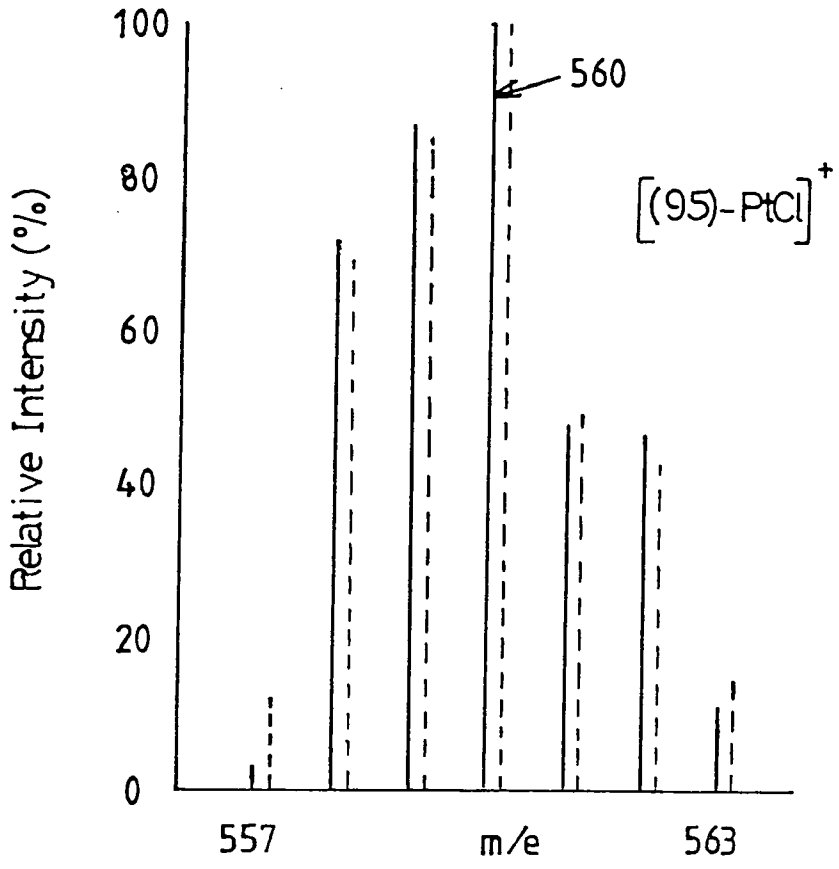

Figure 6.12

Positive ion FAB mass spectrum of complex (160) *recorded in glycerol*; (——) *calculated*, (---) *experimental*.

mass spectrum of complex (160) in a glycerol matrix gave peaks centred at *m/e* 560 and 525 with the expected platinum isotope patterns (as shown for the molecular ion in Figure 6.12), corresponding to $[(95)\text{-PtCl}]^+$ and $[(95)\text{-Pt}]^+$ respectively. Thus, the probable structure of the complex, represented by (160) is exactly analogous to the palladium complex (159), and similar to the $Rh\text{-}CO^+$ complex (151) characterised by X-ray crystallography.

6.4.2 *Ligand* (96), PyS_2O_5

Reaction of one equivalent of $[Pt(t\text{-}BuCN)_2Cl_2]$ with ligand (96) in boiling dichloromethane gave a white solid (161) which rapidly transformed into a yellow oil on contact with air. The positive ion FAB mass spectrum of complex (161) in a glycerol matrix gave peaks at *m/e* 647 and 612 corresponding to $[(96)\text{-}PtCl]^+$ and $[(96)\text{-}Pt]^+$ respectively. The ^1H NMR spectrum of the complex at 298 K in aqueous solution gave a sharply resolved spectrum. The aromatic ring protons appeared as two sets of doublets and triplets and the benzylic methylene proton resonance consisted of two overlapping AB systems, each with a coupling constant of 17.1 Hz. Such behaviour clearly suggests the presence of two distinct complexes in solution.

Reaction of one equivalent of $[PdCl_2(PhCN)_2]$ with ligand (96) in boiling dichloromethane yielded a yellow microcrystalline solid (162) whose positive ion FAB mass spectrum in a glycerol matrix gave peaks centred at *m/e* 558 and 523 with the expected isotope patterns, corresponding to $[(96)\text{-}PdCl]^+$ and $[(96)\text{-}Pd]^+$ respectively. The complex gave analogous behaviour in solution to the platinum complex (161) of the same ligand. In aqueous solution at 298 K, the ^1H NMR spectrum revealed sharply resolved resonances for the polyether ring protons, with two sets of doublets and triplets for the aromatic protons, again implying the presence of two complexes in aqueous solution. The broadened spectrum with CD_2Cl_2 as solvent suggested the existence of one complex only, with the benzylic methylene proton resonance consisting of an AB system. The solid-state structure is most likely analogous to that predicted for the palladium and platinum complexes of ligand (95), PyS_2O_3. The metal cation may bind to the pyridyl-dithio (NS_2) unit, as represented by (161) and (162). The solution-state structures are not

clear, but one complex is likely to be that represented by (161) and (162). A ring *skip* of the polyether chain over the metal-chlorine vector as observed for the $[RhCO]^+$ complex of ligand (96) is either hindered or unobserved on the time-scale of the experiment. We can only postulate partial aquation of the metal-chloride bond; or the presence of two diastereoisomers {sulphur configurations [SS] and [RS]} to account for the second complex. Further experiments are required to clarify the structural nature of these complexes.

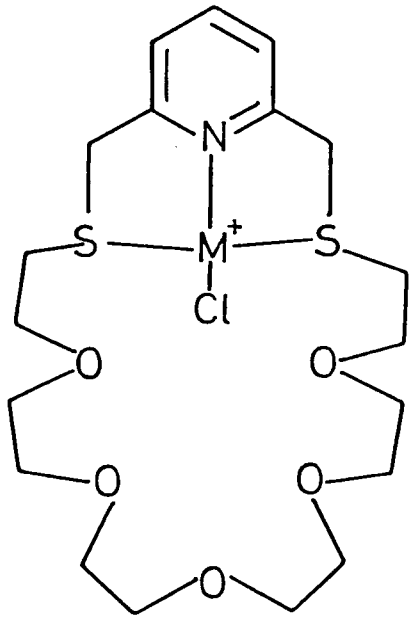

(161) M = Pt

(162) M = Pd

The palladium-chloride complexes (159) and (162) of the PyS_2O_3 and PyS_2O_5 ligands were treated independently with silver(I) nitrate in aqueous solution. Solid deposits of AgCl were removed by filtration and ammonium hexafluorophosphate was added as a solution in water. Yellow precipitates were isolated in each case. Atomic absorption spectrophotometry confirmed the complete loss of chlorine and gave palladium analyses consistent with palladium:ligand ratios of 1:1. The possible binding of a water molecule to the palladium cation in place of

the chlorine atom is currently under consideration. This complex may exhibit simultaneous primary and secondary coordination of the neutral water molecule as described for complex (158), $[(95)\text{-}Rh(H_2O)Cl_2]^+$.

Given that M-Cl bonds (M = Rh, Pt, Pd) may easily be cleaved by the addition of Ag^+ in solution, the complexes described may afford access to some coordinatively unsaturated d^8 complexes of potential catalytic activity, in which a neutral molecule (such as H_2O, NH_3, C_2H_4) or cationic guest (Na^+, K^+) may be closely bound within the macrocyclic ring.[274]

6.5 Complexation Studies of Ligand (92)

The reactions of $[Rh_2Cl_2(CO)_4]$ and $[PdCl_2(PhCN)_2]$ with ligand (92) have been investigated,[41] and the spectral data for the resulting complexes agree with the assignment of the structures represented by (163) and (164). As has already been suggested, it is possible that the two rhodium centres in complex (163) may be constrained to interact.

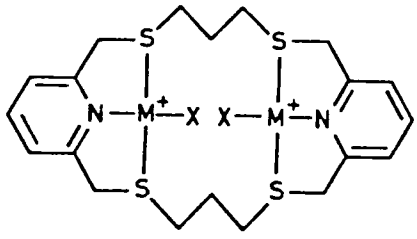

(163) M = Rh(I), X = CO

(164) M = Pd(II), X = Cl

6.5.1 *Palladium Complexes*

The dipalladium complex (164) was treated with an aqueous solution of silver(I) nitrate in order to cleave the Pd–Cl bond. Ethene gas was bubbled through the yellow solution for 30 min after which time silver chloride deposits were removed from the now claret-coloured solution. An excess of ammonium hexafluorophosphate was added as a solution in water whereupon a red solid was isolated. The intention was to form an intramolecular dihydroxy-bridge between the two palladium centres

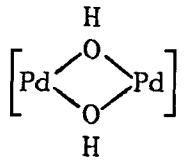

. An analogous intermolecular dirhodium(III)-dihydroxy bridge has been reported by Wieghardt,[283b] synthesised according to the following equations:

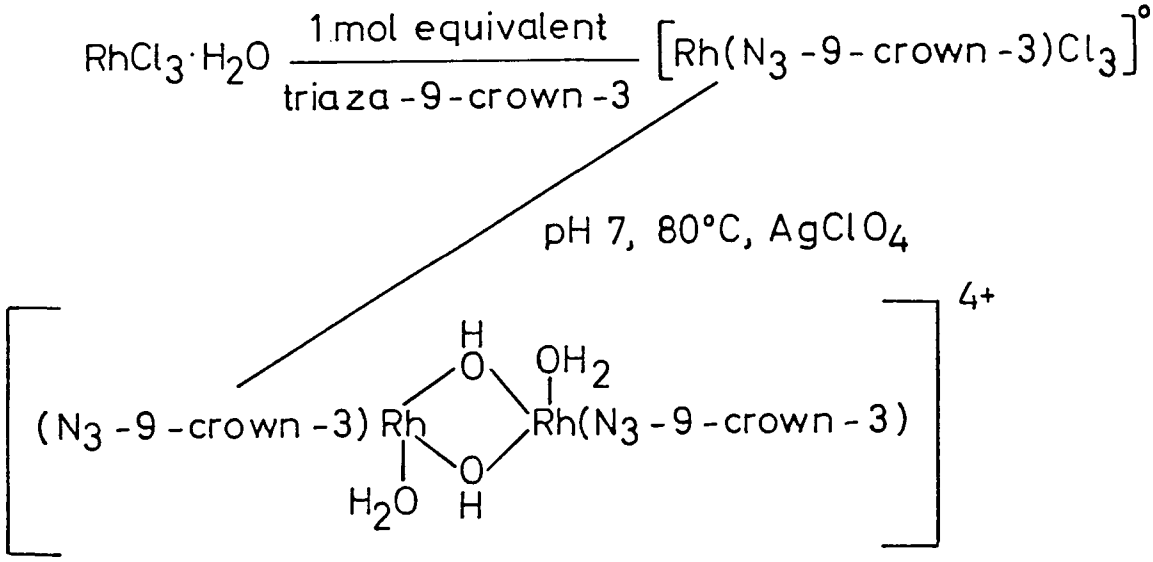

The reaction with complex (164) did not proceed in the absence of ethene which suggests that ethene was required to stabilise a coordinatively-unsaturated palladium intermediate (possibly following Pd-N bond cleavage). Atomic absorption analysis was consistent with the formation of the dipalladium-dihydroxy compound (165), $[(92)\text{-}Pd_2(OH)_2]^{2+}\ 2[PF_6^-]$.

The ^{1}H NMR spectrum recorded in d_6-acetone gave a sharply resolved triplet and doublet for the aromatic ring protons and a broad singlet for the benzylic protons. In contrast, the benzylic resonance for complex (164) appeared as an AB pattern. The AB system observed for the diastereotopic benzylic protons in complex (164) is consistent with all three donor atoms of the pyridyl-dithio unit (NS_2) binding to the palladium centre. The broad singlet observed for the bridged complex (165) suggests that either the N or one of the S atoms may not be bound to the palladium centre, (Section 6.4 discusses the IR data for the pyridine ring frequency stretches).

Reaction of ligand (92) with palladium(II) nitrate trihydrate in aqueous methanol gave a yellow complex (166) whose ^{1}H NMR spectrum in d_6-acetone gave a broadened spectrum (298 - 253 K). The compound may be a dinuclear complex in which the two metal centres are bridged by nitrate groups which may possibly dissociate in solution. The combustion analysis is consistent with the formation of a dinuclear complex $[(92)\text{-}Pd_2(NO_3)_2]^{2+}$ $2[NO_3]^-.2H_2O$.

6.5.2 *Nickel(II), Cobalt(II), and Copper Complexes*

Reaction of ligand (92) with cobalt(II) tetrafluoroborate gave a black solid (167) whose FAB mass spectrum in a 2,2'-thiodiethanol matrix gave a peak at *m/e* 481 corresponding to $[(92)\text{-}Co]^+$. Combustion analysis confirmed the likelihood of a ligand:cobalt ratio of 1:1.

Reaction of ligand (92) with nickel(II) perchlorate gave a violet solid (168) whose FAB MS and analytical data suggested the formation of a complex with a ligand:metal ratio of 1:1.

A mixture of the ditopic macrocycle (92) with copper(II) perchlorate in acetone gave dark green needles of a mononuclear copper(II) complex $[(92)\text{-}Cu][ClO_4]_2$ (169),[41] in which only one of the

pyridine nitrogens appeared to be bound. Reaction with $[Cu(MeCN)_4]BF_4$ gave a yellow mononuclear copper(I) complex, $[(92)\text{-}Cu][BF_4]$ (170) (δ_H s, benzylic protons).[41] It was reported that copper(II) binds to five of the available heteroatoms (S_4N) while copper(I) presumably coordinates to the four sulphur atoms in a favourable distorted-tetrahedral geometry.[41]

Reaction between ligand (92) and copper(II) dichloride gave a green solid (171) whose FAB mass spectrum gave a peak at *m/e* 485, 487 corresponding to $[(92)\text{-}Cu]^+$. The elemental analysis was consistent however with a dinuclear complex in which the copper cations are most likely fully bound by the pyridyl-dithio (NS_2) units, as demonstrated for the copper(II) chloride complex of ligand (95).[265]

6.5.3 *Platinum Complexes*

Reaction of two equivalents of $[PtCl_2(MeCN)_2]$ with ligand (92) in boiling dichloromethane yielded the pale yellow compound $[(92)\text{-}Pt_2Cl_2]Cl_2$ (172) which was soluble in water. The positive ion FAB mass spectrum of complex (172),using a thiodiglycol matrix yielded a molecular ion at *m/e* 884 with the expected platinum isotope pattern (see Figure 6.13). Fragments due to successive loss of chlorine and platinum at *m/e* 847, 653, and 617 with the expected platinum isotope patterns, corresponding to $[(92)\text{-}Pt_2Cl]^+$, $[(92)\text{-}PtCl]^+$, and $[(92)\text{-}Pt]^+$ respectively were also observed. The ^1H and ^{13}C NMR spectra revealed the presence of two distinct complexes in aqueous solution. In the ^1H spectrum, two sets of triplets and doublets were observed for the aromatic ring protons, together with two AB patterns for the benzylic protons with sharply resolved multiplets for the alkyl methylene groups. Over a period of time in solution the ratio of these complexes altered.

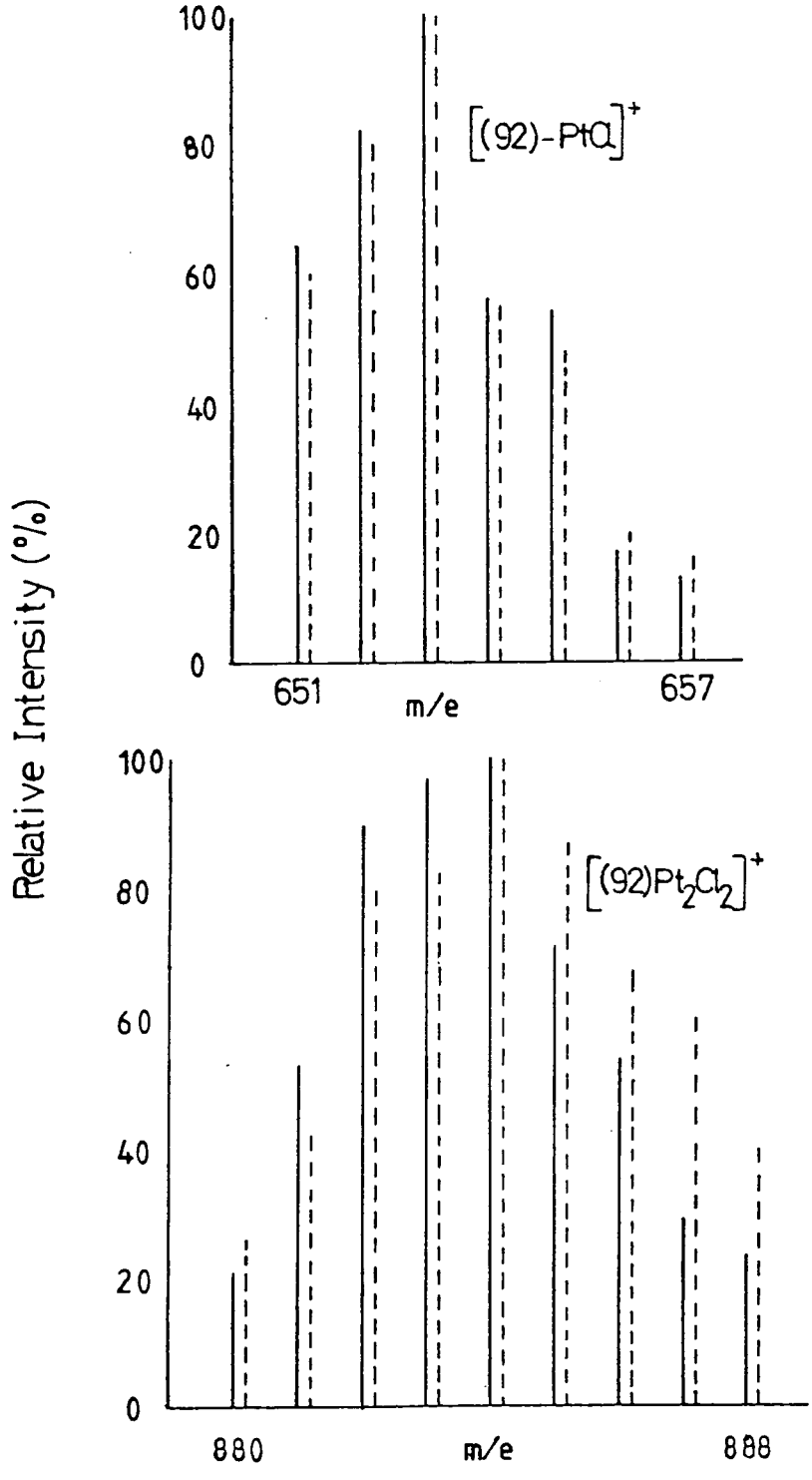

Figure 6.13

Positive ion FAB mass spectrum of complex (172) *recorded in thiodiglycol showing patterns corresponding to* $[(92)\text{-}PtCl]^+$ *and* $[(92)\text{-}Pt_2Cl_2]^+$; (——) *calculated,* (---) *experimental.*

The ^{13}C spectrum showed two signals for the *meta* aromatic carbons, the *ortho* aromatic carbons, the benzylic carbons, and the CH_2S carbons. Resonances for the *para* aromatic carbons and the central $CH_2CH_2CH_2$ carbons occurred as single peaks. It may be the case that complex (172) exists as two diastereoisomers, which may be considered as those formed when the configurations of the sulphur atoms are either [RSRS] or [SRRS]. In the [SRRS] isomer the metal centres may interact whereas the configuration of the [RSRS] isomer forbids any interaction.

6.5.4 *Coordination to the Pyridine Nitrogen Atom of Ligand* (92) *in its Transition Metal Complexes*

The pyridine ring vibrations for ligand (92) and its complexes are given in Table 6.1. Coordination of the metal atom to the pyridine ring nitrogen is indicated by a splitting and shifting of the ring vibrations

Compound	Pyridine Ring Vibrations (cm^{-1})
Ligand (92)	1592, 1572
$[(92)\text{-}Rh_2(CO)_2][PF_6]_2$ (163)[a]	1596, 1562
$[(92)\text{-}Pd_2Cl_2]Cl_2$ (164)[a]	1596, 1562
$[(92)\text{-}Pd_2(OH)_2][PF_6]_2$ (165)	1602, 1573
$[(92)\text{-}Pd_2(NO_3)_2][NO_3]_2$ (166)	1602, 1571
$[(92)\text{-}Co][BF_4]_2$ (167)	1600, 1569
$(92)\text{-}Cu][ClO_4]_2$ (169)[a]	1601, 1592, 1566
$[(92)\text{-}Cu_2Cl_2]Cl_2$ (171)	1602, 1573
$[(92)\text{-}Pt_2Cl_2]Cl_2$ (172)	1602, 1568
$[(92)\text{-}Ag][Ag(NO_3)_2]$[b]	1592, 1573

[a]Data from ref. 41, measured as Nujol mull
[b]Synthesised by D. Parker, unpublished results.

Table 6.1

Infrared absorptions of ligand (92) *and its complexes measured as KBr discs unless otherwise stated.*

as observed for many pyridine-metal complexes.[286-288] The $Cu(II)(ClO_4)_2$ complex (169) of ligand (92) has been described as having one pyridine ring-nitrogen free and one bound.[41] Given this, the ring stretches occurring in the region 1590-1610 cm^{-1} may be diagnostic of ring nitrogen binding. The free ligand. the Cu(II) complex mentioned and the Ag(I) complex all have low ring stretches at 1592 cm^{-1}, consistent with an unbound pyridine ring. The coordination in the Ag(I) complex may be associated with the preference of silver to bind to sulphur atoms.[289] The remaining complexes all have a ring stretch at $\simeq$ 1600 cm^{-1}. These data suggest that in these complexes the cations are bound to the ring nitrogen. The cobalt(II) complex may be octahedral and bound by two NS_2 units (molecular models suggest that this is possible). The palladium complexes may have nitrogen-bound metal centres, but are perhaps bound to only one sulphur atom which is consistent with the reported NMR data.

CHAPTER SEVEN - EXPERIMENTAL

7.1 Experimental Syntheses

7.1.1 *Introduction*

In the proceeding section which describes the synthetic procedures for all compounds used in this work, temperatures are quoted in ^{o}C unless otherwise indicated and alumina refers to Merck Alumina (activity II to III).

Proton NMR spectra and ^{13}C spectra were recorded using a Bruker AC 250 spectrometer operating at 250.134 MHz for protons and 62.896 for the carbon nucleus. Chemical shifts are given in ppm [relative to Me_4Si (TMS) at 0 ppm]. Chemical shifts for protons showing an AB pattern are at the "centre of gravity" of the two peaks associated with each shift and have been calculated using the formula

$$(1 - 3) = (2 - 4) = \sqrt{[(\Delta\upsilon)^2 + J^2]}$$

The peak positions 1 to 4 are numbered from left to right and are given in Hz from TMS. $\Delta\upsilon$ is the chemical shift difference in Hz and J is the scalar coupling constant in Hz. It follows that the shift position of each proton is $\Delta\upsilon/2$ from the mid-point of the pattern.

Electronic spectra were recorded in the stated solvent on a Pye Unicam SP8-100UV spectrophotometer (λ_{max} in nm).

Infrared spectra were recorded in the stated solvent or in the solid-state as a potassium bromide disc on a Perkin-Elmer 577 spectrometer. Fourier transform infrared spectra were recorded on a Mattson Sirius 100 FT IR spectrometer.

Cyclic voltammetry was conducted using a BAS CV-1B Voltammograph, conditions of the experiment are stated with the results.

The magnetic susceptibility datum was acquired using the Evans NMR method for the measurement of magnetic susceptibilities of species in

solution.[290]

ESR spectra were recorded by Mr. C. Williams, University of Durham. Metal determinations were accomplished using a Perkin-Elmer 5000 atomic absorption spectrophotometer.

Mass spectra were recorded on a VG 7070E mass spectrometer, with FAB, DCI, CI, and EI ionisation modes as stated.

7.1.2 *Procedures*

1,11-*Dichloro*-3,6,9-*trioxaundecane* (98) and 1,11-*Diiodo*-3,6,9-*trioxa-undecane* (99).- (98) and (99) were synthesised according to the methods of Calverley and Dale.[124]

10-*Benzyl*-1,4,7-*trioxa*-10-*azacyclododecane* (102) and 1,4,7-*Trioxa*-10-*aza- cyclododecane* (100).- The cyclododecanes, (102) and (100), were synthesised according to the methods of Calverley and Dale.[124]

10-(2-*Hydroxyethyl*)-1,4,7-*trioxa*-10-*azacyclododecane* (106).- (106) was synthesised according to the method of Calverley and Dale.[124] The residue obtained after extraction was chromatographed on basic alumina eluting with dichloromethane - methanol (9:1) to give a pale yellow oil.

10-*Ethoxycarbonylmethyl*-1,4,7-*trioxa*-10-*azacyclododecane* (107).- (107) was synthesised according to the method of Calverley and Dale.[124] The residue obtained after extraction was chromatographed on basic alumina eluting with dichloromethane - methanol (methanol increasing from 0 to 10%) to give 10-*ethoxycarbonylmethyl*-1,4,7-*trioxa*-10-*azacyclododecane* as a colourless oil, (Found: M^+, 261.1569 $\pm$ 0.002; $C_{12}H_{23}NO_5$ requires M^+, 261.1569).

10-*Hydroxycarbonylmethyl*-1,4,7-*trioxa*-10-*azacyclododecane* (108).- The product from the preceeding preparation (107) was treated with concentrated hydrochloric acid (6.0 M) and heated under reflux with stirring of the mixture for 4 h. Evaporation of the excess of hydrochloric acid by azeotroping with methanol gave 10-*hydroxycarbonylmethyl*-1,4,7-*trioxa*-10-*azacyclododecane* as a white solid, δ_C (D_2O) 53.40 (CH_2N ring), 55.79 (CH_2N side-arm), 63.72, 69.07, and 69.57 (CH_2O ring), and 168.12 (C=O); *m/e* 234 (M^+, 70%).

10-*Methoxycarbonylethyl*-1,4,7-*trioxa*-10-*azacyclododecane hydrochloride*.- 1,11-Diiodo-3,6,9-trioxaundecane (99) (18.5 g, 0.045 mol) and 3-aminomethyl- propanoate hydrochloride (6.5 g, 0.047 mol) in dry acetonitrile (500 ml) containing anhydrous sodium carbonate (18 g) were heated under reflux with stirring for 48 h under an atmosphere of nitrogen. After cooling of the mixture to room temperature, the mixture was filtered, the solvent removed under reduced pressure, and the residue chromatographed on basic alumina, eluting with dichloromethane. Evaporation of the eluant gave a residue which was acidified with concentrated hydrochloric acid (5 ml) in methanol (20 ml). Evaporation of the excess of hydrochloric acid by azeotroping with methanol gave a residue which was crystallised from propan-2-ol at -5^o, to give 10-*methoxycarbonylethyl*- 1,4,7-*trioxa*-10-*azacyclododecane hydrochloride* as a yellow crystalline solid, 2.53 g (22%), m.p. 135°C, $\upsilon_{max.}$ (KBr) 1725 (C=O); δ_H (D_2O) 3.00 (2 H, t, *J* 6.7 Hz, CH_2C=O), 3.63 (2 H, t, 6.7 Hz, CH_2N side-arm), 3.78 (3 H, s, OCH_3), and 3.44-4.02 (16 H, m, CH_2O and CH_2N ring); *m/e* 262 (M^+, 10%).

10-*Methoxycarbonylethyl*-1,4,7-*trioxa*-10-*azacyclododecane* (109).- A molar equivalent quantity of solid tetramethylammonium hydroxide was added to

a solution of 10-methoxycarbonylethyl-1,4,7-trioxa-10-azacyclododecane hydrochloride in dichloromethane. After stirring for 15 min during which time the bright yellow colour diminished considerably, the solution was decanted from the residual solid hydroxide. Evaporation of the dichloromethane gave an oil which was redissolved in a small volume of dichloromethane and passed over a small quantity of alumina to give 10-*methoxycarbonylethyl*-1,4,7-*trioxa*-10-*azacyclododecane* as a colourless oil, (Found: M^+, 261.1569 ± 0.002; $C_{12}H_{23}NO_5$ requires M^+, 261.1569); δ_H ($CDCl_3$) 2.48 (2 H, *J* 7.2 Hz, $CH_2C{=}O$), 2.70 (4 H, t, *J* 4.8 Hz, CH_2N ring), 2.86 (2 H, t, *J* 7.2 Hz, CH_2N side-arm), and 3.62-3.68 (15H, m, OCH_3 and CH_2O's); δ_C ($CDCl_3$) 32.13 ($CH_2C{=}O$), 50.98 (CH_2N ring), 51.62 (CH_2N side-arm), 54.63 (OCH_3), 69.81, 69.98, and 70.83 (CH_2O's), and 172.55 (C=O).

10-*Hydroxycarbonylethyl*-1,4,7-*trioxa*-10-*azacyclododecane hydrochloride* (110).- 10-Methoxycarbonylethyl-1,4,7-trioxa-10-azacyclododecane hydrochloride (109) was treated with concentrated hydrochloric acid (6 M) and heated under reflux with stirring for 12 h. Evaporation of the solvent gave 10-*hydroxycarbonylethyl*-1,4,7-*trioxa*-10-*aza-cyclododecane hydrochloride* as colourless crystals, δ_H (D_2O) 2.98 (2 H, t, *J* 6.5 Hz, $CH_2C{=}O$), 3.60 (2 H, t, *J* 6.4 Hz, CH_2N side-arm), and 3.45-4.06 (16 H, m, CH_2N and CH_2O ring); δ_C (D_2O) 27.67 ($CH_2CH_2C{=}O$), 49.06 (CH_2N ring), 54.11 (CH_2N side-arm), 63.17, 68.77, and 68.87 (CH_2O ring), and 173.14 (C=O); *m/e* (DEI) 248 (M^+, 100%).

N,N-*Dimethylbromoacetamide*.- The title compound was synthesised according to the method of Weaver and Whaley.[241]

10-(N,N-*Dimethylethanamide*)-1,4,7-*trioxa*-10-*azacyclododecane* (111).- *N,N*-Dimethylbromoacetamide (0.2 g, 1.2 mmol) was added to a solution of 1,4,7-trioxa-10-azacyclodecane (100)(160 mg, 0.9 mmol) in dry acetonitrile (15 ml) containing anhydrous sodium carbonate (0.3 g)and the resulting mixture was stirred and heated under reflux under a nitrogen atmosphere for 48 h. After cooling of the mixture to 20° the solid was removed by filtration and the filtrate evaporated under reduced pressure. The crude residue was taken up in the minimum amount of dilute hydrochloric acid (0.2 M) and the aqueous solution was washed with chloroform (5 x 25 ml). The aqueous layer was basified with potassium hydroxide solution and the product was extracted with chloroform (5 x 25 ml). The combined organic layers were evaporated under reduced pressure to a small volume, the solid was removed by filtration through a small bed of alumina. Evaporation of the filtrate gave 10-(N,N-*dimethylethanamide*)-1,4,7-*trioxa*-10-*azacyclododecane* as a pale yellow oil, (Found: M^+, 260.17150 ± 0.002; $C_{12}H_{24}N_2O_4$ requires M^+, 260.17361); δ_C (CD_3Cl) 35.58 (CH_3), 36.71 (CH_3), 54.22 (CH_2N), 54.92 (CH_2N), 69.87, 70.31, and 70.98 (CH_2O), and 170.60 (C=O).

1,7-*Dioxa*-4,10-*diazacyclododecane* (112) and 4,10-bis(2-*Hydroxyethyl*)-1,7-*dioxa*-4,10-*diazacyclododecane* (113).- Heterocycles (112) and (113) were synthesised according to the methods of Amble and Dale.[123]

4,10-bis(N,N-*Dimethylethanamide*)-1,7-*dioxa*-4,10-*diazacyclododecane* (114).- *N,N*-Dimethylbromoacetamide (0.57 g, 3.44 mmol) was added to a solution of 1,7-dioxa-4,10-diazacyclododecane (112)(0.30 g, 1.72 mmol) in dry acetonitrile (25 ml) containing anhydrous sodium carbonate (0.38 g) and the mixture was heated under reflux under an atmosphere of

nitrogen with stirring for 48 h. After cooling of the mixture to 20° the mixture was filtered and the solvent removed under reduced pressure. The crude residue was taken up in the minimum volume of dilute hydrochloric acid (0.2 M) and washed with chloroform (5 x 25 ml). The aqueous layer was basified with potassium hydroxide solution and the product was extracted with chloroform (5 x 25 ml). The product was further purified by chromatography on alumina, eluting with dichloromethane-methanol (methanol increasing from 0 to 2%). Evaporation of the organic eluates gave 4,10-bis(N,N-*dimethyl-ethanamide*)-1,7-*dioxa*-4,10-*diazacyclododecane* as a crystalline residue, 0.50 g (85%), m.p. 135°, (Found: M^+, 344.243393 ± 0.002; $C_{16}H_{32}N_4O_4$ requires M^+, 344.2423558); υ_{max} (FT)(nujol) 1641 (C=O stretch); δ_H ($CDCl_3$) 2.89 (8 H, t, *J* 4.64 Hz, CH_2N), 2.93 (6 H, s, NCH_3), 3.06 (6 H, s, NCH_3), 3.45 (4 H, s, $NCH_2C{=}O$), and 3.57 (8 H, t, *J* 4.56 Hz, CH_2O); δ_C ($CDCl_3$) 35.6 (NCH_3), 36.42 (NCH_3), 54.69 (CH_2N), 57.41 ($NCH_2C{=}O$), 68.74 (CH_2O), and 170.23 (C=O).

4,10-bis(N,N-*Dimethylpropanamide*)-1,7-*dioxa*-4,10-*diazacyclododecane* (115).- *N,N*-Dimethylpropenamide (1.46 g, 0.015 mol; freshly distilled) was added to a solution of 1,7-dioxa-4,10-diazacyclododecane (112) (0.50 g, 0.287 mol) in methanol (20 ml), and the stirred mixture was heated under reflux, under a nitrogen atmosphere for 4 h. After cooling of the mixture to 20° the mixture was filtered and the solvent removed under reduced pressure. The crude residue was taken up in the minimum volume of dilute hydrochloric acid (0.1 M) and washed with chloroform (5 x 25 ml). The aqueous layer was basified with potassium hydroxide solution and the product extracted into chloroform (5 x 25 ml). The solution was reduced to small volume under reduced pressure. Chromatography on basic alumina eluting with dichloromethane-methanol

(methanol increasing from 0 to 2%) gave a pale yellow oil which was crystallised from toluene with a trace of ether present to give 4,10-bis(N,N-*dimethylpropanamide*)-1,7-*dioxa*-4,10-*diazacyclododecane* as colourless plates, m.p. 82°, (Found: M^+, 372.2755 ± 0.001; $C_{18}H_{36}N_4O_4$ requires M^+, 372.2753); δ_H ($CDCl_3$) 2.49 (4 H, t, *J* 7.63 Hz, $CH_2C{=}O$), 2.65 (8 H, t, *J* 4.67 Hz, CH_2N ring), 2.83 (4 H, t, *J* 7.64 Hz, CH_2N side-arm), 2.89 (6 H, s, CH_3's), and 3.55 (8 H, t, *J* 4.67 Hz, CH_2O ring); δ_C ($CDCl_3$) 31.88 ($CH_2C{=}O$), 35.95 (CH_3), 37.96 (CH_3), 53.36 (CH_2N ring), 55.83 (CH_2N side-arm), 70.11 (CH_2O), and 172.63 (C=O).

X-Ray Crystal Data.-$C_{18}H_{36}N_4O_4$; *M* = 372.51. Monoclinic, *a* = 8.578 (2), *b* = 9.673 (2), *c* = 13.154 (4) Å, *β* = 107.63 (2)°; V = 1 040.2 Å^3, Z = 2, D_x = 1.19 g cm^{-3}, *F*(000) = 204, μ(Mo-K_α) = 0.8 cm^{-1}. Space group determined uniquely from the systematic absences as $P2_1/n$ (alt. $P2_1/c$, No. 14). The structure was determined by direct methods. Isotropic followed by anisotropic refinement of the non-hydrogen atoms with the hydrogens in geometrically idealised positions converged with *R* = 0.030 and R_w = 0.029 for 880 observed reflexions measured on a CAD4 diffractometer.

1,13-*Dihydroxy*-4,7,10-*trioxatridecane* (117).- Sodium metal (1.43 g, 0.062 mol) was added to propan-1,3-diol (65 ml) under nitrogen and the mixture was stirred at 20° until evolution of hydrogen had ceased. Diethylene glycol ditosylate[291] (12.85 g, 0.031 mol) was added in portions with swirling of the solution and the mixture stirred at 110° for 18 h. After cooling of the resulting mixture to 20°, dichloromethane (200 ml) was added and the mixture was filtered. Solvent was removed under reduced pressure and the residue was distilled to remove the excess of propan-1,3-diol. The residue from the distillation was dissolved in a small quantity of dichloromethane and

passed over a small quantity of basic alumina to afford 1,13-*dihydroxy*-4,7,10-*trioxatridecane* as a colourless oil, 4.4 g (64%), [Found: $(M+1)^+$, 223.155106 ± 0.001; $C_{10}H_{22}O_5$ requires M^+, 223.154550]; δ_H ($CDCl_3$) 1.81 (4 H, t x t, *J* 5.82 Hz, $CH_2CH_2CH_2$), 3.49 (2 H, br s, OH), 3.59-3.66 (12 H, m, CH_2O's), and 3.73 (4 H, t, *J* 5.75 Hz, CH_2OH); δ_C ($CDCl_3$) 31.80 ($CH_2CH_2CH_2$), 60.07 (CH_2OH), 69.00 ($OCH_2CH_2CH_2$), and 69.79 and 70.17 (CH_2OCH_2).

1,13-*Dichloro*-4,7,10-*trioxatridecane* (118).- Thionyl chloride (4.0 g, 0.034 mol) was added dropwise with stirring to a solution of the diol (117) in dry pyridine (10 ml) at 0° and the resulting solution stirred for 24 h. Water (10 ml) was added to the mixture and the solution was extracted with dichloromethane (5 x 10 ml), a further volume of water (10 ml) being added before each extraction. The combined organic extracts were washed with water (25 ml), brine (25 ml), dried (anhydrous $MgSO_4$), and the solvent removed under reduced pressure. The residue was distilled to give 1,13-*dichloro*-4,7,10-*trioxatridecane* as a colourless oil, b.p. 96°/0.001 mm Hg, [Found: $(M+1)^+$, 259.085462 ± 0.001; $C_{10}H_{20}O_3Cl_2$ requires M^+, 259.08467]; δ_H ($CDCl_3$) 2.03 (4 H, t x t, *J* 6.19 Hz, $CH_2CH_2CH_2$), and 3.59-3.67 (16 H, m, CH_2Cl and CH_2O's); δ_C ($CDCl_3$) 32.59 ($CH_2CH_2CH_2$), 41.80 (CH_2Cl), 67.50 ($OCH_2CH_2CH_2$), and 70.25 and 70.45 (OCH_2CH_2O).

1,13-*Diiodo*-4,7,10-*trioxatridecane* (119).- Powdered sodium iodide (1.36 g, 9.1 mmol) was added to a solution of the dichloride (118) (0.96 g, 3.7 mmol) in acetone (6 ml) containing a catalytic amount of tetra-*n*-hexylammonium bromide (15 mg), and the mixture was stirred and heated under reflux for 70h. The mixture was cooled to 20°, the solid was removed by filtration, and the filtrate was concentrated under

reduced pressure. The residue was dissolved in ethyl acetate (10 ml), washed with sodium thiosulphate solution (5 ml; 20%), water (10 ml), brine (10 ml), and dried (anhydrous $MgSO_4$). The solution was evaporated under reduced pressure to give 1,13-*diiodo*-4,7,10-*trioxatridecane* as a yellow oil, δ_H ($CDCl_3$) 2.05 (4 H, t x t, *J* 6.32 Hz, $CH_2CH_2CH_2$), 3.26 (4 H, t, *J* 6.77 Hz, CH_2I), 3.52 (4 H, t, *J* 5.87 Hz, $OCH_2CH_2CH_2$), and 3.58-3.64 (8 H, m, AA'*BB*' pattern, OCH_2CH_2O); δ_C ($CDCl_3$) 3.22 (CH_2I), 33.37 ($CH_2CH_2CH_2$), 70.27 ($OCH_2CH_2CH_2$), and 70.43 and 70.48 (OCH_2CH_2O).

11-*Methoxycarbonylethyl*-1,4,7-*trioxa*-11-*azacyclotetradecane* (116).- 1,13-Diiodo-4,7,10-trioxatridecane (119)(4.74 g, 10.7 mmol) was added to a solution of 3-aminomethylpropanoate hydrochloride (1.5 g, 10.7 mmol) in dry acetonitrile (210 ml) containing anhydrous sodium carbonate (4.4 g) and the mixture was heated under reflux with stirring for 48 h under an atmosphere of nitrogen. After cooling of the mixture to 20° the mixture was filtered and the solvent removed under reduced pressure. The residue was chromatographed on alumina eluting with dichloromethane-methanol (methanol increasing from 0 to 10%). Evaporation of the eluates gave 11-*methoxycarbonylethyl*-1,4,7-*trioxa*-11-*azacyclotetradecane* as a pale yellow oil, υ_{max} 1738 (C=O); δ_C (CD_3OD) 27.95 and 33.69 ($CH_2C{=}O$ and $CH_2CH_2CH_2$), 50.31, 60.20, and 62.27 (CH_2N ring, CH_2N side-arm, and OCH_3), 70.05, 70.36, and 71.08 (CH_2O's), and 174.80 (C=O); *m/e* (CI; isobutane) 290 [$(M + 1)^+$].

Synthesis of [12]-*Ring Macrocyclic Complexes*.- $[(113)_2\text{-}Cu_3]^{2+}$ $2PF_6^-$ (125).- A molar equivalent quantity of copper (II) perchlorate hexahydrate in aqueous ethanol was added to a solution of ligand (113) in aqueous ethanol. On standing of the resulting solution, a green, crystalline solid formed which was collected by filtration,

washed with ethanol, and dried *in vacuo* to give $[(113)_2\text{-}Cu_3]^{2+}$ $2PF_6^-$, λ_{max} 273 nm, ϵ 9.7 x 10^3 dm^3 mol^{-1} cm^{-1}, 720 (120); *m/e* (FAB; glycerol) 811 $[(113)_2\text{-}Cu_3ClO_4]^+$, 711 $[(113)_2\text{-}Cu_3]^{\cdot+}$.

A hot solution of the perchlorate complex in aqueous propan-2-ol was filtered and an excess of ammonium hexafluorophosphate was added as a solution in propan-2-ol. On standing of the solution, green needles formed which were isolated, washed with propan-2-ol, and dried by slow evaporation of the solvent. The powder ESR spectrum is of the axial type with $g_{||}$ = 2.23, $g_{\perp}$ = 2.04, and a normal $A_{||}$ hyperfine splitting was observed (0.015 cm^{-1}). Cyclic voltammetry measurements in H_2O (μ = 0.1 M, NBu^n_4 ClO_4) on a glassy carbon electrode show two quasi-reversible peaks at +0.23 V and -0.04 V (relative to the standard calomel electrode). Coulometric reductions indicate that two Faradays per mole of complex are exchanged at +0.23 V and one Faraday per mole of complex at -0.04 V. Magnetic susceptibility measurements give a magnetic moment at 295 K of 1.1 μ_B (per copper atom).

X-Ray Crystal Data.- $C_{24}H_{48}Cu_3F_{12}N_4O_8P_2$; M = 1001.2. Monoclinic, a = 7.112 (2), b = 18.507 (5), c = 14.106 (4) Å, β = 101.44 (3)°; V = 1819.7 $Å^3$, Z = 2, D_x = 1.83 g cm^{-3}, $F(000)$ = 1018, μ(Mo-K_α) = 19.4 cm^{-1}. Space group determined uniquely from the systematic absences as $P2_1/c$ (No. 14). The structure was determined by the heavy atom method. Isotropic followed by anisotropic refinement of the non-hydrogen atoms with the hydrogens in geometrically idealised positions converged with R = 0.047 and R_w = 0.058 for 1491 observed reflexions measured on a CAD4 diffractometer.

$[(106)_2\text{-}Cu_2]^{2+}$ $2ClO_4^-$ (126).- A solution of copper (II) perchlorate hexahydrate (44.7 mg, 1.2 mmol) in methanol (1 ml) was added to a solution of ligand (106) (88.5 mg, 0.4 mmol) in methanol (1 ml). An

immediate pale green precipitate formed which was collected by filtration, washed with cold methanol, and dried *in vacuo*. Recrystallisation of a small quantity of the solid material from methanol gave $[(106)_2\text{-}Cu_2]^{2+}$ $2ClO_4^-$ as green needles, λ_{max}(MeOH) 263 nm, (ϵ 2 x 10^4), > 800 ($\simeq$ 400); *m/e* (FAB; glycerol) 282,284 $[(106)\text{-}Cu]^+$, 220 $[(106) + H]^+$. Cyclic voltammetry measurements in MeCN (μ = 0.07 M, $NBu^n_4ClO_4$) on a platinum electrode show a quasi-reversible peak at $\simeq$ 0.36 V (relative to the standard calomel electrode).

X-Ray Crystal Data.- $C_{20}H_{40}Cu_2Cl_2N_2O_{16}$; *M* = 762.53. Monoclinic, *a* = 7.551 (3), *b* = 12.213 (2), *c* = 16.158 (3) Å, β = 92.13 (2)°; V = 1489.1 Å^3, Z = 2, D_x = 1.70 g cm^{-3}, *F*(000) = 1576, μ(Mo-K_α) = 16.8 cm^{-1}. Space group determined uniquely from the systematic absences as $P2_1/c$ (No. 14). The structure was determined by the heavy atom method. Isotropic followed by anisotropic refinement of the non-hydrogen atoms with the hydrogens in geometrically idealised positions converged with *R* = 0.059 and R_w = 0.080 for 737 observed reflexions measured on a CAD4 diffractometer.

$[(109)_4\text{-}Cu_4]^{4+}$ $4PF_6^-$ (127).- A solution of copper (II) perchlorate hexahydrate (522 mg, 1.4 mmol) in methanol (1 ml) was added to a solution of ligand (109) (182 mg, 0.7 mmol) in methanol (1 ml). An immediate blue precipitate formed which was removed by filtration, washed with methanol and dried *in vacuo* to give $[(109)_4\text{-}Cu_4]^{4+}$ $4ClO_4^-$, (Found: C, 32.0; H, 4.9; N, 3.9. $C_{11}H_{20}CuNO_5.ClO_4$ requires C, 32.3; H, 4.9; N, 3.4%.); ν_{max} (FT)(KBr) 1606 $\pm$ 1 (C=O stretch). The powder ESR spectrum is of the axial type with $g_{||}$ = 2.21 and $g_\perp$ = 2.09. A hot solution of the perchlorate complex in methanol was filtered and an excess of ammonium hexafluorophosphate was added as a solution in methanol. The addition of a small volume of ethyl acetate led to the

formation of bright blue cubic crystals which were isolated, washed with methanol, and dried by slow evaporation of the solvent, [Found: C, 28.7; H, 4.8; N, 3.2. $(C_{11}H_{20}NO_5Cu)_4.(PF_6)_4$ requires C, 29.0; H, 4.4; N, 3.1%.].

X-Ray Crystal Data. The current R factor is 9.1%, we are now awaiting a low-temperature study.

$[(114)\text{-}Cu]^{2+}$ $2ClO_4^-$ (128).- A solution of copper (II) perchlorate hexahydrate (1.25 molar excess) in methanol (1 ml) was added to a solution of ligand (114) (35 mg, 0.1 mmol) in methanol (1 ml). On standing of the resulting solution a pale turquoise, furry solid formed which was isolated by filtration, washed with methanol, and dried *in vacuo* to give $[(114)\text{-}Cu]^{2+}$ $2ClO_4^-$, (Found: C, 30.7; H, 5.3; N, 8.2. $C_{16}H_{32}ClN_4O_8Cu.H_2O$ requires C, 30.7; H, 5.4; N, 8.9%.); υ_{max} (FT)(KBr) 1 627 $\pm$ 1 (C=O); *m/e* (FAB; glycerol) 407, 409 $[(114)\text{-}Cu)]^+$, 506, 508 $[(114)\text{-}Cu(ClO_4)]^+$.

4-Toluenesulphonyl-N,N-di(ethanol)amide (129), *4-Toluenesulphonyl-N,N-di(chloro-1-oxa-2-butane)amide* (130), *4-Toluenesulphonyl-N,N-di-(cyano-1-oxa-2-butane)amide* (131), *and Dioic-4-toluenesulphonyl-N,N-di-(oxa-3-pentanoic)amide* (132).- These were synthesised according to the methods of Graf and Lehn.[104]

4-Toluenesulphonyl-N,N-di(oxa-3-pentanol)amide (133).- A solution of the diacid (132)(0.5 g, 1.33 mmol) in tetrahydrofuran (8 ml) was cooled to 0^o under an atmosphere of nitrogen. A solution of borane in dimethyl sulphide (5 ml; 10 M) was added dropwise. Reaction was accompanied by a brisk evolution of hydrogen. The slow addition of methanol destroyed the excess of borane and evaporation of the solvent under reduced

pressure gave 4-*toluenesulphonyl*-N,N-*di*(*oxa*-3-*pentanol*)*amide* as a colourless oil, δ_C ($CDCl_3$) 21.10 (CH_3), 48.60 (CH_2N), 61.03 (CH_2OH), 69.52 and 72.06 (CH_2O's) and 126.79, 129.39, 135.85, and 143.13 (aromatic C's); *m/e* (CI; isobutane) 348 [$(M+1)^+$].

4-*Toluenesulphonyl*-N,N-*di*(*chloro*-1-*oxa*-3-*pentane*)*amide* (134).- Thionyl chloride (0.2 ml, 2.8 mmol) was added slowly to a stirred solution of the diol (133)(0.46 g, 1.33 mmol) in dichloromethane (20 ml) containing pyridine (0.5 ml) at 0^o. Stirring of the resulting solution was continued for 30 min with the temperature being maintained at 0^o and for a further 24 h at 20^o. Water (5 ml) was added to the mixture and the solution was extracted with dichloromethane (5 x 10 ml), a further volume of water (5 ml) being added before each extraction. The combined organic fractions were washed with water (20 ml), brine (20 ml), dried (anhydrous $MgSO_4$), and the solvent removed under reduced pressure to give 4-*toluenesulphonyl*-N,N-*di*(*chloro*-1-*oxa*-3-*pentane*)*amide* as a yellow oil which was used without purification in the succeeding preparation, δ_H ($CDCl_3$) 2.40 (3 H, s, CH_3), 3.42 (4 H, t, J 5.72 Hz, CH_2Cl), 3.48-3.71 (12 H, m, CH_2O's and CH_2N's), 7.30 (2 H, d, J 8.10 Hz, half of AA'XX' system, aromatic H), and 7.70 (2 H, d, J 8.13 Hz, half of AA'XX' system, aromatic H); δ_C ($CDCl_3$) 21.05 (CH_3), 42.55 (CH_2Cl), 48.27 (CH_2N), 69.61 and 70.59 (CH_2O's), 126.72, 129.29, 136.48, and 142.98 (aromatic C's).

4-*Toluenesulphonyl*-N,N-*di*(*iodo*-1-*oxa*-3-*pentane*)*amide* (135).- Powdered sodium iodide (0.5 g, 3.3 mmol) was added to a solution of the dichloride (134)(0.5 g, 1.3 mmol) in acetone (5 ml) containing a catalytic amount of tetra-n-hexylammonium bromide (15 mg) and the mixture heated under reflux with stirring for 70 h. The mixture was

cooled to 20°, filtered, and the filtrate evaporated under reduced pressure. The residue was dissolved in ethyl acetate (10 ml), washed with sodium thiosulphate solution (5 ml; 20%), water (5 ml), brine (5 ml), and dried (anhydrous $MgSO_4$). The solvent was evaporated under reduced pressure to give *4-toluenesulphonyl-N,N-di(iodo-1-oxa-3-pentane)amide* as an orange oil, δ_H ($CDCl_3$) 2.32 (3 H, s, CH_3), 3.09 (4 H, t, *J* 6.47 Hz, CH_2I), 3.34 (4 H, t, *J* 5.70 Hz, CH_2N), 3.52-3.57 (8 H, m, CH_2O's), 7.21 (2 H, d, J 8.15 Hz, half of AA'XX' system, aromatic H) and 7.61 (2 H, d, J 8.15 Hz, half of AA'XX' system, aromatic H); δ_C ($CDCl_3$) 2.97 (CH_2I), 21.25 (CH_3), 48.34 (CH_2N), 69.34 and 71.11 (CH_2O's), 126.78, 129.35, 136.58, and 142.93 (aromatic C's).

Pyridacyl Pyridinium Iodide (136) *and* 5-*Methyl*-2,2'-*bipyridine* (137).- These compounds were synthesised according to the methods of Kröhnke.[258]

5-*Bromomethyl*-2,2'-*bipyridine* (138), 5-*Phthalimidomethyl*-2,2'-*bipyridine* (139), 5-*Aminomethyl*-2,2'-*bipyridine Hydrochloride* (140).- Compounds (138), (139), and (140) were synthesised according to literature procedures.[292]

N-Bromosuccinimide (1.96 g, 11 mmol; freshly recrystallised) and azabisisobutyronitrile (50 mg) were added to a solution of 5-methyl-2,2'-bipyridine (137)(1.7 g, 10 mmol) in dry carbon tetrachloride (100 ml), and the resulting solution heated under reflux for 1 h. The progress of the reaction was monitored by following the disappearance of the methyl singlet (δ_H 2.4) and the appearance of the CH_2Br singlet (δ_H 4.46). The mixture was allowed to cool to 20°, filtered, and the filtrate was evaporated under reduced pressure. The resulting product was used without purification in the next stage.

Potassium phthalimide (0.93 g, 5 mmol) was added to a solution of 5-bromomethyl-2,2'-bipyridine (138)(1.25 g, 5 mmol) in dry dimethylformamide (50 ml) and the mixture was heated at 80° for 3h. The resulting mixture was poured onto crushed ice (200 g). A pale orange solid was removed by filtration and crystallised from ethanol to give *5-phthalimidomethyl-2,2'-bipyridine*, 1.35 g (90%), m.p. 199-200°, (Found: C, 72.4; H, 4.1; N, 13.3. $C_{19}H_{13}N_3O_2$ requires C, 72.4; H, 4.1; N, 13.3%.); δ_H ($CDCl_3$) 4.92 (2 H, s, CH_2), 7.29 (1 H, m), 7.80 (1 H, m) and (4 H, AA'*BB*' system, phthalimide H's), 7.91 (1 H, d, *J* 2.26 Hz), 8.36 and 8.37 (2 H, d + d, *J* 8.15 Hz and 7.99 Hz), 8.66 (1 H, d, *J* 4.73 Hz), and 8.77 (1 H, d, *J* 1.93 Hz); *m/e* 315 (M^+, 100%).

A two molar excess of hydrazine hydrate was added to a suspension of the phthalimide (139)(3.0 g, 9.4 mmol) in ethanol (90 ml) and the resulting mixture was heated under reflux for 8 h. After cooling of the mixture to 20°, the solid was removed by filtration and the filtrate was treated with hydrochloric acid (10 ml; 12 M). The resultant mixture was heated under reflux for a further 30 min. The mixture was cooled to 20°, the solid removed by filtration, and the filtrate evaporated under reduced pressure. The residue was crystallised from ethanol to give the required *amine hydrochloride* (140) as orange needles, δ_H (D_2O) 4.42 (2 H, s, CH_2), 8.12 (1 H, m), 8.27 (1 H, d + d, *J* 2.25 Hz), 8.40 (1 H, d, *J* 8.28 Hz), 8.65-8.74 (2 H, m), 8.89 (1 H, m), and 8.93 (1 H, d, *J* 1.83 Hz); δ_C (D_2O) 40.83 (CH_2), 124.05, 125.44, 128.10, 141.37, 143.29, 147.68, and 149.85 (aromatic C's), 132.66 (aromatic C-CH_2, quaternary), and 147.00 and 147.16 (aromatic C2 and C2', quaternary); *m/e* (CI; isobutane) 186 (M^+).

4-(2,2'-*Bipyridine-5-methyl*)-10-(4-*toluenesulphonylamide*)-1,7-*dioxa*-4,10-*diazacyclodecane* (141).- 4-Toluenesulphonyl-*N*,*N*-di(iodo-1-oxa-3-pentane)amide (135)(1.7 g, 3.00 mmol) was added to a solution of 5-aminomethyl-2,2'-bipyridine hydrochloride (140)(0.7 g; 3.16 mmol) in dry acetonitrile (50 ml) containing anhydrous sodium carbonate (1.3 g) and the stirred mixture was heated under reflux for 18 h, under an atmosphere of nitrogen. After cooling of the mixture to 20^{o} the solid was removed by filtration, and the solvent removed under reduced pressure to give an oily solid. The residue was dissolved in chloroform, and the solution was washed with water, dried (anhydrous $MgSO_4$), and the solvent removed under reduced pressure. The residue was chromatographed on basic alumina, eluting with dichloromethane-methanol (methanol increasing from 0 to 1%) to give 4-(2,2'-*bipyridine-5-methyl*)-10-(4-*toluenesulphonylamide*)-1,7-*dioxa*- 4,10-*diazacyclodecane* as a yellow solid, δ_H ($CDCl_3$) 2.32 (3 H, s, CH_3), 2.63 (4 H, t, *J* 4.29 Hz, ring CH_2), 3.19 (4 H, t, *J* 5.00 Hz, ring CH_2), 3.44 (4 H, t, *J* 4.38 Hz, ring CH_2), 3.62 (2 H, s, benzylic CH_2), 3.74 (4 H, t, *J* 5.02 Hz, ring CH_2), 7.22 (2 H, half of AA'XX' system, J_{AX} 8.40 Hz, tosyl aromatic H), 7.61 (2 H, half of AA'XX' system, $J_{A'X'}$ 8.23 Hz, tosyl aromatic H), 7.22 (1 H, m, aromatic H), 7.73 (2 H, m, aromatic H), 8.26 and 8.28 (2 H, d + d, *J* 8.05 and 7.25 Hz, aromatic H), 8.52 (1 H, d, *J* 1.65 Hz), and 8.58 (1 H, d, *J* 5.75 Hz); δ_C ($CDCl_3$) 21.33 (CH_3), 50.48 and 54.74 (CH_2N), 57.94 (benzylic CH_2), 68.60 and 69.82 (CH_2O), 120.63, 120.78, 123.40, 134.81, 136.69, 137.54, 148.99, 149.39, 154.92, and 155.91 (aromatic C), 127.09, 129.52, 135.56, and 143.10 (tosyl aromatic C); *m/e* 255 (23%), 155 (11), 86 (63), and 100 (11).

4-(2,2'-*Bipyridine-5-methyl*)-1,7-*dioxa*-4,10-*diazacyclodecane* (142).- A solution of the tosylated macrocycle (141)(0.69 g, 1.4 mmol), and phenol

(0.68 g, 8.1 mmol) in hydrogen bromide in acetic acid (10 ml; 45%) was heated with stirring of the solution at 80° for 36 h. The solvent was evaporated by azeotroping with toluene. The residue was dissolved in water (15 ml), the solution washed with dichloromethane (4 x 10 ml), and the water removed *in vacuo* to yield an orange gum. This was dissolved in water (15 ml) and tetramethylammonium hydroxide (1.1 equivalents) was added. The mixture was agitated for 15 min and the product extracted by dichloromethane (3 x 10 ml). Evaporation of the solvent gave a brown oil which was crystallised from toluene to give 4-(2,2'-*bipyridine*-5-*methyl*)-1,7-*dioxa*-4,10-*diazacyclodecane* as a white powder, m.p. 101-103°, (Found: C, 66.3; H, 7.5; N, 16.0. $C_{19}H_{26}N_4O_2$ requires C, 66.7; H, 7.6; N, 16.3%.); δ_H ($CDCl_3$) 2.77 (4 H, t, *J* 4.90 Hz, CH_2N ring), 2.91 (4 H, t, *J* 4.61 Hz, CH_2N ring), 3.64 (4 H, t, *J* 4.89 Hz, CH_2O ring), 3.75 (4 H, t, *J* 4.63 Hz, CH_2O ring), 3.79 (2 H, s, benzylic CH_2), 7.24 (1 H, m), 7.71-7.77 (2 H,m), 8.31 (2 H, d, *J* 8.08 Hz), 8.52 (1 H, s), and 8.60 (1 H, d, *J* 4.83 Hz); δ_C ($CDCl_3$) 48.23 (CH_2N ring), 53.03 (benzylic CH_2), 53.47 (CH_2N ring), 66.70 and 67.22 (CH_2O), and 120.80, 120.99, 123.65, 132.88, 136.87, 137.87, 149.17, 149.74, 155.33 and 155.80 (aromatic C); *m/e* (DCI; ammonia) 343 [$(M+1)^+$, 100%].

Synthesis of Fe(II), Cu(II), and Pd(II) Complexes of Ligand (142).- *Fe(II) complex* (143).- Complex (143) was synthesised according to the method of Burstall and Nyholm.[260]

Cu(II) complex (144).- Complex (144) was synthesised according to the method of Hall, Litzow, and Plowan.[261]

Pd(II) complex (145).- Complex (145) was synthesised according to the method of Parker, Lehn, and Rimmer.[41]

2,6-*Dibromomethylpyridine* (146).- 2,6-Dibromomethylpyridine was synthesised according to the method of Newcomb, Gokel, and Cram.[268]

2,6-*Dithiomethylpyridine* (147) and *Disodium* 2,6-*Dithiolatomethylpyridine* (148).- (147) and (148) were synthesised according to the methods outlined by Carroy-Chalansonnet.[54]

21-*Aza*-3,15-*dithia*-6,9,12-*trioxabicyclo*[15.3.1]*heneicosa*-1(21),17,19-*triene* (95).[265,268]- The disodium salt of 2,6-dithiomethylpyridine (148) (1.5 g, 7.0 mmol) was added to a solution of 1,11-diiodo-3,6,9-trioxaundecane (99)(2.9 g, 7.0 mmol) in butan-1-ol (500 ml) and the resulting mixture was stirred and heated under reflux under a nitrogen atmosphere for 6 h. The solvent was removed under reduced pressure, the residue was extracted with chloroform (3 x 30 ml), each time the solution being decanted from the white powdery solid. After filtration, the filtrate was concentrated *in vacuo* and the residue chromatographed on basic alumina eluting with dichloromethane-methanol (0.3% methanol; column packed with toluene) to give a white solid which was crystallised from hexane to give 21-aza-3,15-dithia-6,9,12-trioxabicyclo[15.3.1]heneicosa-1(21),17,19-triene, (Found: C, 54.7; H, 7.0; N, 4.0. Calc. for $C_{15}H_{23}S_2NO_3$: C, 54.4; H, 7.0; N, 4.2%.); δ_H ($CDCl_3$) 2.71 (4 H, t, *J* 7.0 Hz, SCH_2CH_2O), 3.63 (s*, CH_2O), 3.68 (t*, *J* 3.8 Hz, CH_2O), 3.86 (4 H, s, benzylic CH_2), 7.27 (2 H, d, *J* 7.6 Hz, aromatic H), and 7.64 (1 H, t, *J* 7.8 Hz, aromatic H) (* these signals together integrate for 12 H); δ_C ($CDCl_3$) 30.07 (SCH_2CH_2O), 37.54 (benzylic CH_2), 70.13, 70.66, and 70.77 (CH_2O's), and 121.06, 137.64, and 158.34 (aromatic C); *m/e* (CI; isobutane) 330 [$(M+1)^+$, 100%].

Hexaethylene glycol (149) *and Hexaethylene glycol ditosylate* (150).- These two compounds were synthesised according to the methods of Newcomb, Moore, and Cram.[270]

27-Aza-3,21-*dithia*-6,9,12,15,18-*pentaoxabicyclo*[21.3.1]*heptacosa*-1(27),23,25-*triene* (96).- The disodium salt (148)(1.4 g, 6.6 mmol) was added to a solution of hexaethylene glycol ditosylate (150) (3.9 g, 6.6 mmol) in butan-1-ol (250 ml) kept under a nitrogen atmosphere. The resulting mixture was heated under reflux with stirring for 6 h. After removal of the solvent under reduced pressure, the residue was extracted with chloroform (4 x 30 ml), each time the solution being decanted from the white solid. After removal of the solid by filtration, the filtrate was evaporated *in vacuo*. The residue was chromatographed on basic alumina eluting with dichloromethane-methanol (methanol increasing from 0 to 1%; column packed with toluene), to give a yellow oil. Extraction with hot hexane (4 x 25 ml), with decanting of the solution from the oily residue, and evaporation of the solvent *in vacuo* gave 27-aza-3,21-dithia-6,9,12,15,18-pentaoxabicyclo[21.3.1]heptacosa-1(27),23,25-triene as a colourless oil, (Found: C, 54.5; H, 7.3; N, 3.7. Calc. for $C_{19}H_{31}NO_5S_2$: C, 54.7; H, 7.4; N, 3.4%.); δ_H ($CDCl_3$) 2.70 (4 H, t, *J* 6.64 Hz, SCH_2CH_2O), 3.64 (20 H, m, CH_2O's), 3.85 (4 H, s, benzylic CH_2), 7.28 (2 H, d, *J* 8.40 Hz, aromatic H), and 7.64 (1 H, t, *J* 7.3 Hz, aromatic H); δ_C ($CDCl_3$) 30.48 (SCH_2CH_2O), 37.91 (benzylic CH_2), 70.30, 70.49, and 70.62 (CH_2O's), and 121.19, 137.35, and 158.45 (aromatic C); *m/e* (CI; isobutane) 418 [$(M+1)^+$, 100%].

15-Aza-3,9-*dithia*-6-*oxabicyclo*[9.3.1]*pentadeca*-1(15),11,13-*triene* (94)[268] *and* 29,30-*Diaza*-3,9,17,23-*tetrathia*-6,20-*dioxatricyclo*-[23.3.1.1^{11,15}]-*triaconta*-1(29),11,13,15(30),25,27-*hexaene* (94a).- A

solution of 2-mercaptoethyl ether (2.76 g, 20 mmol) in butan-1-ol (50 ml) was stirred with potassium hydroxide (2.44 g, 40 mmol) for 1 h. A solution of 2,6-dibromomethylpyridine (146) (5.3 g, 20 mmol) in butan-1-ol was added over 2 h and the resulting mixture heated at 80° for 18 h. The solid was removed by filtration and the filtrate evaporated *in vacuo*. Chromatography on alumina with elution with toluene-dichloromethane (1:1) gave 15-aza-3,9-dithia-6-oxabicyclo-[9.3.1]pentadeca-1(15),11,13-triene, 1.1 g (23%), δ_H ($CDCl_3$) 2.60 (4 H, t, *J* 8.05 Hz, SCH_2), 3.32 (4 H, t, *J* 8.04 Hz, CH_2O), 3.85 (4 H, s, benzylic CH_2), 7.32 (2 H, d, *J* 7.70 Hz, aromatic H), and 7.73 (1 H, t, *J* 7.78 Hz, aromatic H); δ_C ($CDCl_3$) 27.50 (SCH_2), 36.91 (benzylic CH_2), 67.00 (CH_2O), and 121.91, 138.28, and 157.60 (aromatic C); and 29,30-diaza-3,9,17,23-tetrathia-6,20-dioxatricyclo[23.3.1.$1^{11,15}$]-triaconta-1(29),11,13,15(30),25,27-hexaene, 210 mg (5%), m.p. 106-108°, (Found: C, 54.4; H, 6.2; N, 5.2. Calc. for $C_{22}H_{30}N_2O_2S_4$: C, 54.8; H, 6.2; N, 5.8%.); δ_H ($CDCl_3$) 2.67 (8 H, t, *J* 6.98 Hz, SCH_2), 3.54 (8 H, t, *J*, 6.97 Hz, CH_2O), 3.81 (8 H, s, benzylic CH_2), 7.24 (4 H, d, *J* 7.68 Hz, aromatic H), and 7.63 (2 H, t, *J* 7.68 Hz, aromatic H); δ_C ($CDCl_3$) 30.48 (SCH_2), 37.83 (benzylic C), 70.00 (CH_2O), and 121.12, 137.40, and 158.39 (aromatic C).

Synthesis of Rhodium Complexes of (95)(PyO_3S_2), (96)(PyO_5S_2), (94)($PyOS_2$), and (94a)($Py_2O_2S_4$).-

[(95)-*Rh*(CO)]$^+$ PF_6^- (151).- A solution of tetracarbonyldichloro-dirhodium(I) (39.3 mg, 0.1 mmol) in methanol (1 ml) was added to a solution of the ligand (95) (66.5 mg, 0.2 mmol) in methanol (2 ml). Brisk evolution of carbon monoxide ensued and the solution was stirred for 30 min under nitrogen. An excess of ammonium hexafluorophosphate was added as a solution in methanol and a red microcrystalline

precipitate formed within two minutes. The precipitate was isolated by filtration, washed with ethanol (2 x 1 ml), and dried *in vacuo*. The filtrate was allowed to stand at 0^{o} and ruby-red, diamond-shaped crystals of [(95)-*Rh*(CO)]$^{+}$ PF_6^- were formed, υ_{max} (CH_2Cl_2, acetone, and tetrahydrofuran) 2020 (C≡O stretch); δ_H ($CDCl_3$) 3.15 (4 H, m), 3.38 (4 H, m), 3.53 (4 H, t, *J* 7.80 Hz), 4.18 (4 H, m), 4.79 (2 H, d, *J* 16.98 Hz, half of *AB* system, benzylic CH_2), 5.07 (2 H, d, *J* 17.01 Hz, half of *AB* system, benzylic CH_2), 7.53 (2 H, d, *J* 8.00 Hz, aromatic H) and 7.92 (1 H, t, *J* 7.98 Hz, aromatic H); *m/e* (FAB; glycerol) 460 [(95)-Rh(CO)]$^{+}$.

X-Ray Crystal Data.- $C_{32}H_{46}F_{12}N_2O_8P_2Rh_2S_4$; *M* = 1210.72; tetragonal, *a* = 11.800 (2), *c* = 31.822 (8) Å; V = 4 430.9 Å^3; Z = 4; D_x = 1.81 g cm^{-3}; *F*(000) = 2 432; μ(Mo-K_α) = 10.8 cm^{-1}. Space group determined from the systematic absences as $P4_12_12$ (No. 92). The structure was determined by the heavy atom method. 2844 unique reflexions were measured on a CAD4 diffractometer of which 1737 were used in the refinement to give *R* = 0.027 and R_w = 0.033.

[(96)]-*Rh*(CO)]$^{+}$ PF_6^- (156).- A solution of tetracarbonyldichlorodirhodium(I) (22.4 mg, 0.06 mmol) in methanol (1 ml) was added to a solution of ligand (96) (59.5 mg, 0.14 mmol) in methanol (2 ml). The mixture was stirred vigorously under nitrogen for 30 min. An excess of ammonium hexafluorophosphate was added as a solution in methanol (1 ml). The solution was reduced to a small volume under reduced pressure. A bright red precipitate of [(96)]-*Rh*(CO)]$^{+}$ PF_6^- formed which was collected by filtration [any further contact of the red precipitate with solvent (methanol or dichloromethane) causes transformation to a yellow powder which analyses similarly which suggests that the red compound is the dimeric form of the title compound], υ_{max} (CH_2Cl_2) 2020 cm^{-1} (C≡O

stretch); δ_H^{298} (CD_2Cl_2) 3.12 (4 H, br s, CH_2S), 3.55 and 4.01 (20H, br s, CH_2O's), 4.97 (4 H, d, *J* 6.73 Hz, benzylic CH_2) [sharpens on cooling of the solution to give 4.91 (*J* 18.3 Hz,) and 5.05 (*J* 18.2 Hz)(*AB* system); $\Delta G^{\neq}$ = 63.8 kJ mol^{-1}], 7.60 (2 H, d, *J* 7.88 Hz, *meta* aromatic H),and 7.92 (1 H, t, *J* 7.77 Hz, *para* aromatic H); *m/e* (FAB; glycerol) 548 $[(96)\text{-}Rh(CO)]^+$, 520 $[(96)\text{-}Rh]^+$.

$[(96)\text{-}RhCl_2(H_2O)]^+ PF_6^-$ (158).- A solution of rhodium trichloride trihydrate (41.1 mg, 0.16 mmol) in aqueous methanol was added to a solution of the ether (96)(72.4 mg, 0.17 mmol) in methanol (2 ml). The mixture was heated under reflux for 18 h under an atmosphere of nitrogen. The initial dull pink precipitate which formed redissolved during the course of the reaction to give an orange solution. An excess of ammonium hexafluorophosphate was added as a solution in methanol and the resulting solution was evaporated to a small volume under reduced pressure. The orange crystalline solid was isolated by filtration and washed thoroughly with methanol, and dried to give $[(96)\text{-}RhCl_2(H_2O)]^+ PF_6^-$, δ_H (CD_2Cl_2) 2.87 (2 H, m), 3.66 (22 H, m,), 4.70 (2 H, d, *J* 16.33 Hz, half of *AB* system, benzylic CH_2) 4.92 (2 H, d, *J* 16.16 Hz, half of *AB* system, benzylic CH_2) 7.60 (2 H, d, *J* 8.08 Hz *meta* aromatic H),and 7.93 (1 H, t, *J* 7.89 Hz, *para* aromatic H); *m/e* (FAB; glycerol) 608 $[(96)\text{-}RhCl_2(H_2O)]^+$, 573 $[(96)\text{-}RhCl(H_2O)]^+$, 555 $[(96)\text{-}RhCl]^+$, 520 $[(96)\text{-}Rh]^+$. [The title compound is also formed by aerial oxidation of a methanol solution of complex (156) saturated with chloride ions.]

X-Ray Crystal Data.- $C_{19}H_{33}Cl_2F_6NO_6PRhS_2$; *M* = 754.38; monoclinic, a = 10.767(2), b = 23.479(4), c = 11.577(2) Å, β = 95.04(1)°; V = 2915.4 $Å^3$, Z = 4, D_x = 1.72 g cm^{-3}; F(000) = 1528, μ(Mo-Kα) = 10.3 cm^{-1}. Space group determined uniquely from the systematic absences as $P2_1/n$ (alt. $P2_1/c$, No. 14). The structure was

determined by the heavy atom method. Isotropic followed by anisotropic refinement of the non-hydrogen atoms with the hydrogens in geometrically idealised positions converged with R = 0.024 and R_w = 0.032: 4637 unique reflexions were measured on a CAD4 diffractometer to a 2θ maximum of 54^o. After correction for Lorentz polarisation and absorption effects, 2103 were labelled "observed" and used in the structure solution and refinement.

[(94a)-$Rh_2(CO)_2$]$^{2+}$ $2PF_6^-$ (155).- A solution of tetracarbonyldichloro-dirhodium(I) (19 mg, 0.05 mmol) in methanol (1 ml) was added to a solution of ligand (94a)(24 mg, 0.05 mmol) in methanol (3 ml). The resulting mixture was stirred for 30 min under nitrogen. An excess of ammonium hexafluorophosphate was added as a solution in methanol. A brilliant red precipitate formed immediately and the mixture was allowed to stand for 1 h, during which ruby red crystals of the complex formed. The precipitate was collected by filtration, washed with ethanol (2 x 1 ml), and dried *in vacuo* to give [(94a)-$Rh_2(CO)_2$]$^{2+}$ $2PF_6^-$, (Found: C, 28.4; H, 3.0; N, 2.7. $C_{24}H_{30}F_{12}N_2O_4P_2Rh_2S_4$ requires C, 27.9; H, 2.9; N, 2.7%.); υ_{max} 1993, 2044 (C≡O stretches); δ_H (CD_3COCD_3) 3.43 (8 H, br s, CH_2S), 4.16 (8 H, br s, CH_2O), 5.07 (8 H, br s, benzylic CH_2), 7.72 (4 H, d, *J* 7.5 Hz, *meta* aromatic H), and 8.08 (2 H, t, *J* 7.5 Hz, *para* aromatic H).

[(94)-$Rh(CO)$]$^+$ PF_6^- (152).- A solution of tetracarbonyldichlorodi-rhodium(I) (19.4 mg, 0.05 mmol) in methanol (1 ml) was added to a solution of ligand (94) (24.1 mg, 0.1 mmol) in methanol (4 ml). Reaction was accompanied by a brisk evolution of carbon monoxide and the solution darkened to a deep blue. The solution was agitated for 5 min and a solution of ammonium hexafluorophosphate in methanol was added.

An indigo precipitate formed immediately which was collected by filtration, washed with ethanol (2 x 1 ml) and dried *in vacuo* to give $[(94)\text{-}Rh(CO)]^+ PF_6^-$, (Found: C, 28.3; H, 2.9; N, 2.6. $C_{12}H_{15}F_6NO_2PRhS_2$ requires C, 27.9; H, 2.9; N, 2.7%.); υ_{max} 1740 (C≡O stretch); δ_H (CD_3CN)(rapidly decomposes) 3.53 (s), 3.80 and 3.84 (br d), 4.72 (4 H, q, *AB* system, *J* 18.3 Hz, benzylic CH_2), 7.63 (2 H, d, *J* 7.73 Hz, *meta* aromatic H's), and 7.96 (1 H, t, *J* 7.63 Hz, *para* aromatic H).

Synthesis of Potassium Complex of (96)(PyO_5S_2).- $[(96)\text{-}K]^+ Cl^-$ (157).- A solution of potassium chloride (2 molar excess) in methanol (0.5 ml) was added to a hot methanolic solution of ligand (96). The resulting solution was filtered and colourless cubic crystals of $[(96)\text{-}K]^+ Cl^-$ formed on standing of the solution, δ_H (CD_3OD) 2.78 (4 H, t, *J* 6.84 Hz, SCH_2CH_2O), 3.67 (20 H, m, CH_2O's), 3.91 (4 H, s, benzylic CH_2), 7.39 (2 H, d, *J* 7.63 Hz, *meta* aromatic H), and 7.80 (1 H, t, *J* 7.70 Hz, *para* aromatic H); δ_C (CD_3OD) 31.42 (SCH_2CH_2O), 38.21 (benzylic CH_2), 71.12 (CH_2O's), and 123.06, 139.41, and 159.99 (aromatic C's); *m/e* (FAB; glycerol) 456 $[(96)\text{-}K]^+$.

Synthesis of the Palladium Complexes of (95)(PyO_3S_2) *and* (96)(PyO_5S_2).- $[(95)\text{-}PdCl]^+ Cl^-$ (159).- A solution of *bis*(benzonitrile)-dichloropalladium(II) (43.8 mg, 110 μmol) in dichloromethane (1 ml) was added to a solution of ligand (95) (37.6 mg, 110 μmol) in dichloromethane (2 ml) and the resulting solution was heated under reflux for 15 h under a nitrogen atmosphere. The solution was reduced to a small volume under reduced pressure when a bright yellow solid separated which was collected by filtration, washed with ether (2 x 1 ml), and dried *in vacuo* to give $[(95)\text{-}PdCl]^+ Cl^-$, (Found: C, 34.8; H, 4.5; N, 2.5. $C_{15}H_{23}NO_3S_2PdCl_2.H_2O$ requires C, 34.4; H, 4.7; N, 2.6%.);

λ_{max} (H_2O) 357; δ_H (D_2O) 3.51 (12 H, m), 4.28 (4 H, m), 4.96 (2 H, d, *J* 17.68 Hz, half of *AB* system, benzylic CH_2), 5.12 (2 H, d, *J* 17.56 Hz, half of *AB* system, benzylic CH_2), 7.61 (2 H, d, *J* 8.03 Hz, *meta* aromatic H), and 8.08 (1 H, t, *J* 7.94 Hz, *para* aromatic H); *m/e* (FAB; glycerol) 470 [(95)-PdCl]$^+$, 435 [(95)-Pd]$^+$.

{[(96)-*PdCl*]$^+$}$_2$ $PdCl_4^{2-}$ (162).- A solution of *bis*(benzonitrile)dichloropalladium(II) (88.7 mg, 230 μmol) in dichloromethane (2 ml) was added to a solution of ligand (96) (96.3 mg, 230 μmol) in dichloromethane (2 ml) and the resulting solution was heated under reflux for 15 h under an atmosphere of nitrogen. A yellow precipitate began to form after 1 h. The precipitate was collected by filtration, washed with dichloromethane (1 ml), and dried *in vacuo* to give {[(96)-*PdCl*]$^+$}$_2$ $PdCl_4^{2-}$, (Found: C, 33.1; H, 4.7; N, 1.7; Pd, 24.9. $C_{38}H_{62}Cl_6N_2O_{10}Pd_3S_4$ requires C, 33.4; H, 4.5; N, 2.0; Pd, 23.3%.); λ_{max} (H_2O) 357; δ_H (D_2O) 3.12-3.62 (m), 3.76-4.04 (m), 4.78 and 5.18 (*AB* pattern, benzylic CH_2, *J* 17.95 Hz), 5.03 (s br, benzylic CH_2), 7.42 (d, *J* 8.2 Hz, *meta* aromatic H), 7.44 (d, *J* 8.0 Hz, *meta* aromatic H), 7.86 (t, *J* 8.0 Hz, *para* aromatic H) and 7.87 (t, *J* 8.0 Hz, *para* aromatic H); *m/e* (FAB; glycerol) 557 [(96)-PdCl]$^+$, 523 [(96)-Pd]$^+$, 246 [negative ion; $(PdCl_4)^-$].

Synthesis of the platinum complexes of (95)(PyO_3S_2) *and* (96)(PyO_5S_2).- [(95)-*PtCl*]$^+$ Cl^- (160).- A solution of bis(tertiarybutylcyano)dichloroplatinum(II) (60.8 mg, 0.14 mmol) in dichloromethane (1 ml) was added to a solution of ligand (95) (44.9 mg, 0.14 mmol) in dichloromethane (2 ml) and the resulting solution was heated under reflux for 3 h under an atmosphere of nitrogen. The mixture was filtered and the filtrate was evaporated to small volume under reduced pressure and poured dropwise into ether yielding a creamy white precipitate which was isolated by

filtration, washed with ether, and dried *in vacuo* to give [(95)-*PtCl*]$^+$ Cl^-, (Found: C, 29.0; H, 3.9; N, 2.1. $C_{15}H_{23}Cl_2NO_3PtS_2.H_2O$ requires C, 29.3; H, 4.0; N, 2.2%.); δ_H (D_2O) 3.38 - 3.62 (m), 4.24 (m), 5.05 (2 H, d, *J* 17.61 Hz, half of *AB* system, benzylic CH_2), 5.30 (2 H, d, *J* 17.63 Hz, half of *AB* system, benzylic CH_2), 7.68 (2 H, d, *J* 7.93 Hz, *meta* aromatic H), and 8.15 (1 H, t, *J* 8.00 Hz, *para* aromatic H); *m/e* (FAB; glycerol) 560 [(95)-PtCl]$^+$, 525 [(95)-Pt]$^+$.

[(96)-*PtCl*]$^+$ Cl^- (161).- A solution of bis(tertiarybutylcyano)dichloro-platinum(II) (84.7 mg, 0.20 mmol) in dichloromethane (1 ml) was added to a solution of ligand (96) (81.3 mg, 0.19 mmol) in dichloromethane (2 ml) and the solution heated under reflux for 3 h under an atmosphere of nitrogen. The mixture was filtered and the filtrate was evaporated under reduced pressure, precipitation of a white solid was induced by the addition of ethyl acetate. The solid was collected by filtration, washed with cold ethyl acetate, and dried *in vacuo* to give [(96)-*PtCl*]$^+$ Cl^-, δ_H (D_2O) 3.13-3.59 (m), 3.77-4.05 (m), 4.76 and 4.92 (*AB* pattern, *J* 17.81 Hz, benzylic CH_2), 4.83 and 4.95 (*AB* pattern, *J* 18.07 Hz, benzylic CH_2), 7.48 (d, *J* 8.2 Hz, *meta* aromatic H), 7.51 (d, *J* 8.2 Hz, *meta* aromatic H), 7.95 (t, *J* 8.2 Hz, *para* aromatic H), and 7.96 (t, *J* 8.2 Hz, *para* aromatic H); *m/e* (FAB; glycerol) 648 [(96)-PtCl$^+$], 612 [(96)-Pt$^+$].

25,26-*Diaza*-3,7,15,19-*tetrathiatricyclo*[19.3.1.1^{9,13}]*hexacosa*-1(25),9,11,13(26),21,23-*hexaene* (92).- The title compound was synthesised according to the method of Parker, Lehn, and Rimmer,[41] υ_{max} (FT)(KBr) 1591 and 1572 (pyridine ring stretches).

X-Ray Crystal Data.- The current R factor is 9.7%, we are now awaiting a low-temperature study.

Synthesis of the Transition Metal Complexes of the Py_2S_4 Ligand (92).- $[(92)\text{-}Co]^{2+}$ $2BF_4^-$ (167).- A solution of cobalt(II) tetrafluoroborate (86.6 mg, 0.37 mmol) in acetone (1 ml) was added to a solution of ligand (92) (27.7 mg, 0.07 mmol) in dichloromethane (2 ml). There was an immediate formation of a black precipitate which was collected by filtration, washed with dichloromethane and acetone, and dried *in vacuo* to give the *cobalt complex* (167), (Found: C, 36.3; H, 3.9; N, 3.9. $C_{20}H_{26}B_2CoF_8N_2S_4$ requires C, 36.6; H, 4.0; N, 4.2%.); υ_{max} (KBr) 1600 and 1569 (pyridine ring); λ_{max} (MeOH) 212, 271, and 579; *m/e* (FAB; 2,2'-thiodiethanol) 481 $[(92)\text{-}Co]^{2+}$.

$[(92)\text{-}Ni]^{2+}$ $2ClO_4^-$ (168).- A solution of nickel(II) perchlorate pentahydrate (56.8 mg, 160 μmol) in acetone (1 ml) was added to a solution of the ligand (92) (20.4 mg, 48 μmol) in dichloromethane (2 ml). There was an immediate formation of a pale lilac precipitate which was collected by filtration, washed with dichloromethane and acetone, and dried *in vacuo* to give the *nickel complex* (168), (Found: C, 35.4; H, 3.6; N, 3.4. $C_{20}H_{26}Cl_2N_2NiO_8S_4$ requires C, 35.3; H, 3.8; N, 4.1%.); λ_{max} (H_2O) 202, 265, 310; *m/e* (FAB; 2,2'-thiodiethanol) 481 $[(92)\text{-}Ni]^{2+}$.

$[(92)\text{-}(Cu)_2Cl_2]^{2+}$ $2Cl^-$ (171).- A solution of copper(II) dichloride dihydrate (27.0 mg, 160 μmol) in methanol (1 ml) was added to a solution of the ligand (92)(15.4 mg, 40 μmol) in dichloromethane (1 ml). There was an immediate formation of a pale green precipitate which was collected by filtration, washed with methanol and ethyl acetate, and dried *in vacuo* to give the *copper complex* (171), (Found: C, 36.0; H, 4.2; N, 3.9; Cu, 15.8. $C_{20}H_{26}Cl_4Cu_2N_2S_4.2MeOH$ requires C, 36.0; H, 4.5; N, 3.7; Cu, 16.7%.); υ_{max} (KBr) 1602 and 1573 (pyridine ring stretches);

λ_{max} (H_2O) 656 (390), 407 (4060), 276 (12750), and 190 (23200); *m/e* (FAB; glycerol) 485, 487 $[(92)\text{-}Cu]^+$.

$[(92)\text{-}Pd_2(NO_3)_2]^{2+}$ $2NO_3^-.2H_2O$ (166).- A solution of palladium(II) nitrate trihydrate (21.7 mg, 80 μmol) in aqueous methanol (1 ml) was added to a solution of the ligand (92)(14.0 mg, 30 μmol) in dichloromethane (2 ml). There was an immediate formation of a beige precipitate which darkened on standing to a golden yellow. This was collected by filtration, washed with dichloromethane and dried *in vacuo* to give the *palladium complex* (166), (Found: C, 26.0; H, 3.2; N, 8.6. $C_{20}H_{26}N_6O_{12}Pd_2S_4.2H_2O$ requires C, 26.1; H, 3.3; N, 9.1%.); υ_{max} (KBr) 1602 and 1571 (pyridine ring stretches); δ_H (D_2O) 3.28 (m br), 3.58 (m br), 4.94 (s br), 7.63 (d br, *J* 7.93 Hz), and 8.03 (m br).

$[(92)\text{-}Pd_2Cl_2]^{2+}$ $2Cl^-$ (164).- This complex was synthesised according to the method of Parker.[41]

$[(92)\text{-}Pd_2(OH)_2]^{2+}$ $2PF_6^-$ (165).- The dipalladium complex (164) (*c.* 20 mg) was dissolved in water (1 ml) and silver nitrate (four mole equivalents) in water (1 ml) was added. Silver chloride was deposited and the solution remained yellow. Ethene was bubbled through the solution for 30 min during which the solution became claret in colour. Silver chloride was removed by centrifugation and decanting of the supernatant. An excess of a solution of ammonium hexafluorophosphate in water was added to this solution and a red precipitate formed. The precipitate was collected by filtration, washed thrice with water, and dried *in vacuo* to give the *palladium complex* (165), (Found: C, 25.2; H, 3.1; N, 3.0; Pd, 21.9. $C_{20}H_{28}F_{12}N_2O_2P_2Pd_2S_4$ requires C, 25.05; H, 2.9; N. 2.9; Pd, 22.1%.); υ_{max} (FT; KBr disc) 1602 and 1573 (pyridine ring

stretches); δ_H (CD_3COCD_3) 2.75 (4 H, overlapping t + t, *J* 5.05 Hz, $CH_2CH_2CH_2$), 2.87 (1 H, s, OH), 3.49 (8 H, t, *J* 5.51 Hz, CH_2S's), 5.10 (8 H, s, benzylic CH_2), 7.79 (4 H, d, *J* 7.83 Hz, *meta* aromatic H), and 8.12 (2 H, t, *J* 7.83 Hz, *para* aromatic H).

$[(92)\text{-}Pt_2Cl_2]^{2+}$ $2Cl^-$ (172).- A solution of *bis*(methylcyano)dichloroplatinum(II) (84 mg, 0.241 mmol) in dichloromethane (5 ml) was added to a solution of ligand (92) (50 mg, 118 μmol) in dichloromethane and the solution heated under reflux for 1.5 h under nitrogen. The pale yellow precipitate which formed was collected by filtration, washed with dichloromethane, and dried *in vacuo* to give the *platinum complex* (172), 103 mg (90%), (Found: C, 25.3; H, 3.1; Cl, 14.5; N, 3.3; S, 13.2. $C_{20}H_{26}Cl_4N_2Pt_2S_4$ requires C, 25.2; H, 2.8; N. 2.9; Cl, 14.9; S, 13.4%.); υ_{max} (KBr) 1600 and 1565 (pyridine ring stretches), (CsI) 368, 360, 355 (Pt-Cl stretch); δ_H (D_2O) 2.69 and 3.00 (4 H, m and overlapping t x t, *J* 7.83 Hz, $CH_2CH_2CH_2$), 3.19-3.45 (8 H, m, CH_2S), 4.95 and 5.10 (*AB* pattern, *J* 17.46 Hz and 17.65 Hz, benzylic CH_2), 4.97 and 5.1 (*AB* pattern, *J* 17.97 Hz, benzylic CH_2), 7.68 and 7.76 (4 H, d and d, *J* 8.05 and 8.00 Hz, *meta* aromatic H), and 8.15 and 8.21 (2 H, t and t, *J* 8.01 and 7.98 Hz, *para* aromatic H); δ_C (D_2O) 29.76 ($CH_2CH_2CH_2$), 35.80 and 36.07 (CH_2S), 45.66 and 46.20 (benzylic CH_2), 122.85 and 123.27 (*meta* aromatic C), 140.83 (*para* aromatic C), and 161.63 and 161.95 (*ortho* aromatic C); *m/e* (FAB; thiodiglycol), 881 $[(92)\text{-}Pt_2Cl_2]^+$, 847 $[(92)\text{-}Pt_2Cl]^+$, 812 $[(92)\text{-}Pt_2]^+$, 653 $[(92)\text{-}PtCl]^+$, and 617 $[(92)\text{-}Pt]^+$. Conductimetric measurements confirm the stoichiometry as the 2:1 salt.

7.2 NMR Experiments

Titration curves were obtained using d_4-methanol solutions (2 ml) of the ligands ($\simeq$ 0.1 M) and solid alkali salts [LiCl (BDH); $CaCl_2$ (Aldrich)]. After each addition of salt, the ^{13}C NMR chemical shift (relative to TMS) was measured at 298 K using a Bruker AC 250 instrument operating at 62.896 MHz for the carbon nucleus. The signals that underwent the largest displacement were selected for plotting the curves, unless otherwise indicated.

Kinetic experiments by dynamic ^{13}C NMR spectroscopy were conducted with a ratio of ligand ($\simeq$ 0.1 M) to salt of 2:1, giving at equilibrium a 50:50 mixture of the free and the complexed ligand.

7.3 FAB MS Experiments

The stainless steel tip of a FAB probe was coated with a thin layer of the analytical solution. Positive ion FAB MS was performed using a primary atom beam of Ar (8 keV) on a VG 7070E mass spectrometer coupled to a VG 11-250 data system. At an accelerating voltage of 6 kV, the mass range *m/e* 20-2000 was scanned at 3 s per decade (scan cycle time, 10 s). Twenty successive spectra of each analytical solution were acquired and scans 5 to 15 inclusive were averaged to afford the final spectrum.

7.4 pH-Metric Measurements

The apparatus used was an Orion Expandable Ion Analyzer EA940. The

reference Ag/AgCl electrode was fitted with a bridge containing a non-complexable cation, 0.1 M NMe_4Br in methanol-water (9:1 by volume). The measuring electrode was an Orion 91-02sc pH electrode suitable for measurements in methanol-water. In methanol-water the electrodes were calibrated using an oxalate buffer at pH 3.73 and a succinate buffer at ph 6.73,[293] both buffers in methanol-water (9:1). In this solvent the logarithm of the dissociation constant of water (pK_w) is 15.56 $\pm$ 0.03.[207] All experiments were back titrations by NMe_4OH [0.1 M in methanol-water (9:1)] of solutions containing a sufficient amount of acid to protonate the ligand completely. The standard ligand solution was [0.011 M HNO_3 + 0.01 M ligand + 0.089 M NMe_4Br in methanol-water (9:1)]. The pK values for the ligands were determined on a mixture of ligand solution (15 ml) and NMe_4Br solution (15 ml; 0.1 M) in methanol-water (9:1). For determination of the stability constants, titrations were performed at 1:1 and 2:1 salt/ligand ratios; the solutions were (15 ml ligand + 1.5 ml 0.1 M salt/13.5 ml 0.1 M NMe_4Br) and (15 ml ligand solution + 3 ml 0.1 M salt/12 ml 0.1 M NMe_4Br). The data from the titration curves were analysed with the computer program SUPERQUAD.[210,211]

The error limits are about $\pm$ 0.2 for log K.

7.5 Calorimetric Experiments

Titration calorimetric experiments were carried out by Dr. H.-J. Buschmann, Abteilung für Physikalische Chemie, Universität-GH Siegen, Postfach 101240, D-5900 Siegen, Federal Republic of Germany. Materials: the salts used were $LiClO_4$ (Ventron), $NaNO_3$ (Merck), KI (Merck), RbI (Merck), $Ca(NO_3)_2$ (BDH), $SrBr_2$ (Ventron), $AgNO_3$ (Merck),

and $Ba(ClO_4)_2$ (Merck). The solvent used was MeOH [0.01% H_2O (Merck)]. Procedure: all stability constants and reaction enthalpies were determined using a Tronac Model 450 calorimeter. A solution of the ligand (0.05 - 0.025 M) was added slowly to a solution containing a salt ($1.5 - 4 \times 10^{-3}$ M). The heat Q produced during titration was related to the reaction enthalpy ΔH after correction for all non-chemical heat effects as shown by the following equation:

$$Q_t = \Delta n_t \cdot \Delta H$$

where Δn_t is the number of moles of the complex formed at time, t. During the titration Δn_t varies since it is a function of the stability constant, K.

$$M^{x+} + L \rightleftharpoons ML^{x+} ; \quad K = \frac{[ML^{x+}]}{[M^{x+}][L]}$$

No values for the stability constant can be calculated from the thermogram if log $K > 5.5$. In other cases, the salt concentration in the reaction vessel was so high ($2 - 3 \times 10^{-2}$ M) that every added molecule of the ligand forms a complex. In this case, Δn_t is constant during the titration and only values of the reaction enthalpy can be obtained from the thermogram.

7.6 X-Ray Crystal Structure Determinations

All structures were determined by Professor George Ferguson, Department of Chemistry, University of Guelph, Ontario, Canada. Reflexions were measured on a CAD4 diffractometer. Calculations were made with the SDP suite of programs[294] on a PDP-11/73 computer. The atomic coordinates are available from Dr. D. Parker, Department of Chemistry, University of Durham, South Road, Durham DH1 3LE. Positional

and thermal parameters and molecular dimensions for each structure are given in the Appendix.

PUBLICATIONS, COLLOQUIA, AND CONFERENCES

List of Publications

1. G. Ferguson, C.R. Langrick, D. Parker, and K.E. Matthes, *J. Chem. Soc., Chem. Commun.*, 1985, 1609.

2. A. Carroy, C.R. Langrick, J.M. Lehn, K.E. Matthes, and D. Parker, *Helv. Chim. Acta*, 1986, 69, 580.

3. K.E. Matthes and D. Parker, *Stereochemistry of Organometallic and Inorganic Compounds*, 1987, 2, Chap. 3.

4. G. Ferguson, K.E. Matthes, and D. Parker, accepted for publication in *J. Chem. Soc., Chem. Commun.*, 1987 (COM NO. 658).

5. G. Ferguson, K.E. Matthes, and D. Parker, accepted for publication in *Angew. Chem., Int. Ed. Engl.*, 1987.

6. H.-J. Buschmann, G. Ferguson, K.E. Matthes, and D. Parker, submitted for publication in *Tetrahedron Lett.*, 1987.

COLLOQUIA AND CONFERENCES

The Board of Studies in Chemistry requires that each postgraduate research thesis contain an appendix listing:

(A) all research colloquia, research seminars, and lectures arranged by the Department of Chemistry during the period of the author's residence as a postgraduate student;

(B) all research conferences attended and papers presented by the author during the period when research for the thesis was carried out.

RESEARCH COLLOQUIA, SEMINARS, LECTURES, AND CONFERENCES

(A) Lectures and Seminars organised by the Department of Chemistry during the period 1984-1987.

19.10.84 Dr. A. Germain (Languedoc, Montpellier)
"Anodic Oxidation of Perfluoro Organic Compounds in Perfluoroalkane Sulphonic Acids"

24.10.84 Prof. R.K. Harris (Durham)
"N.M.R. of Solid Polymers"

28.10.84 Dr R. Snaith (Strathclyde)
"Exploring Lithium Chemistry: Novel Structures, Bonding, and Reagents"

7.11.84 * Prof. W.W. Porterfield (Hampden-Sydney College, USA)
"There is no Borane Chemistry (only Geometry)"

7.11.84 Dr. H.S. Munro (Durham)
"New Information from ESCA Data"

21.11.84 Mr. N. Everall (Durham)
Picosecond Pulsed Laser Raman Spectroscopy"

27.11.84 * Dr. W.J. Feast (Durham)
"A Plain Man's Guide to Polymeric Organic Metals"

28.11.84 * Dr. T.A. Stephenson (Edinburgh)
"Some recent Studies in Platinum Metal Chemistry"

12.12.84 Dr. K.B. Dillon (Durham)
"^{31}P NMR Studies of some Anionic Phosphorus Complexes"

11. 1.85 Emeritus Prof. H. Suchitzky (Salford)
"Fruitful Fissions of Benzofuroxanes and Isobenzimidazoles (*Umpolung* of *o*-phenylenediamine)"

13. 2.85 Dr. G.W.J. Fleet (Oxford)
"Synthesis of some Alkaloids from Carbohydrate"

19. 2.85 Dr. D.J. Mincher (Durham)
"Stereoselective Syntheses of Some Novel Anthracyclinones Related to the Anti-cancer Drug Adriamycin and to the Steffimycin Antibiotics"

27. 2.85 * Dr. R.E. Mulvey (Durham)
"Some Unusual Lithium Complexes"

6. 3.85 Dr. P.J. Kocienski (Leeds)
"Some Synthetic Applications of Silicon-Mediated Annulation Reactions"

7. 3.85 Dr. P.J. Rodgers (I.C.I. plc Agricultural Division, Billingham)
"Industrial Polymers from Bacteria"

12. 3.85 Prof. K.J. Packer (B.P. Ltd./East Anglia)
"NMR Investigations of the Structure of Solid Polymers"

14. 3.85 * Prof. A.R. Katritzky F.R.S. (Florida)
"Some Adventures in Heterocyclic Chemistry"

20. 3.85 Dr. M. Poliakoff (Nottingham)
New Methods for Detecting Organometallic Intermediates in Solution"

28. 3.85 * Prof. H. Ringsdorf (Mainz)
"Polymeric Liposomes as Models for Biomembranes and Cells"

24. 4.85 Dr. M.C. Grossel (Bedford College, London)
"Hydroxypyridine Dyes - Bleachable One-Dimensional Metals?"

25. 4.85 Major S.A. Shackelford (U.S. Air Force)
"*In Situ* Mechanistic Studies on Condensed Phase Thermochemical Reaction Processes: Deuterium Isotope Effects in HMX Decomposition, Explosives and Combustion"

1. 5.85 Dr. D. Parker (I.C.I plc, Petrochemical and Plastics Division, Wilton)
"Applications of Radioisotopes in Industrial Research"

7. 5.85 Prof. G.E. Coates (formerly of Wyoming, U.S.A.)
"Chemical Education in England and America: Successes and Deficiencies"

8. 5.85 Prof. D. Tuck (Windsor, Ontario)
"Lower Oxidation State Chemistry of Indium"

8. 5.85 Prof. G. Williams (U.C.W., Aberwystwyth)
"Liquid Crystalline Polymers"

9. 5.85 Prof. R.K. Harris (Durham)
"Chemistry in a Spin: Nuclear Magnetic Resonance"

14. 5.85 Prof. J. Passmore (New Brunswick, U.S.A.)
The Synthesis and Characterisation of some Novel Selenium-Iodine Cations, aided by 77-Se NMR Spectroscopy"

15. 5.85 Dr. J.E. Packer (Auckland, New Zealand)
"Studies of Free Radical Reactions in Aqueous Solution Using Ionising Radiation"

17. 5.85 Prof. I.D. Brown (McMaster University, Canada)
"Bond Valence as a Model for Inorganic Chemistry"

21. 5.85 * Dr. D.L.H. Williams (Durham)
"Chemistry in Colour"

22. 5.85 Dr. M. Hudlicky (Blacksburg, U.S.A.)
Preferential Elimination of Hydrogen Fluoride from Vicinal Bromofluorocompounds"

22. 5.85 Dr. R. Grimmett (Otago, New Zealand)
"Some Aspects of Nucleophilic Substitution in Imidazoles"

4. 6.85 Dr. P.S. Belton (Food Research Institute, Norwich)
"Analytical Photoacoustic Spectroscopy"

13. 6.85 Dr. D. Woolins (Imperial College, London)
"Metal - Sulphur - Nitrogen Complexes"

14. 6.85 Prof. Z. Rappoport (Hebrew University, Jerusalem)
"The Rich Mechanistic World of Nucleophilic Vinylic Substitution"

19. 6.85 Dr. T.N. Mitchell (Dortmund)
"Some Synthetic and NMR-Spectroscopic Studies of Organotin Compounds"

26. 6.85 Prof. G. Shaw (Bradford)
"Synthetic Studies on Imidazole Nucleosides and the Anitbiotic Coformycin"

12. 7.85 Dr. K. Laali (Hydrocarbon Research Institute, University of Southern California, U.S.A.)
"Recent Developments in Superacid Chemistry and Mechanistic Considerations in Electrophilic Aromatic Substitutions: A Progress Report"

13. 9.85 Dr. V.S. Parmar (Delhi)
"Enzyme Assisted ERC Synthesis"

17.10.85 * Dr. C.J. Ludman (Durham)
"Some Thermochemical Aspects of Explosions"

24.10.85 * Dr. J. Dewing (UMIST)
"Zeolites - Small Holes, Big Opportunities"

30.10.85 * Dr. S.N. Whittleton (Durham)
"An Investigation of a Reaction Window"

31.10.85 * Dr. P. Timms (Bristol)
"Some Chemistry of Fireworks"

5.11.85 Prof. M.J. O'Donnell (Indiana-Purdue University, U.S.A.)
"New Methodology for the Synthesis of Amino Acids"

7.11.85 * Prof. G. Ertl (Munich, W. Germany)
"Heterogeneous Catalysis"

14.11.85 * Dr. S.G. Davies (Oxford)
"Chirality Control and Molecular Recognition"

20.11.85 Dr. J.A.H. McBride (Sunderland Polytechnic)
"A Heterocyclic Tour on a Distorted Tricycle - Biphenylene"

21.11.85 * Prof. K.H. Jack (Newcastle)
"Chemistry of Si-Al-O-N Engineering Ceramics"

28.11.85 * Dr. B.A.J. Clark (Kodak Ltd.)
"Chemistry and Principles of Colour Photography"

28.11.85 * Prof. D.J. Waddington (York)
"Resources for the Chemistry Teacher"

15. 1.86 Prof. N. Sheppard (East Anglia)
"Vibrational and Spectroscopic Determinations of the Structures of Molecules Chemisorbed on Metal Surfaces"

23. 1.86 * Prof. Sir Jack Lewis (Cambridge)
"Some More Recent Aspects in the Cluster Chemistry of Ruthenium and Osmium Carbonyls"

29. 1.86 Dr. J.H. Clark (York)
"Novel Fluoride Ion Reagents"

30. 1.86 * Dr. N.J. Phillips (Loughborough)
"Laser Holography"

12. 2.86 Dr. J. Yarwood (Durham)
"The Structure of Water in Liquid Crystals"

12. 2.86 Dr. O.S. Tee (Concordia University, Montreal, Canada)
"Bromination of Phenols"

13. 2.86 * Prof. R. Grigg (Queen's, Belfast)
"Thermal Generation of 1,3-Dipoles"

19. 2.86 Prof. G. Procter (Salford)
"Approaches to the Synthesis of Some Natural Products"

20. 2.86 * Dr. C.J.F. Barnard (Johnson Matthey Group)
"Platinum Anti-Cancer Drug Development"

26. 2.86 Ms. C. Till (Durham)
"ESCA and Optical Emission Studies of the Plasma Polymerisation of Perfluoroaromatics"

27. 2.86 * Prof. R.K. Harris (Durham)
"The Magic of Solid-State NMR"

5. 3.86 Dr. D. Hathway (Durham)
"Herbicide Selectivity"

5. 3.86 * Dr. M. Schroder (Edinburgh)
"Studies on Macrocyclic Compounds"

6. 3.86 * Dr. B. Iddon (Salford)
"The Magic of Chemistry"

12. 3.86 * Dr. J.M. Brown (Oxford)
"Chelate Control in Homogeneous Catalysis"

14. 5.86 Dr. P.R.R. Langridge-Smith (Edinburgh)
"Naked Metal Clusters - Synthesis, Characterisation, and Chemistry"

9. 6.86 Prof. R. Schmutzler (Braunschweig, W. Germany)
"Mixed Valence Diphosphorus Compounds"

23. 6.86 Prof. R.E. Wilde (Texas Technical University, U.S.A.)
"Molecular Dynamic Processes from Vibrational Bandshapes"

16.10.86 * Prof. N.N. Greenwood (University of Leeds)
"Glorious Gaffes in Chemistry"

23.10.86 Prof. H.W. Kroto (University of Sussex)
"Chemistry in Stars, Between Stars and in the Laboratory"

29.10.86 Prof. E.H. Wong (University of New Hampshire, U.S.A.)
"Coordination Chemistry of P-O-P Ligands"

5.11.86 Prof. Döpp (University of Duisburg)
"Cyclo-Additions and Cyclo-Reversions Involving Capto-Dative Alkenes"

6.11.86 Dr. R.M. Scrowston (University of Hull)
"From Myth and Magic to Modern Medicine"

13.11.86 * Prof. Sir Geoffrey Allen (Unilever Research)
"Biotechnology and the Future of the Chemical Industry

20.11.86 Dr. A. Milne and Mr. S. Christie (International Paints)
"Chemical Serendipity - A Real Life Case Study"

26.11.86 Dr. N.D.S. Canning (University of Durham)
"Surface Adsorption Studies of Relevance to Heterogeneous Ammonia Synthesis"

27.11.86 Prof. R.L. Williams (Metropolitan Police Forensic Science)
"Science and Crime"

3.12.86 Dr. J. Miller (Dupont Central Research, U.S.A.)
"Molecular Ferromagnets: Chemistry and Physical Properties"

8.12.86 Prof. T. Dorfmüller (University of Bielefeld)
"Rotational Dynamics in Liquids and Polymers"

22. 1.87 Prof. R.H. Ottewill (University of Bristol)
"Colloid Science: A Challenging Subject"

28. 1.87 Dr. W. Clegg (University of Newcastle-upon-Tyne)
"Carboxylate Complexes of Zinc Charting a Structural Jungle"

4. 2.87 Prof. A. Thomson (University of East Anglia)
"Metalloproteins and Magneto-optics"

5. 2.87 * Dr. P. Hubberstey (University of Nottingham)
"Demonstration Lecture on Various Aspects of Alkali Metal Chemistry"

11. 2.87 Dr. T. Shepherd (University of Durham)
"Pteridine Natural Products: Synthesis and Use in Chemotherapy"

12. 2.87 Dr. P.J. Rodgers (I.C.I. Billingham)
"Industrial Polymers from Bacteria"

17. 2.87 Prof. E.H. Wong (Unviersity of New Hampshire, U.S.A.)
"Symmetrical Shapes from Molecules to Art and Nature"

19. 2.87 Dr. M. Jarman (Institute of Cancer Research)
"The Design of Anti-Cancer Drugs"

4. 3.87 Dr. R. Newman (University of Oxford)
"Change and Decay: A Carbon-13 CP/MAS NMR Study of Humification and Coalification Processes"

5. 3.87 Prof. S.V. Ley (Imperial College)
"Fact and Fantasy in Organic Synthesis"

9. 3.87 Prof. F.G. Bordwell (Northeastern University, U.S.A.)
"Carbon Anions, Radicals, Radical Anions and Radical Cations"

11. 3.87 Dr. R.D. Cannon (University of East Anglia)
"Electron Transfer in Polynuclear Complexes"

12. 3.87 Dr. E.M. Goodger (Cranfield Institute of Technology)
"Alternative Fuels for Transport"

17. 3.87 Prof. R.F. Hudson (University of Kent)
"Aspects of Organophosphorus Chemistry"

18. 3.87 Prof. R.F. Hudson (University of Kent)
"Homolytic Rearrangements of Free-Radical Stability"

3. 4.87 * Prof. G. Ferguson (University of Guelph, Canada)
"X-Ray Crystallography for the Organic Chemist"

6. 5.87 Dr. R. Bartsch (University of Sussex)
"Low Co-ordinated Phosphorus Compounds"

7. 5.87 * Dr. M. Harmer (I.C.I. Chemicals and Polymer Group)
"The Rôle of Organometallics in Advanced Materials"

11. 5.87 Prof. S. Pasynkiewicz (Technical University, Warsaw)
"Thermal Decomposition of Methyl Copper and Its Reactions with Trialkylaluminium"

27. 5.87 Dr. M. Blackburn (University of Sheffield)
"Phosphonates as Analogues of Biological Phosphate Esters"

24. 6.87 Prof. S.M. Roberts (University of Exeter)
"Synthesis of Novel Anti-Viral Agents"

26. 6.87 Dr. C. Krespan (E.I. Dupont de Nemours)
"Nickel(0) and Iron(0) as Reagents in Organofluorine Chemistry"

* Indicates colloquia attended by the author.

(B) Conferences Attended

1. Graduate Symposium, Durham, March, 1985.

2. XI International Symposium on Macrocyclic Chemistry, Firenze, Italy, September 1986.
   Poster presented: The Synthesis and Complexation of a Series of Selective Mononucleating Macrocycles.

3. Graduate Symposium, Durham, March, 1987.
   Lecture presented: Metal Binding with Functionalised [12]-Ring Macrocycles.

REFERENCES

1. C.J. Pedersen, *J. Am. Chem. Soc.*, 1967, 89, 7017.

2. R. Hilgenfeld and W. Saenger, *Top. Curr. Chem.*, 1982, 101, 1.

3. J.M. Lehn, La Recherche, 1981, 12, 1213.

4. H.K. Wipf, A. Olivier, and W. Simon, *Helv. Chim. Acta*, 1970, 53, 1605.

5. P. Oggenfuss, W.E. Morf, U. Oesch, D. Ammann, E. Pretsch, and W. Simon, *Anal. Chim. Acta*, 1986, 180, 299.

6. M. Guggi, U. Fiedler, E. Pretsch, and W. Simon, *Anal. Lett.*, 1975, 8, 857.

7. N.N.L. Kirsch, R.J.J. Funck, E. Pretsch, and W. Simon, *Helv. Chim. Acta*, 1977, 60, 2326.

8. J.G. Schindler, G. Stork, H.-J. Strüh, and W. Schäl, *Z. Anal. Chem.*, 1978, 290, 45.

9. A.F. Zhukov, D. Erne, D. Ammann, M. Guggi, E. Pretsch, and W. Simon, *Anal. Chim. Acta*, 1981, 131, 117.

10. U. Olsher, *J. Am. Chem. Soc.*, 1982, 104, 4006.

11. D. Erne, D. Ammann, A.F. Zhukov, F. Behm, E. Pretsch, and W. Simon, *Helv. Chim. Acta*, 1982, 65, 538.

12. K.M. Aalmo and J. Krane, *Acta Chem. Scand.*, 1982, A36, 227.

13. A. Shanzer, D. Samuel, and R. Korenstein, *J. Am. Chem. Soc.*, 1983, 105, 3815.

14. K. Kimura, S. Kitazawa, and T. Shono, *Chem. Letters*, 1984, 639.

15. K. Hiratani, K. Taguchi, H. Sugihara, and K. Iio, *Bull. Chem. Soc. Japan*, 1984, 57, 1976.

16. E. Metzger, D. Ammann, U. Schefer, E. Pretsch, and W. Simon, *Chimia*, 1984, 38, 440.

17. M. Canessa, N. Adragna, H.S. Solomon, T.M. Connolly, and D.C. Tosteson, *New England J. Medic.*, 1980, 302, 772.

18. S. Kitazawa, K. Kimura, H. Yanoad, and T. Shono, *J. Am. Chem. Soc.*, 1984, 106, 6978.

19. "Lithium Research and Therapy", ed. F.N. Johnson, Academic Press, London, 1975.

20. D. Ammann, R. Bissig, Z. Cimerman, U. Fiedler, M. Guggi, W.E. Morf, M. Oehme, H. Osswald, E. Pretsch, and W. Simon, in "Ion and Enzyme Electrodes in Biology and Medicine", ed. M. Kessler *et al.*, Urban and Schwarzenberg, Munich, 1976, p. 22.

21. W. Simon, D. Ammann, M. Oehme, and W.E. Morf, *Annals New York Academy of Sciences*, 1978, 307, 52.

22. D. Ammann, M. Guggi, E. Pretsch, and W. Simon, *Anal. Lett.*, 1975, 8, 709.

23. D. Ammann, W.E. Morf, P. Anker, P.C. Meier, E. Pretsch, and W. Simon, *Ion-Selective Electrode Rev.*, 1983, 5, 3.

24. J.D.R. Thomas, *Anal. Proc. (London)*, 1985, 22, 356.

25. G.J. Moody and J.D.R. Thomas, *Ion-Selective Electrode Rev.*, 1979, 1, 3.

26. J. Petranek and O. Ryba, *Anal. Chim. Acta*, 1981, 128, 129.

27. K. Kimura, K. Kumami, S. Kitazawa, and T. Shono, *J. Chem. Soc., Chem. Commun.*, 1984, 442.

28. U. Schefer, D. Ammann, E. Pretsch, U. Oesch, and W. Simon, *Anal. Chem.*, 1986, 58, 2282.

29. M. Guggi, U. Fiedler, E. Pretsch, and W. Simon, *Anal. Lett.*, 1975, 8, 857.

30. IUPAC Analytical Division, Commission on Analytical Nomenclature, *Pure Appl. Chem.*, 1976, 48, 127.

31. K. Schwochau, *Top. Curr. Chem.*, 1984, 124, 93.

32. K.G. Allum, R.D. Hancock, I.V. Howell, S. McKenzie, R.D. Pitkethly, and P.J. Robinson, *J. Organomet. Chem.*, 1973, 87, 203.

33. J.M. Brown and H. Molinari, *Tetrahedron Lett.*, 1979, 2933.

34. Y. Koyamoko and Y. Yasuda, *Suiyo Kaishi*, 1977, 18, 523.

35. R.A. Bartsch, G.S. Heo, S.I. Kaug, Y. Lin, and J. Strzelbicki, *J. Org. Chem.*, 1982, 97, 457.

36. M. Kirch and J.M. Lehn, *Angew. Chem., Int. Ed. Engl.*, 1975, 14, 355.

37. J.M. Lehn, in "IUPAC Frontiers of Chemistry", ed. K.L. Laidler, Pergamon Press, Oxford, 1982, p. 265.

38. P.K. Coughlin, J.C. Dewan, S.J. Lippard, E.I. Watanabe, and J.M. Lehn, *J. Am. Chem. Soc.*, 1979, 101, 265.

39. R.J. Motekaitis, A.E. Martell, J.P. Lecomte, and J.M. Lehn, *Inorg. Chem.*, 1983, 22, 609.

40. B.A. Boyce, A. Carroy, J.M. Lehn, and D. Parker, *J. Chem. Soc., Chem. Commun.*, 1984, 1546.

41. D. Parker, J.M. Lehn, and J. Rimmer, *J. Chem. Soc. Dalton Trans.*, 1985, 1517.

42. J.P. Lecomte, J.M. Lehn, D. Parker, J. Guilhem, and C. Pascard, *J. Chem. Soc., Chem. Commun.*, 1983, 296.

43. D. Parker, *J. Chem. Soc., Chem. Commun.*, 1985, 1129.

44. S.J. McLain, *J. Am. Chem. Soc.*, 1983, 105, 6355.

45. J. Powell and C.J. May, *J. Am. Chem. Soc.*, 1982, 104, 2636.

46. C.S. Kraihanzel, E. Sinn, and M.G. Gray, *J. Am. Chem. Soc.*, 1981, 103, 960.

47. D.A. Wrobelski and T.B. Rauchfuss, *J. Am. Chem. Soc.*, 1982, 104, 2314.

48. J. Comarmond, P. Plumere, J.M. Lehn, Y. Agnus, R. Louis, R. Weiss, O. Kahn, and I. Morgenstern-Badarau, *J. Am. Chem. Soc.*, 1982, 104, 6330.

49. E.I. Solomon, in "Copper Proteins, Metal Ions in Biology", ed. T.G. Spiro, Wiley, New York, 1981, vol. 3, pp. 41-108.

50. J.A. Fee, *Struct. Bonding (Berlin)*, 1975, 23, 1.

51. J.M. Lehn, *Acc. Chem. Res.*, 1978, 11, 49.

52. J.M. Lehn, *Pure Appl. Chem.*, 1978, 50, 871.

53. J.M. Lehn, *Pure Appl. Chem.*, 1980, 52, 2441.

54. A. Carroy, Thèse de Doctorat, Université Louis Pasteur, Strasbourg, 1984.

55. D.E. Fenton, *Adv. Inorg. Bioinorg. Mech.*, 1983, 2, 187.

56. M.G.B. Drew, M. McCann, and S.M. Nelson, *J. Chem. Soc., Chem. Commun.*, 1979, 481.

57. J.M. Lehn, *Structure and Bonding*, 1973, 16, 1.

58. J.M. Lehn, *Pure Appl. Chem.*, 1977, 49, 857.

59. A. Carroy, C.R. Langrick, J.M. Lehn, K.E. Matthes, and D. Parker, *Helv. Chim. Acta*, 1986, 69, 580.

60. C.K. Chang, *J. Chem. Soc., Chem. Commun.*, 1977, 800.

61. C.K. Chang, M.S. Kuo, and C.B. Wang, *J. Heterocyclic Chem.*, 1977, 14, 943.

62. C.K. Chang, *J. Heterocyclic Chem.*, 1977, 14, 1285.

63. J.P. Collman, C.M. Elliot, T.R. Halbert, B.S. Tovrog, *Proc. Natl. Acad. Sci. USA*, 1977, 74, 18.

64. J.P. Collman. M. Marrocco, P. Denisevich, C. Koval, and F.C. Anson, *J. Electroanal. Chem.*, 1979, 101, 117.

65. J.P. Collman, F. Basolo, E. Bunnenberg, T.J. Collins, J.H. Dawson, P.E. Ellis, M.L. Marrocco, A. Moscowitz, J.L. Sessler, and T. Szymanski, *J. Am. Chem. Soc.*, 1981, 103, 5636.

66. J.P. Collman, C.S. Bencosme, R.R. Durand, R.P. Kreh, and F.C. Anson, *J. Am. Chem. Soc.*, 1983, 105, 2699.

67. R.R. Durand, C.S. Bencosme, J.P. Collman, and F.C. Anson, *J. Am. Chem. Soc.*, 1983, 105, 2710.

68. J. Powell, A. Kuksis, C.J. May, S.C. Nyburg, and S.J. Smith, *J. Am. Chem. Soc.*, 1981, 103, 5941.

69. J. Powell, S.C. Nyburg, and S.J. Smith, *Inorg. Chim. Acta*, 1983, 76, 75.

70. A. Carroy and J.M. Lehn, *J. Chem. Soc., Chem. Commun.*, 1986, 1232.

71. J.M. Lehn and J. Comarmond, unpublished work, cited in ref. 53.

72. L. Wei, A. Bell, S. Warner, I.D. Williams, and S.J. Lippard, *J. Am. Chem. Soc.*, 1986, 108, 8302.

73. P.J. Sadler, *Inorg. Perspect. Biol. Med.*, 1978, 1, 233.

74. G. Kolks, C.R. Frihart, H.N. Rabinowitz, and S.J. Lippard, *J. Am. Chem. Soc.*, 1976, 98, 5720.

75. G. Kolks, S.J. Lippard, J.V. Waszczak, and H.R. Lilienthal, *J. Am. Chem. Soc.*, 1982, 104, 717.

76. J.C. Dewan and S.J. Lippard, *Inorg. Chem.*, 1980, 19, 2079.

77. G. Kolks, C.R. Frihart, P.K. Coughlin, and S.J. Lippard, *Inorg. Chem.*, 1981, 20, 2933.

78. P.K. Coughlin, S.J. Lippard, A.E. Martin, and J.E. Bulkowski, *J. Am. Chem. Soc.*, 1980, 102, 7617.

79. P.K. Coughlin, A.E. Martin, J.C. Dewan, E.I. Watanabe, J.E. Bulkowski, J.M. Lehn, and S.J. Lippard, *Inorg. Chem.*, 1984, 23, 1004.

80. P.K. Couglin and S.J. Lippard, *Inorg. Chem.*, 1984, 23, 1446.

81. A.E. Martin and S.J. Lippard, *J. Am. Chem. Soc.*, 1984, 106, 2579.

82. P.K. Coughlin, J.C. Dewan, S.J. Lippard, E.I. Watanabe, and J.M. Lehn, *J. Am. Chem. Soc.*, 1979, 101, 265.

83. A.E. Martin and S.J. Lippard, in "Copper Cordination Chemistry: Biochemical and Inorganic Perspectives", ed. K.D. Karlin and J. Zubieta, Adenine Press, New York, 1983, p. 395.

84. A. Shanzer, D. Samuel, and R. Korenstein, *J. Am. Chem. Soc.*, 1983, 105, 3815.

85. V.T. Ivanov, *Ann. N.Y. Acad. Sci.*, 1975, 264, 221.

86. C.J. Pedersen and H.K. Frensdorff, *Angew. Chem., Int. Ed. Engl.*, 1972, 11, 16.

87. F. Vögtle and E. Weber, *Angew. Chem., Int. Ed. Engl.*, 1979, 18, 753.

88. D. Bright and M.R. Truter, *J. Chem. Soc. B*, 1970, 1544; and *Nature*, 1970, 225, 176.

89. B. Dietrich, J.M. Lehn, and J.P. Sauvage, *Tetrahedron Lett.*, 1969, 2885.

90. B. Dietrich, J.M. Lehn, and J.P. Sauvage, *Tetrahedron Lett.*, 1969, 2889.

91. J.M. Lehn and J.P. Sauvage, *J. Am. Chem. Soc.*, 1975, 97, 6700.

92. B. Dietrich, J.M. Lehn, J.P. Sauvage, and J. Blanzat, *Tetrahedron*, 1973, 29, 1629.

93. B. Dietrich, J.M. Lehn, J.P. Sauvage, *Tetrahedron*, 1973, 29, 1647.

94. D. Moras and R. Weiss, *Acta Crystallogr.*, 1973, B29, 400.

95. E. Kauffmann, J.M. Lehn, and J.P. Sauvage, *Helv. Chim. Acta*, 1976, 59, 1099.

96. G. Anderegg, *Helv. Chim. Acta*, 1975, 58, 1218.

97. D. Moras, B. Metz, and R. Weiss, *Acta Crystallogr.*, 1973, B29, 388.

98. E. Mei, A.I. Popov, and J.L. Dye, *J. Am. Chem. Soc.*, 1977, 99, 6532.

99. E. Kauffmann, J.L. Dye, J.M. Lehn, and A.I. Popov, *J. Am. Chem. Soc.*, 1980, 102, 2274.

100. E. Mei, L. Liu, J.L. Dye, and A.I. Popov, *J. Solution Chemistry*, 1977, 6, 771.

101. F. Mathieu, B. Metz, D. Moras, and R. Weiss, *J. Am. Chem. Soc.*, 1978, 100, 4912.

102. D.J. Cram and K.N. Trueblood, *Top. Curr. Chem.*, 1981, 98, 43.

103. D.J. Cram, *Science*, 1983, 219, 1177.

104. E. Graf and J.M. Lehn, *J. Am. Chem. Soc.*, 1975, 97, 5022.

105. D.J. Cram, T. Kaneda, G.M. Lein, and R.C. Helgeson, *J. Chem. Soc., Chem. Commun.*, 1979, 948.

106. D.J. Cram, T. Kaneda, R.C. Helgeson, and G.M. Lein, *J. Am. Chem. Soc.*, 1979, 101, 6752.

107. D.J. Cram, I.B. Dicker, C.B. Knobler, and K.N. Trueblood, *J. Am. Chem. Soc.*, 1982, 104, 6828.

108. G.M. Lein and D.J. Cram, *J. Chem. Soc., Chem. Commun.*, 1982, 301.

109. D.J. Cram, G.M. Lein, T. Kaneda, R.C. Helgeson, C.B. Knobler, E. Maverick, and K.N. Trueblood, *J. Am. Chem. Soc.*, 1981, 103, 6228.

110. G.M. Lein and D.J. Cram, *J. Chem. Soc., Chem. Commun.*, 1982, 301.

111. D.J. Cram, I.B. Dicker, G.M. Lein, C.B. Knobler, and K.N. Trueblood, *J. Am. Chem. Soc.*, 1982, 104, 6827.

112. D.J. Cram, S.P. Ho, C.B. Knobler, E. Maverick, and K.N. Trueblood, *J. Am. Chem. Soc.*, 1986, 108, 2989.

113. D.J. Cram and S.P. Ho, *J. Am. Chem. Soc.*, 1986, 108, 2998.

114. J.M. Lehn, J.P. Sauvage, and B. Dietrich, *J. Am. Chem. Soc.*, 1970, 92, 2916.

115. J.M. Ceraso and J.L. Dye, *J. Am. Chem. Soc.*, 1973, 95, 4432.

116. J.P. Kitzinger and J.M. Lehn, *J. Am. Chem. Soc.*, 1974, 96, 3313.

117. V.M. Loyola, R.G. Wilkins, and R. Pizer, *J. Am. Chem. Soc.*, 1975, 97, 7382.

118. B.G. Cox and H. Schneider, *J. Am. Chem. Soc.*, 1977, 99, 2809.

119. J.M. Lehn, *Pure Appl. Chem.*, 1979, 51, 979.

120. J.M. Girodeau, J.M. Lehn, and J.P. Sauvage, *Angew. Chem., Int. Ed. Engl.*, 1975, 14, 764.

121. J.M. Lehn, J. Simon, and J. Wagner, *Angew. Chem., Int. Ed. Engl.*, 1973, 12, 578.

122. J.P. Behr, J.M. Lehn, and P. Vierling, *J. Chem. Soc., Chem. Commun.*, 1976, 621.

123. E. Amble and J. Dale, *Acta Chem. Scand.*, 1979, B33, 698.

124. M.J. Calverley and J. Dale, *Acta Chem. Scand.*, 1982, B36, 241.

125. T.J. Lotz and T.A. Kaden, *Helv. Chim. Acta*, 1978, 61, 1376.

126. S.J. Leigh and I.O. Sutherland, *J. Chem. Soc., Perkin Trans. 1*, 1979, 1089.

127. G.W. Gokel, D.M. Dishong, and C.J. Diamond, *J. Chem. Soc., Chem. Commun.*, 1980, 1053.

128. D.M. Dishong, C.J. Diamond, M.I. Cinoman, and G.W. Gokel, *J. Am. Chem. Soc.*, 1983, 105, 586.

129. D.M. Dishong, C.J. Diamond, and G.W. Gokel, *Tetrahedron Lett.*, 1981, 22, 1663.

130. R.A. Schultz, D.M. Dishong, and G.W. Gokel, *J. Am. Chem. Soc.*, 1982, 104, 625.

131. R.A. Schultz, D.M. Dishong, and G.W. Gokel, *Tetrahedron Lett.*, 1981, 22, 2623.

132. A. Masuyama, Y. Nakatsuji, and M. Okahara, *Tetrahedron Lett.*, 1981, 22, 4665.

133. F. Montanari and P.J. Tundo, *J. Org. Chem.*, 1982, 47, 1298.

134. S.J. Jungk, J.A. Moore, and R.D. Gandour, *J. Org. Chem.*, 1983, 48, 1116.

135. T. Maeda, M. Ouchi, K. Kimura, and T. Shono, *Chem. Lett.*, 1981, 11, 1573.

136. K. Fukunishi, B.P. Czech, and S.L. Regen, *J. Org. Chem.*, 1981, 46, 1218.

137. B.P. Czech, A. Czech, and R.A. Bartsch, *Tetrahedron Lett.*, 1983, 24, 1327.

138. see ref. 102.

139. S. Kitazawa, K. Kimura, H. Yano, and T. Shono, *J. Am. Chem. Soc.*, 1984, 106, 6978.

140. B. Bowsher, A.J. Rest, and B.G. Main, *J. Chem. Soc., Dalton Trans.*, 1984, 1421.

141. see ref. 14.

142. G.W. Gokel, D.M. Goli, C. Minganti, and L. Echegoyen, *J. Am. Chem. Soc.*, 1983, 105, 6786.

143. G. Michaux and J. Reisse, *J. Am. Chem. Soc.*, 1982, 104, 6895.

144. G. Wipff, P. Weiner, and P. Kollman, *J. Am. Chem. Soc.*, 1982, 104, 3249.

145. J.D. Dunitz and P. Seiler, *Acta Crystallogr.*, 1974, B30, 2739.

146. J. Dale, *Israel J. Chem.*, 1980, 20, 3.

147. J.C.A. Boeyens and S.M. Dobson, *Stereochemistry of Organometallic and Inorganic Compounds*, 1987, 2, 1.

148. J.D. Dunitz, M. Dobler, P. Seiler, and R.P. Phizackerley, *Acta Crystallogr.*, 1974, B30, 2733.

149. R.M. Izatt, R.E. Terry, B.L. Haymore, L.D. Hansen, N.K. Dulley, A.G. Avondet, and J.J. Christensen, *J. Am. Chem. Soc.*, 1976, 98, 7620.

150. K.H. Wong, G. Konizer, and J. Smid, *J. Am. Chem. Soc.*, 1970, 92, 666.

151. R.D. Hancock, *Pure Appl. Chem.*, 1986, 58, 1445.

152. R.A. Bartsch, B.P. Czech, S.I. Kang, L.E. Stewart, W. Wolkowiak, W.A. Charewicz, G.S. Heo, and B. Son, *J. Am. Chem. Soc.*, 1985, 107, 4997.

153. G. Shoham, W.N. Lipscomb, and U. Olsher, *J. Am. Chem. Soc.*, 1983, 105, 1247.

154. G. Shoham, D.W. Christianson, R.A. Bartsch, G.S. Heo, U. Olsher, and W.N. Lipscomb, *J. Am. Chem. Soc.*, 1984, 106, 1280.

155. G. Shoham, W.N. Lipscomb, and U. Olsher, *J. Chem. Soc., Chem. Commun.*, 1983, 208.

156. P. Groth, *Acta Chem. Scand.*, 1981, A35, 460.

157. P. Groth, *Acta Chem. Scand.*, 1981, A35, 463.

158. A.E. Martell and R.M. Smith, "Critical Stability Constants", Vol. 1-5, Plenum Press, New York, 1974, 1975, 1977, 1978, 1982.

159. R.D. Gandour, F.R. Fronczek, V.J. Gatto, C. Minganti, R.A. Schultz, B.D. White, K.A. Arnold, D. Mazzocchi, S.R. Miller, and G.W. Gokel, *J. Am. Chem. Soc.*, 1986, 108, 4078.

160. V.J. Gatto, K.A. Arnold, A.M. Viscariello, S.R. Miller, C.R. Morgan, and G.W. Gokel, *J. Org. Chem.*, 1986, 51, 5373.

161. R.A. Schultz, E. Schlegel, D.M. Dishong, and G.W. Gokel, *J. Chem. Soc., Chem. Commun.*, 1982, 242.

162. A. Kaifer, H.D. Durst, L. Echegoyen, D.M. Dishong, R.A. Schultz, and G.W. Gokel, *J. Org. Chem.*, 1982, 47, 3195.

163. D.M. Goli, D.M. Dishong, C.J. Diamond, and G.W. Gokel, *Tetrahedron Lett.*, 1982, 23, 5243.

164. F.R. Fronczek, V.J. Gatto, R.A. Schultz, S.J. Jungk, W.J. Colucci, R.D. Gandour, and G.W. Gokel, *J. Am. Chem. Soc.*, 1983, 105, 6717.

165. F.R. Fronczek, V.J. Gatto, C. Minganti, R.A. Schultz, R.D. Gandour, and G.W. Gokel, *J. Am. Chem. Soc.*, 1984, 106, 7244.

166. G. Ferguson, C.R. Langrick, K.E. Matthes, and D. Parker, *J. Chem. Soc., Chem. Commun.*, 1985, 1609.

167. G. Ferguson, K.E. Matthes, and D. Parker, unpublished results.

168. L. Echegoyen, A. Kaifer, H. Durst, R.A. Schultz, D.M. Goli, and G.W. Gokel, *J. Am. Chem. Soc.*, 1984, 106, 5100.

169. J.M. Lehn and J.P. Kintzinger, *J. Am. Chem. Soc.*, 1974, 96, 3313.

170. A.I. Popov, *Pure Appl. Chem.*, 1979, 51, 101.

171. M.C. Fedarko, *J. Magn. Reson.*, 1973, 12, 30.

172. V.J. Gatto and G.W. Gokel, *J. Am. Chem. Soc.*, 1984, 106, 8240.

173. B.P. Czech, A. Czech, B. Son, H.K. Lee, and R.A. Bartsch, *J. Heterocyclic Chem.*, 1986, 23, 465.

174. J. Strzelbicki and R.A. Bartsch, *Anal. Chem.*, 1981, 53, 2251.

175. W.A. Charewicz, G.S. Heo, and R.A. Bartsch, *Anal. Chem.*, 1982, 54, 2094.

176. W.A. Charewicz and R.A. Bartsch, *Anal. Chem.*, 1982, 54, 2300.

177. J. Strzelbicki and R.A. Bartsch, *J. Membrane Sci.*, 1982, 10, 35.

178. W.A. Charewicz and R.A. Bartsch, *J. Membrane Sci.*, 1983, 12, 323.

179. B.P. Czech, B. Son, and R.A. Bartsch, *Tetrahedron Lett.*, 1983, 24, 2923.

180. R.A. Bartsch, W.A. Charewicz, and S.I. Kang, *J. Membrane Sci.*, 1984, 17, 97.

181. J. Koszuk, B.P. Czech, W. Walkowiak, D.A. Babb, and R.A. Bartsch, *J. Chem. Soc., Chem. Commun.*, 1984, 1504.

182. M.J. Pugia, G. Ndip, H.K. Lee, I.W. Yang, and R.A. Bartsch, *Anal. Chem.*, 1986, 58, 2723.

183. K. Kimura, M. Tanaka, S. Iketani, and T. Shono, *J. Org. Chem.*, 1987, 52, 836.

184. W. Walkowiak and R.A. Bartsch, unpublished results, cited in ref. 182..

185. B.G. Cox, H. Schneider, and J. Stroka, *J. Am. Chem. Soc.*, 1978, 100, 4746.

186. U. Olsher and J. Jagur-Grodzinski, *J. Chem. Soc. Dalton Trans.*, 1981, 501.

187. R.E. Lenkinski, G.A. Elgavish, and J. Reuben, *J. Magn. Reson.*, 1978, 32, 367.

188. J. Reuben, *J. Am. Chem. Soc.*, 1973, 95, 3534.

189. G. Borgen, J. Dale, and G. Teien, *Acta Chem. Scand.*, 1979, B33, 15.

190. H. Stamm, W. Lamberty, and J. Stafe, *Tetrahedron*, 1976, 32, 2045.

191. C.J. Cresswell and A.L. Allred, *Phys. Chem.*, 1962, 66, 1469.

192. J.M. Lehn and M.E. Stubbs, *J. Am. Chem. Soc.*, 1974, 96, 4011.

193. M.J. Calverley and J. Dale, *J. Chem. Soc., Chem. Commun.*, 1981, 684.

194. D.H. Williams and I. Fleming, in "Spectroscopic Methods in Organic Chemistry", Third edition, McGraw-Hill, London, 1980.

195. J.M. Miller, *Adv. in Inorg. Chem. and Radiochem.*, 1984, 28, 1.

196. I.A.S. Lewis and S. Puccia, Organic Mass Spectroscopy, V.G. Analytical Applications Notes, No. 15.

197. D.H. Williams, A.F. Findeis, S. Naylor, and B.W. Gibson, *J. Am. Chem. Soc.*, 1987, 109, 1980.

198. M. Barber, R.S. Bordoli, R.D. Sedgewick, and A.N. Tyler, *J. Chem. Soc., Chem. Commun.*, 1981, 325.

199. R.A.W. Johnstone and M.E. Rose, *J. Chem. Soc., Chem. Commun.*, 1983, 1268.

200. J. Meili and J. Seibl, *Int. J. Mass Spec. and Ion Phys.*, 1983, 46, 367.

201. C.J. Pedersen, *J. Am. Chem. Soc.*, 1970, 92, 391.

202. S.S. Moore, T.L. Tarnowski, M. Newcomb, and D.J. Cram, *J. Am. Chem. Soc.*, 1977, 99, 6398.

203. K. Yokota, T. Kakuchi, M. Yamanaka, and T. Takada, *Makromol. Chem., Rapid Commun.*, 1986, 7, 633.

204. M.J. Pugia, B.E. Knudsen, C.V. Cason, and R.A. Bartsch, *J. Am. Chem. Soc.*, 1987, 52, 541.

205. B.P. Czech, D.A. Babb, B. Son, and R.A. Bartsch, *J. Org. Chem.*, 1984, 49, 4805.

206. see ref. 204.

207. J.M. Lehn and J. Simon, *Helv. Chim. Acta*, 1977, 60, 141.

208. see ref. 39.

209. C.A. Chang and V.O. Ochaya, *Inorg. Chem.*, 1986, 25, 355.

210. P. Gans, A. Sabatini, and A. Vacca, *Inorg. Chem.*, 1983, 79, 219.

211. P. Gans, A. Sabatini, and A. Vacca, *J. Chem. Soc., Dalton Trans.*, 1985, 1195.

212. A. Laouenan and E. Suet, *Talanta*, 1985, 32, 245.

213. I.G. Sayce, *Talanta*, 1968, 15, 1397.

214. R.J. Motekaitis and A.E. Martell, *Can. J. Chem.*, 1982, 60, 2403.

215. R.J. Motekaitis and A.E. Martell, *Can. J. Chem.*, 1982, 60, 168.

216. G.J. Moody and J.D.R. Thomas, "Selective Ion Sensitive Electrodes", Merrow Publishing Co., Watford, England, 1971.

217. K.A. Arnold, L. Echegoyen, and G.W. Gokel, *J. Am. Chem. Soc.*, 1987, 109, 3713; and K.A. Arnold, L. Echegoyen, F.R. Fronczek, R.D. Gandour, V.J. Gatto, B.D. White, and G.W. Gokel, *J. Am. Chem. Soc.*, 1987, 109, 3716..

218. H.K. Frensdorff, *J. Am. Chem. Soc.*, 1971, 93, 600.

219. K. Srinivasan and G.A. Rechnitz, *Anal. Chem.*, 1969, 41, 1203.

220. K.M. Aalmo and J. Krane, *Acta Chem. Scand.*, 1982, A36, 227.

221. J.J. Christensen, R.M. Izatt, L.D. Hansen, and J.A. Partridge, *J. Phys. Chem.*, 1966, 70, 2003.

222. R.M. Izatt, D.P. Nelson, J.H. Rytting, B.L. Haymore, and J.J. Christensen, *J. Am. Chem. Soc.*, 1971, 93, 1619.

223. R.M. Izatt, R.E. Terry, D.P. Nelson, Y. Chan, D.J. Eatough, J.S. Bradshaw, L.D. Hansen, and J.J. Christensen, *J. Am. Chem. Soc.*, 1976, 98, 7626.

224. H.-J. Buschmann, *Inorg. Chim. Acta*, 1985, 98, 43.

225. H.-J. Buschmann, *Inorg. Chim. Acta*, 1985, 102, 95.

226. H.-J. Buschmann, *Thermochimica Acta*, 1986, 102, 179.

227. H.-J. Buschmann, *Thermochimica Acta*, 1986, 107, 219.

228. H.-J. Buschmann, *Inorg. Chim. Acta*, 1986, 125, 31.

229. C.J. van Staveren, D.N. Reinhoudt, J. van Eerden, and S. Harkema, *J. Chem. Soc., Chem. Commun.*, 1987, 974.

230. C.J. van Staveren, D.E. Fenton, D.N. Reinhoudt, J. van Eerden, and S. Harkeme, *J. Am. Chem. Soc.*, 1987, 109, 3456.

231. F. Martinelli, G. Mestroni, A. Camus, and G. Zassinovich, *J. Organomet. Chem.*, 1981, 220, 383.

232. R.L. DeKock and H.B. Gray, in "Chemical Structure and Bonding", The Benjamin/Cummings Publishing Company, Menlo Park, California, 1980.

233. J.P. Collman, R.G. Finke, J.N. Cawse, and J.I. Brauman, *J. Am. Chem. Soc.*, 1978, 100, 4766.

234. M.Y. Darenbourg, H.L.C. Barros, *Inorg. Chem.*, 1979, 18, 3286.

235. S.B. Butts, S.H. Strauss, E.M. Holt, R.E. Stimson, N.W. Alcock, and D.F. Shriver, *J. Am. Chem. Soc.*, 1980, 102, 5093.

236. J.A. Marsella, J.C. Huffman, K.G. Caulton, B. Longato, and J.R. Norton, *J. Am. Chem. Soc.*, 1982, 104, 6360.

237. D.M. Hamilton, W.S. Willis, and G.D. Stucky, *J. Am. Chem. Soc.*, 1981, 103, 4255.

238. S. Buϕen, J. Dale, P. Groth, and J. Krane, *J. Chem. Soc., Chem. Commun.*, 1982, 1172.

239. H.-J. Buschmann, *Stereochemistry of Organometallic and Inorganic Compounds*, 1987, 2, 103.

240. M.C. Day, J.H. Medley, and N. Ahmad, *Can. J. Chem.*, 1983, 61, 1719.

241. W.E. Weaver and W.M. Whaley, *J. Am. Chem. Soc.*, 1947, 69, 515.

242. J. Dale, J. Eggestad, S.B. Fredriksen, and P. Groth, *J. Chem. Soc., Chem. Commun.*, in the press.

243. J. Dale, personal communication.

244. C.K. Schauer and O.P. Anderson, *J. Am. Chem. Soc.*, 1987, 109, 3647.

245. R.M. Izatt, J.S. Bradshaw, S.A. Nielsen, J. D. Lamb, and J.J. Christensen, *Chem. Rev.*, 1985, 85, 271.

246. M.J. Calverley and J. Dale, *J. Chem. Soc., Chem. Commun.*, 1981, 684 and 1084.

247. P.Groth, *Acta Chem. Scand.*, 1981, A35, 717.

248. W.A. Baker and F.T. Helm, *J. Am. Chem. Soc.*, 1975, 97, 2295.

249. N. Matsumoto, Y. Nishida, S. Kida, and I. Ueda, *Bull. Chem. Soc. Japan*, 1976, 49, 117.

250. J.P. Gisselbrecht, M. Gross, A.H. Alberto, and J.M. Lehn, *Inorg. Chem.*, 1980, 19, 1386.

251. K.P. Balakrishnan, L. Siegfried, and T.A. Kaden, *Helv. Chim. Acta*, 1984, 67, 1060.

252. D. Parker, A.H. Alberts, and J.M. Lehn, *J. Chem. Soc., Dalton Trans.*, 1985, 2311.

253. J. Comarmond, Thèse de Doctorat, Université Louis Pasteur, Strasbourg, 1981.

254. O. Kahn, *Inorg. Chim. Acta*, 1982, 62, 3.

255. P.J. Hay, J.C. Thibeault, and R. Hoffmann, *J. Am. Chem. Soc.*, 1975, 97, 4884.

256. V.H. Crawford, H.W. Richardson, J.R Wasson, D.J. Hodgson, and W.E. Hatfield, *Inorg. Chem.*, 1976, 15, 2107.

257. F.A. Cotton and G. Wilkinson, in "Advanced Inorganic Chemistry", Fourth edition, John Wiley and Sons, New York, 1980.

258. F. Kröhnke, *Synthesis (Reviews)*, 1976, 1; and *Angew. Chem., Int. Ed. Engl.*, 1963, 2, 380.

259. J.G. Eaves, H.S. Munro, and D. Parker, *Inorg. Chem.*, 1987, 26, 644.

260. F.H. Burstall and R.S. Nyholm, *J. Chem. Soc.*, 1952, 3570.

261. J.R. Hall, M.R. Litzow, and R.H. Plowan, *Aust. J. Chem.*, 1965, 18, 1331.

262. R.E. Wolf Jr., J.R. Hartman, J.M.E. Storey, B.M. Foxman, and S.R. Cooper, *J. Am. Chem. Soc.*, 1987, 109, 4328.

263. R.E. DeSimone and M.D. Glick, *J. Am. Chem. Soc.*, 1975, 97, 942.

264. R.E. DeSimone and M.D. Glick, *J. Am. Chem. Soc.*, 1976, 98, 762.

265. G. Weber, *Inorg. Chim. Acta*, 1982, 58, 27.

266. A.S. Craig, G. Ferguson, K.E. Matthes, and D. Parker, unpublished results.

267. M.Newcomb, G.W. Gokel, and D.J. Cram, *J. Am. Chem. Soc.*, 1974, 96, 6810.

268. E. Weber and F. Vögtle, *Chem. Ber.*, 1976, 109, 1803.

269. M. Newcomb, S.S. Moore, and D.J. Cram, *J. Am. Chem. Soc.*, 1977, 99, 6405.

270. G. Ferguson, K.E. Matthes, and D. Parker, *J. Chem. Soc., Chem. Commun.*, in the press (1987, COM NO. 658).

271. K.R. Mann, J.A. Thich, R.A. Bell, C.L. Coyle, and H.B. Gray, *Inorg. Chem.*, 1980, 19, 2462.

272. R.W. DeHaven and V.L. Goedken, *Inorg. Chem.*, 1979, 18, 827.

273. K.A. Beveridge, G.W. Bushnell, S.R. Stobart, J.L. Attwood, and M.J. Zaworotko, *Organometallics*, 1983, 2, 1447.

274. J.F. Stoddart, *Angew. Chem., Int. Ed. Engl.*, 1986, 25, 487.

275. B.L. Allwood, F.H. Kohnke, J.F. Stoddart, and D.L. Williams, *Angew. Chem., Int. Ed. Engl.*, 1985, 24, 581.

276. B.L. Allwood, H.M. Colquhoun, S.M. Doughty, F.H. Kohnke, A.M.Z. Slawin, J.F. Stoddart, D.J. Williams, and R. Zarzycki, *J. Chem. Soc., Chem. Commun.*, 1987, 1054.

277. B.L. Allwood, N. Spencer, H. Shahriari-Zavareh, J.F. Stoddart, and D.J. Williams, *J. Chem. Soc., Chem. Commun.*, 1987, 1061.

278. M.J. Gunter, L.N. Mander, K.S. Murray, and P.E. Clark, *J. Am. Chem. Soc.*, 1981, 103, 6784.

279. J.S. Miller and A.J. Epstein, *Progr. Inorg. Chem.*, 1976, 20, 1.

280. S.F. Rice and H.B. Gray, *J. Am. Chem. Soc.*, 1981, 103, 1593.

281. see ref. 271.

282. G. Ferguson, K.E. Matthes, and D. Parker, *Angew. Chem., Int. Ed. Engl.*, in the press.

283. Other Rh(III) aquo complexes: (a) C.K. Thomas and J.A. Stanko, *J. Coordination Chem.*, 1973, 2, 211 ans 231; (b) K. Wieghardt, W. Schmidt, B. Nuber, B. Prickner, and B. Weiss, *Chem. Ber.*, 1980, 113, 36; (c) G.H.Y. Lin, J.D. Leggett, and R.M. Wing, *Acta Crystallogr.*, 1973, B29, 1023; and (d) T. Glowiak, M.Kubiak, and T. Szymanska-Buzar, *Acta Crystallogr.*, 1977, B33, 1732.

284. H.M. Colquhoun, S.M. Doughty, A.M.Z. Slawin, J.F. Stoddart, and D.J. Williams, *Angew. Chem., Int. Ed. Engl.*, 1985, 24, 135.

285. N.W. Alcock, J.M. Brown, and J.C. Jeffery, *J. Chem. Soc., Dalton Trans.*, 1976, 583.

286. P.E. Figgins and D.H. Busch, *J. Phys. Chem.*, 1961, 65, 2236.

287. N.S. Gill and H.J. Kingdom, *Aust. J. Chem.*, 1966, 19, 2197.

288. G. Vasapollo, P. Giannocaro, C.F. Nobile, and G. Sacco, *Inorg. Chim. Acta*, 1981, 48, 125.

289. K.E. Matthes and D. Parker, *Stereochemistry of Organometallic and Inorganic Compounds*, 1987, 2, 187.

290. D.F. Evans, *J. Chem. Soc.*, 1959, 2003.

291. I.J. Burdon, A.C. Coxon, J.F. Stoddart, and C.M. Wheatley, *J. Chem. Soc. Perkin Trans. 1*, 1977, 220.

292. J.C. Sheehan and W.A. Bolhofer, *J. Am. Chem. Soc.*, 1950, 72, 2786.

293. C.L. DeLigny, P.F.M. Luykx, M. Rehbach, and A.A. Wieneke, *Recueil*, 1960, 79, 713.

294. B.A. Frenz, in "Computing in Crystallography", Delft University Press, Delft, The Netherlands, 1976, pp. 64-71.

APPENDIX - CRYSTAL DATA

1. Macrocyclic Ligand (115)

Table

Positional Parameters and Their Estimated Standard Deviations

Atom	x	y	z	B(A2)
N1	-0.0178(2)	0.0491(2)	0.1506(1)	3.69(4)
C2	-0.1140(3)	0.1684(3)	0.1000(2)	4.55(6)
C3	-0.1348(3)	0.1748(3)	-0.0175(2)	4.51(6)
O4	-0.2543(2)	0.0760(2)	-0.0693(1)	4.87(4)
C5	-0.2602(3)	0.0454(3)	-0.1761(2)	4.83(6)
C6	-0.1575(3)	-0.0783(3)	-0.1826(2)	4.66(6)
C7	-0.0689(3)	-0.0043(3)	0.2389(2)	4.85(6)
C8	-0.2173(3)	-0.0966(3)	0.2007(2)	5.17(6)
C9	-0.1719(3)	-0.2330(3)	0.1623(2)	4.33(6)
O10	-0.0491(2)	-0.2936(2)	0.2155(1)	6.12(5)
N11	-0.2658(2)	-0.2854(2)	0.0691(2)	4.58(5)
C12	-0.2196(4)	-0.4150(3)	0.0330(2)	6.51(8)
C13	-0.4189(3)	-0.2262(3)	0.0039(2)	6.31(8)

These coordinates correspond to half the centrosymmetric molecule; symmetry operation -x, -y, -z, will generate the other half.

Anisotropically refined atoms are given in the form of the isotropic equivalent thermal parameter defined as:

(4/3) * [a2*B(1,1) + b2*B(2,2) + c2*B(3,3) + ab(cos gamma)*B(1,2) + ac(cos beta)*B(1,3) + bc(cos alpha)*B(2,3)]

Molecular Dimensions

(a) Bond Lengths (Å)

N1	C2	1.457(3)
N1	C6*	1.461(3)
N1	C7	1.455(3)
C2	C3	1.503(3)
C3	O4	1.416(3)
O4	C5	1.421(3)
C5	C6	1.503(4)
C7	C8	1.511(3)
C8	C9	1.506(4)
C9	O10	1.223(3)
C9	N11	1.345(3)
N11	C12	1.438(4)
N11	C13	1.451(3)

(b) Bond Angles (°)

C2	N1	C6*	111.7(2)
C2	N1	C7	112.3(2)
C6*	N1	C7	111.8(2)
N1	C2	C3	112.1(2)
C2	C3	O4	108.1(2)
C3	O4	C5	114.8(2)
O4	C5*	C6	112.1(2)
N1*	C6	C5	113.6(2)
N1	C7	C8	111.8(2)
C7	C8	C9	110.6(2)
C8	C9	O10	119.5(2)
C8	C9	N11	119.4(2)
O10	C9	N11	121.0(2)
C9	N11	C12	118.7(2)
C9	N11	C13	125.1(2)
C12	N11	C13	116.1(2)

The * refers to the atom at equivalent position $-x, -y, -z$.

Deposition Data

Calculated Hydrogen Coordinates (C-H = 0.95 Å)

Atom	x	y	z
H21	-0.0603	0.2501	0.1327
H22	-0.2189	0.1628	0.1100
H31	-0.0339	0.1541	-0.0300
H32	-0.1698	0.2646	-0.0438
H51	-0.2211	0.1231	-0.2052
H52	-0.3704	0.0272	-0.2164
H61	-0.1900	-0.1104	-0.2541
H62	-0.1767	-0.1484	-0.1372
H71	-0.0945	0.0712	0.2771
H72	0.0184	-0.0560	0.2848
H81	-0.2969	-0.0522	0.1436
H82	-0.2612	-0.1124	0.2577
H121	-0.1182	-0.4446	0.0809
H122	-0.3013	-0.4822	0.0305
H123	-0.2084	-0.4036	-0.0361
H131	-0.4381	-0.1412	0.0343
H132	-0.4129	-0.2099	-0.0660
H133	-0.5058	-0.2885	0.0006
H134	-0.4622	-0.2815	-0.0578
H135	-0.4945	-0.2230	0.0437
H136	-0.4000	-0.1351	-0.0168

Atoms are numbered according to the heavier atom to which they are bonded. The hydrogens on C13 (H131 to H136) are disordered over two sites and had 0.5 occupancies. Overall B(iso) values of 5 and 7 $Å^2$ were assigned to the non-methyl and methyl hydrogens respectively.

Deposition Data

General Temperature Factor Expressions - U's

Name	U(1,1)	U(2,2)	U(3,3)	U(1,2)	U(1,3)	U(2,3)
N1	0.0492(9)	0.045(1)	0.0489(9)	0.0028(9)	0.0185(7)	-0.001(1)
C2	0.065(1)	0.046(1)	0.066(1)	0.008(1)	0.027(1)	-0.006(1)
C3	0.068(1)	0.042(1)	0.064(1)	0.007(1)	0.023(1)	0.002(1)
O4	0.0564(8)	0.065(1)	0.0658(9)	-0.0059(9)	0.0217(7)	-0.007(1)
C5	0.051(1)	0.065(2)	0.058(1)	0.002(1)	0.002(1)	-0.001(1)
C6	0.062(1)	0.050(1)	0.066(1)	-0.007(1)	0.020(1)	-0.006(1)
C7	0.078(1)	0.062(2)	0.048(1)	0.000(1)	0.025(1)	-0.004(1)
C8	0.069(1)	0.069(2)	0.068(1)	-0.002(1)	0.035(1)	0.003(1)
C9	0.055(1)	0.054(1)	0.058(1)	-0.003(1)	0.020(1)	0.011(1)
O10	0.073(1)	0.068(1)	0.076(1)	0.011(1)	-0.0004(9)	0.013(1)
N11	0.051(1)	0.059(1)	0.061(1)	0.004(1)	0.0122(8)	0.005(1)
C12	0.087(2)	0.070(2)	0.085(2)	-0.002(2)	0.017(1)	-0.008(2)
C13	0.063(2)	0.093(2)	0.076(2)	0.003(2)	0.009(1)	0.006(2)

The form of the anisotropic thermal parameter is:

exp[-2PI2{h2a2U(1,1) + k2b2U(2,2) + l2c2U(3,3) + 2hkabU(1,2) + 2hlacU(1,3) + 2klbcU(2,3)}] where a, b, and c are reciprocal lattice constants.

Deposition Data

Torsion Angles

C7	N1	C2	C3	-147.4
C6*	N1	C2	C3	86.0
C2	N1	C7	C8	81.4
C6*	N1	C7	C8	-152.1
C2	N1	C6*	C5*	-147.4
C7	N1	C6*	C5*	85.8
N1	C2	C3	O4	76.6
C2	C3	O4	C5	-165.5
C3	O4	C5	C6	93.8
O4	C5	C6	N1*	-76.3
N1	C7	C8	C9	72.7
C7	C8	C9	O10	45.2
C7	C8	C9	N11	-133.8
C8	C9	N11	C12	179.3
C8	C9	N11	C13	-5.3
O10	C9	N11	C12	0.3
O10	C9	N11	C13	175.8

2. $[(113)_2\text{-}Cu(II)_3]^{2+}\ [PF_6^-]_2$ (125)

Table of Positional Parameters and Their Estimated Standard Deviations

Atom	x	y	z	B(A2)
CU1	0.000	0.000	0.000	6.21(4)
CU2	-0.3398(1)	0.04474(5)	-0.14712(7)	3.47(2)
P	0.0901(3)	0.1595(1)	-0.5198(2)	4.49(5)
F(1)	0.028(1)	0.0853(4)	-0.5623(7)	12.0(2)
F(2)	-0.1242(7)	0.1777(3)	-0.5180(4)	7.3(1)
F(3)	0.156(1)	0.2334(4)	-0.4816(8)	16.0(3)
F(4)	0.3060(7)	0.1405(4)	-0.5225(5)	8.5(2)
F(5)	0.114(1)	0.1280(6)	-0.4171(5)	13.0(3)
F(6)	0.0642(9)	0.1896(5)	-0.6223(5)	14.1(2)
O(1)	-0.1786(8)	-0.0375(3)	-0.1088(4)	5.3(1)
O(2)	-0.1761(9)	0.0778(3)	-0.0318(5)	6.7(2)
O(3)	-0.2466(7)	0.0994(3)	-0.2887(4)	4.3(1)
O(4)	-0.7132(8)	0.0381(4)	-0.1399(4)	6.7(2)
N(1)	-0.4663(8)	-0.0225(3)	-0.2607(4)	3.7(1)
N(2)	-0.4470(8)	0.1506(4)	-0.1480(5)	4.0(1)
C(1)	-0.239(1)	-0.1016(4)	-0.1555(7)	6.0(2)
C(2)	-0.336(1)	-0.0855(5)	-0.2544(8)	6.9(3)

Table of Positional Parameters and Their Estimated Standard Deviations (cont.)

Atom	x	y	z	B(A2)
C(3)	-0.483(1)	0.0105(5)	-0.3566(6)	5.7(2)
C(4)	-0.312(1)	0.0533(5)	-0.3694(6)	5.1(2)
C(5)	-0.329(1)	0.1693(5)	-0.2984(7)	6.0(2)
C(6)	-0.337(1)	0.1977(5)	-0.2007(7)	5.5(2)
C(7)	-0.396(1)	0.1727(5)	-0.0434(7)	5.7(2)
C(8)	-0.199(1)	0.1457(5)	0.0028(6)	4.9(2)
C(9)	-0.658(1)	-0.0513(6)	-0.2461(7)	7.6(3)
C(10)	-0.792(1)	0.0025(6)	-0.2254(7)	6.7(3)
C(11)	-0.773(1)	0.1109(8)	-0.1378(8)	9.3(4)
C(12)	-0.653(1)	0.1597(5)	-0.1831(7)	6.1(2)
H11	-0.3239	-0.1260	-0.1226	
H12	-0.1311	-0.1317	-0.1578	
H21	-0.4100	-0.1264	-0.2784	
H22	-0.2426	-0.0759	-0.2910	
H31	-0.5912	0.0414	-0.3658	
H32	-0.5033	-0.0273	-0.4024	
H41	-0.3456	0.0812	-0.4258	

Table of Positional Parameters and Their Estimated Standard Deviations (cont.)

Atom	x	y	z
H42	-0.2117	0.0205	-0.3755
H51	-0.4559	0.1667	-0.3363
H52	-0.2540	0.2005	-0.3293
H61	-0.3957	0.2439	-0.2085
H62	-0.2095	0.2019	-0.1656
H71	-0.4866	0.1517	-0.0097
H72	-0.3985	0.2232	-0.0383
H81	-0.1862	0.1442	0.0708
H82	-0.1049	0.1770	-0.0139
H91	-0.6338	-0.0841	-0.1940
H92	-0.7157	-0.0755	-0.3038
H101	-0.8173	0.0359	-0.2772
H102	-0.9072	-0.0213	-0.2193
H111	-0.7650	0.1247	-0.0722
H112	-0.9025	0.1143	-0.1714
H121	-0.6800	0.1515	-0.2510
H122	-0.6861	0.2083	-0.1709

Starred atoms were refined isotropically.
Anisotropically refined atoms are given in the form of the isotropic equivalent thermal parameter defined as:
(4/3) * [a2*B(1,1) + b2*B(2,2) + c2*B(3,3) + ab(cos gamma)*B(1,2) + ac(cos beta)*B(1,3) + bc(cos alpha)*B(2,3)]

Table of Bond Distances in Angstroms

Atom1	Atom2	Distance	Atom1	Atom2	Distance	Atom1	Atom2	Distance
CU1	O(1)	1.918(4)	O(3)	C(4)	1.424(8)	C(5)	C(6)	1.483(11)
CU1	O(1)	1.918(4)	O(3)	C(5)	1.417(9)	C(7)	C(8)	1.506(10)
CU1	O(2)	1.902(5)	O(4)	C(10)	1.390(10)	C(9)	C(10)	1.451(13)
CU1	O(2)	1.902(5)	O(4)	C(11)	1.416(15)	C(11)	C(12)	1.474(15)
CU2	O(1)	1.918(4)	N(1)	C(2)	1.480(9)	P	F(1)	1.529(6)
CU2	O(2)	1.904(5)	N(1)	C(3)	1.466(9)	P	F(2)	1.566(4)
CU2	O(3)	2.444(4)	N(1)	C(9)	1.515(10)	P	F(3)	1.510(7)
CU2	O.4)	2.681(5)	N(2)	C(6)	1.470(10)	P	F(4)	1.583(5)
CU2	N(1)	2.086(5)	N(2)	C(7)	1.505(9)	P	F(5)	1.540(6)
CU2	N(2)	2.101(5)	N(2)	C(12)	1.458(9)	P	F(6)	1.526(6)
O(1)	C(1)	1.382(8)	C(1)	C(2)	1.459(11)			
O(2)	C(8)	1.369(9)	C(3)	C(4)	1.492(10)			

Numbers in parentheses are estimated standard deviations in the least significant digits.

Table of Bond Angles in Degrees

Atom1	Atom2	Atom3	Angle
F(2)	P	F(4)	179.4(3)
F(2)	P	F(5)	89.5(3)
F(2)	P	F(6)	90.1(3)
F(3)	P	F(4)	88.6(3)
F(3)	P	F(5)	92.2(6)
F(3)	P	F(6)	88.7(5)
F(4)	P	F(5)	90.7(3)
F(4)	P	F(6)	89.7(3)
F(5)	P	F(6)	179.0(5)

Cont/d···

Atom1	Atom2	Atom3	Angle
O(1)	CU1	O(1)[#]	180.0(4)
O(1)	CU1	O(2)	77.6(2)
O(1)	CU1	O(2)[#]	102.4(2)
O(1)[#]	CU1	O(2)	102.4(2)
O(1)[#]	CU1	O(2)[#]	77.6(2)
O(2)	CU1	O(2)[#]	180.0(4)
O(1)	CU2	O(2)	77.6(2)
O(1)	CU2	O(3)	108.3(2)
O(1)	CU2	O(4)	119.6(2)
O(1)	CU2	N(1)	83.4(2)
O(1)	CU2	N(2)	159.7(2)
O(2)	CU2	O(3)	110.3(2)
O(2)	CU2	O(4)	113.1(2)
O(2)	CU2	N(1)	161.0(2)
O(2)	CU2	N(2)	82.3(2)
O(3)	CU2	O(4)	118.8(2)
O(3)	CU2	N(1)	76.4(2)
O(3)	CU2	N(2)	76.5(2)
O(4)	CU2	N(1)	73.8(2)
O(4)	CU2	N(2)	71.5(2)
N(1)	CU2	N(2)	116.8(2)
CU1	O(1)	CU2	101.6(2)
CU1	O(1)	C(1)	141.8(4)
CU2	O(1)	C(1)	115.7(4)
CU1	O(2)	CU2	102.7(2)
CU1	O(2)	C(8)	136.9(4)
CU2	O(2)	C(8)	120.2(4)
CU2	O(3)	C(4)	107.8(4)
CU2	O(3)	C(5)	106.4(4)
C(4)	O(3)	C(5)	113.9(6)
CU2	O(4)	C(10)	102.9(5)
CU2	O(4)	C(11)	105.1(5)
C(10)	O(4)	C(11)	113.4(8)
C(2)	N(1)	C(3)	108.7(6)
C(2)	N(1)	C(9)	106.3(7)
C(3)	N(1)	C(9)	111.1(6)
C(6)	N(2)	C(7)	106.6(6)
C(6)	N(2)	C(12)	111.1(7)
C(7)	N(2)	C(12)	109.4(6)
O(1)	C(1)	C(2)	108.9(6)
N(1)	C(2)	C(1)	112.9(7)
N(1)	C(3)	C(4)	114.3(6)
O(3)	C(4)	C(3)	111.6(6)
O(3)	C(5)	C(6)	108.9(6)
N(2)	C(6)	C(5)	112.3(6)
N(2)	C(7)	C(8)	110.9(6)
O(2)	C(8)	C(7)	108.3(6)
N(1)	C(9)	C(10)	113.6(8)
O(4)	C(10)	C(9)	109.3(7)
O(4)	C(11)	C(12)	111.8(8)
N(2)	C(12)	C(11)	114.3(8)
F(1)	P	F(2)	89.6(3)
F(1)	P	F(3)	177.4(5)
F(1)	P	F(4)	89.8(3)
F(1)	P	F(5)	89.9(5)
F(1)	P	F(6)	89.2(5)
F(2)	P	F(3)	92.0(3)

Table of General Temperature Factor Expressions - U's

Name	U(1,1)	U(2,2)	U(3,3)	U(1,2)	U(1,3)	U(2,3)
CU1	0.092(1)	0.0395(7)	0.075(1)	-0.0086(9)	-0.0536(8)	0.0034(7)
CU2	0.0364(4)	0.0484(5)	0.0407(5)	-0.0070(5)	-0.0077(4)	0.0058(5)
P	0.053(1)	0.058(1)	0.058(1)	0.014(1)	0.005(1)	0.007(1)
F(1)	0.119(5)	0.107(4)	0.224(7)	-0.002(4)	0.024(5)	-0.074(4)
F(2)	0.062(3)	0.100(4)	0.121(4)	0.026(3)	0.032(3)	0.032(3)
F(3)	0.117(5)	0.114(5)	0.38(1)	-0.020(5)	0.066(6)	-0.109(5)
F(4)	0.058(3)	0.142(5)	0.118(5)	0.034(3)	0.007(3)	-0.004(4)
F(5)	0.117(5)	0.298(9)	0.080(4)	0.062(6)	0.020(4)	0.066(5)
F(6)	0.097(4)	0.309(8)	0.136(5)	0.063(5)	0.041(4)	0.128(5)
O(1)	0.068(4)	0.047(3)	0.066(3)	0.001(3)	-0.036(3)	-0.004(3)
O(2)	0.098(4)	0.043(3)	0.084(4)	0.004(3)	-0.056(3)	-0.005(3)
O(3)	0.053(3)	0.056(3)	0.056(3)	-0.002(3)	0.017(3)	0.001(3)
O(4)	0.056(3)	0.142(5)	0.056(4)	-0.047(3)	0.007(3)	-0.014(4)
N(1)	0.034(3)	0.062(4)	0.035(3)	-0.013(3)	-0.009(3)	0.003(3)
N(2)	0.027(3)	0.066(4)	0.057(4)	0.005(3)	0.002(3)	-0.001(3)
C(1)	0.078(6)	0.046(5)	0.083(6)	-0.019(5)	-0.035(5)	0.007(5)
C(2)	0.094(7)	0.051(5)	0.098(7)	-0.008(6)	-0.025(6)	-0.013(5)

Table of General Temperature Factor Expressions - U's (Continued)

Name	U(1,1)	U(2,2)	U(3,3)	U(1,2)	U(1,3)	U(2,3)
C(3)	0.080(6)	0.087(6)	0.047(5)	-0.013(6)	0.003(5)	-0.004(5)
C(4)	0.059(5)	0.090(6)	0.048(5)	0.002(5)	0.017(4)	-0.005(5)
C(5)	0.102(7)	0.067(5)	0.060(5)	-0.007(6)	0.021(5)	0.015(5)
C(6)	0.080(6)	0.051(5)	0.071(6)	0.019(5)	0.003(5)	0.007(5)
C(7)	0.048(5)	0.099(6)	0.068(6)	0.001(5)	0.005(4)	-0.032(5)
C(8)	0.073(6)	0.065(5)	0.045(5)	-0.007(5)	0.000(4)	-0.004(4)
C(9)	0.082(6)	0.127(7)	0.068(6)	-0.067(5)	-0.010(5)	-0.011(6)
C(10)	0.032(4)	0.142(9)	0.080(6)	-0.022(6)	0.009(4)	-0.009(7)
C(11)	0.051(5)	0.22(1)	0.085(7)	-0.034(7)	0.021(5)	-0.059(7)
C(12)	0.048(5)	0.104(7)	0.073(6)	0.030(5)	-0.004(4)	-0.024(5)

The form of the anisotropic thermal parameter is:
exp[-2PI2{h2a2U(1,1) + k2b2U(2,2) + l2c2U(3,3) + 2hkabU(1,2) + 2hlacU(1,3) + 2klbcU(2,3)}] where a, b, and c are reciprocal lattice constants.

Table of Least-Squares Planes

The equation of the plane is of the form: $A*x + B*y + C*z - D = 0$

where A,B,C & D are constants and x,y & z are orthogonalized coordinates.

Plane No.	A	B	C	D	Atom	x	y	z	Distance	Esd
1	0.7426	0.3338	-0.5806	0.0000	**Atoms in Plane**					
					CU1	0.0000	0.0000	0.0000	0.000	0.000
					CU2	-2.0048	0.8280	-2.0340	-0.032	0.001
					N(1)	-2.5870	-0.4157	-3.6044	0.033	0.006
					N(2)	-2.7649	2.7870	-2.0461	0.065	0.006
					O(1)	-0.9658	-0.6945	-1.5046	-0.076	0.006
					O(2)	-1.1633	1.4398	-0.4394	-0.128	0.006
					Other Atoms					
					O(3)	-0.9464	1.8387	-3.9917	2.228	0.005
					O(4)	-4.6810	0.7043	-1.9344	-2.118	0.006

Chi-Squared Values:

Plane No.	Chi-Squared
1	1924.

Table of Torsional Angles in Degrees

Atom 1	Atom 2	Atom 3	Atom 4	Angle
O(2)	CU1	O(1)	CU2	5.3
O(2)	CU1	O(1)	C(1)	-162.9
O(1)	CU1	O(2)	CU2	-5.3
O(1)	CU1	O(2)	C(8)	179.5
O(2)	CU2	O(1)	CU1	-5.3
O(2)	CU2	O(1)	C(1)	166.6
N(1)	CU2	O(1)	CU1	175.5
N(1)	CU2	O(1)	C(1)	-12.6
N(2)	CU2	O(1)	CU1	1.5
N(2)	CU2	O(1)	C(1)	173.3
O(1)	CU2	O(2)	CU1	5.3
O(1)	CU2	O(2)	C(8)	-178.5
N(1)	CU2	O(2)	CU1	7.7
N(1)	CU2	O(2)	C(8)	-176.1
N(2)	CU2	O(2)	CU1	-172.3
N(2)	CU2	O(2)	C(8)	3.9
O(1)	CU2	N(1)	C(2)	-10.4
O(1)	CU2	N(1)	C(3)	-129.0
O(1)	CU2	N(1)	C(9)	104.2
O(2)	CU2	N(1)	C(2)	-12.7
O(2)	CU2	N(1)	C(3)	-131.3
O(2)	CU2	N(1)	C(9)	101.9
N(2)	CU2	N(1)	C(2)	167.3
N(2)	CU2	N(1)	C(3)	48.7
N(2)	CU2	N(1)	C(9)	-78.1
O(1)	CU2	N(2)	C(6)	82.7
O(1)	CU2	N(2)	C(7)	-30.5
O(1)	CU2	N(2)	C(12)	-130.5
O(2)	CU2	N(2)	C(6)	89.3
O(2)	CU2	N(2)	C(7)	-23.8
O(2)	CU2	N(2)	C(12)	-143.9
N(1)	CU2	N(2)	C(6)	-90.7
N(1)	CU2	N(2)	C(7)	156.2
N(1)	CU2	N(2)	C(12)	36.1
C(3)	N(1)	C(9)	H91	162.2
C(3)	N(1)	C(9)	H92	43.6
CU2	N(2)	C(6)	C(5)	52.9
CU2	N(2)	C(6)	H61	172.3
CU2	N(2)	C(6)	H62	-67.3
C(7)	N(2)	C(6)	C(5)	163.9
C(7)	N(2)	C(6)	H61	-76.7
C(7)	N(2)	C(6)	H62	43.6
C(12)	N(2)	C(6)	C(5)	-77.0
C(12)	N(2)	C(6)	H61	42.4
C(12)	N(2)	C(6)	H62	162.7
CU2	N(2)	C(7)	C(8)	39.8
CU2	N(2)	C(7)	H71	-79.0
CU2	N(2)	C(7)	H72	160.6
C(6)	N(2)	C(7)	C(8)	-75.1
C(6)	N(2)	C(7)	H71	166.2
C(6)	N(2)	C(7)	H72	45.7
C(12)	N(2)	C(7)	C(8)	164.7
C(12)	N(2)	C(7)	H71	45.9
C(12)	N(2)	C(7)	H72	-74.5
CU2	N(2)	C(12)	C(11)	50.6
CU2	N(2)	C(12)	H121	-70.6
CU2	N(2)	C(12)	H122	171.5
C(6)	N(2)	C(12)	C(11)	176.3
C(6)	N(2)	C(12)	H121	55.2
C(6)	N(2)	C(12)	H122	-62.8
C(7)	N(2)	C(12)	C(11)	-66.2
C(7)	N(2)	C(12)	H121	172.6
C(7)	N(2)	C(12)	H122	54.7
O(1)	C(1)	C(2)	N(1)	-42.5
O(1)	C(1)	C(2)	H21	-162.2
O(1)	C(1)	C(2)	H22	77.9
H11	C(1)	C(2)	N(1)	78.4
H11	C(1)	C(2)	H21	-41.3

Cont/d···

CU1	O(1)	C(1)	H11	79.5
CU1	O(1)	C(1)	H12	-41.2
CU2	O(1)	C(1)	C(2)	33.0
CU2	O(1)	C(1)	H11	-87.6
CU2	O(1)	C(1)	H12	151.7
CU1	O(2)	C(8)	C(7)	-167.6
CU1	O(2)	C(8)	H81	-47.2
CU1	O(2)	C(8)	H82	73.3
CU2	O(2)	C(8)	C(7)	17.9
CU2	O(2)	C(8)	H81	138.3
CU2	O(2)	C(8)	H82	-101.3
C(5)	O(3)	C(4)	C(3)	-91.0
C(5)	O(3)	C(4)	H41	29.4
C(5)	O(3)	C(4)	H42	149.5
C(4)	O(3)	C(5)	C(6)	150.9
C(4)	O(3)	C(5)	H51	30.8
C(4)	O(3)	C(5)	H52	-89.0
C(11)	O(4)	C(10)	C(9)	148.7
C(11)	O(4)	C(10)	H101	29.2
C(11)	O(4)	C(10)	H102	-92.4
C(10)	O(4)	C(11)	C(12)	-85.7
C(10)	O(4)	C(11)	H111	153.9
C(10)	O(4)	C(11)	H112	35.0
CU2	N(1)	C(2)	C(1)	31.1
CU2	N(1)	C(2)	H21	150.3
CU2	N(1)	C(2)	H22	-89.0
C(3)	N(1)	C(2)	C(1)	153.1
C(3)	N(1)	C(2)	H21	-87.6
C(3)	N(1)	C(2)	H22	33.0
C(9)	N(1)	C(2)	C(1)	-87.2
C(9)	N(1)	C(2)	H21	32.1
C(9)	N(1)	C(2)	H22	152.7
CU2	N(1)	C(3)	C(4)	41.0
CU2	N(1)	C(3)	H31	-79.4
CU2	N(1)	C(3)	H32	162.1
C(2)	N(1)	C(3)	C(4)	-75.3
C(2)	N(1)	C(3)	H31	164.3
C(2)	N(1)	C(3)	H32	45.7
C(9)	N(1)	C(3)	C(4)	168.1
C(9)	N(1)	C(3)	H31	47.6
C(9)	N(1)	C(3)	H32	-70.9
CU2	N(1)	C(9)	C(10)	51.5
CU2	N(1)	C(9)	H91	-69.5
CU2	N(1)	C(9)	H92	171.8
C(2)	N(1)	C(9)	C(10)	165.2
C(2)	N(1)	C(9)	H91	44.1
C(2)	N(1)	C(9)	H92	-74.5
C(3)	N(1)	C(9)	C(10)	-76.8
H12	C(1)	C(2)	N(1)	-162.2
H12	C(1)	C(2)	H21	78.2
H12	C(1)	C(2)	H22	-41.7
N(1)	C(3)	C(4)	O(3)	-45.5
N(1)	C(3)	C(4)	H41	-166.5
N(1)	C(3)	C(4)	H42	74.1
H31	C(3)	C(4)	O(3)	74.1
H31	C(3)	C(4)	H41	-46.9
H31	C(3)	C(4)	H42	-166.3
H32	C(3)	C(4)	O(3)	-165.6
H32	C(3)	C(4)	H41	73.3
H32	C(3)	C(4)	H42	-46.0
O(3)	C(5)	C(6)	N(2)	-58.3
O(3)	C(5)	C(6)	H61	-178.4
O(3)	C(5)	C(6)	H62	62.8
H51	C(5)	C(6)	N(2)	61.7
H51	C(5)	C(6)	H61	-59.3
H51	C(5)	C(6)	H62	-177.1
H52	C(5)	C(6)	N(2)	-179.5
H52	C(5)	C(6)	H61	61.4
H52	C(5)	C(6)	H62	-57.4
N(2)	C(7)	C(8)	O(2)	-39.0
N(2)	C(7)	C(8)	H81	-159.3
N(2)	C(7)	C(8)	H82	80.2
H71	C(7)	C(8)	O(2)	80.2
H71	C(7)	C(8)	H81	-40.2
H71	C(7)	C(8)	H82	-160.6
H72	C(7)	C(8)	O(2)	-160.2
H72	C(7)	C(8)	H81	79.4
H72	C(7)	C(8)	H82	-41.0
N(1)	C(9)	C(10)	O(4)	-61.1
N(1)	C(9)	C(10)	H101	59.1
N(1)	C(9)	C(10)	H102	178.5
H91	C(9)	C(10)	O(4)	59.7
H91	C(9)	C(10)	H101	180.0
H91	C(9)	C(10)	H102	-60.7
H92	C(9)	C(10)	O(4)	178.8
H92	C(9)	C(10)	H101	-60.9
H92	C(9)	C(10)	H102	58.4
O(4)	C(11)	C(12)	N(2)	-50.2
O(4)	C(11)	C(12)	H121	70.8
O(4)	C(11)	C(12)	H122	-171.2
H111	C(11)	C(12)	N(2)	69.9
H111	C(11)	C(12)	H121	-169.2
H111	C(11)	C(12)	H122	-51.2
H112	C(11)	C(12)	N(2)	-170.5
H112	C(11)	C(12)	H121	-49.5
H112	C(11)	C(12)	H122	68.4

3. $[(106)_2\text{-}Cu(II)_2]^{2+}\ [PF_6^-]_2$ (126)

Positional Parameters and Their Estimated Standard Deviations

Atom	x	y	z	B(A2)
Cu	0.0719(3)	0.1025(2)	0.4705(1)	3.90(4)
CL	0.3878(6)	0.5061(4)	0.3272(3)	5.5(1)
O1	0.026(2)	-0.042(1)	0.4342(6)	8.0(4)
O2	0.375(2)	0.116(1)	0.4977(9)	10.2(5)
O3	0.124(2)	0.2540(9)	0.5363(8)	7.1(4)
O4	-0.133(2)	0.236(1)	0.4257(7)	6.0(3)
O11	0.243(3)	0.483(1)	0.369(1)	18.3(6)
O12	0.378(3)	0.450(2)	0.255(1)	16.3(7)
O13	0.540(2)	0.481(2)	0.365(1)	18.8(7)
O14	0.390(2)	0.615(1)	0.3124(9)	10.2(5)
N	0.151(2)	0.127(1)	0.3544(8)	5.1(4)
C1	0.066(3)	-0.067(2)	0.354(1)	7.2(6)
C2	0.140(4)	0.022(2)	0.314(1)	11.9(7)
C3	0.329(3)	0.169(2)	0.353(1)	9.9(7)
C4	0.443(3)	0.135(2)	0.415(2)	10.9(8)
C5	0.413(3)	0.205(3)	0.554(2)	15(1)
C6	0.286(3)	0.260(2)	0.571(2)	10.3(7)
C7	0.005(3)	0.343(2)	0.529(1)	8.9(7)
C8	-0.131(3)	0.326(2)	0.482(2)	9.8(7)
C9	-0.099(3)	0.260(2)	0.346(1)	8.7(7)
C10	0.030(4)	0.212(3)	0.318(1)	15(1)

Anisotropically refined atoms are given in the form of the isotropic equivalent thermal parameter defined as:
(4/3) * [a2*B(1,1) + b2*B(2,2) + c2*B(3,3) + ab(cos gamma)*B(1,
+ ac(cos beta)*B(1,3) + bc(cos alpha)*B(2,3)]

Bond Distances in Angstroms

Atom1	Atom2	Distance	Atom1	Atom2	Distance
Cu ...	Cu*	2.904(3)	CL	O13	1.32(2)
Cu	O1	1.881(12)	CL	O14	1.35(2)
Cu	O1*	1.886(12)	O1	C1	1.38(2)
Cu	O2	2.322(13)	O2	C4	1.46(3)
Cu	O3	2.164(12)	O2	C5	1.44(4)
Cu	O4	2.345(12)	O3	C6	1.33(3)
Cu	N	2.012(13)	O3	C7	1.42(2)
CL	O11	1.34(2)	O4	C8	1.43(3)
CL	O12	1.36(2)	O4	C9	1.36(3)

Numbers in parentheses are estimated standard deviations in the least significant digits.

The coordinates of the atoms marked with a star are obtained from the coordinate table by applying the transformation -x, -y, 1-z.

Atom1	Atom2	Distance
N	C2	1.44(2)
N	C3	1.44(3)
N	C10	1.49(3)
C1	C2	1.39(3)
C3	C4	1.36(3)
C5	C6	1.21(4)
C7	C8	1.27(3)
C9	C10	1.23(4)

Table

Bond Angles in Degrees

Atom1	Atom2	Atom3	Angle	Atom1	Atom2	Atom3	Angle
Cu*	Cu	O1	39.6(4)	O3	Cu	N	106.0(5)
Cu*	Cu	O1	39.5(4)	O4	Cu	N	79.9(5)
Cu*	Cu	O2	112.2(4)	O11	CL	O12	108.(1)
Cu*	Cu	O3	129.7(4)	O11	CL	O13	115.(1)
Cu*	Cu	O4	116.9(3)	O11	CL	O14	108.(1)
Cu*	Cu	N	124.2(4)	O12	CL	O13	107.(1)
O1*	Cu	O1	79.2(5)	O12	CL	O14	110.(1)
O1	Cu	O2	107.2(6)	O13	CL	O14	107.(1)
O1	Cu	O3	168.7(5)	Cu	O1	Cu*	100.8(5)
O1	Cu	O4	116.4(5)	Cu	O1	C1	117.(1)
O1	Cu	N	84.6(5)	Cu*	O1	C1	142.(1)
O1*	Cu	O2	106.7(6)	Cu	O2	C4	102.(1)
O1*	Cu	O3	90.4(5)	Cu	O2	C5	110.(1)
O1*	Cu	O4	104.7(5)	C4	O2	C5	113.(2)
O1*	Cu	N	163.5(5)	Cu	O3	C6	114.(1)
O2	Cu	O3	71.6(5)	Cu	O3	C7	121.(1)
O2	Cu	O4	129.9(5)	C6	O3	C7	124.(2)
O2	Cu	N	80.8(5)	Cu	O4	C8	110.(1)
O3	Cu	O4	70.2(4)	Cu	O4	C9	107.(1)

Atom1	Atom2	Atom3	Angle
C8	O4	C9	117. (2)
Cu	N	C2	106. (1)
Cu	N	C3	112. (1)
Cu	N	C10	106. (1)
C2	N	C3	110. (2)
C2	N	C10	115. (2)
C3	N	C10	108. (2)
O1	C1	C2	111. (2)
N	C2	C1	121. (2)
N	C3	C4	116. (2)
O2	C4	C3	119. (2)
O2	C5	C6	115. (2)
O3	C6	C5	127. (3)
O3	C7	C8	115. (2)
O4	C8	C7	119. (2)
O4	C9	C10	115. (2)
N	C10	C9	132. (2)

Numbers in parentheses are estimated standard deviations in the least significant digits.

The coordinates of the atoms marked with a * are obtained from the coordinate table by applying the symmetry transformation $-x, -y, 1-z$.

Table of Least-Squares Planes

The equation of the plane is of the form: A*x + B*y + C*z - D = 0

where A,B,C & D are constants and x,y & z are orthogonalized coordinates.

Plane No.	A	B	C	D	Atom	x	y	z	Distance	Esd
					----------Atoms in Plane----------					
1	-0.9081	0.3116	-0.2798	0.0000	CU	0.5605	1.2516	-0.4768	0.014	0.002
					O1	0.2362	-0.5069	-1.0621	-0.075	0.014
					N	1.2294	1.5500	-2.3506	0.025	0.014
					O3	0.9165	3.1022	0.5867	-0.030	0.012
					Chi Squared = 85.					
					----------Other Atoms----------					
					O2	2.8348	1.4199	-0.0371	-2.121	0.013
					O4	-0.9579	2.8859	-1.1996	2.105	0.012

Table of Torsional Angles in Degrees

Atom 1	Atom 2	Atom 3	Atom 4	Angle	Atom 1	Atom 2	Atom 3	Atom 4	Angle
C5	O2	C4	C3	-101.1	C10	N	C3	C4	148.4
C4	O2	C5	C6	108.4	C2	N	C10	C9	113.3
C7	O3	C6	C5	-150.7	C3	N	C10	C9	-123.1
C6	O3	C7	C8	169.1	O1	C1	C2	N	-5.9
C9	O4	C8	C7	-99.8	N	C3	C4	O2	-34.4
C8	O4	C9	C10	120.8	O2	C5	C6	O3	-8.1
C3	N	C2	C1	128.4	O3	C7	C8	O4	-16.7
C10	N	C2	C1	-109.3	O4	C9	C10	N	5.1
C2	N	C3	C4	-85.2					

4. $\{[(95)\text{-}Rh(CO)]^{+}\}_2\ [PF_6^-]_2$ (151)

Positional Parameters and Their Estimated Standard Deviations

Atom	x	y	z	B(A2)
Rh	0.32632(4)	0.14553(4)	0.52222(1)	2.623(7)
N1	0.3737(4)	0.0816(4)	0.4646(1)	2.7(1)
C2	0.4621(5)	0.1287(6)	0.4438(2)	3.7(1)
C3	0.5023(6)	0.0812(7)	0.4074(2)	5.2(2)
C4	0.4505(7)	-0.0151(8)	0.3924(2)	6.0(2)
C5	0.3588(6)	-0.0602(6)	0.4121(2)	4.8(2)
C6	0.3218(5)	-0.0097(5)	0.4487(2)	3.1(1)
C7	0.2175(5)	-0.0519(6)	0.4699(2)	3.8(1)
S8	0.1959(1)	0.0013(1)	0.52252(5)	3.18(3)
C9	0.2486(5)	-0.1102(5)	0.5563(2)	3.5(1)
C10	0.3683(5)	-0.1512(5)	0.5496(2)	3.7(1)
O11	0.3713(4)	-0.2249(4)	0.5152(2)	4.9(1)
C12	0.4720(5)	-0.2890(5)	0.5107(3)	4.7(2)
C13	0.5517(5)	-0.2388(5)	0.4797(2)	4.4(2)
O14	0.6094(4)	-0.1453(4)	0.4973(2)	4.3(1)
C15	0.6952(6)	-0.1033(6)	0.4711(2)	4.4(2)
C16	0.7589(6)	-0.0125(6)	0.4934(3)	4.8(2)
O17	0.6952(4)	0.0896(3)	0.4990(2)	4.4(1)

Table of Positional Parameters and Their Estimated Standard Deviations (cont.)

Atom	x	y	z	B(A2)
C18	0.6303(5)	0.0944(6)	0.5360(2)	3.8(1)
C19	0.5946(6)	0.2141(5)	0.5436(2)	3.8(1)
S20	0.4750(1)	0.2694(1)	0.51403(5)	3.67(4)
C21	0.5111(6)	0.2389(6)	0.4600(2)	4.3(2)
C22	0.2833(5)	0.2005(5)	0.5737(2)	3.3(1)
O23	0.2545(4)	0.2343(4)	0.6046(1)	5.5(1)
P	0.4800(2)	0.5497(2)	0.37611(6)	4.24(4)
F1	0.3676(4)	0.4800(5)	0.3767(2)	10.7(2)
F2	0.4116(5)	0.6572(4)	0.3850(2)	9.6(2)
F3	0.4905(6)	0.5334(6)	0.4242(1)	10.2(2)
F4	0.5471(5)	0.4367(5)	0.3672(2)	10.3(2)
F5	0.4687(5)	0.5635(6)	0.3277(1)	9.3(2)
F6	0.5909(4)	0.6196(6)	0.3751(2)	10.8(2)

Anisotropically refined atoms are given in the form of the isotropic equivalent thermal parameter defined as:

(4/3) * [a2*B(1,1) + b2*B(2,2) + c2*B(3,3) + ab(cos gamma)*B(1,2) + ac(cos beta)*B(1,3) + bc(cos alpha)*B(2,3)]

Molecular dimensions.

(a) Bond Lengths (Å)

Rh	Rh*	3.3320(6)	C6	C7	1.489(9)
Rh	N1	2.060(4)	C7	S8	1.807(7)
Rh	S8	2.295(2)	S8	C9	1.808(6)
Rh	S20	2.298(2)	C9	C10	1.508(9)
Rh	C22	1.833(6)	C10	O11	1.398(8)
N1	C2	1.355(8)	O11	C12	1.417(8)
N1	C6	1.339(7)	C12	C13	1.486(10)
C2	C3	1.372(9)	C13	O14	1.412(8)
C2	C21	1.514(10)	O14	C15	1.402(8)
C3	C4	1.376(12)	C15	C16	1.489(10)
C4	C5	1.358(11)	C16	O17	1.431(8)
C5	C6	1.379(9)	O17	C18	1.406(8)

C18	C19	1.493(9)
C19	S20	1.818(7)
S20	C21	1.807(7)
C22	O23	1.116(7)
P	F1	1.560(6)
P	F2	1.531(6)
P	F3	1.549(5)
P	F4	1.576(6)
P	F5	1.554(5)
P	F6	1.547(6)

(b) Bond Angles ( )

Rh*	Rh	N1	91.8(1)	N1	C6	C5	121.4(6)
Rh*	Rh	S8	92.72(4)	N1	C6	C7	118.4(5)
Rh*	Rh	S20	91.92(4)	C5	C6	C7	120.0(6)
Rh*	Rh	C22	88.6(2)	C6	C7	S8	114.8(4)
N1	Rh	S8	85.1(1)	Rh	S8	C7	99.2(2)
N1	Rh	S20	85.7(1)	Rh	S8	C9	108.2(2)
N1	Rh	C22	179.2(2)	C7	S8	C9	104.5(3)
S8	Rh	S20	169.77(6)	S8	C9	C10	118.1(4)
S8	Rh	C22	94.2(2)	C9	C10	O11	109.4(5)
S20	Rh	C22	95.0(2)	C10	O11	C12	115.7(5)
Rh	N1	C2	119.6(4)	O11	C12	C13	112.7(5)
Rh	N1	C6	120.5(4)	C12	C13	O14	110.7(6)
C2	N1	C6	119.9(5)	C13	O14	C15	112.9(5)
N1	C2	C3	120.8(6)	O14	C15	C16	109.6(6)
N1	C2	C21	118.7(5)	C15	C16	O17	113.6(5)
C3	C2	C21	120.4(6)	C16	O17	C18	115.1(5)
C2	C3	C4	118.4(7)	O17	C18	C19	109.1(5)
C3	C4	C5	121.2(7)	C18	C19	S20	118.3(5)
C4	C5	C6	118.2(7)	Rh	S20	C19	107.8(2)

Rh	S20	C21	99.3(2)
C19	S20	C21	103.8(3)
C2	C21	S20	113.9(5)
Rh	C22	O23	178.3(6)
F1	P	F2	89.2(3)
F1	P	F3	89.4(4)
F1	P	F4	89.1(3)
F1	P	F5	89.7(3)
F1	P	F6	179.4(3)
F2	P	F3	87.8(3)
F2	P	F4	178.2(3)
F2	P	F5	92.9(3)
F2	P	F6	90.4(3)
F3	P	F4	91.9(4)
F3	P	F5	178.9(4)
F3	P	F6	91.0(3)
F4	P	F5	87.3(3)
F4	P	F6	91.3(3)
F5	P	F6	89.8(3)

The * refers to equivalent position: y, x, 1-z.

Deposition Data:

Calculated Hydrogen Coordinates (C-H 0.95 A)

Atom	x	y	z
H3	0.5642	0.1142	0.3927
H4	0.4792	-0.0508	0.3678
H5	0.3212	-0.1248	0.4009
H71	0.2216	-0.1322	0.4712
H72	0.1540	-0.0304	0.4532
H91	0.1999	-0.1737	0.5527
H92	0.2435	-0.0835	0.5843
H101	0.3934	-0.1900	0.5740
H102	0.4163	-0.0882	0.5444
H121	0.4525	-0.3632	0.5015
H122	0.5088	-0.2932	0.5371
H131	0.5102	-0.2143	0.4557
H132	0.6053	-0.2946	0.4714
H151	0.6623	-0.0731	0.4462
H152	0.7455	-0.1630	0.4639
H161	0.8249	0.0047	0.4776
H162	0.7800	-0.0402	0.5203
H181	0.6743	0.0684	0.5590
H182	0.5650	0.0478	0.5330
H191	0.6579	0.2609	0.5374
H192	0.5761	0.2204	0.5725
H211	0.5912	0.2349	0.4577
H212	0.4835	0.2987	0.4428

Deposition Data:

General Temperature Factor Expressions - U's

Name	U(1,1)	U(2,2)	U(3,3)	U(1,2)	U(1,3)	U(2,3)
Rh	0.0309(2)	0.0310(2)	0.0378(2)	0.0001(2)	0.0021(2)	-0.0025(2)
N1	0.038(3)	0.033(2)	0.032(2)	0.002(2)	0.005(2)	0.005(2)
C2	0.046(4)	0.056(4)	0.037(3)	0.004(3)	0.002(3)	0.008(3)
C3	0.066(5)	0.092(6)	0.042(4)	0.007(5)	0.015(4)	0.014(4)
C4	0.094(6)	0.103(6)	0.032(4)	0.032(5)	-0.001(4)	-0.012(4)
C5	0.078(5)	0.060(4)	0.044(4)	0.014(4)	-0.012(4)	-0.010(3)
C6	0.050(4)	0.038(3)	0.030(3)	0.014(3)	-0.009(3)	-0.005(3)
C7	0.046(3)	0.053(4)	0.046(4)	-0.010(3)	-0.009(3)	0.002(3)
S8	0.0323(7)	0.0419(8)	0.0465(8)	-0.0032(6)	-0.0020(8)	0.0007(8)
C9	0.050(4)	0.045(4)	0.038(3)	-0.005(3)	0.004(3)	0.009(3)
C10	0.050(3)	0.040(3)	0.049(3)	-0.004(3)	-0.010(3)	0.002(3)
O11	0.040(2)	0.070(3)	0.077(3)	0.008(2)	-0.011(2)	-0.021(3)
C12	0.037(3)	0.035(3)	0.106(6)	0.002(3)	-0.006(4)	-0.006(4)
C13	0.049(4)	0.036(3)	0.081(4)	0.008(3)	-0.022(4)	-0.017(4)
O14	0.042(2)	0.046(2)	0.075(3)	-0.013(2)	0.007(2)	-0.010(3)
C15	0.056(4)	0.044(4)	0.070(4)	0.003(3)	0.005(4)	-0.004(4)
C16	0.038(3)	0.040(4)	0.104(6)	-0.000(3)	0.012(4)	-0.005(4)
O17	0.056(3)	0.036(2)	0.077(3)	0.003(2)	0.013(3)	0.005(2)

(continued..)

Name	U(1,1)	U(2,2)	U(3,3)	U(1,2)	U(1,3)	U(2,3)
C18	0.034(3)	0.049(4)	0.060(4)	-0.001(3)	0.004(3)	0.005(3)
C19	0.045(4)	0.045(4)	0.053(4)	-0.005(3)	-0.005(3)	-0.009(3)
S20	0.0399(8)	0.0313(8)	0.068(1)	-0.0033(7)	-0.0006(8)	-0.0010(8)
C21	0.045(4)	0.061(4)	0.056(4)	-0.006(3)	0.007(3)	0.019(4)
C22	0.045(3)	0.035(3)	0.047(3)	0.002(3)	-0.006(3)	-0.010(3)
O23	0.076(3)	0.079(3)	0.053(3)	0.005(3)	0.011(3)	-0.026(3)
P	0.059(1)	0.060(1)	0.042(1)	-0.0057(9)	0.0130(9)	-0.010(1)
F1	0.094(3)	0.137(4)	0.173(5)	-0.062(3)	0.052(4)	-0.065(3)
F2	0.128(4)	0.078(3)	0.161(5)	0.024(3)	0.035(4)	-0.028(4)
F3	0.162(5)	0.173(6)	0.051(3)	-0.013(5)	0.000(3)	-0.002(4)
F4	0.151(5)	0.106(4)	0.134(4)	0.057(4)	0.001(4)	-0.024(4)
F5	0.120(4)	0.179(5)	0.056(3)	0.010(4)	0.007(3)	0.009(4)
F6	0.085(3)	0.179(5)	0.148(4)	-0.061(3)	0.039(3)	-0.052(4)

The form of the anisotropic thermal parameter is:

$\exp[-2\pi^2(h^2a^2U(1,1) + k^2b^2U(2,2) + l^2c^2U(3,3) + 2hkabU(1,2) + 2hlacU(1,3) + 2klbcU(2,3))]$ where a, b, and c are reciprocal lattice constants.

Deposition Data:

Torsion Angles ( )

S8	Rh	N1	C2	-176.9	C22	Rh	Rh*	N1*	-7.0
S8	Rh	N1	C6	-0.5	C22	Rh	Rh*	S8*	-92.1
S20	Rh	N1	C2	-1.3	C22	Rh	Rh*	S20*	78.8
S20	Rh	N1	C6	175.1	C22	Rh	Rh*	C22*	173.8
C22	Rh	N1	C2	-155.3	Rh	N1	C2	C3	173.8
C22	Rh	N1	C6	21.1	Rh	N1	C2	C21	-10.1
Rh*	Rh	N1	C2	90.5	C6	N1	C2	C3	-2.6
Rh*	Rh	N1	C6	-93.1	C6	N1	C2	C21	173.5
N1	Rh	S8	C7	-6.7	Rh	N1	C6	C5	-174.0
N1	Rh	S8	C9	101.9	Rh	N1	C6	C7	10.1
S20	Rh	S8	C7	-32.0	C2	N1	C6	C5	2.4
S20	Rh	S8	C9	76.6	C2	N1	C6	C7	-173.5
C22	Rh	S8	C7	173.6	N1	C2	C3	C4	0.1
C22	Rh	S8	C9	-77.8	C21	C2	C3	C4	-176.0
Rh*	Rh	S8	C7	84.8	N1	C2	C21	S20	18.9
Rh*	Rh	S8	C9	-166.5	C3	C2	C21	S20	-165.0
N1	Rh	S20	C19	-98.6	C2	C3	C4	C5	2.7
N1	Rh	S20	C21	9.2	C3	C4	C5	C6	-2.9
S8	Rh	S20	C19	-73.3	C4	C5	C6	N1	0.3
S8	Rh	S20	C21	34.5	C4	C5	C6	C7	176.2
C22	Rh	S20	C19	81.1	N1	C6	C7	S8	-16.4
C22	Rh	S20	C21	-171.1	C5	C6	C7	S8	167.5
Rh*	Rh	S20	C19	169.8	C6	C7	S8	Rh	13.6
Rh*	Rh	S20	C21	-82.4	C6	C7	S8	C9	-98.0
N1	Rh	C22	O23	-79.0	Rh	S8	C9	C10	-50.1
S8	Rh	C22	O23	-57.4	C7	S8	C9	C10	54.9
S20	Rh	C22	O23	127.0	S8	C9	C10	O11	-78.8
Rh*	Rh	C22	O23	35.2	C9	C10	O11	C12	-166.8
N1	Rh	Rh*	N1*	172.3	C10	O11	C12	C13	-98.3
N1	Rh	Rh*	S8*	87.2	O11	C12	C13	O14	77.3
N1	Rh	Rh*	S20*	-102.0	C12	C13	O14	C15	172.9
N1	Rh	Rh*	C22*	-7.0	C13	O14	C15	C16	-174.6
S8	Rh	Rh*	N1*	87.2	O14	C15	C16	O17	-70.4
S8	Rh	Rh*	S8*	2.0	C15	C16	O17	C18	88.9
S8	Rh	Rh*	S20*	172.9	C16	O17	C18	C19	164.7
S8	Rh	Rh*	C22*	-92.1	O17	C18	C19	S20	79.5
S20	Rh	Rh*	N1*	-102.0	C18	C19	S20	Rh	52.3
S20	Rh	Rh*	S8*	172.9	C18	C19	S20	C21	-52.4
S20	Rh	Rh*	S20*	-16.2	Rh	S20	C21	C2	-16.6
S20	Rh	Rh*	C22*	78.8	C19	S20	C21	C2	94.4

The * refers to equivalent position: -x, y, 1-z

Table of Least-Squares Planes

The equation of the plane is of the form: A*x + B*y + C*z - D = 0

where A, B, C & D are constants and x, y & z are orthogonalized coordinates.

Plane No.	A	B	C	D	Atom	x	y	z	Distance	Esd
1	-0.6374	0.6251	-0.4504	-8.9032	----------Atoms in Plane----------					
					RH	3.8505	1.7173	16.6180	0.037	0.000
					N1	4.4096	0.9624	14.7844	0.035	0.005
					S8	2.3119	0.0150	16.6275	-0.051	0.001
					S20	5.6049	3.1786	16.3573	-0.050	0.002
					C22	3.3430	2.3662	18.2552	0.029	0.006
					Chi Squared = 9174.					
					----------Other Atoms----------					
					RH*	1.7173	3.8506	15.2038	3.368	0.000
2	-0.6376	0.6254	-0.4498	-8.9021	----------Atoms in Plane----------					
					N1	4.4096	0.9624	14.7844	0.043	0.005
					S8	2.3119	0.0150	16.6275	-0.041	0.001
					S20	5.6049	3.1786	16.3573	-0.041	0.002
					C22	3.3430	2.3662	18.2552	0.040	0.006
					Chi Squared = 1578.					
					----------Other Atoms----------					
					RH	3.8505	1.7173	16.6180	0.046	0.000
					RH*	1.7173	3.8506	15.2038	3.377	0.000

Dihedral Angles Between Planes:

Plane No.	Plane No.	Dihedral Angle
1	2	0.0

5. $[(96)\text{-}RhCl_2(H_2O)]^+ [PF_6^-]$ (158)

Table

Positional Parameters and Their Estimated Standard Deviations

Atom	x	y	z	B(A2)
Rh	0.31715(3)	0.00217(2)	-0.26616(3)	2.363(6)
CL1	0.1177(1)	-0.03698(7)	-0.2927(1)	3.79(3)
CL2	0.5162(1)	0.04163(6)	-0.2413(1)	3.62(3)
S8	0.3609(1)	-0.02790(6)	-0.0752(1)	3.02(3)
S26	0.3166(1)	0.02175(6)	-0.4632(1)	3.33(3)
P	-0.1171(2)	0.16719(7)	-0.2723(1)	4.08(4)
F1	-0.1898(4)	0.2258(2)	-0.2740(4)	8.8(1)
F2	0.0050(4)	0.2033(2)	-0.2813(4)	8.4(1)
F3	-0.2395(4)	0.1321(2)	-0.2636(4)	7.4(1)
F4	-0.0415(4)	0.1109(2)	-0.2667(5)	11.2(2)
F5	-0.1328(5)	0.1640(2)	-0.4073(4)	9.8(1)
F6	-0.1038(5)	0.1727(2)	-0.1366(4)	9.8(1)
OW	0.2402(4)	0.0782(2)	-0.2166(4)	5.4(1)
O11	0.1643(3)	0.0273(2)	0.0248(3)	4.44(9)
O14	0.2460(3)	0.1437(2)	0.0339(3)	4.53(9)
O17	0.3908(4)	0.1799(2)	-0.1373(3)	4.89(9)
O20	0.4092(4)	0.2211(2)	-0.3780(4)	6.7(1)
O23	0.2202(4)	0.1402(2)	-0.4567(3)	5.1(1)
N1	0.3892(4)	-0.0735(2)	-0.3112(3)	2.74(9)
C2	0.3777(5)	-0.0897(2)	-0.4225(4)	3.3(1)
C3	0.4286(5)	-0.1408(3)	-0.4561(5)	4.7(1)
C4	0.4874(6)	-0.1750(3)	-0.3736(6)	5.3(2)
C5	0.4980(6)	-0.1584(3)	-0.2592(5)	4.8(1)
C6	0.4502(5)	-0.1067(2)	-0.2280(5)	3.5(1)

Atom	x	y	z	B(A2)
C7	0.4685(5)	-0.0841(3)	-0.1079(5)	4.2(1)
C9	0.2308(6)	-0.0665(3)	-0.0201(5)	4.6(1)
C10	0.1791(5)	-0.0292(3)	0.0687(5)	4.7(1)
C12	0.1509(6)	0.0651(3)	0.1178(5)	5.7(2)
C13	0.1335(6)	0.1228(3)	0.0741(6)	5.7(2)
C15	0.2289(6)	0.1978(3)	-0.0195(5)	4.7(1)
C16	0.3492(6)	0.2188(2)	-0.0552(5)	4.7(1)
C18	0.5018(6)	0.1968(3)	-0.1861(6)	6.2(2)
C19	0.4814(7)	0.2420(3)	-0.2775(7)	6.8(2)
C21	0.2818(7)	0.2301(3)	-0.3775(6)	6.5(2)
C22	0.2145(6)	0.2001(3)	-0.4760(6)	6.2(2)
C24	0.1753(6)	0.1103(3)	-0.5565(5)	5.4(2)
C25	0.1669(6)	0.0478(3)	-0.5264(5)	4.8(1)
C27	0.3029(5)	-0.0528(2)	-0.5072(4)	3.9(1)

Anisotropically refined atoms are given in the form of the isotropic equivalent thermal parameter defined as:

(4/3) * [a2*B(1,1) + b2*B(2,2) + c2*B(3,3) + ab(cos gamma)*B(1,2) + ac(cos beta)*B(1,3) + bc(cos alpha)*B(2,3)]

Molecular Dimensions

(a) Interatomic Distances (A)

Rh	CL1	2.332(1)
Rh	CL2	2.330(1)
Rh	S8	2.329(1)
Rh	S26	2.327(1)
Rh	OW	2.070(4)
Rh	N1	2.025(4)
S8	C7	1.817(6)
S8	C9	1.830(6)
S26	C25	1.817(6)
S26	C27	1.826(6)
P	F1	1.583(4)
P	F2	1.575(4)
P	F3	1.566(4)
P	F4	1.551(5)
P	F5	1.558(4)
P	F6	1.571(5)
O11	C10	1.425(8)
O11	C12	1.413(8)
O14	C13	1.423(8)
O14	C15	1.418(7)
O17	C16	1.418(7)
O17	C18	1.422(8)

O20	C19	1.428(8)
O20	C21	1.388(9)
O23	C22	1.424(8)
O23	C24	1.401(7)
N1	C2	1.339(6)
N1	C6	1.363(6)
C2	C3	1.388(8)
C2	C27	1.491(7)
C3	C4	1.361(8)
C4	C5	1.376(9)
C5	C6	1.378(8)
C6	C7	1.485(8)
C9	C10	1.495(9)
C12	C13	1.451(9)
C15	C16	1.478(9)
C18	C19	1.502(10)
C21	C22	1.475(10)
C24	C25	1.511(9)
OW ...	F4	3.133(6)
OW ...	O17	2.986(6)
OW ...	O23	3.128(6)

(b) Bond Angles ( )

CL1	Rh	CL2	179.50(5)	F1	P	F4	177.5(3)
CL1	Rh	S8	96.48(5)	F1	P	F5	91.1(3)
CL1	Rh	S26	91.48(5)	F1	P	F6	86.7(3)
CL1	Rh	OW	89.4(1)	F2	P	F3	179.2(2)
CL1	Rh	N1	89.4(1)	F2	P	F4	91.4(2)
CL2	Rh	S8	84.02(5)	F2	P	F5	88.7(3)
CL2	Rh	S26	88.04(5)	F2	P	F6	91.0(3)
CL2	Rh	OW	90.5(1)	F3	P	F4	89.4(2)
CL2	Rh	N1	90.7(1)	F3	P	F5	91.2(3)
S8	Rh	S26	166.76(5)	F3	P	F6	89.0(3)
S8	Rh	OW	92.9(1)	F4	P	F5	90.7(3)
S8	Rh	N1	85.9(1)	F4	P	F6	91.5(3)
S26	Rh	OW	97.7(1)	F5	P	F6	177.8(3)
S26	Rh	N1	83.6(1)	C10	O11	C12	109.2(4)
OW	Rh	N1	178.2(2)	C13	O14	C15	111.7(4)
Rh	S8	C7	95.9(2)	C16	O17	C18	114.4(5)
Rh	S8	C9	112.6(2)	C19	O20	C21	114.4(5)
C7	S8	C9	103.6(3)	C22	O23	C24	111.0(5)
Rh	S26	C25	112.8(2)	Rh	N1	C2	119.5(3)
Rh	S26	C27	94.4(2)	Rh	N1	C6	119.5(3)
C25	S26	C27	99.4(3)	C2	N1	C6	121.0(4)
F1	P	F2	86.9(2)	N1	C2	C3	120.7(5)
F1	P	F3	92.3(2)	N1	C2	C27	117.8(5)

C3	C2	C27	121.4(5)
C2	C3	C4	118.9(5)
C3	C4	C5	120.1(6)
C4	C5	C6	120.1(5)
N1	C6	C5	119.1(5)
N1	C6	C7	118.2(5)
C5	C6	C7	122.6(5)
S8	C7	C6	114.9(4)
S8	C9	C10	107.1(4)
O11	C10	C9	109.6(5)
O11	C12	C13	109.8(5)
O14	C13	C12	110.4(5)
O14	C15	C16	109.7(5)
O17	C16	C15	108.0(5)
O17	C18	C19	113.7(5)
O20	C19	C18	111.5(6)
O20	C21	C22	110.1(6)
O23	C22	C21	109.8(5)
O23	C24	C25	108.6(5)
S26	C25	C24	110.5(4)
S26	C27	C2	110.4(4)

Deposition Data.

Calculated Hydrogen Coordinates (C-H, O-H 0.95(2) A)

Atom	x	y	z
H3	0.4225	-0.1516	-0.5354
H4	0.5211	-0.2104	-0.3950
H5	0.5382	-0.1825	-0.2016
H71	0.5508	-0.0694	-0.0960
H72	0.4589	-0.1147	-0.0558
H91	0.2593	-0.1013	0.0142
H92	0.1685	-0.0740	-0.0814
H101	0.2347	-0.0288	0.1371
H102	0.1004	-0.0435	0.0862
H121	0.2236	0.0636	0.1704
H122	0.0805	0.0542	0.1567
H131	0.1097	0.1467	0.1345
H132	0.0698	0.1229	0.0119
H151	0.1981	0.2238	0.0339
H152	0.1707	0.1946	-0.0857
H161	0.4086	0.2209	0.0103
H162	0.3383	0.2554	-0.0893
H181	0.5366	0.1642	-0.2198
H182	0.5587	0.2110	-0.1255
H191	0.5600	0.2544	-0.2991
H192	0.4388	0.2732	-0.2466
H211	0.2649	0.2697	-0.3838
H212	0.2545	0.2160	-0.3070
H221	0.2517	0.2088	-0.5451
H222	0.1297	0.2119	-0.4833
H241	0.2306	0.1151	-0.6152
H242	0.0950	0.1241	-0.5833
H251	0.1427	0.0268	-0.5948
H252	0.1063	0.0428	-0.4722
H271	0.3325	-0.0571	-0.5816
H272	0.2178	-0.0639	-0.5105
HW1	0.2881	0.1105	-0.1914
HW2	0.2341	0.0970	-0.2895
HW3	0.1548	0.0881	-0.2318

The atoms were assigned Biso values of 6.0 A .
The two hydrogens of the water molecule are disordered over three sites with occupancies (from peak-densities) 0.72, 0.80 and 0.48 for HW1, HW2 and HW3 respectively

Deposition Data

General Temperature Factor Expressions - U's

Name	U(1,1)	U(2,2)	U(3,3)	U(1,2)	U(1,3)	U(2,3)
Rh	0.0266(2)	0.0354(2)	0.0276(2)	-0.0030(2)	0.0015(1)	-0.0018(2)
CL1	0.0331(7)	0.0673(9)	0.0434(7)	-0.0143(7)	0.0009(6)	0.0016(7)
CL2	0.0319(6)	0.0568(9)	0.0489(7)	-0.0114(6)	0.0033(6)	-0.0036(7)
S8	0.0398(7)	0.0435(7)	0.0311(7)	-0.0019(7)	0.0007(6)	0.0001(6)
S26	0.0434(7)	0.0516(9)	0.0310(7)	-0.0077(7)	0.0010(6)	0.0025(6)
P	0.0471(8)	0.0493(9)	0.0573(9)	-0.0084(8)	-0.0017(7)	0.0106(8)
F1	0.116(3)	0.067(3)	0.151(4)	0.022(3)	0.016(3)	0.007(3)
F2	0.079(3)	0.116(3)	0.128(3)	-0.045(2)	0.024(2)	-0.007(3)
F3	0.072(2)	0.098(3)	0.113(3)	-0.036(2)	0.019(2)	-0.004(3)
F4	0.104(3)	0.089(3)	0.240(5)	0.048(2)	0.063(3)	0.060(3)
F5	0.188(4)	0.123(3)	0.061(2)	-0.062(3)	-0.008(3)	0.006(3)
F6	0.149(4)	0.153(4)	0.068(2)	-0.041(3)	-0.002(3)	0.015(3)
OW	0.068(3)	0.068(3)	0.068(3)	0.005(2)	0.003(2)	-0.007(2)
O11	0.055(2)	0.063(2)	0.053(2)	0.001(2)	0.017(2)	0.005(2)
O14	0.056(2)	0.055(2)	0.062(2)	-0.000(2)	0.011(2)	0.002(2)
O17	0.068(2)	0.055(2)	0.066(2)	-0.017(2)	0.027(2)	-0.014(2)
O20	0.086(3)	0.099(4)	0.072(3)	0.005(3)	0.028(2)	-0.011(3)
O23	0.080(3)	0.062(3)	0.051(2)	0.015(2)	-0.003(2)	0.014(2)
N1	0.034(2)	0.036(2)	0.035(2)	-0.003(2)	0.009(2)	-0.009(2)
C2	0.043(3)	0.046(3)	0.038(3)	-0.006(3)	0.007(2)	-0.009(3)
C3	0.066(4)	0.063(4)	0.050(3)	-0.005(3)	0.012(3)	-0.022(3)
C4	0.075(4)	0.049(4)	0.079(4)	0.009(3)	0.006(4)	-0.019(3)
C5	0.058(4)	0.058(4)	0.063(4)	0.020(3)	-0.002(3)	-0.001(3)
C6	0.042(3)	0.035(3)	0.054(3)	0.004(3)	-0.004(3)	-0.004(3)
C7	0.058(3)	0.057(4)	0.044(3)	0.017(3)	-0.006(3)	0.001(3)
C9	0.072(4)	0.064(4)	0.041(3)	-0.020(3)	0.007(3)	0.009(3)
C10	0.053(3)	0.075(4)	0.052(3)	-0.007(3)	0.014(3)	0.016(3)
C12	0.071(4)	0.083(5)	0.070(4)	0.009(4)	0.038(3)	0.002(4)
C13	0.073(4)	0.072(4)	0.077(4)	0.009(4)	0.032(3)	0.002(4)
C15	0.065(4)	0.061(4)	0.056(3)	0.006(3)	0.014(3)	-0.017(3)
C16	0.084(4)	0.040(3)	0.055(4)	-0.005(3)	0.006(3)	-0.010(3)
C18	0.075(4)	0.072(5)	0.092(5)	-0.018(4)	0.030(4)	-0.024(4)
C19	0.096(5)	0.067(5)	0.100(5)	-0.013(4)	0.038(4)	0.000(4)
C21	0.096(5)	0.069(5)	0.084(5)	0.015(4)	0.032(4)	0.008(4)
C22	0.086(5)	0.072(5)	0.076(4)	0.026(4)	0.005(4)	0.012(4)
C24	0.066(4)	0.073(4)	0.062(4)	0.008(4)	-0.016(3)	0.024(3)
C25	0.052(3)	0.078(4)	0.050(3)	-0.004(3)	-0.016(3)	0.015(3)
C27	0.054(3)	0.060(4)	0.034(3)	-0.009(3)	0.004(3)	-0.011(3)

The form of the anisotropic thermal parameter is:

exp[-2PI2(h2a2U(1,1) + k2b2U(2,2) + l2c2U(3,3) + 2hkabU(1,2) + 2hlacU(1,3) + 2klbcU(2,3))] where a, b, and c are reciprocal lattice constants.

Deposition Data

Torsion Angles in the Macrocyclic Ligand

C9	S8	C7	C6	90.5
C7	S8	C9	C10	147.3
C27	S26	C25	C24	-151.7
C25	S26	C27	C2	-151.5
C12	O11	C10	C9	-163.1
C10	O11	C12	C13	-179.0
C15	O14	C13	C12	174.4
C13	O14	C15	C16	177.6
C18	O17	C16	C15	175.7
C16	O17	C18	C19	-77.3
C21	O20	C19	C18	92.5
C19	O20	C21	C22	-172.1
C24	O23	C22	C21	-170.2
C22	O23	C24	C25	-172.3
C6	N1	C2	C3	-0.5
C6	N1	C2	C27	176.3
C2	N1	C6	C5	-1.5
C2	N1	C6	C7	175.2
N1	C2	C3	C4	2.0
C27	C2	C3	C4	-174.7
N1	C2	C27	S26	32.1
C3	C2	C27	S26	-151.1
C2	C3	C4	C5	-1.4
C3	C4	C5	C6	-0.7
C4	C5	C6	N1	2.1
C4	C5	C6	C7	-174.4
N1	C6	C7	S8	21.5
C5	C6	C7	S8	-161.9
S8	C9	C10	O11	46.6
O11	C12	C13	O14	-70.3
O14	C15	C16	O17	61.6
O17	C18	C19	O20	-66.8
O20	C21	C22	O23	70.5
O23	C24	C25	S26	-55.3

Deposition data: Least-Squares Planes

The equation of the plane is of the form: $Ax + By + Cz - D = 0$

where A,B,C & D are constants and x,y & z are orthogonalized coordinates.

Plane No.	A	B	C	D	Atom	x	y	z	Distance	Esd
1	-0.9068	-0.4117	-0.0906	-3.1401		Atoms in Plane				
					Rh	3.6854	0.0510	-3.0695	0.055	0.001
					N1	4.5067	-1.7253	-3.5890	0.089	0.004
					OW	2.8069	1.8360	-2.4980	0.065	0.004
					S8	3.9629	-0.6551	-0.8677	-0.105	0.001
					S26	3.8796	0.5106	-5.3420	-0.104	0.001
					Chi Squared =	33872.				
						Other Atoms				
					CL1	1.5644	-0.8682	-3.3752	2.385	0.001
					CL2	5.8037	0.9775	-2.7827	-2.273	0.001
					C9	2.5055	-1.5603	-0.2318	1.532	0.006
					C25	2.3319	1.1231	-6.0704	1.113	0.006
2	0.8804	0.4534	-0.1388	3.6904		Atoms in Plane				
					N1	4.5067	-1.7253	-3.5890	-0.007	0.004
					C2	4.4958	-2.1071	-4.8720	-0.011	0.005
					C3	5.0787	-3.3049	-5.2604	0.013	0.006
					C4	5.6278	-4.1089	-4.3090	0.000	0.006
					C5	5.6252	-3.7184	-2.9891	-0.009	0.006
					C6	5.0792	-2.5055	-2.6295	0.011	0.005
					Rh	3.6854	0.0510	-3.0695	0.004	0.001
					Chi Squared =	103.				
						Other Atoms				
					C7	5.1539	-1.9742	-1.2448	0.125	0.006
					C27	3.7768	-1.2401	-5.8495	-0.115	0.005

Dihedral angle between planes 1 and 2 is 166.5 degrees
i.e. a 13.5 degree rotation from planarity.